IMPERIAL

Department of Aeronautics

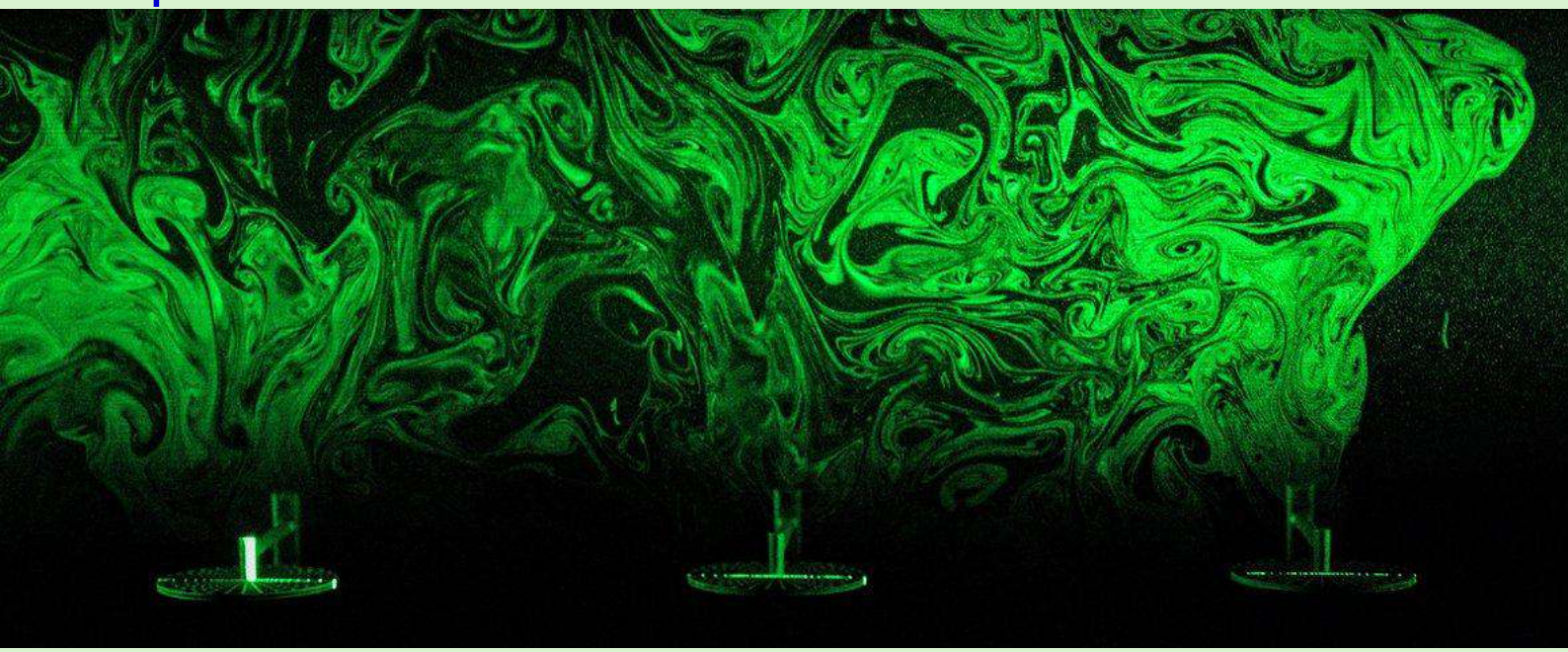

Recent Advances in Turbulent Wind Farm Dynamics Colloquium

22-24 April 2026

Booklet of Abstracts

Editors: Oliver Buxton, Martin Bourhis, Michael Hölling, & Richard Stevens

UKRI Engineering and Physical Sciences Research Council

ERCOFTAC

EUROPEAN MECHANICS SOCIETY

Table of Contents

Wind Farm Entrainment

Raúl Bayoán Cal [1]

[1] Department of Mechanical and Materials Engineering , Portland State University, Portland, OR, USA

email-address of the corresponding author: rcal@pdx.edu

Abstract:
Wind farms interact with the incoming resource, the atmospheric boundary layer. In doing so, the mechanism for recovery in the wakes is entrainment. This mechanism is hereby discussed under various scenarios starting with terrestrial wind farms and arriving at the case of offshore wind farms, where offshore wind has the potential to unlock the vast wind energy resources over deep waters. Achieving the potential of this technology requires a deeper understanding of how the dynamics introduced by coupling between the wind, wakes, and turbine platform affect wake interactions and farm level power output.

Experiments performed in the Portland State wind and wave tunnel to explore these dynamics under various wave conditions. The farm is constructed of a four-by-three layout spaced at 5D in x and 3D in z, with 15 cm diameter turbines. The farm's flow field is measured using 2D-3C particle image velocimetry. Individual turbine motion is captured using optical tracking, and power output is measured through generators placed in the nacelle of each turbine. Flow field results are described in terms of both ensemble and wave-phase-averaged quantities. Phase averaging is shown to reveal different wave-dependent behavior and structures that are not evident in the ensemble sense thus revealing insights into entrainment.

Figure 1: *Scaled offshore wind farm.*

Characteristics of the temporal evolution of the turbulent/non-turbulent interface in a planar wake

Jiangang Chen [1] and Oliver R. H. Buxton [2]

[1] Institute of Extreme Mechanics, School of Aeronautics, Northwestern Polytechnical University, Xi'an, China
[2] Department of Aeronautics, Imperial College London, London, United Kingdom

email-adress of the corresponding authour: jiangang.chen@nwpu.edu.cn

An essential feature of turbulent flow is that it continuously entrains and mixes with the surrounding environmental fluid. The local rate of entrainment of the environmental fluid into the turbulent region depends in the first place on the local dynamics of the interfacial layer, usually referred to as the turbulent/non-turbulent interface (TNTI), which undergoes intensive spatial-temporal evolution during the development of the turbulent flow [1, 2]. How the local dynamics of the TNTI evolves over time, and how such evolution is related to the dynamics of the turbulence in the bulk region remain open questions. A better understanding of the associated physics is of practical importance, such as for developing more accurate models to predict the downstream expansion of the wake of a wind turbine.

In the present work, we experimentally investigated the characteristics of the temporal evolution of the TNTI in a planar wake. In the experiment, a vertically arranged circular cylinder was electrically towed through a quiescent water flume at a constant speed $U_D = 0.6m/s$, corresponding to a global Reynolds number Re ($\equiv U_D d/\nu$ where d is the cylinder diameter) of about 6000. A flourescent dye (Rohdamine 6G) was released from the rear surface of the cylinder to mark the turbulent wake (figure 1a). A simultaneous measurement of the velocity field and the dye concentration field was performed using a two-camera planar particle image velocimetry (PIV) system and a planar laser-induced fluorescence (PLIF) system, respectively (figure 1a). The fields of view of the two PIV cameras were combined to form a larger one of $9d$-by-$3d$ (figure 1b). The sampling frequency of the PIV and PLIF systems was 200Hz.

Some results are shown in figures 2 and 3. The identified TNTI at different time instants is displayed in figure 2, where $t^* \equiv tU_D/d$ is the non-dimensional time. Note that $t^* = 0$ is losely defined as the the moment when the cylinder passes through the measurement plane. It is clear that the TNTI spreads towards the environmental fluid as t^* increases. As expected, the magnitude of the vorticity of the wake decays as the TNTI spreads. A natural question arises that how the decay of the bulk turbulence is related to the temporal evolution of the TNTI. The characteristic of the evolution of the TNTI is first reflected in the variation of its spatial location with respect to time, which is shown in figure 3(a). $\langle y_{I,exact} \rangle$ represents the mean location of the TNTI over one PIV image. It is observed that $\langle y_{I,exact} \rangle (t^*)$ is characterized by three distinct stages: (i) $t^* < T1$, $\langle y_{I,exact} \rangle$ is almost constant in this stage; (ii) $T1 < t^* < T2$, $\langle y_{I,exact} \rangle$ increases rapidly with t^*; (iii) $t^* > T2$, $\langle y_{I,exact} \rangle$ increases at a much slower rate than that in stage (ii) with a sharp transition at $t^* = T2$. It is interesting to see that the instants $T1$ and $T2$, which distinguish the three stages of the temporal evolution of the TNTI of the wake, almost exactly demarcate the different decay behavior of the turbulent kinetic energy in the bulk region of the flow (figure 3b). The physics behind the observed correlation between the evolution of the TNTI and the decay of the turbulence in the bulk region will be investigated in detail in the presentation.

References

[1] da Silva, C. B., Hunt, J. C. R., Eames, I. and Westerweel, J., (2014), Interfacial Layers Between Regions of Different Turbulence Intensity. *Annu. Rev. Fluid Mech., vol. 46, pp. 567–590.*

[2] Chen, J. G. and Buxton, O. R. H., (2024), Turbulent/turbulent entrainment in a planar wake. *J. Fluid Mech., vol. 1000, A26.*

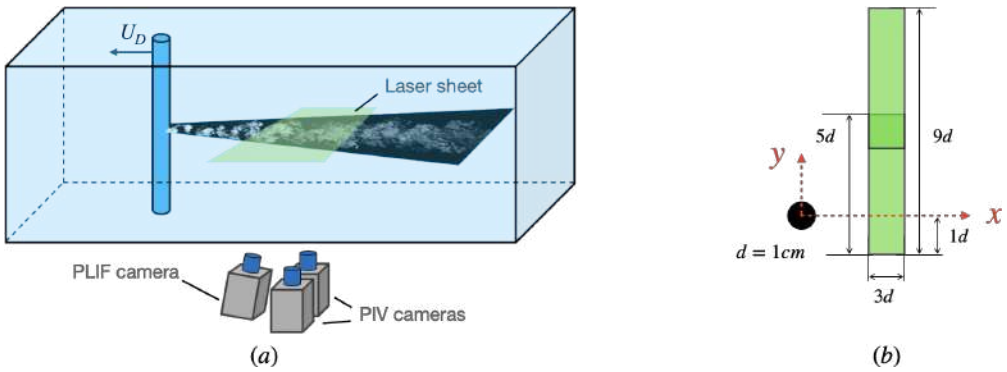

Figure 1: *(a) Skematic setup of the experiment; (b)the arrangement of the cylinder and the field of view of the PIV cameras.*

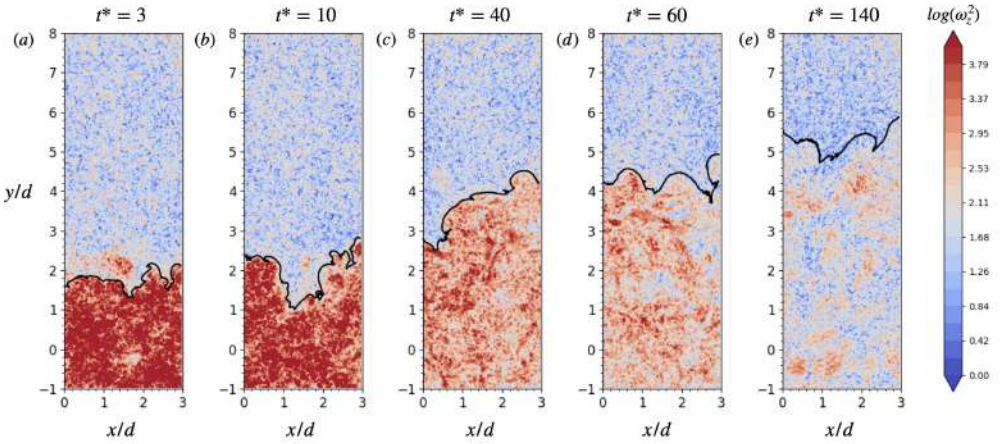

Figure 2: *The turbulent/non-turbulent interface between the wake and the environmental fluid at different time instances.*

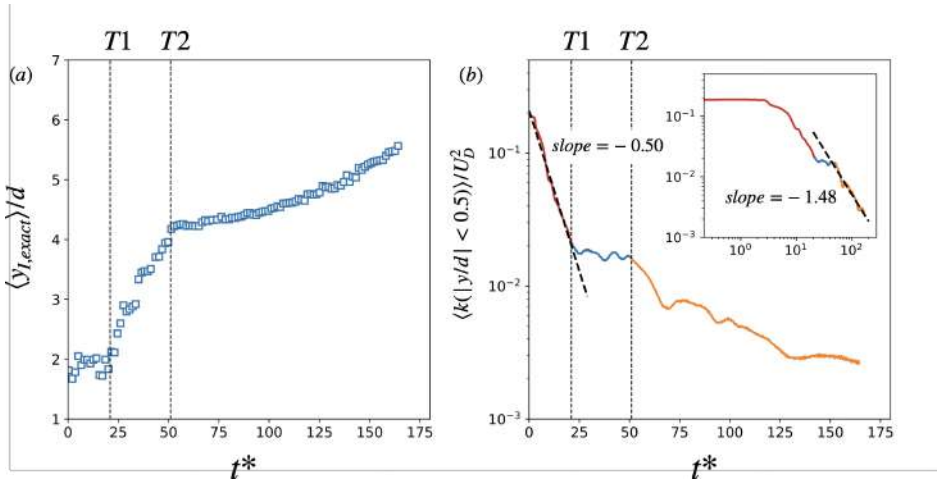

Figure 3: *Evolution of the (a)mean turbulent/non-turbulent interface location and (b) turbulent kinetic energy over time.*

The entrainment of mass, momentum, and kinetic energy into turbulent wakes

Oliver R. H. Buxton [1], and Jiangang Chen [2]

[1] Department of Aeronautics, Imperial College London, London, United Kingdom
[2] School of Aeronautics, Northwestern Polytechnical University, Xi'an, China

email-address of the corresponding author: o.buxton@imperial.ac.uk

Abstract:

The spreading of wind turbine wakes with downstream distance, along with the coupled diminishment of the wake's velocity deficit, is a vitally important factor in the design of wind-farm layouts. Exposure of a wind turbine to the turbulent wake of an upstream machine leads to a reduction in power production [2], due to the incident velocity deficit, as well as an acceleration of the rate at which fatigue damage is accumulated [3], due to the unsteady forcing of the turbine's mechanical components. Exposure to an upstream wake, or incoming atmospheric turbulence, means that wind turbine wakes are almost always exposed to a turbulent background. Accordingly, the spreading of the wake (and associated wake recovery) is governed by the entrainment physics that take place at the turbulent/turbulent interface (TTI) at the wake's outermost boundary. Engineering models that accurately capture wake spreading must therefore grapple with these entrainment physics.

This study reports on a combined particle image velocimetry (PIV)/planar laser induced fluorescence (PLIF) campaign of experiments seeking to understand the nature of the entrainment of mass, streamwise momentum, and kinetic energy into a turbulent wake. For simplicity, a wake produced by a circular cylinder is used (with a Reynolds number based off the cylinder diameter D of $Re_D = 3.8 \times 10^3$), although the results have subsequently been shown to be transferable to more realistic model wind-turbine wakes [1]. The cylinder is exposed to different "flavours" of freestream turbulence, parametrised by the turbulence intensity k and length scale $\mathcal{L}$ of the incident grid-generated (decaying) turbulence. Figure 1(a) illustrates the different flavours of freestream turbulence (FST) studied whilst (b) presents the various measurement stations, centred on $x/D = \{6.5, 10, 20, 30, 40\}$, that were interrogated set against the backdrop of an exemplar PLIF image of the wake.

Given an entrainment mass flux of $\dot{M}$, we derive a theoretical basis for the efficiencies with which rates of streamwise momentum $\dot{P}_x$ and kinetic energy $\dot{K}$ are entrained into the wake, relative to the mass, from an idealised non-turbulent background, i.e. the ratios $\dot{P}_x/\dot{M} = U_\infty$ and $\dot{K}/\dot{M} = \frac{1}{2}U_\infty^2$ where U_∞ is the incident wind speed. Our results, presented in figures 2(b) and (c), show that the presence of FST affects the rate at which mass is entrained into the wake, with an enhanced mass flux (relative to the non-turbulent background) in the near wake and a reduced mass flux in the far wake. However, our results show that the efficiencies with which momentum and kinetic energy are entrained into the wake, relative to mass, are largely preserved such that $\dot{P}_x$ and $\dot{K}$ are slaved to $\dot{M}$. This efficiency is broken in the near wake where the presence of coherent motions means that kinetic energy is entrained into the wake more efficiently when FST is present than from an idealised non-turbulent background. These results have important consequences for the modelling of wake recovery into both individual wind-turbine wakes and wind-farm wakes which rely on the entrainment hypothesis, $\dot{M} = E\mathcal{V}$ where E is an entrianment coefficient and $\mathcal{V}$ is a suitable velocity scale within the wake. If the presence of FST enhances the entrainment efficiency of $\dot{K}$ then it is not appropriate to simply model $\dot{K} = \frac{1}{2}U_\infty^2 E\mathcal{V}$.

References

[1] Bourhis, M., Messmer, T., Hölling, M., and Buxton, O. (2025). Impact of free-stream turbulence and thrust coefficient on wind turbine-generated wakes. *Journal of Fluid Mechanics*, 1023:A3.

[2] Stevens, R., Gayme, D., and Meneveau, C. (2014). Large eddy simulation studies of the effects of alignment and wind farm length. *Journal of Renewable and Sustainable Energy*, 6(2).

[3] Thomsen, K. and Sørensen, P. (1999). Fatigue loads for wind turbines operating in wakes. *Journal of Wind Engineering and Industrial Aerodynamics*, 80(1-2):121–136.

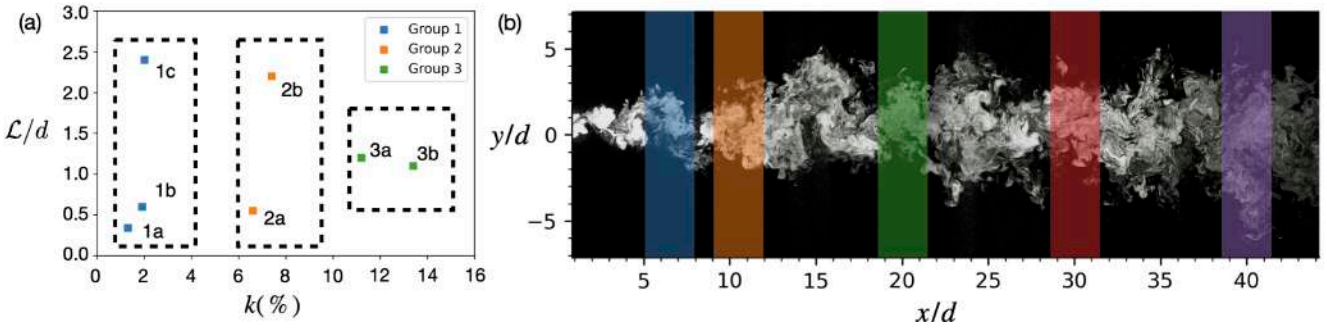

Figure 1: (a) $\{\mathcal{L}, k\}$ parameter space spanned for the various cases ("flavours") of FST studied.

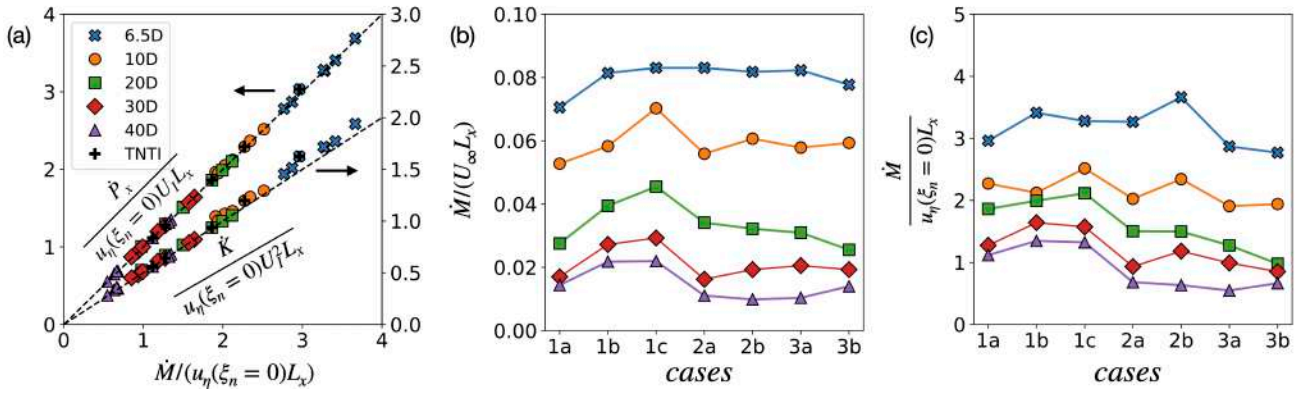

Figure 2: (a) Entrainment mass $\dot{M}$, streamwise momentum $\dot{P}_x$, and kinetic energy $\dot{K}$ fluxes for the FST cases denoted in figure 1(a), including the no-grid (non-turbulent background) case 1a. $\dot{M}$ for the various FST cases normalised by (b) large-scale (invariant) quantities and (c) the local Kolmogorov velocity scale u_η extracted from the wake boundary.

Large-scale variability and turbulence structure in environmental flows relevant to wind energy

Abstract

This talk will focus on recent insights into the characterization and interpretation of turbulence in environmental flows relevant to wind turbines and wind farms, with emphasis on how the treatment of large-scale flow variability influences inferred turbulence structure and spectral dynamics. I will first focus on the impact of detrending methodologies on turbulence quantities, specifically the autocorrelation function ρ_{uu} and the velocity spectrum $\phi(f)$, which are fundamental descriptors of inflow turbulence conditions. Conventional approaches, including frequency-based high-pass filtering and polynomial detrending, are evaluated against an alternative approach based on empirical mode decomposition (EMD). The analysis demonstrates that intervals of acceleration and deceleration, commonly observed in atmospheric boundary layers and tidal or riverine flows, can significantly bias turbulence statistics when standard detrending procedures are applied, altering ρ_{uu} and $\phi(f)$, and thereby affecting the estimation of derived turbulence quantities. The EMD-based approach provides a robust strategy to remove large-scale trends while preserving dynamically relevant turbulent scales. Then, I will present a theoretical formulation that extends a generalized velocity spectrum model, capable of reproducing the debated k^{-1} spectral scaling through the statistical superposition of scale-dependent eddy clusters. The approach links scale-invariant clustering of energy-containing motions to the emergence of the k^{-1} regime without relying on prescribed eddy-correlation structures or classical inertial-range assumptions. Validation using atmospheric boundary-layer and riverine datasets shows that the formulation reproduces observed spectral regimes and identifies the conditions under which k^{-1} scaling emerges or disappears, providing new insights into turbulence organization and offering improved tools for interpreting inflow turbulence and loading conditions in wind turbine and wind farm environments.

A Physics-Based Inverse Framework for Tailoring Mean Flow Profiles using Active Grids

Paweł Baj [1]

[1] Institute of Aeronautics and Applied Mechanics, Warsaw University of Technology, Warsaw, Poland

email-address of the corresponding author: pawel.baj@pw.edu.pl

Abstract:
The reliable prediction of wind farm performance, urban pedestrian comfort, and UAV flight stability critically depends on the accurate experimental reproduction of Atmospheric Boundary Layer (ABL) characteristics in wind tunnels. Active grids (AGs), composed of arrays of independently controllable rotating blades (see Figure 2), have emerged as powerful tools for this purpose, offering unprecedented flexibility in generating sheared mean flows and high-intensity turbulence. However, while stochastic actuation protocols (e.g., Makita-style) are well-established for maximizing turbulence levels, the targeted shaping of specific mean velocity profiles remains a significant challenge. The lack of a robust, physics-based inverse mapping from a desired velocity profile $U(y)$ to the required blade actuation angles $\theta(y)$ has historically forced researchers to rely on heuristic approaches or "black-box" iterative methods, which often lack generality and predictive power.

In this work, we introduce a novel, deterministic numerical framework for active grid control that bridges this gap. We extend the classical passive-grid theory of McCarthy [1] to explicitly account for the aerodynamic forcing of AG. Our model incorporates the lift forces generated by blade inclination, which are critical for flow redirection and redistribution. The physical domain is modeled as a two-dimensional channel partitioned by the grid into upstream Ω^- and downstream Ω^+ regions, as illustrated in the schematic in Figure 1. The flow is treated as inviscid, rotational, and incompressible, with the grid acting as a discontinuity plane that introduces a localized pressure drop and a jump in lateral velocity. The perturbation stream function $\Psi^\pm$ in each subdomain is governed by a linear Helmholtz-type equation:

$$\frac{\partial^2 \Psi^\pm}{\partial x_1^2} + \frac{\partial^2 \Psi^\pm}{\partial x_2^2} = \frac{(U^\pm)''}{U^\pm}\Psi^\pm, \quad \boldsymbol{u}^{*\pm} = [\Psi_y^\pm, -\Psi_x^\pm] \tag{1}$$

The upstream and downstream domains are coupled at the interface $x_1 = 0$ via nonlinear conservation laws for mass, momentum, and energy. The model utilizes lift and drag coefficients derived from a database of RANS simulations, rather than theoretical flat-plate approximations.

The problem is discretized using the Finite Element Method (FEM). A key feature of our approach is the use of static condensation to reduce the large coupled system to a compact set of nonlinear equations for the blade angles alone. This enables rapid solution generation—orders of magnitude faster than full CFD inversions—making the method suitable for real-time experimental planning. We demonstrate that this framework allows for the predictive design of blade angle distributions to achieve specific target flows. Figure 3 presents a validation case where a power-law ABL profile is reproduced in the Environmental Wind Tunnel at Warsaw University of Technology. The results indicate superior agreement compared to classical static blockage approximations (McCarthy's method).

References

[1] McCarthy J.H., (1964), Steady flow past non-uniform wire screens, *Journal of Fluid Mechanics, vol. 19, pp. 491-512*

[2] Huret G. et al., (2023): Numerical study of the generation of sheared turbulent flows by means of non-uniform grids, *Fluid Dynamics Research, vol. 55, 055502*

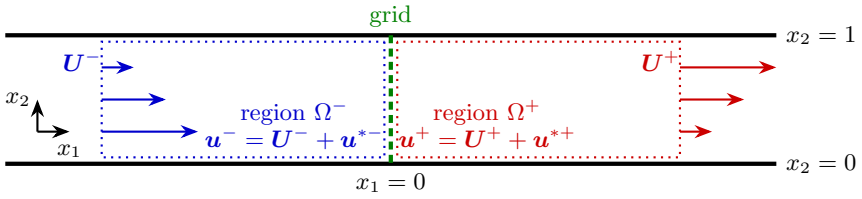

Figure 1: *Schematic representation of the flow domain partitioned into upstream Ω^- and downstream Ω^+ regions. The total velocity field $\boldsymbol{u}^{\pm}(x, y)$ is split into a prescribed far-field profile $U^{\pm}(y)$ and the perturbation $\boldsymbol{u}^{*\pm}(x, y)$.*

Figure 2: *Experimental setup: The 8×8 axis active grid installed in the Environmental Wind Tunnel at WUT.*

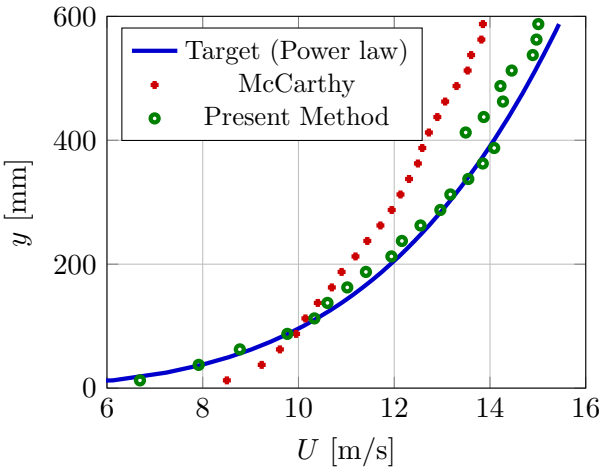

Figure 3: *Experimental validation: Reproduction of a power-law ABL profile. Comparison between target, McCarthy's method, and the proposed inverse framework.*

Investigation of a swirling wake under the effect of upstream disturbances

K. Abdelaziz [1], C. Raibaudo [1] and P. Bénard [2] and N. Mazellier [1],

[1] PRISME, University of Orléans, Orléans, FRANCE
[2] CORIA, University of Rouen, Rouen, FRANCE

email-address of the corresponding author: nicolas.mazellier@univ-orleans.fr

Abstract:
Over the past decades, wake of porous disc has been used as a popular surrogate of wind turbine both numerically [1] and experimentally [2]. More recently, the addition of swirl in a passive manner has proved to be an effective way of mimicking the main characteristics of the mean flow downstream real-scale wind turbines [3]. While emphazing the key role of swirl in the early stage of the wake development, this study was performed in laminar inflow conditions thereby far from field conditions. To tackle this issue, we report an experimental investigation of the wake downstream a porous disc with controlled perturbations injected in the incoming flow.

To this end, an active grid was used to generate periodic perturbations superimposed on a turbulent inflow (see Figure 1). This grid consist of square flaps whose movements are driven by eight independent motors. In this study, a flapping motion was imposed at a frequency $f_e = 3$ Hz with a peak-to-peak amplitude α of up to 45°. It is important to notice that this frequency is much lower than that featuring the integral length scale of the turbulent flow generated by the grid when the flaps remain static. Therefore, this experiment is intended to mimic only the effect of low-frequency pertubations such as wake meandering in wind farms [4]. As illustrated in Figure 2(a), a X-probe hot-wire was used to assess the impact of these disturbances on the properties of the wake generated downstream the porous disk. In addition, a single-probe hot-wire was installed near the disc, but away from its wake, to provide a reference signal characterizing the incoming disturbance. Let us introduce the cross-correlation between the incoming fluctuation $u'(x_0,t)$ and the fluctuation of the swirl velocity $w'(x,t)$ such that

$$R_{uw}(x,\tau) = \frac{\langle u'(x_0,t)\, w'(x,t+\tau)\rangle}{\sqrt{\left\langle u'(x_0,t)^2\right\rangle}\sqrt{\left\langle w'(x,t)^2\right\rangle}}. \tag{1}$$

(2)

This cross-correlation was used as a metric to evaluate the influence of the low-frequency incoming disturbance on the wake properties. A typical example of such cross-correlation is displayed in Figure 2(b) for both non-swirling and swirling porous discs. Whilst in both cases the disturbance persists in the wake of the porous disc, it is evident that, in the absence of a swirling motion [3], the incident disturbance is significantly dampened. This phenomenon could lead to complex interactions at the scale of a wind farm by inducing long-range interactions. A more detailed analysis will be presented during the workshop.

References

[1] Réthoré, P. E., van der Laan, P., Troldborg, N., Zahle, F., and Sørensen, N. N. (2014). Verification and validation of an actuator disc model. *Wind Energy, 17(6), 919-937.*

[2] Aubrun, S., Loyer, S., Hancock, P. E., and Hayden, P. (2013). Wind turbine wake properties: Comparison between a non-rotating simplified wind turbine model and a rotating model. *Journal of Wind Engineering and Industrial Aerodynamics, 120, 1-8.*

[3] Noriega, E. F., and Mazellier, N. (2025). Scaling analysis of the swirling wake of a porous disc: application to wind turbines. *Journal of Fluid Mechanics, 1003, A34.*

[4] Foti, D., Yang, X., Shen, L., and Sotiropoulos, F. (2019). Effect of wind turbine nacelle on turbine wake dynamics in large wind farms. *Journal of Fluid Mechanics, 869, 1-26.*

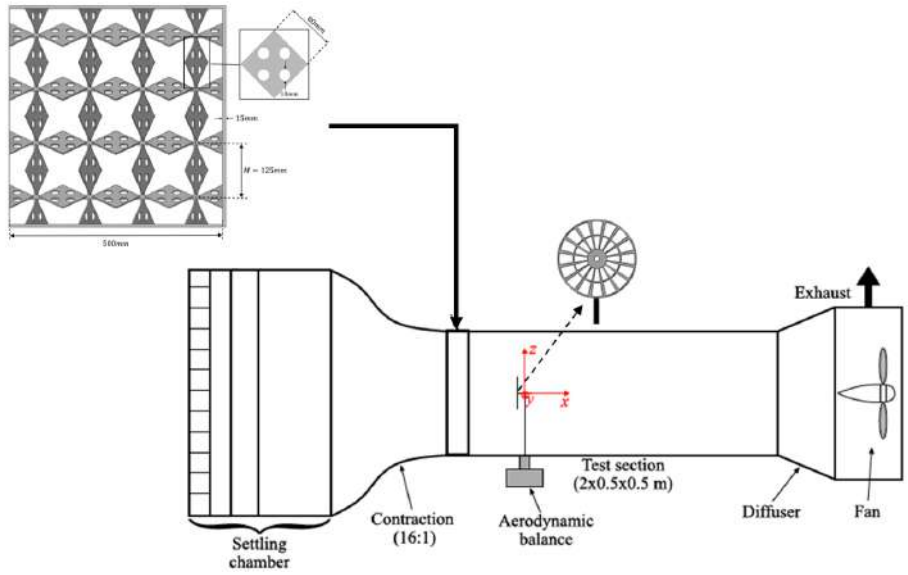

Figure 1: Schematic of the wind tunnel experiment. To generate controlled inflow disturbances, an active grid was installed at the inlet of the test section.

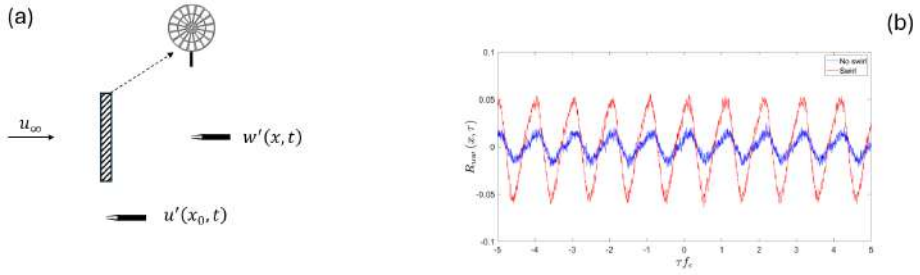

Figure 2: (a) Schematic of the metrology used to estimate the influence of the incoming disturbances of the wake properties. A single probe hot-wire was installed on the side of the porous disk and was used as a reference. A X-probe hot-wire was located in the wake. (b) Typical cross-correlation coefficients between the fluctuating reference velocity signal and the fluctuation of the swirl velocity component ($\alpha = 25°$).

On the Evolution and Receptivity of Turbulence in Wakes, with Application to Wind Turbine Flows

I. Neunaber [1], R.J. Hearst [2]

[1] Department of Engineering Mechanics, KTH Royal Institute of Technology, Stockholm, Sweden
[2] Department of Energy and Process Engineering, Norwegian University of Science and Technology, Trondheim, Norway

email-address of the corresponding author: neunaber@kth.se

Abstract:
Wakes have been the subject of sustained investigation for more than a century, yet their central importance has been renewed by the rapid expansion of wind energy, wherein the interaction of turbulent wakes governs both power production and structural loading within wind farms, e.g., [1]. In this context, wake turbulence constitutes an intrinsically multi-scale phenomenon, arising from the interplay between coherent structures, shear-driven instabilities, and external turbulent forcing across a wide range of spatial and temporal scales, e.g., [2]. Despite extensive study, the physical mechanisms governing the evolution and interaction of turbulence in wakes remain incompletely understood.

This presentation examines these mechanisms through controlled wind tunnel experiments on porous discs (a photo of the set-up of exemplary experiments is shown in figure 1), which serve as canonical models of wake-generating objects, e.g., [7]. Measurements demonstrate that wake evolution depends not only on inflow turbulence, but also on the internal structure of the wake-generating object itself [7, 5, 3]. Discs with comparable drag coefficients but different radial blockage distributions produce fundamentally different wake development, revealing that wake turbulence is not determined solely by integral momentum deficit, but also by the initial distribution of blockage. The influence of inflow turbulence may be consistently interpreted as modifying the effective origin of turbulence development, providing a physical basis for the virtual origin concept in wake modelling [6].

More fundamentally, the experiments reveal that wakes exhibit pronounced receptivity to external perturbations, cf., figure 2. The wake of the nominally non-shedding porous disc acquires distinct spectral signatures when placed in proximity to shedding wakes, demonstrating that wake turbulence is not solely an intrinsic product of local instability, but may be driven and structured by external forcing [4]. Linear stability analysis confirms that these wakes selectively amplify perturbations within preferred frequency ranges, thereby establishing receptivity as a governing mechanism in wake evolution and interaction.

The relevance of these findings to wind energy applications is demonstrated through applying linear stability analysis to profiles obtained from lidar measurements of wind turbine wakes, which show receptivity to structures of Strouhal numbers around 0.3, cf. figure 3. These observations suggest that wake turbulence in wind farms emerges from a dynamic interplay between intrinsic instability and external forcing. This perspective has direct implications for the prediction, modelling, and control of turbulent wakes in wind energy flows.

References

[1] Vermeer L., Sørensen J. and Crespo A. (2003) Wind turbine wake aerodynamics, *Science, vol. 366 pp. 443*

[2] Veers P., Dykes K., Lantz E. *et al.* (2019) Grand challenges in the science of wind energy, *Prog. Aero. Sci., vol. 39 pp. 467e510*

[3] Berstad F.O., Hearst R.J., and Neunaber I. (2025) Wake merging and turbulence transition downstream of side-by-side porous discs, *J Fluid Mech 1015:A39*

[4] Neunaber I., Yadala S., Hearst R.J. (2025) Induced periodicity in wakes, *J Fluid Mech 1022:R3*

[5] Vinnes M. K., Neunaber I., Lykke H-M. H. and Hearst R. J. (2023) Characterizing porous disk wakes in different turbulent inflow conditions with higher-order statistics, *Exp Fluids 64, 25*

[6] Neunaber I., Hölling M. and Obligado M. (2024) Leading effect for wind turbine wake models, *Renew Energy, vol. 223 pp. 119935*

[7] Aubrun, S., Bastankhah, M., Cal, R.B. *et al.* (2019): Round-robin tests of porous disc models, *Journal of Physics: Conference Series*, Vol. 1256, No. 1, p. 012004

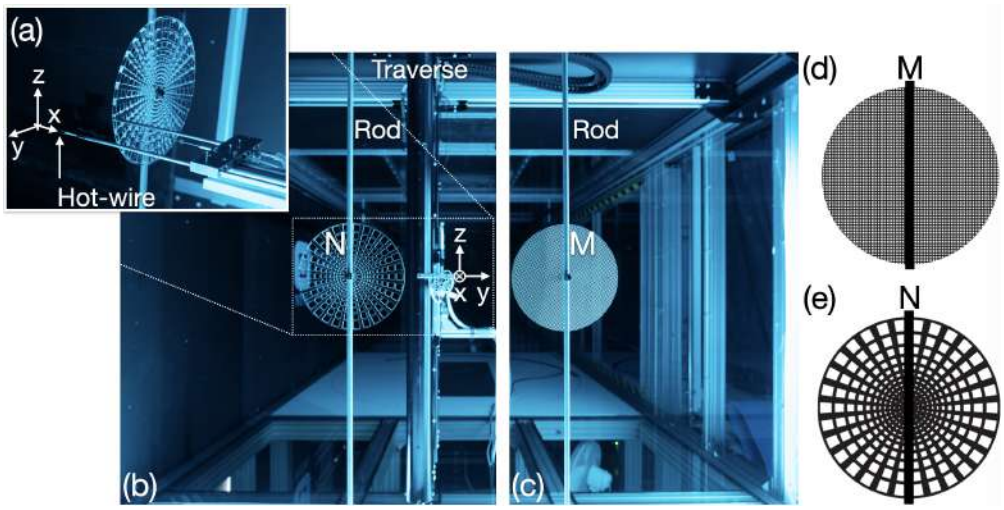

Figure 1: *Photograph and schematic of the two discs and the set-up with the hot-wire mounted on a traverse; from [3] published under CC-BY-4.0 license.*

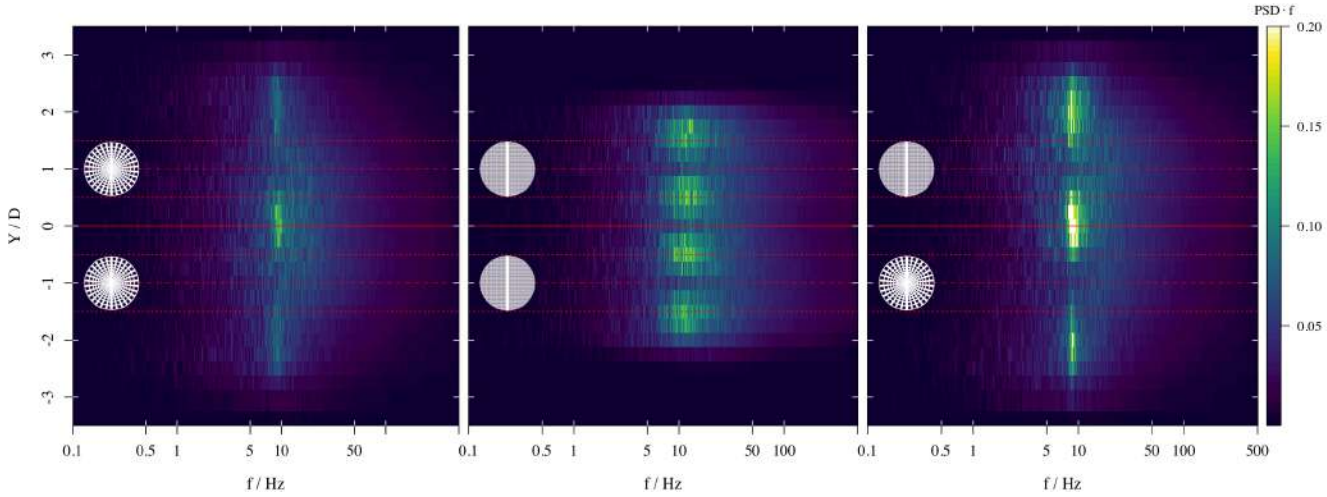

Figure 2: *Pre-multiplied spectrograms of the three investigated disc combinations.*

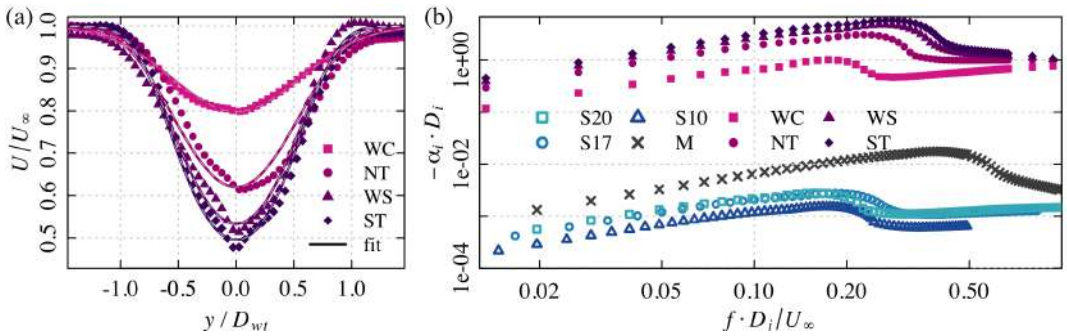

Figure 3: *Wind turbine wake profiles and fits (a) and results from the linear stability analysis of these wake profiles and profiles from solid discs and the uniform porous disc (b); from [4] (CC-BY-4.0 license).*

Time-resolved PIV Measurements of the Wake Response of a Porous Disc to Extreme Wind Shear (EWS) Gusts

M. Yazdanpanah[1,2], C. Evcimen[1], M. Perçin[1,2] and O. Uzol[1,2]

[1] Department of Aerospace Engineering, Middle East Technical University (METU), Ankara, Turkey
[2] METU Center for Wind Energy Research (RÜZGEM), Middle East Technical University (METU), Ankara, Turkey

email-address of the corresponding author: uzol@metu.edu.tr

Abstract:
Extreme Wind Shear (EWS), defined in IEC 61400-1 [1] is a transient perturbation across the rotor diameter superimposed on the mean power-law profile, with amplitude scaled by turbulence class parameters. Its influence on wake dynamics and turbulence evolution remains insufficiently documented experimentally. Numerical investigations of transient shear effects on turbine wakes by Sezer-Uzol & Uzol [2] showed pronounced wake skewing and altered recovery behavior under time-varying shear inflow. High-fidelity CFD studies incorporating IEC-type extreme shear conditions further indicate that transient shear can induce dynamically non-equilibrium wake states, enhanced turbulence production, and asymmetric momentum redistribution (Zareian et al. [3]; Tong [4]). More recent LES investigations of turbines subjected to strong directional and vertical shear confirm significant wake asymmetry and altered turbulence transport mechanisms (Chanprasert et al. [5]). Despite these advances, controlled laboratory measurements resolving the time-dependent wake response to IEC-defined EWS gusts remain scarce. The present study provides time-resolved 2D2C Particle Image Velocimetry (PIV) measurements of the wake response of a porous disc subjected to repeatable EWS gusts in an open-return type atmospheric wind tunnel that has a 1 m $\times$ 1 m cross-section test section (Figure 1). An active turbulence grid is used to generate deterministic transient vertical shear profiles representative of scaled IEC EWS conditions (Figure 1). Time-resolved planar PIV measurements in the vertical mid-plane downstream of the disc capture the evolution of the velocity field, turbulent kinetic energy and Reynolds shear stresses during and after the gust. The study is expected to contribute to the physical understanding of transient shear–wake interaction, contributing to improved modeling of wind-farm dynamics under extreme atmospheric events.

References

[1] International Electrotechnical Commission (IEC), (2019): *IEC 61400-1: Wind Turbines – Part 1: Design Requirements*, IEC, Geneva.

[2] Sezer-Uzol N. and Uzol O., (2013), Effect of steady and transient wind shear on the wake structure and performance of a horizontal-axis wind turbine rotor, *Wind Energy*, vol. 16, pp. 1–17. :contentReference[oaicite:1]index=1

[3] Zareian F., Rasam B., He H. and Liu G., (2024), A detached-eddy simulation study on assessing the impact of extreme wind conditions on wind turbine aerodynamic response and wake evolution, *Energy*, vol. 290, 130210. :contentReference[oaicite:2]index=2

[4] Tong G., Wang L., Zhao Y. and Liu J., (2025), High-fidelity IDDES simulation evaluating impacts of extreme wind conditions on wind turbine aerodynamic response and wake evolution, *Energy*, vol. 302, 131945. :contentReference[oaicite:3]index=3

[5] Chanprasert W., Sharma R. N., Cater J. E. and Norris S. E., (2022), Large-eddy simulation of wind turbine wake interaction in directionally sheared inflows, *Renewable Energy*, vol. 201, pp. 1096–1110. :contentReference[oaicite:4]index=4

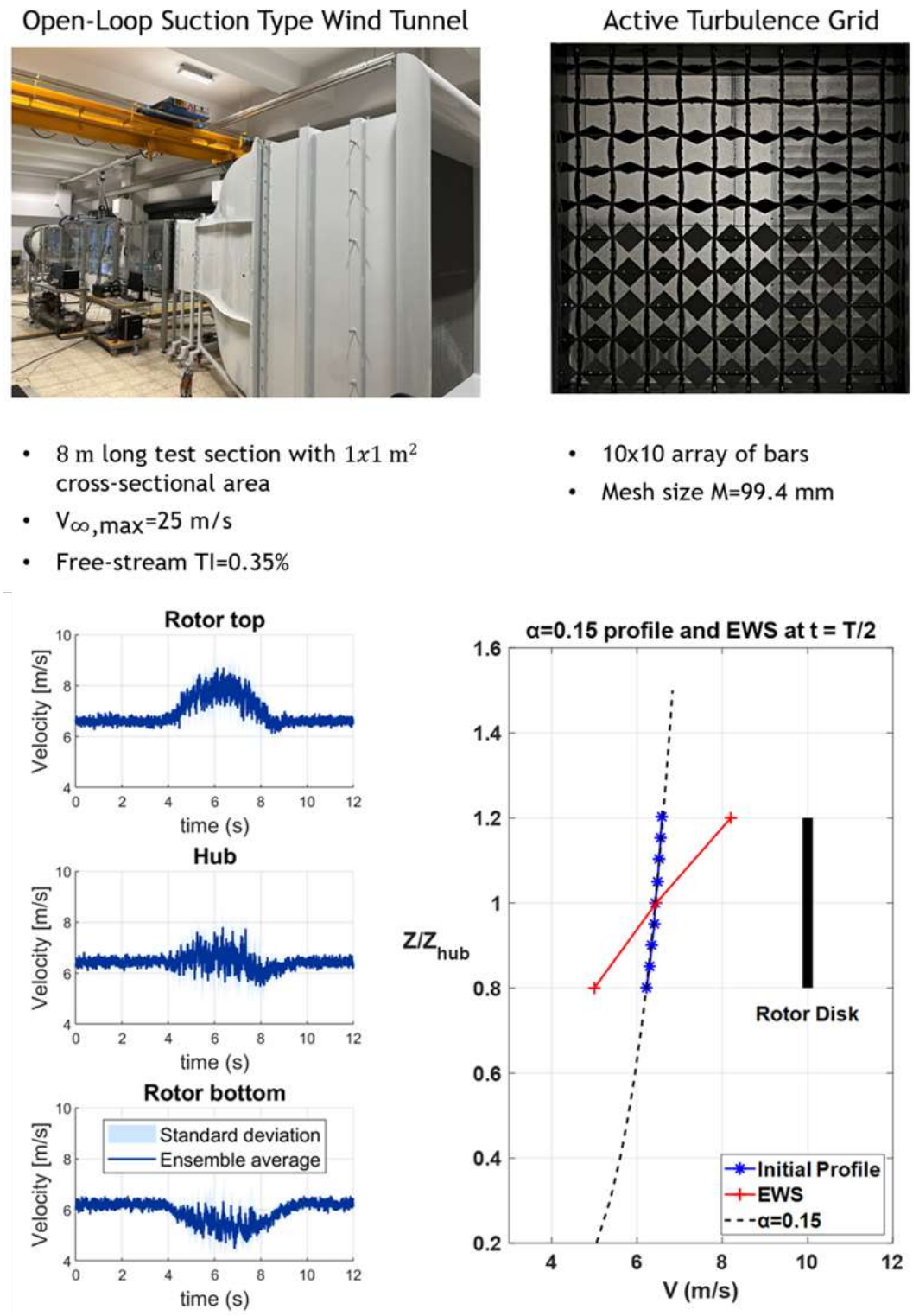

Figure 1: *The wind tunnel, the active turbulence grid and sample measurement result for EWS event*

Dissipation scaling in wind turbine wakes exposed to free-stream turbulence

Martin Bourhis[1], and Oliver R. H. Buxton[1]

[1] Department of Aeronautics, Imperial College London, UK

email address of the corresponding author: m.bourhis@imperial.ac.uk

Abstract:

Wind turbines are typically arranged in densely packed arrays to maximise energy yield within constrained lease areas whilst minimising infrastructure and operational costs. This clustering causes turbulent wakes to impinge on downstream machines, reducing power output and increasing fatigue loading. A thorough understanding of the underlying physics governing wake spreading is therefore essential for developing accurate wake models, and ultimately for the design and optimisation of wind farms.

The decay of the centreline mean velocity deficit, Δu_C, with downstream distance, x, has been extensively studied in the context of self-similar axisymmetric turbulent wakes developing in a quiescent ambient flow. Classically, this was predicted by Townsend [1] and George [2] to be $\Delta u_C \sim x^{-2/3}$ for high-Reynolds-number flows past solid axisymmetric bodies. This result was obtained by using a closure on the self-similar form of the dissipation rate (ε) of turbulent kinetic energy (K) within the wake: $\varepsilon = C_\varepsilon \frac{K^{3/2}}{\mathcal{L}}$, where C_ε is assumed to be a constant, and $\mathcal{L}$ is the integral length scale of the turbulence (*equilibrium* scaling). More recently, however, it has been shown that C_ε is not always a constant, but can instead be a function of the ratio of two Reynolds numbers: a global Reynolds number Re_D (based on the rotor diameter D for a wind turbine), and a local turbulent Reynolds number Re_L, defined using local turbulent velocity and length scales, such that $C_\varepsilon \sim Re_D^m / Re_L^n \neq$ const. [3]. This scaling for C_ε violates the classical Richardson–Kolmogorov equilibrium phenomenology for the TKE cascade and is accordingly referred to as a *non-equilibrium* dissipation scaling. Substituting this scaling into George's self-similar framework yields alternative decay laws for Δu_C. In particular, wakes produced by porous or fractal objects at sufficiently high Reynolds number have been found to follow $\Delta u_C \sim x^{-1}$, associated with $C_\varepsilon \sim \sqrt{Re_D}/Re_\lambda$, where Re_λ is the Taylor Reynolds number [4].

This study experimentally investigates the nature of TKE dissipation in the wake of a model wind turbine exposed to various turbulent inflows generated by an active grid. Figure 1 shows the location of the turbine model relative to the grid, along with the locations of the single-component hot-wire measurement stations. Inflows are parametrised in terms of FST intensity $I_\infty = u'/U_\infty$, where u' is the r.m.s. of the velocity fluctuations, and FST integral length scale $\mathcal{L}_\infty$, obtained by integrating the autocorrelation function of the velocity fluctuations (Figure 2). The nature of TKE dissipation is found to vary significantly across wakes and to be strongly sensitive to the FST conditions (Figure 3). Under low-turbulence inflows ($I_\infty \leq 6\%$, cases S1 to L6), the outer wake exhibits non-equilibrium dissipation scaling ($C_\varepsilon \sim \sqrt{Re_D}/Re_\lambda$), whilst the inner wake recovers equilibrium dissipation behaviour ($C_\varepsilon \sim$ const.). Interestingly, the non-equilibrium dissipation region coincides with a region of high intermittency, *i.e.* high Λ^2 (Figure 4). Λ^2 is defined from the kurtosis of the velocity increments and is a metric that characterises the intermittency of the velocity increments over the time lag τ, Under highly turbulent inflows (cases L7 & L8), however, the background turbulence dominates the wake turbulence, suppressing the intermittency ring and precluding any clear dissipation scaling. In the presentation, the results for the full range of inflow and operating conditions, together with the link between the ring of elevated C_ε and high intermittency, will be discussed.

References

[1] Townsend, A.A.R. (1976), *The Structure of Turbulent Shear Flow*, Cambridge University Press.

[2] George, W.K. (1989), The self-preservation of turbulent flows and its relation to the initial conditions and coherent structures, *Advances in Turbulence*, 39–73.

[3] Vassilicos, J.C. (2015), Dissipation in turbulent flows, *Annual Review of Fluid Mechanics* **46**, 95–114.

[4] Nedić, J., Vassilicos, J.C. and Ganapathisubramani, B. (2013), Axisymmetric turbulent wakes with new nonequilibrium similarity scalings, *Physical Review Letters* **111**(14).

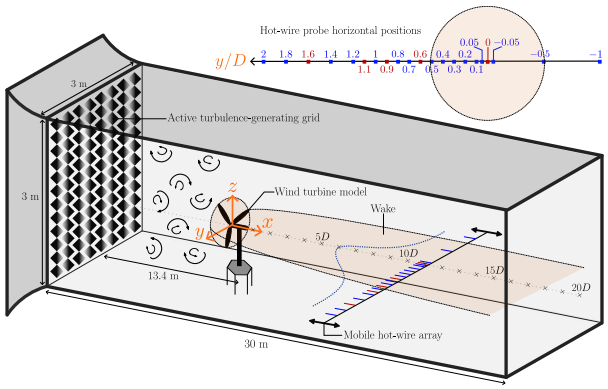

Figure 1: *Experimental setup.*

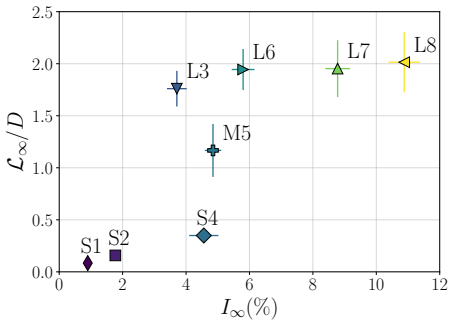

Figure 2: *Free-stream turbulence parameter space* $\{I_\infty(\%), \mathcal{L}_\infty/D\}$.

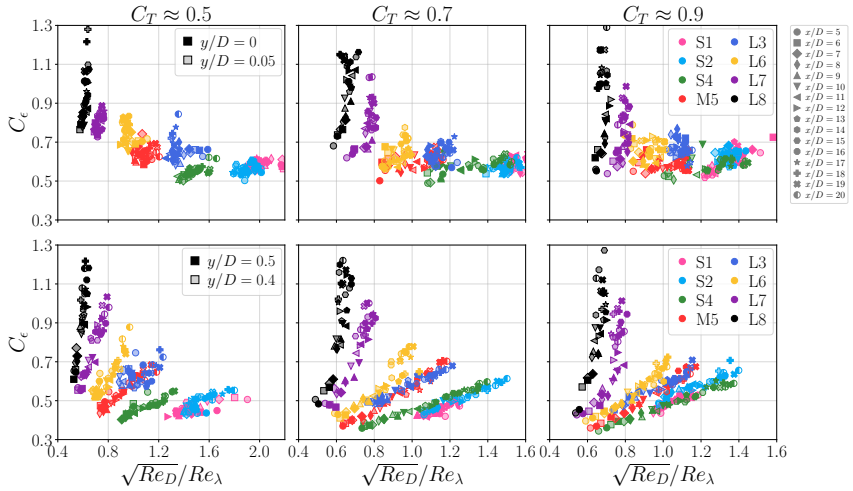

Figure 3: C_ε *as a function of* x *near the wake centreline (top row) and in the outer wake (bottom row) for the different FST flavours shown in Figure 2 and turbine thrust coefficients. Data are extracted over* $5 \leq x/D \leq 20$.

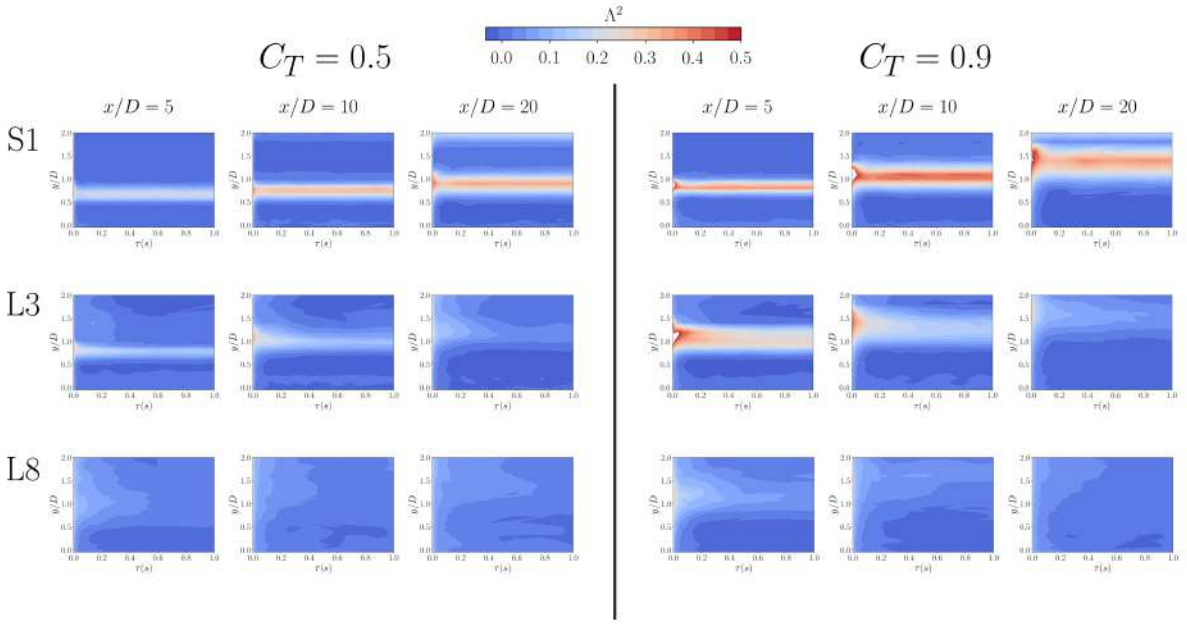

Figure 4: *Intermittency parameter* Λ^2 *plotted as a function of time lag* τ *for three FST cases and two different turbine thrust coefficients.*

Wind tunnel modelling of stable boundary layers and their effects on turbine wake flow

M. Placidi [1*], and P. E. Hancock [1] and P. Hayden [1]

[1] School of Engineering, University of Surrey, Guildford, UK

[*] Email-address of the corresponding author: m.placidi@surrey.ac.uk

Introduction and background:
Wake flows are a reality in most wind farm operations due to land/ocean availability, restrictions and economic considerations. Wakes can be responsible for power losses of up to 30% [1] and significantly increased fatigue loads [2]. To further complicate the matter, atmospheric boundary layers (onshore and offshore) are rarely in thermally neutral conditions [3, 4], i.e. without any vertical potential temperature gradient, and the thermal stability is understood to affect wake recovery rate, flow entrainment, and turbulence loads [2], amongst other quantities. To further investigate the effect of thermal stability on wake flows, laboratory experiments are carried out herein.

Methodology:
Experiments were conducted in the EnFlo wind tunnel, 20m × 3.5m × 1.5m (length x width x height), at the University of Surrey. This EPSRC unique National Facility enables simulations of boundary layers under neutral and non-neutral thermal conditions, with a stable case considered in this study. Deep boundary layers are modelled via a combination of spires and surface roughness, as detailed in [5], and shown in figure 1. The turbine model (with a diameter of $D = 416$ mm) used herein has flat plate-like blades to account for the lower laboratory Reynolds number compared to the field, runs at a tip speed ratio of 6, and has an estimated thrust coefficient of 0.48, as discussed in [5]. Velocity measurements are captured via two independent 1-D Doppler anemometers (FiberFlow, Dantec Dynamics), measuring the streamwise component of velocity, allowing for 2-point correlations to be quantified.

Results:
Figure 2 shows the imposed relative inlet temperature profiles employed for the thermally neutral and stable (with surface Obukhov length, $L_0 = 870$mm) boundary layers. The Z coordinate is centred at the turbine's hub height. The corresponsing non-dimensional mean and fluctuating profiles (in the absence of any wind turbine) are reported in figure 3 for x=1D (≈10.4 m downstream of the tunnel inlet). Little difference with stability is noted in the mean profiles (blue), with the exclusion of the near-wall region; however, the turbulent fluctuations are drastically damped in the stable case; this is expected. Figure 4 shows 2-D interpolated contours for the wake profiles downstream of a single wind turbine for both neutral (colours) and stable (superimposed white contour levels) cases. For the latter, a more persistent wake is observed – see the streamwise stretching of the countours. The talk will consider the effect of thermal stability on higher-order quantities and 2-point velocity correlations in the wake flow.

References

[1] R. J. Barthelmie and L. E. Jensen, "Evaluation of wind farm efficiency and wind turbine wakes at the nysted offshore wind farm," *Wind Energy*, vol. 13, no. 6, pp. 573–586, 2010.

[2] R. J. A. M. Stevens and C. Meneveau, "Flow structure and turbulence in wind farms," *Annual Review of Fluid Mechanics*, vol. 49, no. 1, pp. 311–339, 2017.

[3] A. Peña, R. Floors, A. Sathe, S. E. Gryning, R. Wagner, M. S. Courtney, X. G. Larsén, A. N. Hahmann, and C. B. Hasager, "Ten years of boundary-layer and wind-power meteorology at høvsøre, denmark," *Boundary-Layer Meteorology*, vol. 158, no. 1, pp. 1–26, 2016.

[4] L. Alblas, W. Bierbooms, and D. Veldkamp, "Power output of offshore wind farms in relation to atmospheric stability," *Journal of Physics: Conference Series*, vol. 555, pp. 012004 – 9, 12 2014.

[5] M. Placidi, P. E. Hancock, and P. Hayden, "Wind turbine wakes: experimental investigation of two-point correlations and the effect of stable thermal stability," *Journal of Fluid Mechanics*, vol. 970, p. A30, 2023.

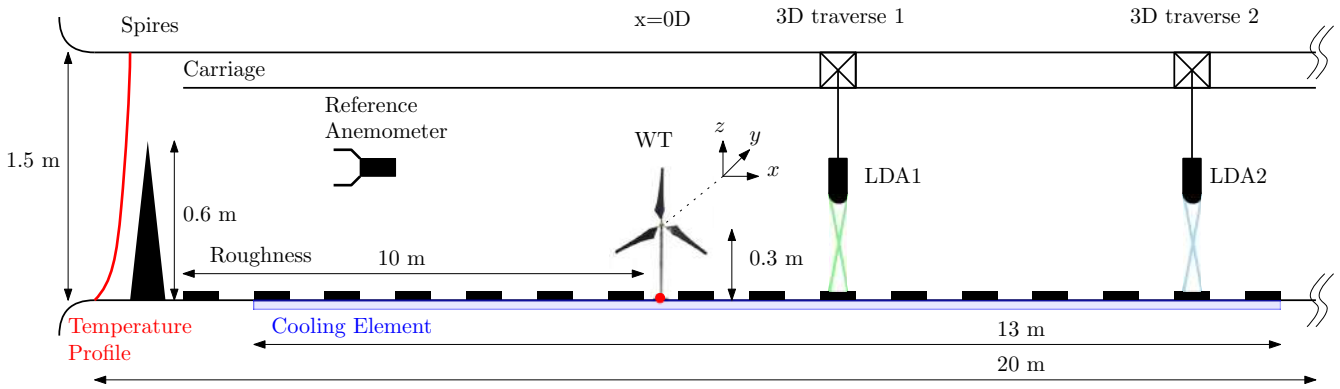

Figure 1: *Sketch of the experimental setup (including thermal treatment for the stable boundary layer). Modified from [5].*

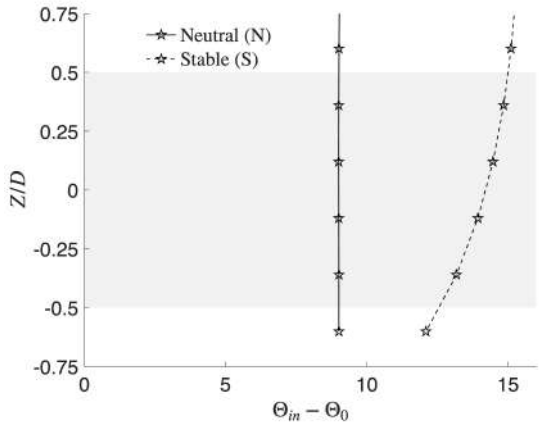

Figure 2: *Relative inlet temperature profiles, Θ_{in}, to floor temperature, Θ_0. The grey area indicates the turbine rotor.*

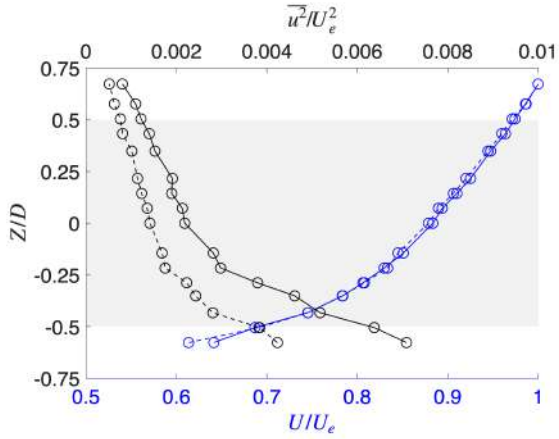

Figure 3: *Mean (blue) and fluctuating (black) velocities in neutral (solid) and stable (dashed) conditions. Grey area as in figure 2.*

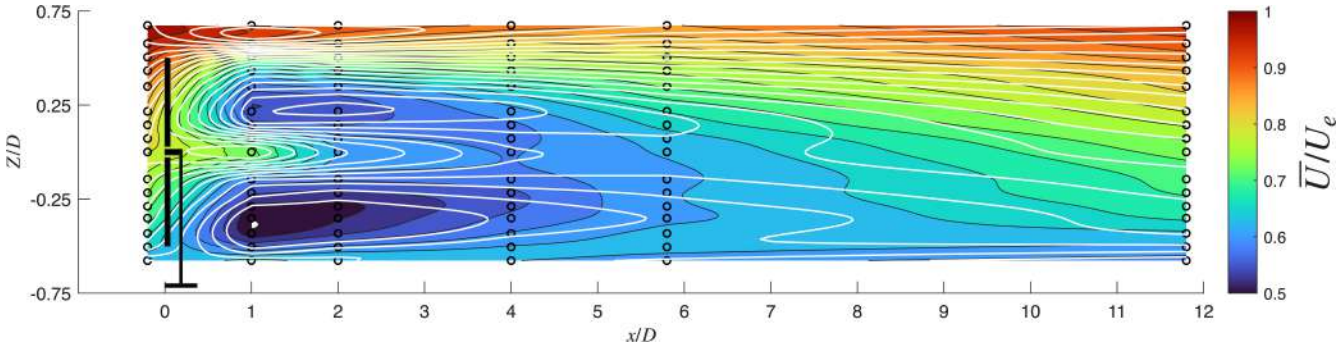

Figure 4: *Interpolated 2-D contours of mean streamwise velocity measurements. Measurement points are indicated by ∘ marks. Colours indicate the neutral case, with the stable case superimposed in white lines. Contours spacing 0.025.*

Tip vortex breakdown at high Reynolds numbers for various inflow conditions

M. Grunwald [1,2], C. E. Brunner [2]

[1] Department of Physics, University of Göttingen, Göttingen, Germany
[2] Max Planck Institute for Dynamics and Self-Organization, Göttingen, Germany

email-adress of the corresponding authour: claudia.brunner@ds.mpg.de

Abstract:
Understanding the re-energization of wind turbine wakes is crucial for the design and control of wind farms. Close to the rotor, this process is determined by the dynamics of the tip vortices. Shear [1], turbulence intensity [2] and the tip speed ratio [3] have all been found to have an effect on the breakdown of the tip vortices. However, these effects have not been studied in highly turbulent inflow conditions, which are crucial to resemble the flow in the atmospheric boundary layer. Here, we experimentally investigate the downstream evolution of the tip vortices for different inflow conditions at a turbine diameter-based Reynolds number of $\mathrm{Re}_D = 2.9 \times 10^6$. The experiments were performed in the Variable Density Turbulence Tunnel at the Max Planck Institute for Dynamics and Self-Organization, which uses pressurized SF_6 as the working fluid. An active turbulence grid was used to generate atmospheric inflow conditions with varying levels of mean shear and turbulence intensity. Hot wire measurements of the streamwise velocity component were conducted in the inflow and at the upper edge of the wake of a model wind turbine MoWiTO 0.6 for various tip speed ratios and are used to investigate the scaling of tip vortex breakdown in the near wake. The obtained mean velocity and turbulence intensity profiles for the inflow are shown in Figure 1. Five different inflow cases are created. Because turbulence in the inflow is generated not only by the active grid, but also by the mean velocity shear, it is practically impossible to keep the turbulence intensity constant across the vertical profile of the test section. However, we expect the behaviour of the tip vortices at the upper edge of the rotor to be primarily sensitive to the turbulence intensity at their height. The case of medium shear and turbulence intensity serves as a reference case. Two cases differ in their turbulence intensity but have approximately the same mean shear across the rotor plane, while the two remaining cases have varying mean shear but approximately the same turbulence intensity at the top edge of the rotor. Figure 2a shows spectra measured at the upper edge of the wake of the model wind turbine for different downstream positions as well as the corresponding inflow spectrum for the reference case. At the blade pass frequency $f_{\mathrm{bp}} = 3f_{\mathrm{rotor}}$ a clear peak is visible close to the rotor which corresponds to the tip vortices [4]. For increasing downstream distance from the rotor, the peak gets less pronounced. The decrease of the peak heights with downstream position is shown more explicitly in Figure 2b. Three different scaling regimes can be identified, which we link to an initial advection phase, the vortex breakdown and a decaying turbulence regime. Figure 3 shows the decrease of the peak heights for all created inflow cases and the tip speed variations. While the scaling in the vortex breakdown regime is only weakly affected by variations in mean velocity shear and turbulence intensity, higher tip speed ratios lead to faster breakdown. Our results underline the importance of the inflow conditions for the tip vortex breakdown process. Even small changes in turbulence intensity impact how far downstream the signature of the tip vortices persists in the wake, so that scalings observed under laminar inflow conditions are unlikely to accurately describe the vortex breakdown process in highly turbulent atmospheric conditions. Under highly turbulent conditions, tip vortex breakdown appears to be initiated very close to the rotor. This work has been accepted for publication in the Physical Review Fluids (`https://doi.org/10.1103/5phx-7dhk`).

References

[1] A. Parinam et al., (2023), Large-Eddy Simulations of wind turbine wakes in sheared inflows, *J. Phys.: Conf. Ser., vol. 2505 pp. 012039*

[2] S. Gambuzza, B. Ganapathisubramani, (2023), The influence of free stream turbulence on the development of a wind turbine wake, *J. Fluid Mech., vol. 963, pp. A19*

[3] N. Biswas, O. R. H. Buxton, (2024), Effect of tip speed ratio on coherent dynamics in the near wake of a model wind turbine, *J. Fluid Mech., vol. 979 pp. A34*

[4] A. Piqué, M. A. Miller, M. Hultmark, (2022), Dominant flow features in the wake of a wind turbine at high Reynolds numbers, *J. Renew. Sustain. Energy, vol. 14 (3), pp. 033304*

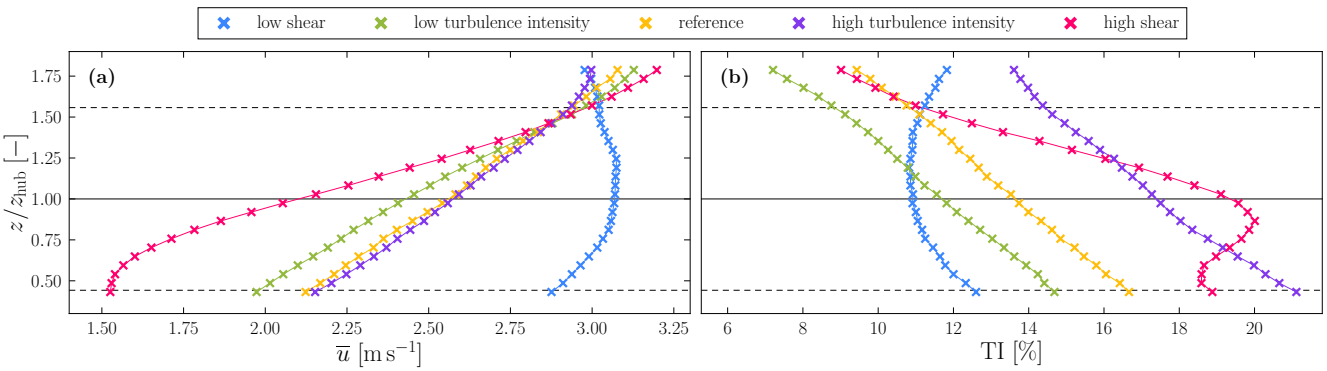

Figure 1: (a) mean velocity and (b) turbulence intensity profiles in the inflow. The solid black line marks the hub height of the model wind turbine, while the dashed black lines show the rotor swept area.

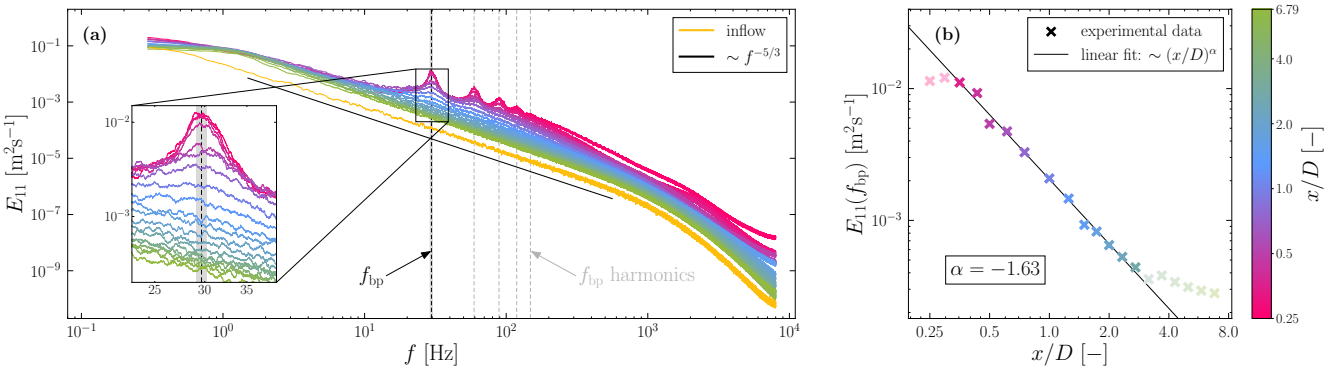

Figure 2: (a) inflow spectrum and wake spectra at the top of the rotor for the reference case at different downstream positions. f_{bp} is the blade pass frequency. The interval shown around f_{bp} corresponds to the region in which the average value is taken for the determination of the peaks. (b) local maxima of the wake spectra around the blade pass frequency. Only the data points shown with solid markers are used for the linear fit.

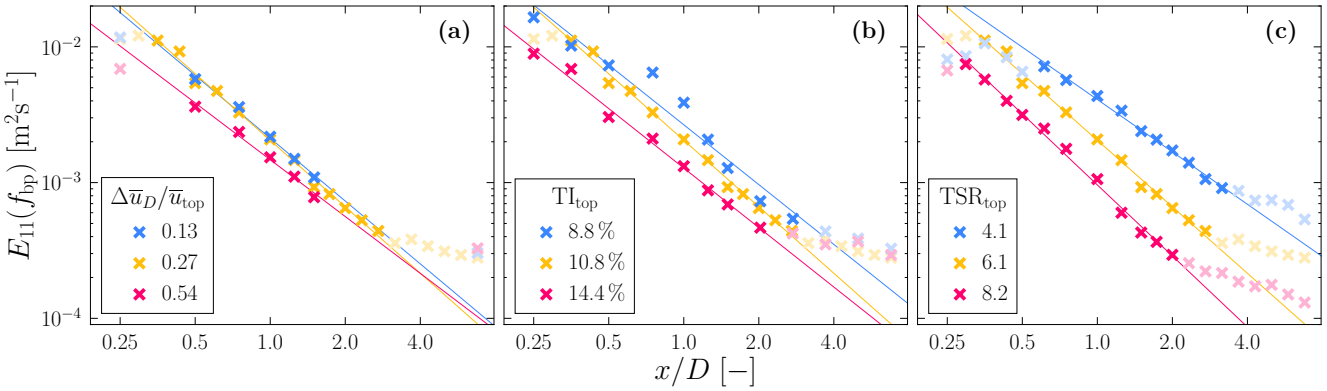

Figure 3: Spectral peak heights corresponding to tip vortices at different downstream positions for varying (a) shear, (b) turbulence intensity and (c) tip speed ratio. The lines correspond to power law fits. Only the data points shown with solid markers are used for the linear fit.

The mean and spectral properties of vortex structures behind a yawed wind turbine

L. Liu[1], C. Li[1], A. Gao[1], X. Lu[1] and R. J. A. M. Stevens[2]

[1]Department of Modern Mechanics, University of Science and Technology of China, Hefei 230027, Anhui, PR China
[2]Physics of Fluids Group, Max Planck Center Twente for Complex Fluid Dynamics, J. M. Burgers Center for Fluid Dynamics, University of Twente, P.O. Box 217, 7500 AE Enschede, The Netherlands

email-address of the corresponding author: luoqinliu@ustc.edu.cn

Abstract:

Yaw control is a promising strategy for wind farm power optimization, but its effectiveness is limited by an incomplete understanding of the complex vortex dynamics in the wakes of yawed turbines. This study aims to bridge this gap by providing a combined analysis of the time-averaged and spectral properties of these wake vortices, linking them to power output and structural loading concerns. First, we introduce a physical model that predicts the evolution of tip vortices from generation to destabilization. This model integrates an enhanced blade element momentum theory [1] for yawed conditions with a point-vortex framework [2] and a skewed vortex cylinder theory [3]. Validation against large eddy simulations confirms its accuracy in capturing the mean vorticity distribution and wake deflection. Second, we employ a sparsity-promoting dynamic mode decomposition [4] to dissect the transient dynamics. This spectral analysis identifies four critical mode types governing wake evolution: the averaged mode, shear modes, harmonic modes, and merging modes. Under yawed conditions, these modes exhibit pronounced asymmetry, which facilitates a direct interaction between tip and root vortex structures. We show that this interaction plays a crucial role during the formation process of the counter-rotating vortex pair observed in yawed wakes. By unifying the complementary perspectives of mean structure and spectral dynamics, this work delivers a more complete physical description of yawed turbine wakes, with direct implications for improving yaw-based control strategies for both power augmentation and fatigue load mitigation.

References

[1] Lu, J., Li, C., Li, X., Liu, H., Zhang, G., Liu, N. and Liu, L. (2023), Analytical model for the power production of a yaw-misaligned wind turbine, *Physics of Fluids, vol. 35, pp. 127109*

[2] Zong, H. and Porté-Agel, F. (2020), A point vortex transportation model for yawed wind turbine wakes, *Journal of Fluid Mechanics, vol. 890, pp. A8*

[3] Branlard, E. and Gaunaa, M. (2016), Cylindrical vortex wake model: skewed cylinder, application to yawed or tilted rotors, *Wind Energy, vol. 19, pp. 345–358*

[4] Jovanović, M. R., Schmid, P. J. and Nichols, J. W. (2014), Sparsity-promoting dynamic mode decomposition, *Physics of Fluids, vol. 26, pp. 024103*

The effect of turbulence on wing tip vortices

R. Jason Hearst

Department of Energy & Process Engineering, Norwegian University of Science & Technology, Trondheim, Norway

email-address of the corresponding author: jason.hearst@ntnu.no

Abstract:
The instantaneous near-field of a wind turbine wake is characterised by a series of vortical structures. The most iconic of these structures are the wing tip vortices, which are present at all scales from utility scale turbines [1] to 45 mm rotors at lab-scale [2]. Despite their omnipresence in wind turbine wakes and indeed wind farms, they are most often studied in (near-)laminar flow. As such, information on how the tip vortices behave in turbulent flows reminiscent of the atmosphere remains limited.

Using a set-up similar to that of Bailey and Tavoularis [3], we investigate the spatial structure of a wing tip vortex in homogeneous turbulent flows with significantly higher turbulence intensity (up to 13%) using an active grid [4, 5]; see Figure 1. Experiments are conducted with stereo particle image velocimetry in multiple transverse planes to capture the evolution of the wing tip vortex. It is demonstrated that although the vortex appears more diffuse in a fixed lab-frame as the incoming turbulence intensity is increased, in a conditional-frame centred on the vortex core, there is minimal difference in the vortex with changing incoming conditions (Figure 2). This suggests that the vortex is merely advected (meanders) more when turbulence is present, and its dynamics are not substantially different. Moreover, when examining the spatial modes from proper orthogonal decomposition conducted on the streamwise vorticity field, it is demonstrated that when turbulence is present upstream of the wing, the exact same modes occur, in the same order. However, they occur closer to the wing when incoming turbulence is added [5]. Only with extreme turbulence do these modes become more diffuse in the fixed lab-frame, and even then they are the same modes, simply more diffuse. This further suggests that the primary action of the turbulent is to initiate the meandering instability.

Applying this set-up to spinning model turbine blades allows us to explore the phenomenon of "vanishing" vortices in wind turbine wakes. Here, we refer to the often reported phenomenon whereby the spectral signature in the wake of a wind turbine has the most energy at the turbine rotational frequency rather than the blade pass frequency. Using time-resolved volumetric particle tracking velocimetry (Shake-the-Box), we capture the near-wake of a frequently used model turbine (Figure 3) and find that tip vortices can vanish in surprisingly short distances (~ 1 diameter) downstream of the blades in turbulent conditions [6, 7].

References

[1] J. Hong, M. Toloui, L. P. Chamorro, M. Guala, K. Howard, S. Riley, J. Tucker, and F. Sotiropoulos, "Natural snowfall reveals large-scale flow structures in the wake of a 2.5-MW wind turbine," *Nat. Commun.*, vol. 5, p. 4216, 2014.

[2] S. Helvig, M. K. Vinnes, A. Segalini, N. A. Worth, and R. J. Hearst, "A comparison of lab-scale free rotating wind turbines and actuator disks," *J. Wind Eng. Ind. Aero.*, vol. 209, no. 104485, 2021.

[3] S. C. C. Bailey and S. Tavoularis, "Measurements of the velocity field of a wing-tip vortex, wandering in grid turbulence," *J. Fluid Mech.*, vol. 601, pp. 281–315, 2008.

[4] S. Yadala, S. Dehareng, I. Neunaber, G. K. Jankee, R. Kaufmann, M. Couliou, and R. J. Hearst, "The effect of turbulence on a flexible finite wing: forces, deflections and the wingtip vortex," *J. Fluid Mech.*, vol. 1019, p. A38, 2025.

[5] M. Couliou, S. Yadala, G. K. Jankee, I. Neunaber, and R. J. Hearst, "The effect of freestream turbulence on wing-tip vortex meandering and deformation," *Int. J. Heat Fluid Flow*, vol. 117, p. 110013, 2026.

[6] J. N. Hillestad, S. Yadala, I. Neunaber, L. Li, R. J. Hearst, and N. A. Worth, "Volumetric visualization of vanishing vortices in wind turbine wakes," *Phys. Rev. Fluids*, vol. 9, p. L052701, 2024.

[7] J. N. Hillestad, S. Yadala, L. Li, R. J. Hearst, and N. A. Worth, "Volumetric three-dimensional experimental measurement of vortex dynamics in a rotating wake," *Phys. Rev. Fluids*, vol. 11, p. 014701, 2026.

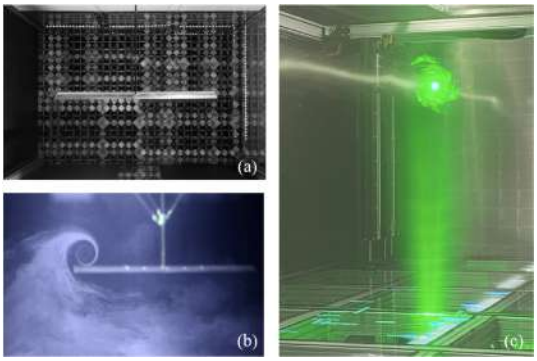

Figure 1: *Experimental set-up showing (a) the wing downstream of the active grid, (b) the wing tip vortex roll-up, and (c) visualisation of the vortex in a laser sheet. Adapted from [5].*

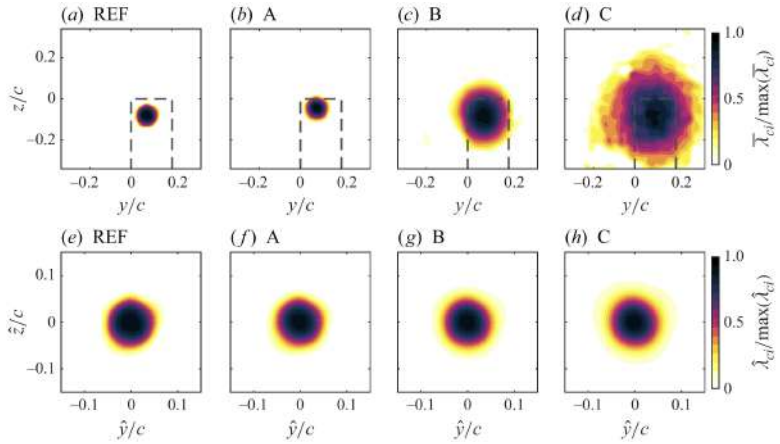

Figure 2: *Mean swirling strength field of the wing tip vortex for increasing incoming turbulence intensity (from REF to C): (a-d) in the fixed lab-frame, (e-h) in the conditional vortex-centred frame. Adapted from [4].*

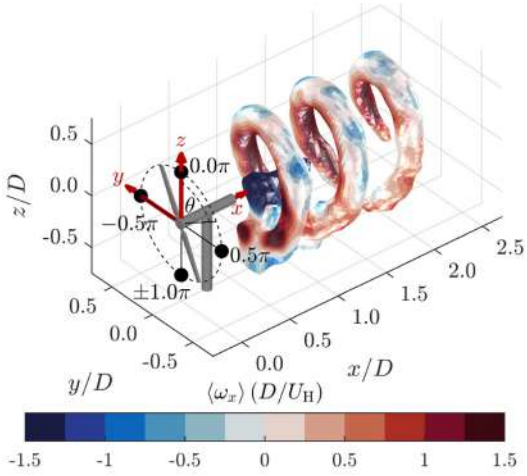

Figure 3: *Volumetric particle tracking velocimetry of a model wind turbine. Isosurface of the wing tip vortex, colour by streamwise vorticity. Adapted from [6].*

Inviscid influences on wind farm flows

J. Bleeg [1] and C. Montavon [2]

[1] Group Research and Development, DNV, Bristol, UK
[2] Energy Systems, DNV, Arnhem, NL

email-address of the corresponding author: james.bleeg@dnv.com

Abstract:
Turbulence rightly receives a lot of attention in investigations of wind farm flows; however, non-turbulent influences can also have a significant impact on these flows. The role of inviscid effects in wind farm flows has been highlighted in many studies, particularly over the last several years. This presentation expands upon some of this research, using results from a large number of Reynolds-Average Navier-Stokes (RANS) simulations. For example, it is well-established that terrain-induced pressure gradients can substantially influence wake recovery [1, 2]; we take the matter a step further to look at the (related) impact of terrain on blockage. Figure 1, which derives from [3], shows the impact of terrain on both wake and blockage effects for a tightly spaced row of turbines in three different locations: on the windward side of a quasi-2D hill, on the leeward side of the hill, and in flat terrain. In each case, the single row of turbines is simulated in a conventionally neutral boundary layer. The wake recovery is very sensitive to the position of the row relative to the hill and departs substantially from that of the flat terrain case. The same can be said for the upstream blockage effect. The presentation discusses the physical drivers behind these trends, including terrain-induced streamwise pressure variation and other inviscid effects related to stable stratification.

The presentation also explores the physical drivers behind the development and recovery of wind farm wakes. Wind farm wake recovery has long been assumed to be dominated by the turbulent transport of momentum, and engineering models for wind farm flows largely reflect this assumption. However, recent studies, including [4, 5], indicate that inviscid effects can also contribute materially to the recovery of a wind farm wake. The presentation adds to the discussion by means of control volume analyses of RANS-simulated wakes from a large hypothetical offshore wind farm operating in a variety of atmospheric conditions. The analysis confirms that vertical turbulent transport of momentum is an important contributor to wind farm wake recovery in many of the simulations. However, stratification above the boundary layer can significantly limit this contribution, and other contributors to the recovery of a wind farm wake are found to be at least as important as turbulent momentum transport in these RANS results. In addition, the analysis underlines the importance of considering the wind farm simulation results relative to the back-to-back freestream simulation when assessing various contributors to wind farm wake recovery.

References

[1] Shamsoddin S. and Porte-Agel F., (2018), Wind turbine wakes over hills, *J. Fluid Mech, vol. 855, pp. 671-702.*

[2] Bayron P., Kelso, R. and Chin R., (2023), Experimental study on the evolution of the wind turbine wake under streamwise pressure gradients, *Energy Convers. Manag.: X, vol. 20.*

[3] Bleeg J., (2026), A numerical study of the influence of terrain on wakes, blockage, wind farm efficiency, and turbine efficiency, *Wind Energy Sci., Pre-print*

[4] Lanzilao L. and Meyers J., (2025), Wind-farm wake recovery mechanisms in conventionally neutral boundary layers, *J. Fluid Mech., vol. 1015.*

[5] Smith R. and Gribben B., (2026), Coriolis recovery of wind farm wakes, *Wind Energy Sci., vol. 11.*

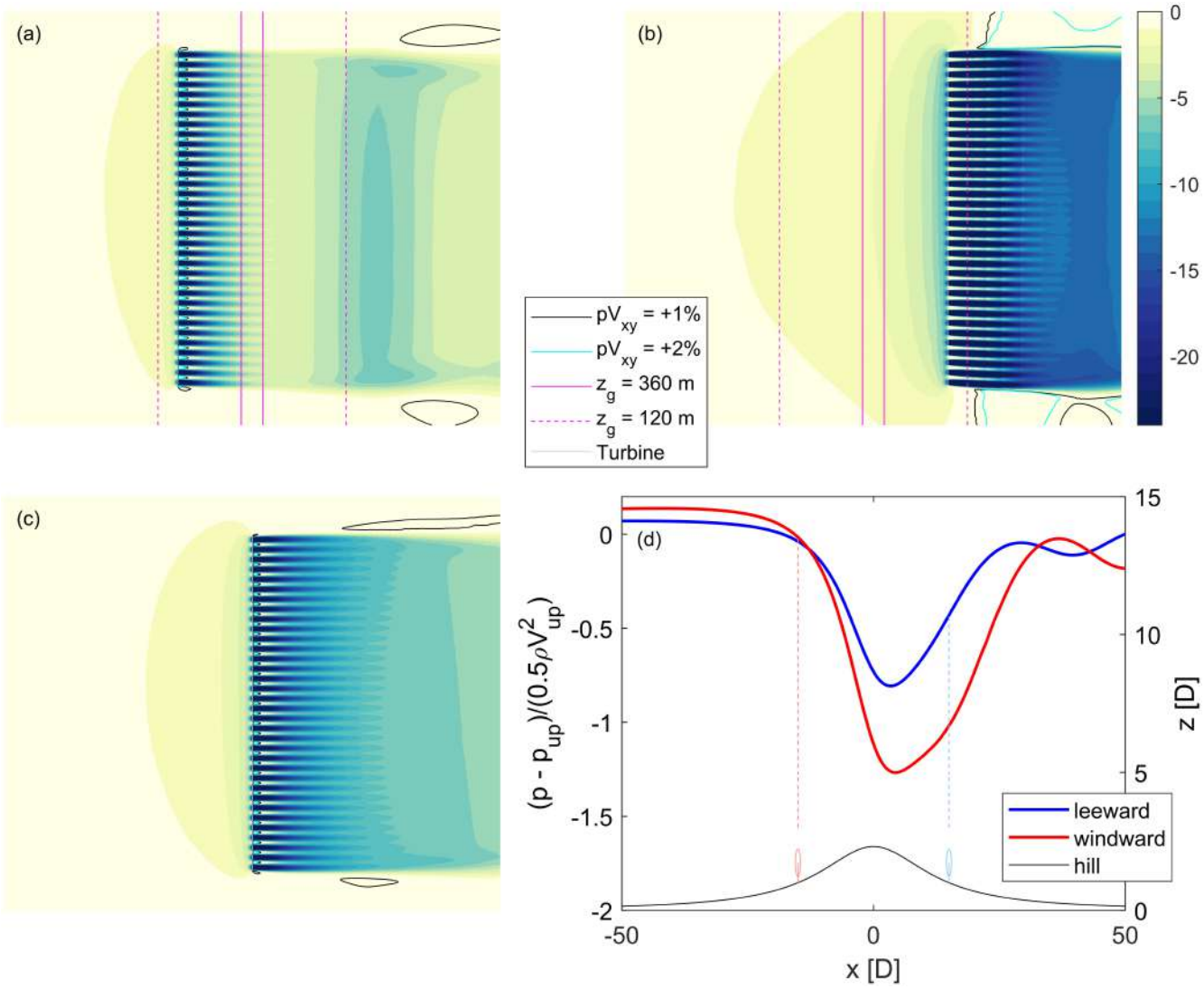

Figure 1: *Top view of the percent change in wind speed relative to freestream (i.e. the percent change in wind speed due to the presence of the wind farm) on the hub-height, terrain-following surface for a row of turbines on the windward side of a quasi-2D hill (a), a row on the leeward side (b), and a row in flat terrain (c). The bottom right plot (d) shows the freestream pressure coefficient along the hill profile relative to conditions at the upstream boundary for the windward (red) and leeward (blue) cases. The thin black line is the hill profile. In (a) and (b) the magenta lines are ground elevation contours; the hill crest is located between the two solid magenta lines. Flow is from left to right in all plots.*

Integration of a Meandering-Capturing Wake Model into Model Predictive Control for Dynamic Wind-Farm Operation

Philippe Chatelain [1], Maud Moens [1] and Maxime Lejeune [2]

[1] Institute of Mechanics, Materials and Civil Engineering, UCLouvain, Louvain-la-Neuve, Belgium
[2] von Karman Institute for Fluid Dynamics, Rhode-Saint-Genèse, Belgium

email-address of the corresponding author: philippe.chatelain@uclouvain.be

Abstract:
Wind-farm-scale control increasingly requires flow-aware strategies able to react to the turbulent, unsteady and heterogeneous nature of atmospheric inflow. Classical control strategies - based on steady-state wake models - perform well for power maximization in steady conditions [1] but degrade in dynamically evolving situations [2, 3] and cannot reliably support short-horizon tasks such as power tracking. This motivates integrating unsteady wake physics, including wake meandering, into real-time control architectures.

This work incorporates the medium-fidelity, meandering-capturing wake model *OnWaRDS* [4] into a Model Predictive Control (MPC) framework. *OnWaRDS* is a computationally efficient Lagrangian wake model that predicts wake advection, meandering, and turbine–turbine interactions several minutes ahead while assimilating rotor-based flow measurements to estimate inflow conditions [5]. In addition to these model-based predictions, the controller and its underlying flow predictions are assessed in a realistic turbulent flow field generated by high-fidelity Large-Eddy Simulations (LES) coupled to an Actuator Disk representation [6].

Because adjoint-based MPC would require significant restructuring of the model, the control is implemented using the derivative-free Covariance Matrix Adaptation Evolution Strategy (CMA–ES). This approach leverages *OnWaRDS*' predictive capabilities while allowing efficient optimization in nonlinear, unsteady wind-farm environments.

The controller is evaluated in a two-turbine NREL-5MW layout under turbulent inflow. Two control scenarios are considered: (i) yaw-based wake steering for power maximization, and (ii) power-setpoint tracking through collective pitch control. As shown in Fig. 1, the yaw-based MPC achieves a mean farm-level power increase of approximately 10% relative to standard operation. The predicted wake fields generated by the controller (Fig. 2) reveal that this gain is achieved by optimally redirecting the upstream wake, increasing the downstream turbine's power recovery. In the regulation scenario, the farm follows a prescribed power trajectory within a tight tolerance band (Fig. 1), while reduced induction leads to weaker wake deficits (Fig. 2). The yaw-command evolution (Fig. 3) shows that once the optimal setpoint is reached, control activity remains minimal, indicating stable and actuator-efficient operation.

These results highlight the potential of turbulence-resolving wake models embedded within MPC for achieving dynamically responsive wind-farm control. Ongoing work focuses on the imposition of actuation-rate constraints, evaluation under transient inflow and operational scenarios, and the integration of real-time load proxies to enable multi-objective control balancing power extraction and fatigue mitigation.

Acknowledgements

This work was supported by the Fonds de la Recherche Scientifique - FNRS under Grant No 40014012. The present research benefited from computational resources made available on Lucia, the Tier-1 supercomputer of the Walloon Region, infrastructure funded by the Walloon Region under the grant agreement No 1910247, and computational resources provided by the Consortium des Équipements de Calcul Intensif (CÉCI), funded by the Fonds de la Recherche Scientifique de Belgique (F.R.S.-FNRS) under Grant No. 2.5020.11

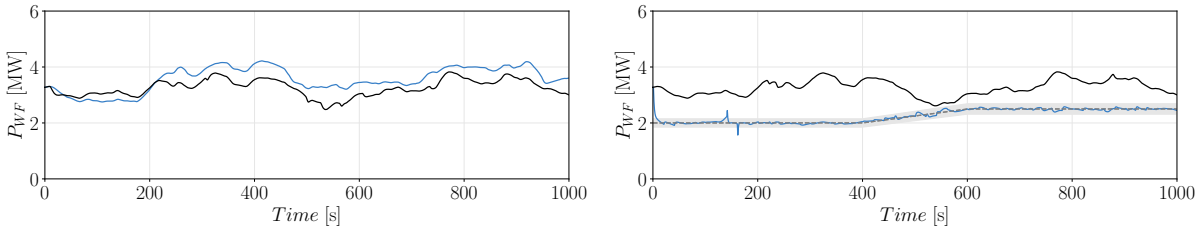

Figure 1: **Wind farm power for yaw control (YAW, left) and power-regulation control (REGUL, right).** These time series correspond to 1000 s simulations of two inline NREL-5MW turbines separated by 7D and subjected to 8 m/s inflow with 6% turbulence intensity. Controlled cases (blue lines) are compared against a baseline greedy controller for the turbines (STD, black lines). In the **YAW** case, the controller increases the total farm power relative to the STD baseline. In the **REGUL** case, the farm accurately tracks the prescribed power command (grey dashed line) within ±7.5%.

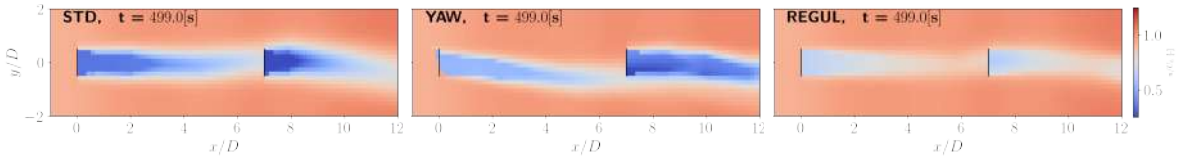

Figure 2: **Instantaneous streamwise velocity fields (STD, YAW, REGUL), predicted using *OnWaRDS*.** In **STD** operation, the downstream turbine experiences a strong, centered wake deficit. Under **YAW** control, the upstream wake is deflected laterally, significantly increasing downstream recovery. Under **REGUL** control, reduced induction leads to a weaker wake deficit. These differences illustrate how MPC leverages predicted meandering dynamics.

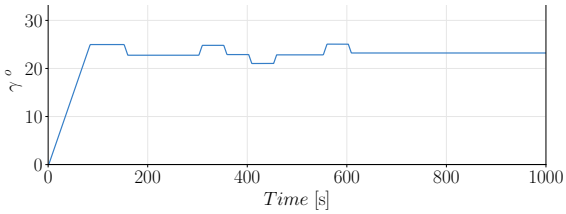

Figure 3: **Yaw-angle command for the upstream turbine (YAW case).** The controller converges to an optimal yaw misalignment of approximately 22°, and actuator activity becomes minimal once this optimum is reached. The stable yaw behavior shows that unsteady wake-aware MPC achieves similar optima as steady-state methods while dynamically adapting to turbulence.

References

[1] C. R. Shapiro, G. Starke, and D. Gayme. Turbulence and control wind farms. *Annual Review Of Control, Robotics, and Autonomous Systems*, 5:579–602, 2022.

[2] M. Becker, M. Lejeune, P. Chatelain, D. Allaerts, R. Mudafort, and J.-W. van Wingerden. A dynamic open-source model to investigate wake dynamics in response to wind farm flow control strategies. *Wind Energy Science*, 10(6):1055–1075, 2025.

[3] M. Lejeune, A. Frère, M. Moens, and P. Chatelain. Are steady-state wake models and lookup tables sufficient to design profitable wake steering strategies? a large eddy simulation investigation. *Journal of Physics: Conference Series*, 2767(9):092075, jun 2024.

[4] M. Lejeune, M. Moens, and P. Chatelain. A meandering-capturing wake model coupled to rotor-based flow-sensing for operational wind farm flow prediction. *Front. Energy Res.*, 10, 2022.

[5] M. Moens, M. Lejeune, and P. Chatelain. An advanced farm flow estimator for the real-time evaluation of the potential wind power of a down-regulated wind farm. *Journal of Physics : Conference Series*, 2767(3):032044, 2024.

[6] M. Moens and P. Chatelain. Correlations between wake phenomena and fatigue loads within large wind farms: A large-eddy simulation study. *Front. Energy Res.*, 10, 2022.

Modelling the Aerodynamics of high loaded wind turbines

Kostas Steiros [1]

[1] Aeronautics Department, Imperial College London, London, UK

email-address of the corresponding author: k.steiros@imperial.ac.uk

Abstract:
Many aerodynamic predictive tools used in the wind energy industry are based on the actuator disk theory of Rankine-Froude. Some examples are the Blade Element Momentum (BEM) theory model for the turbine power prediction, the Frandsen model used in the prediction of the wake momentum deficit of wind turbines, and the Werle blockage correction model. While low-fidelity, the above models are orders of magnitude faster/cheaper than the alternatives of field/laboratory experiments and grid-based numerical simulations, and are thus expected to remain popular in the decades to come. However, the above models are only accurate at small induction factors, i.e. small turbine loading, as at higher induction factors some of the assumptions behind the Rankine-Froude theory are violated. While most large horizontal axis turbines indeed operate at low induction factors, there are cases where the permissible value is exceeded; these include vertical axis wind turbines, tidal turbines, and micro wind turbines used in urban settings. An alternative aerodynamic theory is needed there, to model the relevant flow physics.

In this talk, I will first revise the Rankine-Froude theory to extend its validity to high induction factors. I will then derive novel BEM, wake deficit and blockage models, valid at arbitrary rotor loadings. The results will be validated via a combination of laboratory and numerical experiments of wind turbines and porous plates.

The porous disc as a physical model of a wind turbine: From the concept validation to the floating wind turbine applications

Sandrine Aubrun [1]

[1] Nantes Université, École Centrale Nantes, CNRS, LHEEA, UMR 6598, F-44000 Nantes, France

email-address of the corresponding author: sandrine.aubrun@ec-nantes.fr

Abstract:
Wind tunnel experiments are considered as a standard method to produce reliable results in controlled conditions if leading similarity laws are respected and if an acceptable degree of physical modeling is applied to the incoming flow and to the object of interest. Within the field of wind energy, wind turbines are immersed in the Atmospheric Boundary Layer (ABL), and consequentially, the turbine and the ABL flow must be modeled. The wakes evolving downstream of wind turbines interact with the ABL and while the near-wake properties are mainly driven by the WT rotor aerodynamics (rotating blade wakes), the far-wake properties are mainly driven by the interactions between the ambient atmospheric boundary layer (ABL) flow and the wakes [1]. As typical wind turbine models for wind tunnel applications are scaled with a ratio between 1:100 and 1:1000, Reynolds similarity cannot be fulfilled, and some adjustments are therefore needed to reproduce realistic load distributions on the WT rotor. The limitations of small Reynolds numbers and geometrical simplifications result in the improper reproduction of the near wake ($x/D < 3-4$).

However, studies show that these small models are appropriate to model the far-wake properties and are therefore acceptable when studying the wake interactions at a wind farm scale [2, 3]. Nevertheless, an alternative to rotating wind turbine models is the use of porous discs as Wake-Generating Turbine models (Fig. 1). The wake flow generated by a porous disc belongs to the category of canonical flows, and so are subject to a long lasting literature that can benefit to the studies on wind turbine wakes. The porous disc combines the advantages of the geometric simplicity (design, fabrication, reproducibility, etc.), of a relative Reynolds number independency, and of an absence of blade-related signatures or instabilities in its wake flow. It makes the porous disc an ideal physical model to isolate the wake flow instabilities and dynamics related to the rotor scale from those related to the blade scale.

Grounded on these features, the presentation will cover twenty years of experimental investigations conducted by the author's group on the wakes of porous discs, aiming at contributing to a better understanding of the wind turbine wake dynamics. It will address the comparison between the wake of a porous disc and of a rotating wind turbine [2], the evidence of the wake meandering inferred by the inflow turbulent eddies [4, 5], and the analysis of the wake dynamics inferred by specific disc motions (yaw manoeuvres used for wake steering [6], floating wind turbines, Fig. 2, [7, 8, 9]).

References

[1] Porté-Agel F., Bastankhah M. and Shamsoddin S., (2020), Wind-Turbine and Wind-Farm Flows: A Review, *Boundary-Layer Meteorology, 174, pp.1-59*

[2] Aubrun S., Loyer S., Hancock P.E., Hayden P., (2013), Wind turbine wake properties: Comparison between a non-rotating simplified wind turbine model and a rotating model, *Journal of Wind Engineering and Industrial Aerodynamics, 120, pp. 1-8*

[3] Stevens and Meneveau, (2017), Flow Structure and Turbulence in Wind Farms, *Annual Review of Fluid Mechanics 49:311-339*

[4] España G., Aubrun S., Loyer S., Devinant P., (2012), Wind tunnel study of the wake meandering downstream of a modelled wind turbine as an effect of large scale turbulent eddies, *Journal of Wind Engineering and Industrial Aerodynamics, 101, pp. 24-33*

[5] Muller Y.-A., Aubrun S., Masson C., (2015), Determination of real-time predictors of the wind turbine wake meandering, *Experiments in Fluids, 56 (3), pp. 1-11*

[6] Macrí S., Aubrun S., Leroy A., Girard N., (2021), Experimental investigation of wind turbine wake and load dynamics during yaw maneuvers, *Wind Energy Science, 6 (2), pp. 585-599*

[7] Schliffke B., Conan B. and Aubrun S., (2024), Floating wind turbine motion signature in the far-wake spectral content – a wind tunnel experiment, *Wind Energy Science, 9 (3), pp. 519 - 532*

[8] Hubert A., Conan B.and Aubrun S., (2025), Spatiotemporal behavior of the far wake of a wind turbine model subjected to harmonic motions: Phase averaging applied to stereo particle image velocimetry measurements, *Wind Energy Science, 10 (7), pp. 1351 - 1368*

[9] Hubert A., Conan B.and Aubrun S., (2026), Experimental investigation of harmonic surge motions on the far wake of a wind turbine model and analysis of a resulting subharmonic wake response, *Wind Energ. Sci. Discuss. [preprint]*

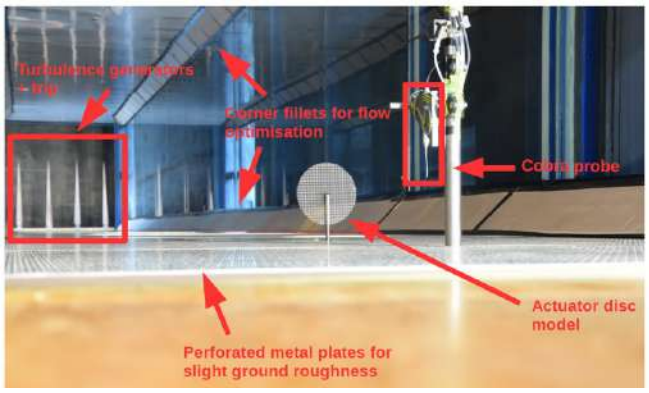

Figure 1: *Wind tunnel set-up of a porous disc used as a Wake-Generating Turbine model*

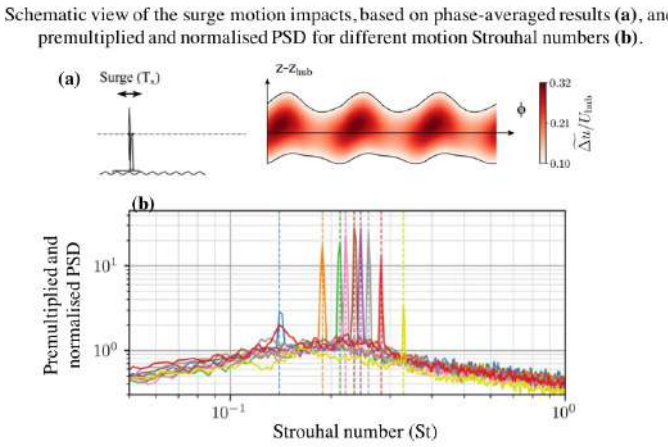

Figure 2: *Graphical abstract of an experimental study about the influence of the surge motion on the wake dynamics of a wind turbine model [9]*

Advances in hybrid testing for floating wind turbines

Federico Taruffi [1] and Axelle Viré [1]

[1] Wind Energy Section, Delft University of Technology, Delft, The Netherlands

email-address of the corresponding author: f.taruffi@tudelft.nl

Abstract:

The deployment of offshore floating wind turbines (FOWTs) is widely regarded as key to enabling large-scale renewable energy exploitation in deep waters. The strong interaction between floater motions and rotor aerodynamics introduces complex phenomena that current numerical models still struggle to capture, including motion-induced unsteady thrust variations [1] and their possible impact on wake development and downstream rotor loads and performance. Recent premature maintenance needs on a floating pilot farm further highlight the urgency for experimental data to improve dynamic load prediction. Traditional experimental approaches, such as wave-basin scale testing, suffer from unavoidable scaling conflicts between aerodynamic and hydrodynamic phenomena, while large-scale in-field demonstrators remain costly and full-scale data from pilots is extremely limited. Hybrid testing has recently emerged as a powerful solution: part of the system is reproduced physically at scale while the remaining part is simulated in real time. For aerodynamic-oriented studies, this enables wind tunnel experiments in which the aerodynamic loads of a scaled physical rotor are measured while an actuator system imposes the floater motions. To ensure realistic two-way coupling between aerodynamics and platform dynamics, hybrid tests incorporate hardware-in-the-loop (HIL) coupling, where floater motions are computed in real time taking into account the measured aerodynamic loads [2].

Our recently developed hybrid/HIL wind tunnel setup follows a force-feedback–motion-actuation architecture (Figure 2), integrating a thrust-scaled 1.2m diameter scale model with a six-degree-of-freedom hexapod and a real-time floater dynamics solver, complemented by an inertia-based aerodynamic force estimation method to address the scaling mismatch [3]. This system has enabled detailed investigations of aerodynamic damping, and combined wind-and-wave tests have also been demonstrated, showing the potential of hybrid/HIL setups to explore realistic operational regimes. In the broader framework of hybrid testing, wind tunnel data will be used to improve the aerodynamic modelling in hybrid wave basin setups, and, in turn, the wave basin data will improve the hydrodynamic modelling in wind tunnel. Challenges in the wind tunnel HIL modelling remain, the most crucial of which is to improve the accuracy in the aerodynamic force estimation. To this end, there is ongoing work on the development of a data-driven force correction model that could outperform current inertia-based methods.

Recent experiments investigated the floating motions effects on wake dynamics using volumetric particle-tracking velocimetry, and the effect on dynamic loading of a downstream rotor with the tandem hybrid setup in Figure 1. Results revealed that, in smooth flow, low-frequency surge and pitch motions, representative of floater natural modes, can accelerate wake recovery by increasing near-wake turbulence (Figure 3). These motions also imprint clear signatures on the downstream turbine. In contrast, wave-frequency motions generate minimal wake alteration and effect on the downstream rotor. Dynamic yawing, relevant for wake-steering control, affects downstream loading through mean-thrust changes and modulation sidebands. The wake measurements are also being used for the tuning of surrogate porous disks capable of reproducing the static and moving rotor wake characteristics. Porous disks are necessary to move to wind tunnel experiments reproducing the whole farm aerodynamics, where it is needed to reduce the scale of the models to a dimension where rotors are not suitable.

By combining improved HIL modelling, state-of-the-art wake-measurement techniques, multi-turbine testing and optimised surrogates, hybrid testing is set to become the leading experimental approach for future research into floating wind turbines and wind farms.

References

[1] Taruffi F., Combette R. and Viré A., (2024), Experimental and CFD analysis of a floating offshore wind turbine under imposed motions, *Journal of Physics: Conference Series, vol. 2767*

[2] Belloli M., Bayati I., Facchinetti A., Fontanella A., Giberti H., La Mura F., Taruffi F. and Zasso A., (2020), A hybrid methodology for wind tunnel testing of floating offshore wind turbines, *Ocean Engineering, vol. 210*

[3] Taruffi F., Thinakaran S. and Viré A., (2025), On the development of a hardware-in-the-loop wind tunnel setup to study the aerodynamic response of floating offshore wind turbines, *Wind Energy Science Discussions*

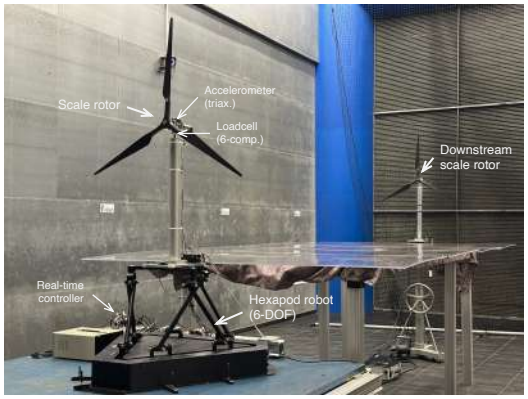

Figure 1: *TU Delft's hybrid setup in tandem configuration*

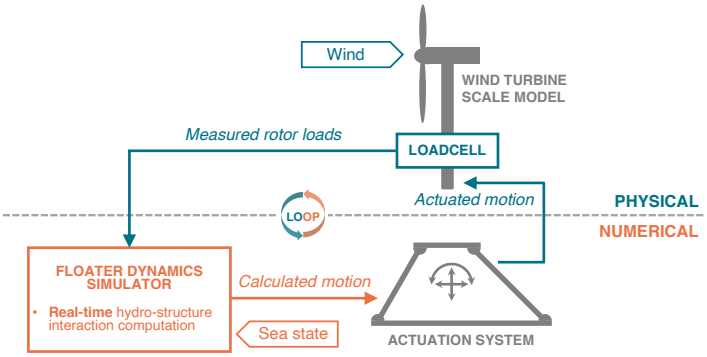

Figure 2: *Scheme of the hardware-in-the-loop architecture*

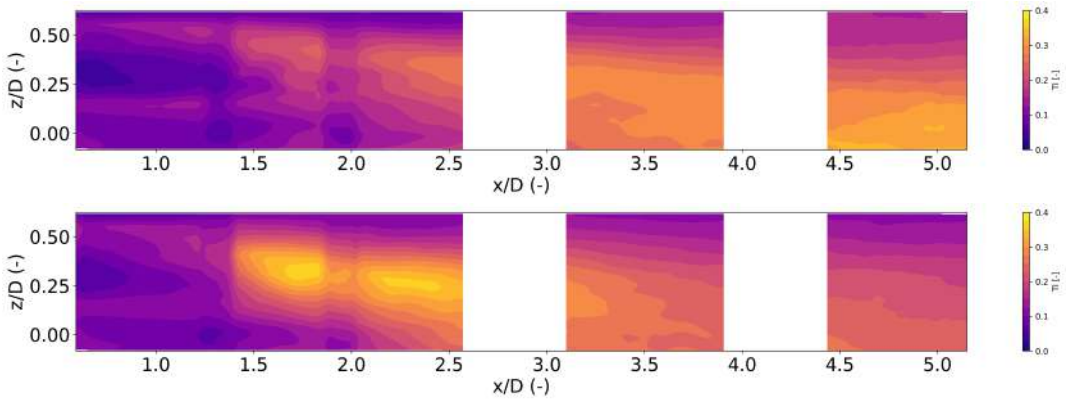

Figure 3: *Turbulence intensity in the wake of a static (top) and surging at St=0.6 (bottom) rotor*

Improved wake mixing by coherent flow structures induced by periodic excitations in the wake of a floating wind turbine

T Messmer [1,2], J. Peinke [1,2] and M. Hölling [1,2]

[1] School of Mathematics and Science, Institute of Physics, Carl von Ossietzky Universität Oldenburg, 26129 Oldenburg, Germany
[2] ForWind - Center for Wind Energy Research, Küpkersweg 70, 26129 Oldenburg, Germany

email-address of the corresponding author: thomas.messmer@uol.de

Abstract:
The growing interest in floating wind turbines opens new questions regarding the impact of platform motion on the wake generated and rotor aerodynamics [1]. Ocean waves and turbulent wind lead to complex 6-degree-of-freedom platform motion dynamics, these movements cover a wide range of frequencies and amplitudes, which depend on platform type and size and environmental conditions. The complex motions can be simplified by considering a single degree of freedom and idealised harmonic movement. Mathematically, for a given degree-of-freedom, idealised motion writes: $\xi(t) = A^* D \sin(2\pi St/(D/U_\infty)t)$ with $A^* = A_p/D$ the reduced amplitude, ratio of motion amplitude A_p and rotor diameter D, $St = f_p D/U_\infty$ the platform Strouhal number with f_p the platform motion frequency and U_∞ the incoming wind speed.

Previous CFD and experimental work from [2, 3] showed that for $St \in [0.2, 0.6]$ rotor motions initiate the formation of large-scale coherent flow structures, whose types depend on the direction of motion. These energetic structures are involved in a faster transition to the far-wake and enhanced wake recovery, both positive effects for wind farm efficiency improvements. The current literature still lacks an understanding of the mechanisms behind the formation of these structures, their role on the enhanced wake recovery, and the interplay with free-stream turbulence. These topics are interconnected and, if better understood, can lead to an improvement in floating offshore wind turbine (FOWT) design, control strategies and engineering models for improved assessment of floating wind farm performance.

In this work, we carried out wind tunnel experiments with a model floating wind turbine to study wake dynamics and recovery using hot-wire anemometry. The experiments were conducted in Milan and Oldenburg, using 3-d and 1-d hot-wires, respectively. We focused on surge (fore-aft) and sway (sideways) motion with $St = 0.3$ and vary the turbulence intensity in the freestream, $TI_\infty \in [1.1, 5.8]\%$ using an active grid at the inlet. Figure 1 shows the experimental set-up. At the wind farm Colloquium, we aim to detail the formation of the excited coherent structures behind the periodically excited wind turbine, their role in the enhanced wake recovery (improving wake mixing) and the interplay with freestream turbulence.

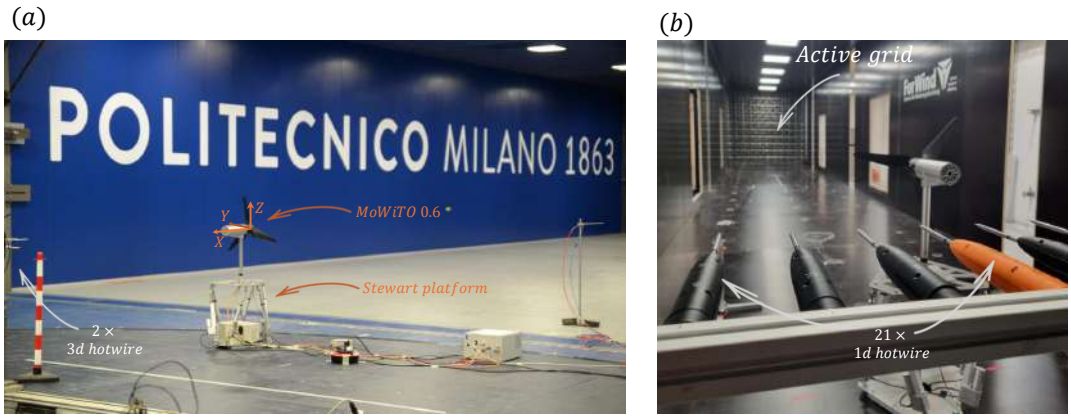

Figure 1: *Experimental set-up, (a) Milan, (b) Oldenburg*

References

[1] Stefano Cioni, Francesco Papi, and et al., (2023): On the characteristics of the wake of a wind turbine undergoing large motions caused by a floating structure: an insight based on experiments and multi-fidelity simulations from the oc6 phase iii project. *Wind Energy Science.*

[2] Zhaobin Li, Guodan Dong, and Xiaolei Yang., (2022): Onset of wake meandering for a floating offshore wind turbine under side-to-side motion., *Journal of Fluid Mechanics, 934:A29.*

[3] Thomas Messmer, Michael Hölling, and Joachim Peinke., (2024): Enhanced recovery caused by nonlinear dynamics in the wake of a floating offshore wind turbine. *Journal of Fluid Mechanics, 984:A66,*

Energy and Momentum Transfer in the Wakes of Floating Offshore Wind Turbines

D. Green[1], T. Rafferty[1], M. Zormpa[1] and C. Vogel[1]

[1] Department of Engineering Science, University of Oxford, Oxford, UK

email-address of the corresponding author: dylan.green@eng.ox.ac.uk

Abstract:
The platform motions of floating offshore wind turbines can induce unsteady wake dynamics, with important implications for the power production and unsteady loading of downstream turbines. Experiments under low-turbulence conditions have shown that prescribed monochromatic platform motions generate large-scale coherent wake structures, and that characteristic utility-scale motion frequencies can excite unstable wake modes, producing responses that are significantly larger than the imposed motion amplitude [1]. However, the way in which these motion-induced coherent structures interact with the sheared, turbulent inflows typical of offshore environments remains unclear. This study therefore aims to investigate the influence of platform motions on momentum and energy transport within the wakes of turbines subject to offshore inflow conditions.

Large-eddy simulations are used to simulate wake evolution in representative offshore conditions. The inflow is generated using a precursor simulation. A shear stress wall boundary condition based on Monin–Obukhov similarity theory is used, with a roughness length of 0.001 m (Figures 1 and 2). The turbine is modelled using the actuator line method in either fixed-bottom operation or undergoing prescribed monochromatic rolling or pitching motions.

Momentum transport within the wakes is analysed using the transport tube theory of [2]. Figure 3 shows downstream cross-sections of axial momentum transport tubes seeded at the perimeter of the rotor-swept area. While the pitching and fixed-bottom cases exhibit similar transport structures, the rolling case shows pronounced transverse stretching, indicating differences in momentum entrainment due to roll-induced wake meandering. This behaviour is further reflected in Figure 4, which shows that rolling motions generate substantially higher levels of coherent kinetic energy than pitching motions of comparable amplitude. Here, the coherent kinetic energy is calculated under the triple decomposition of the velocity field into time-averaged, phase-averaged, and fluctuating components [3].

These results highlight the importance of platform motion orientation in shaping wake coherence, with implications for wake interactions and power variability in floating offshore wind farms, and are consistent with previous findings [4]. Future work will apply the same methodologies to provide deeper insight into the mechanisms through which shear, turbulence, and motion-induced coherent structures interact, clarifying the role of platform motions under offshore conditions.

References

[1] Messmer T., Hölling M. and Peinke J., (2024), Enhanced recovery caused by nonlinear dynamics in the wake of a floating offshore wind turbine, *Journal of Fluid Mechanics, vol. 984*

[2] Meyers J., and Meneveau C. (2013), Flow visualization using momentum and energy transport tubes and applications to turbulent flow in wind farms. *Journal of Fluid Mechanics, vol. 715*

[3] Reynolds W. C., and Hussain A. K. M. F. (1972), The Mechanics of an Organized Wave in Turbulent Shear Flow. Part 3. Theoretical Models and Comparisons with Experiments. *Journal of Fluid Mechanics, vol. 54*

[4] Messmer T., Peinke J., Croce A., and Hölling M. (2025), The role of motion-excited coherent structures in improved wake recovery of a floating wind turbine. *Journal of Fluid Mechanics, vol. 1018*

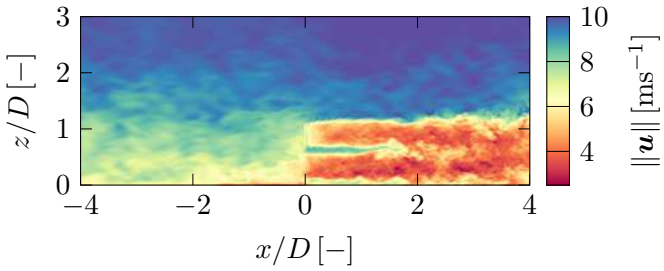

Figure 1: *Snapshot of instantaneous velocity magnitude field around a fixed-bottom turbine (IEA* 15 MW*) in sheared turbulent inflow. Forcing is applied to target a hub height velocity of* $8\,\mathrm{m\,s^{-1}}$.

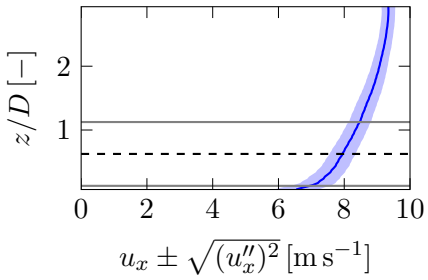

Figure 2: *Inflow mean velocity profile. The shaded region represents one standard deviation from the mean.*

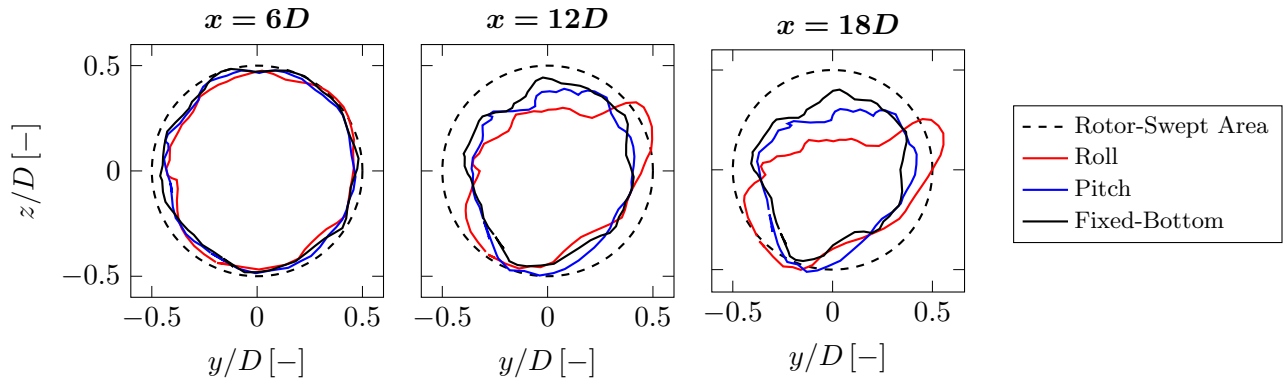

Figure 3: *Time-averaged axial momentum transport tube cross-sections at three downstream locations, originating from seeds placed along the perimeter of the rotor swept area. By construction, no axial-momentum crosses the surfaces of the tubes. Shrinking of the tubes downstream represents the transfer of momentum into the wake from the freestream. The rolling turbine case shows lateral stretching of the transport tube as a result of the motion-induced meandering wake mode. In contrast, pitching motions do not appear to significantly alter the mantle cross sections.*

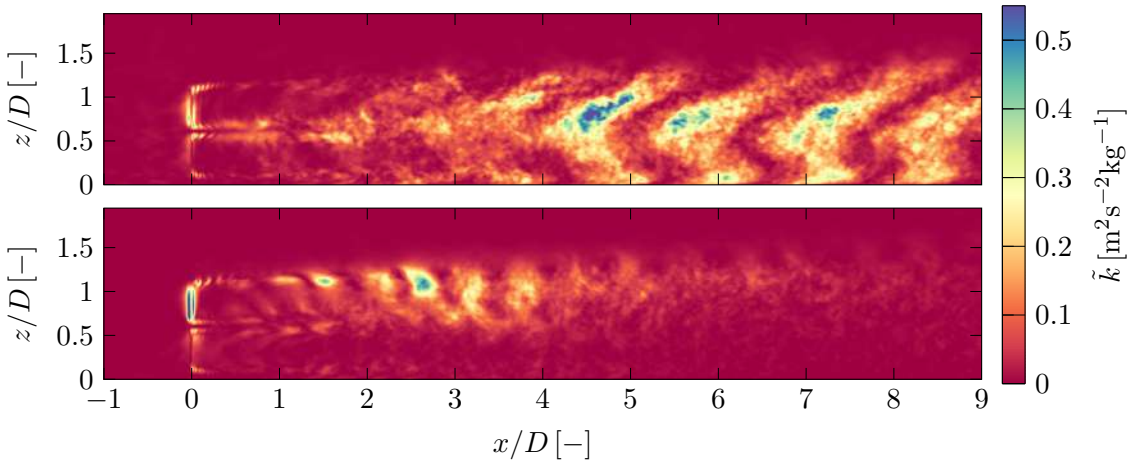

Figure 4: *Snapshot of spatial distribution of coherent kinetic energy, for a rolling (top) and pitching (bottom) turbine. Despite similar motion-induced velocity magnitude, the rolling motions produces significantly more coherent energy within the wake.*

Evaluating the effect of relative Platform Pitch Motion on Floating Offshore Wind Farm Power Output

Y., Zhang[1], M. Ayala [1] C. Meneveau [1] and D. F. Gayme [1]

[1] Department of Mechanical Engineering and Ralph O'Connor Sustainable Energy Institute (ROSEI), Johns Hopkins University, Baltimore, USA

email-address of the corresponding author: dennice@jhu.edu

Abstract:

Predicting the power output of floating offshore wind farms is complicated by the complex coupling between wind and wave induced six degree of freedom turbine motion, which is also affected by inter-turbine wave/wake interactions. There is a growing body of literature focusing on the wake growth of floating turbines under imposed harmonic motion exciting different degrees of freedom (i.e. pitch, surge, roll, and sway), e.g., [1][2]. Wake development and farm power output for ocean wave induced platform pitch motions [3] in the fully developed region of large wind farms (deep array) has also been investigated. Despite this increased research many open questions remain regarding both the flow physics of floating offshore wind turbines interacting with the marine atmospheric boundary layer, and the best computational tools (in terms striking a balance between accuracy versus computational burden) to investigate these phenomena across the wide range of spatial and temporal scales of interest [4].

In this study we employ Large Eddy Simulations (LES) to examine the level of detail required to represent multi-region turbine operation of floating turbines in the simplified setting of harmonic wave motion that imposes different relative phases between floating turbines that are limited to platform pitching motion. We simulate an 8 turbine (4 row, 2 column) array operating in a Fully Developed Wind Turbine Array Boundary Layer (FD-WTABL) via LES with periodic streamwise and spanwise boundary conditions. A PI pressure gradient controller is used to maintain target velocity at the top of the computational domain. The Moving Surface Drag Model (MOSD) of Ayala et al (2024) [5] is applied at the bottom surface. Turbine pitch is prescribed as a harmonic motion with defined amplitude and phase with frequency matched to the ocean wave. Figure 1 provides a sketch of the computational domain (a) and an illustration of the wave induced turbine platform pitching (b). An inertia-induced lag is incorporated via an exponential time filter applied to the disk-averaged velocity based on an imposed timescale. The turbine/platform system representation employs an actuator disk model (ADM) of the IEA 15MW reference turbine mounted on the UMaine VolturnUS-S reference platform.

The results demonstrate that floating wind turbines exhibit substantial velocity oscillations due to platform motion, leading to large variations in the relative velocity normal to the turbine rotor plane that dictate power output. When turbines operate near rated power, these oscillations lead to frequent transitions between operational Regions 2 and 3 that need to be accounted for to prevent over prediction of power output, see sample results in figures 2 and 3. Accordingly, LES frameworks must incorporate time-varying C_T and C_P in order to accurately predict farm level performance. We propose time-varying and turbine operating-regime aware C_T and C_P models and use them in an LES study investigating variations in power output and low order statistics due to different harmonic wave inputs that affect the relative phase of the turbines.

References

[1] Messmer T., Hölling M. and Peinke J., (2024): Enhanced recovery caused by nonlinear dynamics in the wake of a floating offshore wind turbine, *J. Fluid Mech., vol. 984, pp. A66*

[2] Wei N. J. , EI Makdah A. , Hu J. C., Kaiser F., Rival D E. and Dabiri, J O., (2024): Wake dynamics of wind turbines in unsteady streamwise flow conditions, *J. Fluid Mech., vol. 1000, pp. A66*

[3] Xiao S. and Yang D. (2019): Large-eddy simulation-based study of effect of swell-induced pitch motion on wake-flow statistics and power extraction of offshore wind turbines, *Energies, vol. 12, no. 7*

[4] Deskos G., Lee J.C.Y., Draxl C. and Sprague, M.A (2021): Review of wind–wave coupling models for large-eddy simulation of the marine atmospheric boundary layer, *J. Atmospheric Sciences, vol. no. 10, pp. 3025 - 3045*

[5] M Ayala M., Z Sadek Z., O Ferčák O., Cal R. B.,Gayme D, F. and C Meneveau, (2024): A moving surface drag model for LES of wind over waves, *Boundary-Layer Meteorology, vol. 190 no. 10, pp. 39*

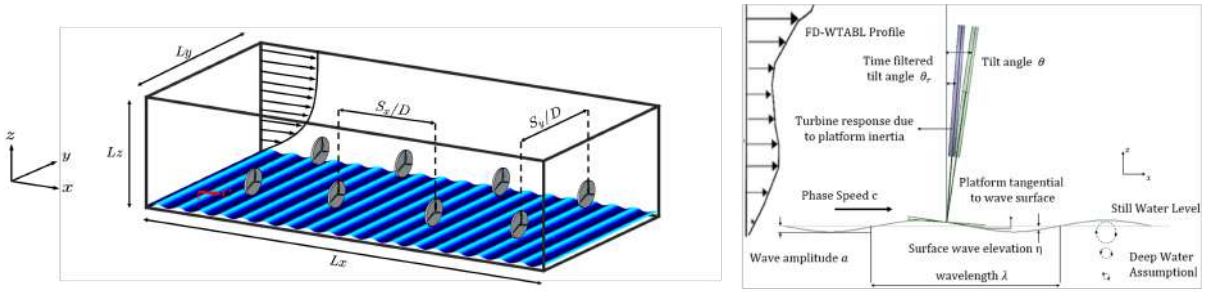

Figure 1: a) Schematic representation of the computational domain used to simulate the FD-WTMABL. b) Schematic of the pitching motion of an individual turbine.

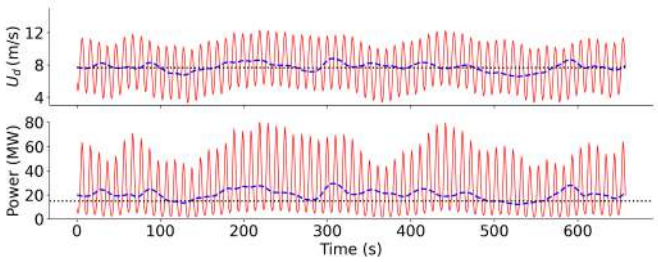

Figure 2: Wind velocity and farm level power output for a farm that assumes typical region 2 control (i.e. a constant C_T and C_p Model)

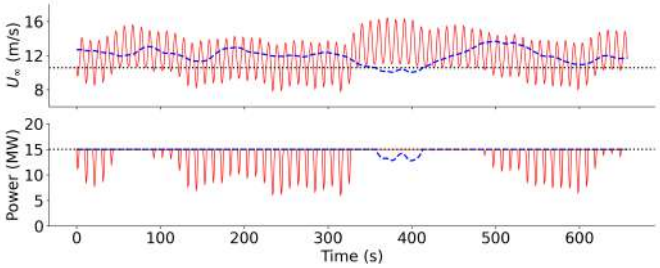

Figure 3: Wind velocity and farm power output for a fixed bottom offshore wind farm using a time-varying and turbine operating-regime aware C_T and C_p model

Generalised actuator disk theory: wake development with turbulent entrainment

M. Bastankhah[1], D.F. Gayme[2], and C. Meneveau[2]

[1] Department of Engineering, Durham University, Durham DH1 3LE, UK
[2] Department of Mechanical Engineering and ROSEI, Johns Hopkins University, Baltimore, MD 21218, USA

email-address of the corresponding author: meneveau@jhu.edu

Abstract:
Classical actuator disk theory [1] provides an idealised description of turbine rotor performance. It treats a rotor as an infinitesimally-thin permeable disk and applies the governing flow equations over a streamtube encompassing the disk. A well-known limitation of the theory is its assumption of ideal flow downstream of the disk, which restricts its applicability to short downwind distances before turbulence and mixing processes governing the wake evolution take hold. Turbulent axisymmetric wakes, by contrast, represent an extensively-studied canonical free shear flow but its applications is limited to the far-wake dynamics [2]. In this work, we introduce a generalised actuator disk theory based on a "hybrid" stream-tube and wake control volume, that seamlessly integrates classical actuator disk analysis with wake turbulence modelling at arbitrary distances from the rotor.

The mass and momentum equations are formulated for the hybrid CV encompassing the streamtube and the wake, upstream and downstream of the actuator disk, as shown in Figure 1. Upwind of the disk, as in Froude's theory, we assume there is no mass exchange between the CV and the surroundings, so the CV is the streamtube encompassing the rotor disk. This assumption implies that turbulent mixing does not play a significant role upstream of the disk [3]. Downstream of the rotor disk, however, the CV is not a streamtube but is assumed to coincide with the outer boundary of the wake, where turbulence drives entrainment of the ambient flow through the lateral surface of the CV, until the wake is fully recovered [4]. Wake recovery is modelled as the result of turbulent entrainment across the lateral surface of the CV with an entrainment velocity that depends on both the wake shear and the ambient turbulence. By integrating mass and momentum balances between far upstream and an arbitrary downstream position x, we derive a generalised Bernoulli-type equation that accounts for both energy extraction by the disk and energy injection into the wake via turbulent mixing. An additional pressure equation is obtained by solving a simplified, axisymmetric form of the pressure Poisson equation. Together, the system consists of three governing relations which can be solved to obtain the streamwise evolution of velocity $U(x)$, pressure $P(x)$, and CV diameter $\sigma(x)$ for given values of the induction factor a or thrust coefficient C_T. The model predicts a physically consistent wake evolution, with an initial flow deceleration due to pressure recovery followed by re-acceleration from turbulent entrainment, along with a gradual wake expansion (see sample comparisons with data in Figure 2). Also, the asymptotic far-wake behaviour depends on free-stream turbulence levels: if entrainment is driven solely by wake shear, the wake width expands as $x^{1/3}$, while it tends to be $\propto x$ when including background turbulence.

The new theory also provides a framework to determine the C_T–a relationship [6] by enforcing the condition that the axial component of the net pressure force on the lateral control surface asymptotically vanishes as $x \to \infty$. The results show that for large values of a or C_T, results become highly sensitive to the level of turbulent entrainment in the near-rotor downstream wake region. The resulting model [4], while still idealised, can be used to predict variations in velocity, pressure, and cross-sectional flow area as function of position, both upstream and downstream of the rotor disk. Furthermore, by accounting for turbulent entrainment in the wake development, it provides more realistic predictions of thrust and power coefficients for highly-loaded disks.

References

[1] Okulov, V. L. & Van Kuik, G. A, (2012), The Betz-Joukowsky limit: ..., *Wind Energy* **15**, pp 335 – 344.

[2] Stevens, R. & Meneveau, C. 2017 Flow structure and turbulence in wind farms. *ARFM* **49**, pp.

[3] Bastankhah, M. & Porte-Agel, F. (2017), Wind tunnel study .... *PoF* **29**, 065105.

[4] Bastankhah, M., Hydon, P.E., Shapiro, C., Gayme, D.F. & Meneveau, C. (2025), Generalised actuator disk theory: wake development with turbulent entrainment (submitted, under review) *Arxiv* 2510.08213v1.

[5] Li, Y., Zhang, F., Li, Zh. & Yang, X. (2024), Impacts of inflow... *JFM* **999**, A30.

[6] Liew, J., Heck, K. S. & Howland, M. F. (2024), Unified momentum model ... *Nature Communic.* **15** (1), 6658.

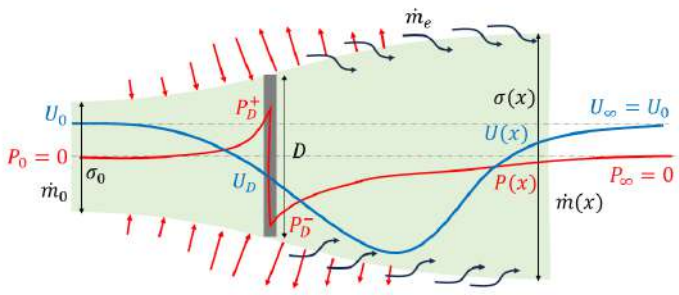

Figure 1: Schematic of the control volume (CV) used in the new proposed actuator disk theory (shaded region). The upstream part of the CV is a streamtube, while the downstream part follows the wake borders and therefore there is flow entrainment from the lateral area. The outlet is at an arbitrary downstream location with a diameter of $\sigma(x)$, pressure $P = P(x)$ and velocity $U = U(x)$. The disk is located at $x = 0$.

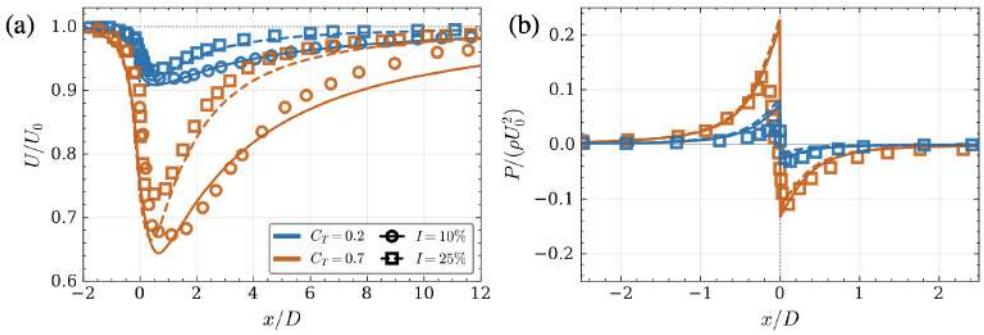

Figure 2: Comparison of actuator-disk model predictions (lines) against LES data of [5] (markers) for (left panel) normalised velocity U/U_0 and (right panel) normalised pressure $P/(\rho U_0^2)$. Results are presented for two thrust coefficients, $C_T = 0.2$ (blue) and $C_T = 0.7$ (orange), at ambient turbulence intensities of $I = 10\%$ (LES: circles, Model: solid lines) and $I = 25\%$ (LES: squares, Model: dashed lines).

Impact of freestream turbulent scales on wind turbine wakes, wind farm flows and power generation: insights and outlook

Emily Louise Hodgson [1], Søren Juhl Andersen [1]

[1] Technical University of Denmark, Department of Wind and Energy Systems, Anker Engelunds Vej 1, 2800 Kgs Lyngby, Denmark

email-address of the corresponding author: emlh@dtu.dk

Abstract:
The impact of turbulence intensity on wind turbine wakes, both for a single wind turbine and a wind farm, is well understood: a higher turbulence intensity leads to greater energy entrainment into the individual wake or farm, which improves wake recovery. This occurs both through the faster breakdown of the tip vortices and shortening of the near-wake, as well as improving entrainment into the far-wake. However, in addition to the turbulence intensity, in recent years a number of both experimental [1, 2] and computational [3] studies on single turbine wakes have shown that the predominant turbulent scales also play an important role, in isolation from turbulence intensity. Turbulent scales are often characterised using the integral time or length scale, T_u or L_u, and normalised with respect to turbine diameter D and freestream velocity U, to relate to the convective time scale D/U or as a Strouhal number $f_T D/U$, where $f_T = 1/T_u$. Longer turbulent scales $f_T D/U \approx 0.1$ show a slower wake evolution, particularly regarding the breakdown of tip vortices and the near-wake length. Shorter integral time scales in the range $f_T D/U = 0.5 - 1.0$ show faster near-wake breakdown, improved wake recovery and - in some studies - greater wake meandering [1, 2, 3]. In Hodgson *et al.* (2023) [3], the near-wake length was $2R$ (where R is the turbine radius) shorter comparing the shortest and longest inflow integral time scales ($f_T D/U = 0.5$ and $f_T D/U = 0.1$ respectively). This led to an improved overall wake recovery that resulted in a 9% increase in mean rotor-averaged velocity and a 35% increase in power at 12R downstream.

After reaching these conclusions for a single turbine wake, a logical next step is to study wind farm flows. Research on the dynamics of entrainment into large wind farms has shown structures larger than the diameter, but constrained by the turbine spacing, to be the most consequential energy-carrying structures into the wind farm from above [4, 5]. The dynamics present in the inflow are broken up by the interaction with the rotor, and through the wind farm structures develop associated with both the individual turbine wakes and the turbine spacing. Additionally, studies on wind farm flow control strategies have shown that control actions applied on a particular turbine only substantially impact the row immediately behind, with impact quickly decreasing through the farm [6, 7]. Therefore, in the context of studying turbulent scales, it is important to investigate firstly whether the freestream integral time scales impacts wind farm flows, and for how deep into the farm that influence persists. Secondly, to study the development of flow dynamics through a turbine row, and whether there is any interaction between atmospheric scales and the self-generated structures in the wind farm.

Hodgson *et al.* (2025) [8] attempts to address these research objectives by examining the impact of the freestream turbulence integral length scale on the flow and power output of a wind farm which consists of a row of 10 turbines with two spacings, $S_x = 8R$ and $S_x = 12R$. Integral length scales in the range $L_u \in [3.2, 12]R$ are studied, equivalent to $f_T D/U \in [0.625, 0.17]$. Turbulence intensity is a constant 3.4% across all inflows. Flow, power output, spectra and correlations are examined. The study shows that the wake recovery of the first turbine, and hence the power output of the second turbine, are strongly influenced by the freestream integral length scale, in agreement with the conclusions for a single turbine. Over the first four turbines, total power output increases by 8.6% and 6.0% respectively for the two spacings, between the shortest and longest freestream integral length scales. However, further into the turbine row, the influence of the freestream decreases as the dynamics become dominated by wake-generated turbulence, and frequencies associated with the turbine spacing.

Despite the many recent advances in the state of art, there are many unaddressed or partially addressed questions that remain, particularly regarding the extension of these conclusions to real wind farms in atmospheric flows, which the presentation hopes to invite a discussion on. For example, to what extent do these results change in more realistic inflows including shear and veer? How relatively important are turbulent scales compared to parameters such as turbulence intensity, stability, and ABL height? Are these parameters so closely linked that in reality one (e.g. ABL stability) dominates over the others? Is it possible to combine the new knowledge about the influence of turbulent dynamics with the development of control strategies to improve wake recovery?

References

[1] Stefano Gambuzza and Bharathram Ganapathisubramani. The influence of free stream turbulence on the development of a wind turbine wake. *J. Fluid Mech.*, 963:A19, 2023.

[2] Martin Bourhis, Thomas Messmer, Michael Hölling, and Oliver R. H. Buxton. Impact of freestream turbulence and thrust coefficient on wind turbine-generated wakes, 2025.

[3] Emily L. Hodgson, Mads H Aa Madsen, and Søren J. Andersen. Effects of turbulent inflow time scales on wind turbine wake behavior and recovery. *Physics of Fluids*, 35(9), sep 2023.

[4] A. Jensen Newman, Donald A. Drew, and Luciano Castillo. Pseudo spectral analysis of the energy entrainment in a scaled down wind farm. *Renew. Energy*, 70:129–141, 10 2014.

[5] Søren J. Andersen, Jens N. Sørensen, and Robert F. Mikkelsen. Turbulence and entrainment length scales in large wind farms. *Phil. Trans. R. Soc. A*, 375(2091):20160107, apr 2017.

[6] Cristina L. Archer and Ahmad Vasel-Be-Hagh. Wake steering via yaw control in multi-turbine wind farms: Recommendations based on large-eddy simulation. *Sust. Energy Tech. Assess.*, 33:34–43, 2019.

[7] W. Munters and J. Meyers. Towards practical dynamic induction control of wind farms: analysis of optimally controlled wind-farm boundary layers and sinusoidal induction control of first-row turbines. *Wind Energy Science*, 3(1):409–425, 2018.

[8] Emily Louise Hodgson, Niels Troldborg, and Søren Juhl Andersen. Impact of freestream turbulence integral length scale on wind farm flows and power generation. *Renewable Energy*, 238:121804, 2025.

Recent Advances in Faster-than-Realtime LES of Wind Farm Flows

S. Ivanell [1], H. Korb [1], H. Asmuth [1], M. M. Mohamamdi [1], J. Bastin [1], D. Lopez [1], Q. Zhaojie [1] and G.P. Navarro Diaz [2].

[1] Uppsala University, Department of Earth Sciences, Wind Energy Division, Visby, Sweden
[2] Vattenfall Europe Windkraft GmbH, Hamburg, Germany

email-adress of the corresponding authour: stefan.ivanell@geo.uu.se

Abstract:

Numerical simulations, in particular Large Eddy Simulation (LES), is one of the pillars of wind farm flow research. However, as wind turbines and wind farms grow in size, so does the computational cost of performing such simulations. The lattice Boltzmann method (LBM) on graphics processing units (GPUs) is one of the most promising contenders for a novel methodology to drastically reduce the computational cost of wind farm simulations.
This presentation reviews the capabilities of the LBM for wind energy applications. The presentation will include a review of key developments that enable the use of LBM for wind energy applications such as the cumulant LBM [7] and present recent work by our research group to include wind energy applications, like the implementation of the actuator line method (ALM) [1] and improved wall modelling [4]. Recently, we also presented simulations of thermally stratified atmospheric boundary layers [8], see Figure 2. We are also increasing the complexity and flexibility of the simulations with LBM, for example, by incorporating forest and more actuator models [11, 10].
Several validation and benchmark studies show that LBM can achieve comparable accuracy as conventional solvers, while reducing computational cost and time by more than one order of magnitude [5, 9, 6], see Figure 1. These advancements enable the examination of large-scale phenomena and even farm-to-farm simulations at unprecedented resolution and computational efficiency, and enabling the industrial application of LES, as demonstrated in [2]. Furthermore, we are able to generate large amounts of highly accurate training data, for example for machine learning methods [3].
Looking forward, the talk outlines key developments required to fully exploit lattice Boltzmann methods for next-generation wind energy simulations. These include improved wall-modeling strategies, coupling with custom aeroelastic solvers, mesoscale coupling, and further improvements in computational efficiency. The presentation concludes with a perspective on how LBM may contribute to more accurate, scalable, and industrially relevant simulations for wind energy research and design in the coming years.

References

[1] Henrik Asmuth et al. “Actuator Line Simulations of Wind Turbine Wakes Using the Lattice Boltzmann Method”. In: *Wind Energy Science* 5.2 (May 26, 2020), pp. 623–645.
[2] Henrik Asmuth et al. “How Fast Is Fast Enough? Industry Perspectives on the Use of Large-eddy Simulation in Wind Energy”. In: *Journal of Physics: Conference Series* 2505.1 (May 2023), p. 012001.
[3] Henrik Asmuth et al. “WakeNet 0.1 - A Simple Three-dimensional Wake Model Based on Convolutional Neural Networks”. In: *Journal of Physics: Conference Series* 2265.2 (May 1, 2022), p. 022066.
[4] Henrik Asmuth et al. “Wall-Modeled Lattice Boltzmann Large-Eddy Simulation of Neutral Atmospheric Boundary Layers”. In: *Physics of Fluids* 33.10 (Oct. 1, 2021), p. 105111.
[5] Henrik Asmuth et al. “Wind Turbine Response in Waked Inflow: A Modelling Benchmark against Full-Scale Measurements”. In: *Renewable Energy* 191 (May 1, 2022), pp. 868–887.
[6] Jean Bastin et al. “A Consistent Performance Comparison of GPU-Resident Lattice Boltzmann and Navier–Stokes Large-Eddy Simulation Solvers for Wind Energy Applications”. In: *Torque Conference Proceedings* (2026). In review.
[7] Martin Geier et al. “The Cumulant Lattice Boltzmann Equation in Three Dimensions: Theory and Validation”. In: *Computers & Mathematics with Applications* 70.4 (Aug. 2015), pp. 507–547.
[8] Henry Korb et al. “Large Eddy Simulation of Thermally Stratified Atmospheric Boundary Layers with a Lattice Boltzmann Method”. In: *Wind Energy Science Discussions* (2025). In Review.
[9] Henry Korb et al. “Validation of a Lattice Boltzmann Solver Against Wind Turbine Response and Wake Measurements”. In: *Journal of Physics: Conference Series* 2505.1 (May 2023), p. 012008.
[10] Damian Lopez-Hermida et al. “Actuator Disk Simulations Using the Lattice Boltzmann Method: Implementation and Validation”. In: *Torque Conference Proceedings* (2026). In review.
[11] Mohammad Mehdi Mohammadi et al. “Efficient Lattice Boltzmann LES of Wind Farm Wakes and Performance in Forest Canopies with Varying PAD Profiles”. In: *Torque Conference Proceedings* (2026). In review.

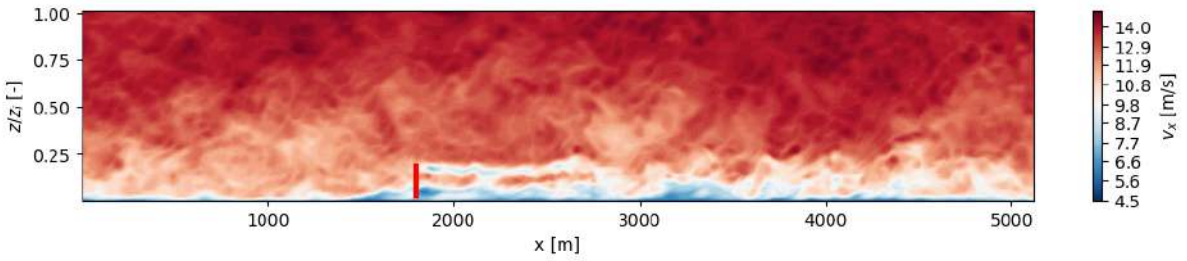

Figure 1: Velocity deficit in the wake of a single turbine in an atmospheric boundary layer. From [6]

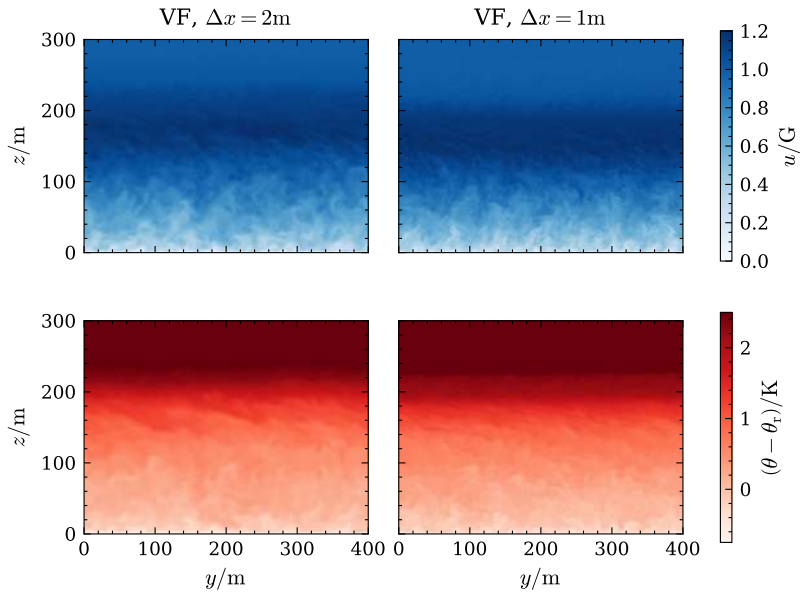

Figure 2: Velocity and temperature planes of simulations of the GABLS1 testcase simulated using VirtualFluids. From [8]

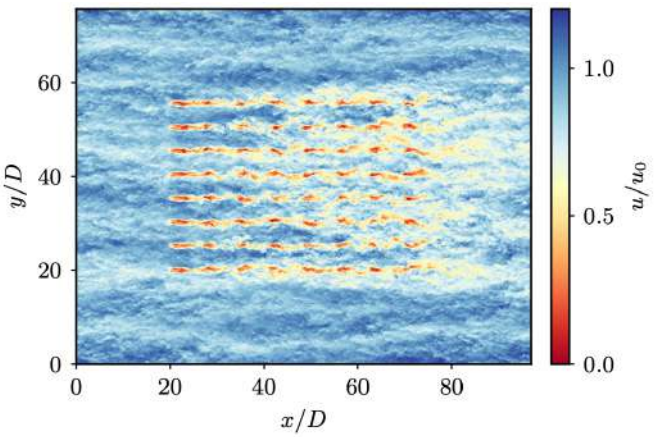

Figure 3: Velocity deficit in a wind farm of 64 DTU 10 MW wind turbines. From [2]

Perspectives on data-driven modelling of atmospheric flows around wind turbines.

Søren Juhl Andersen [1], Juan Pablo Murcia Leon [2], Juan Felipe Cespedes[2], Anna Lena Hölldobler[1], and Niklas Pissarski [1]

[1] Department of Wind and Energy Systems, Technical University of Denmark, Kgs Lyngby, Denmark
[2] Department of Wind and Energy Systems, Technical University of Denmark, Roskilde, Denmark

email-adress of the corresponding authour: sjan@dtu.dk

Abstract:
High-fidelity large-eddy simulations (LES) remain state-of-the-art for simulating atmospheric turbulence and the interaction with individual wind turbines and entire wind farms. However, the computational cost of LES prohibit the full scale deployment of LES for prediction, design, and control purposes.

Various data-driven methods have long offered promising perspectives and avenues for model developments aimed at reducing computational costs, while maintaining high accuracy. Classical approaches such as Proper Orthogonal Decomposition (POD), derive spatial coherent structures in terms of an orthogonal basis, which can form the foundation for Reduced Order Models (ROMs). A fundamental challenge is to construct ROMs, which not only compress data and reconstruct the input data approximately, i.e. the same flow case, but ROMs which can cover unseen cases. The Predictive and Stochastic Reduced Order Model (PS-ROM) [1] combines a global POD basis covering multiple flow scenarios with a stochastic engine, see outline of PS-ROM in Figure 1. The global basis enables prediction of wake aerodynamics for unseen cases with LES accuracy and the stochastic engine generates realizations to converge statistical distributions of power and damage equivalent loads (DEL), see Figure 2. The global basis has been shown to effectively cover different flow scenarios with errors much smaller than the truncation error [2], i.e. how many modes are included in the ROM. The global basis also provide clear physical insights into the flow. The model correctly captures dynamic interaction and how flow features propagate through a wind farm as well as how different POD modes are activated and highlight different flow conditions, i.e. front row turbines, single wake or deep array wakes, as shown in Figure 3 from [3].

Modern machine-learning methods such as autoencoders have been shown to greatly outperform POD for low Reynolds number flow scenarios, e.g. flow over collinear flat plates[4], but there is limited research on autoencoders for capturing the dynamics of highly turbulent flows. Autoencoders can be considered a nonlinear generalization of POD, and the compression (step 2) of PS-ROM could potentially be improved by utilizing autoencoders. New results provide a direct comparison between autoencoders and POD for reconstructing highly turbulent wake aerodynamics. Autoencoders give only modest improvements for small latent spaces, whereas POD becomes superior as more modes are included. The results will be quantified and explained using a newly developed metric, which can be applied a priori to assess whether the potential of autoencoders is sufficiently high to warrant the effort.

References

[1] Andersen S J and Murcia Leon J P 2022 *Wind Energy Science* **7** 2117–2133

[2] Céspedes Moreno J F, Murcia León J P and Andersen S J 2025 *Wind Energy Science* **10** 597–611

[3] Andersen S J and Murcia Leon J P 2023 *Journal of Physics: Conference Series* **2505**(1) 012050 ISSN 1742-6588

[4] Solera-Rico A, Vila C S, Gómez-López M, Wang Y, Almashjary A, Dawson S T M and Vinuesa R 2024 *Nature Communications* **15** 1361 ISSN 2041-1723

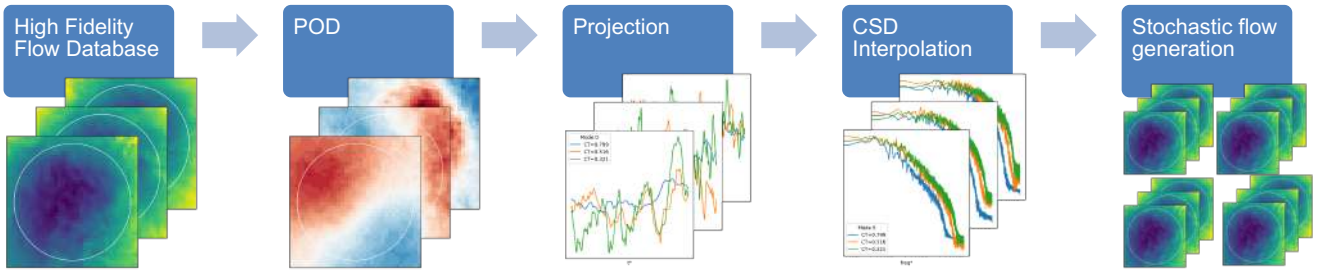

Figure 1: *Five step flowchart of the Predictive and Stochastic Reduced Order Model (PS-ROM) adapted from [1].*

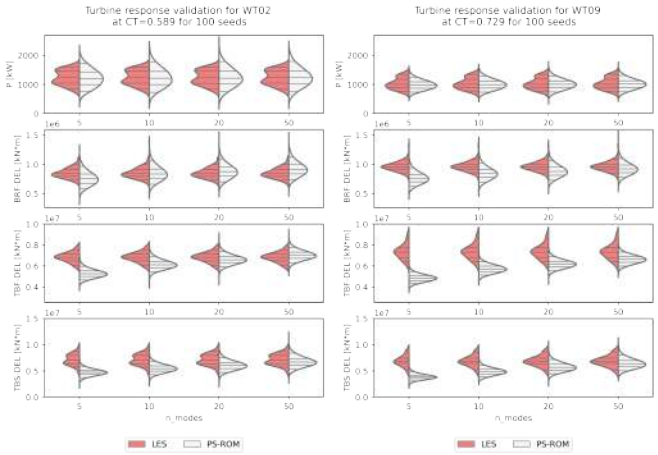

Figure 2: *Comparing distributions of power and DEL of unseen LES (red distributions) against PS-ROM (in white) for different number of POD modes. Figure adapted from [1].*

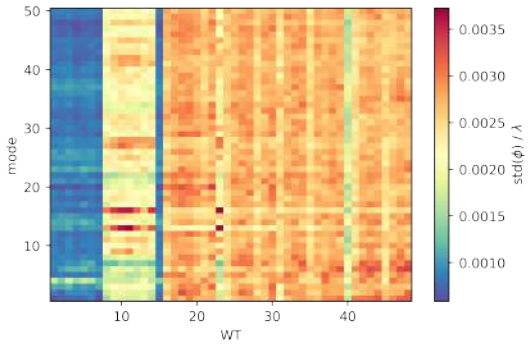

Figure 3: *Normalized standard deviation of first 50 modal time series for 48 turbines (WT) in the Lillgrund wind farm, Figure adapted from [3].*

LES-Modelling of offshore wind farms using a high order continuous spectral element solver

Matias O. Avila [1], Abel Gargallo-Peiró [1] and Oriol Lehmkuhl [1]

[1] Large-scale Computational Fluid Dynamics Group, CASE Dept, Barcelona Supercomputing Center (BSC-CNS), Barcelona, Spain

email-address of the corresponding author: matias.avila@bsc.es

Abstract:

The presence of offshore Wind farms can displace the capping inversion upward, generating gravity waves (GWs) that affect both wind velocity and power distribution. This interaction intensifies the blockage effect, highlighting the necessity of numerical models that accurately simulate these phenomena. This study develops a large-eddy simulation (LES) framework to simulate offshore wind farms in the presence of GWs. Simulation of GWs requires numerical domains that extend to approximately 25 km in altitude. Such simulations typically involve around 1 billion (10^9) mesh nodes, and even more. These computational demands necessitate highly parallel-efficient tools.

The filtered incompressible Navier-Stokes equations are numerically solved using SOD2D (**S**pectral high-**O**rder co**D**e **2** solve partial **D**ifferential equations)[1], an open-source, low-dissipation spectral element mcode developed in-house, designed to run on GPU architectures. SOD2D uses Gauss Legendre Lobatto quadrature, aligning Gauss point positions with nodal positions. This leads to much faster assembly but causes aliasing effects, which are mitigated by using a skew-symmetric splitting of the convective terms. For temporal discretization, a semi-implicit third-order operator-splitting approach is used, allowing equal-order interpolation of pressure and velocity. To prevent numerical oscillations due to dominant convection, the momentum equation is stabilized using a very low-dissipation local projection method [2].

Inflow conditions are generated by solving a concurrent precursor domain that simulates the atmospheric boundary layer without wind turbines. The inflow profile is prescribed at each time step at the nodes of the inflow boundary. GWs reflections are minimized by applying Rayleigh damping layers near the top boundaries. In these simulations, damping layers are not applied at the outflow and inflow boundaries, as described by Lanzilao [3]. The absence of these damping layers does not result in numerical pollution in the simulations.

In domains with a height of 25 km, fully structured meshes produce highly vertically stretched elements in the upper region, resulting in high aspect ratios and poor matrix condition numbers. To address this, conformal hexahedral mesh coarsening is applied in the free atmosphere and damping layer regions, as illustrated in Figure 1, leveraging the code's support for unstructured meshes. This approach yields lower aspect ratio elements, significantly reduces the number of degrees of freedom, improves matrix conditioning, and decreases computational cost. Numerical oscillations arise in mesh transition regions due to buoyancy forces; these are mitigated by implementing a low-pass filter.

Wind turbines are modelled using a uniformly loaded actuator disk. The model is validated with results in the wake of a Vestas V80-2MW wind turbine, obtained by Wu and Porte-Agel. The Wind Speed and TI obtained with SOD2D are very similar to the reference in the near and far wake.

To achieve a higher resolution around the actuator discs, a novel approach based on mesh deformation is adopted. Mesh deformation is conducted treating the computational mesh as a fictitious elastic solid. This technique concentrates resolution near the disks, while maintaining smooth element gradation and high element quality throughout the domain. Fig. 2 illustrates the effect of elastic mesh deformation.

A real offshore wind farm is simulated using SOD2D. Figure 3 shows the wind farm layour, and the Patterns of Production obtained with SOD2D, engineering models and SCADA. Figure 4 displays the pressure field distribution in a vertical plane, demonstrating the presence of GWs.

References

[1] Gasparino L., Spiga F. and Lehmkuhl O., (2024), SOD2D: A GPU-enabled Spectral Finite Elements Method for compressible scale-resolving simulations, *Computer Physics Communications 297 109067*

[2] Blanco-Casares A. et al., (2026), Projection-based stabilization for high-order incompressible flow solvers, *In review, https://doi.org/10.48550/arXiv.2509.04352*

[3] Lanzilao, L. and Meyers, J., (2024), A parametric large-eddy simulation study of wind-farm blockage and gravity waves in conventionally neutral boundary layers, *Journal of Fluid Mechanics 979 A54*

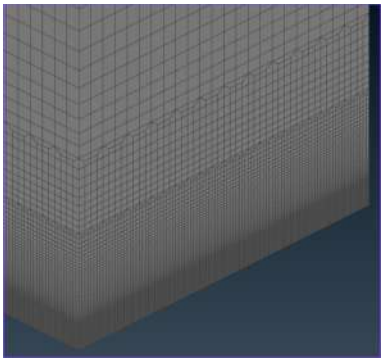

Figure 1: Detail of conformal mesh coarsening when using fourth order hexahedral elements.

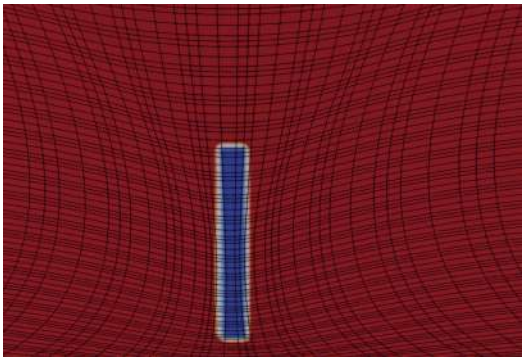

Figure 2: Mesh detail in a vertical plane after applying elastic mesh deformation.

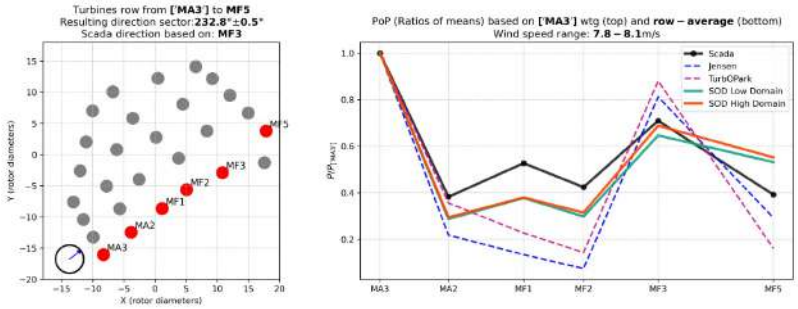

Figure 3: Layout of the wind farm (left). Pattern of production (right) obtained along the wind turbine row in red using SOD2D, Jensen and TurboPark models, and SCADA.

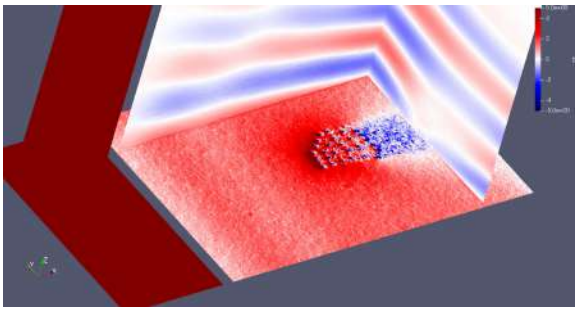

Figure 4: Pressure field obtained with SOD2D in a real offshore wind farm using a domain of 23km height.

Large-scale wind farm atmosphere interactions

Davide Selvatici, Jens Kasper, Richard J.A.M. Stevens [1*]

Physics of Fluids Group, Max Planck Center Twente for Complex Fluid Dynamics, J. M. Burgers Center for Fluid Dynamics, University of Twente

email-address of the corresponding author: r.j.a.m.stevens@utwente.nl

Wind farm performance is strongly influenced by atmospheric turbulence, which governs the vertical transport of kinetic energy and replenishes the energy extracted by turbines. High-resolution large-eddy simulations (LES) provide crucial insights into wind farm-atmosphere interactions. I will discuss how we use LES to improve our understanding and develop analytical models to quantify large-scale interactions among wind farms, the atmosphere, and clouds.

Recent measurements and simulations of wind farm wakes have revealed atmospheric interactions not observed in wakes behind isolated turbines. This raises the question: How do wake recovery and its underlying physical mechanisms vary with wind farm size? We employ LES to study the wake recovery behind 25 different-sized wind farms, ranging from an isolated turbine to an 81-turbine wind farm, in a deep conventional neutral boundary layer. An analysis of wake recovery mechanisms indicates a clear distinction between turbine-scale and wind-farm-scale wake-recovery physics, see figure 1. Turbine wake recovery is primarily driven by spanwise turbulent entrainment of energy, and to a lesser extent by vertical entrainment. We found spanwise mechanisms to be negligible for wake recovery behind large wind farms, which is instead governed by vertical turbulent entrainment and by notable vertical mechanical energy fluxes. Furthermore, we assess the accuracy of several farm-level engineering models in predicting hub-height wind farm wake recovery. We show that large wind farms can influence the atmosphere at higher altitudes far downstream, even after the wind speed at hub height has mostly recovered. Our findings significantly further the understanding of wake recovery physics and may help improve the tools used for siting wind farms within clusters.

In figure 1 we integrate all source and sink terms $\delta\mathbb{E}$ over the wake length L_{wake}: $\mathbb{E} = \int_{L_{\text{wake}}} \delta\mathbb{E}(x')\mathrm{d}x$, Here, $\mathbb{M}_x$ equals the total power required to raise the streamwise mechanical energy flux back up from its value immediately behind the wind farm to the value at $x' = L_{\text{wake}}$. Logically, $\mathbb{M}_x$ increases significantly with both N_T and M_T, since both increase the size of the wake.

We show that offshore wind farms alter cloud-topped boundary layers, producing atmospheric footprints that extend tens of kilometers around the farm, including wave-like patterns visible in satellite imagery. Using high-resolution large-eddy simulations, we demonstrate that these structures originate from gravity waves triggered by the upward deflection of the inflow due to wind-farm blockage. The waves propagate through the boundary layer and into the cloud layer, deforming the inversion height and altering the cloud liquid water content. As a result, radiative fluxes within the cloud layer are modified, leading to significant changes in cloud albedo. At the surface, latent and sensible heat fluxes increase within the farm and decrease downstream, and rainwater content exhibits a similar pattern. Figure 2 shows these large-scale impacts of the wind farm on atmospheric flows and clouds. These effects are poorly represented in climate and weather models because their resolution is too coarse to capture the relevant physics. The simulations presented here reveal the underlying mechanisms and provide a foundation for developing improved parameterizations of wind-farm impacts in mesoscale models.

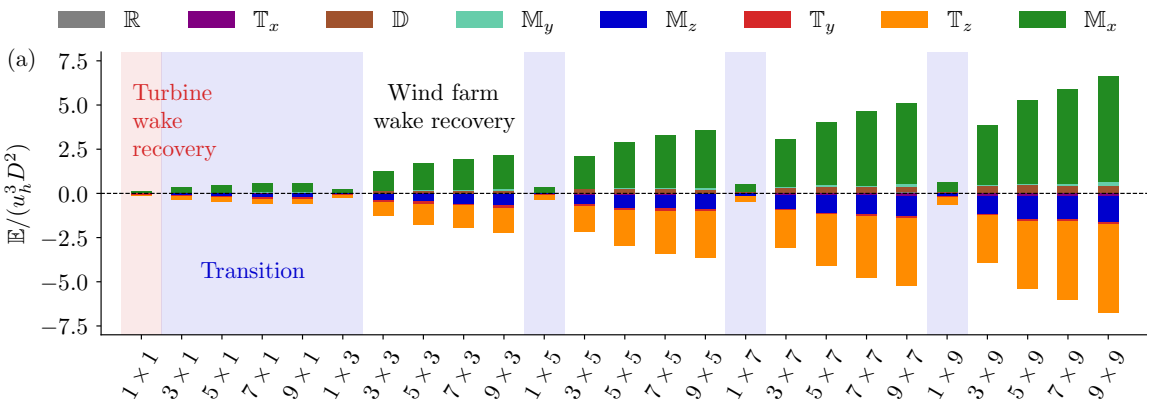

Figure 1: *Comparison of the total source and sink terms $\mathbb{E}$ among all simulated wind farms, normalized with hub-height velocity u_h and turbine diameter D. Here, $\delta\mathbb{M}_x$ denotes the streamwise mechanical-energy flux, $\delta\mathbb{M}_{yz}$ the lateral/vertical mechanical-energy flux, $\delta\mathbb{T}_x$ the total turbulent transport in streamwise directions, $\delta\mathbb{T}_x$ the total turbulent transport in spanwise directions, $\delta\mathbb{T}_z$ the total turbulent transport in vertical direction, $\delta\mathbb{D}$ the dissipation.*

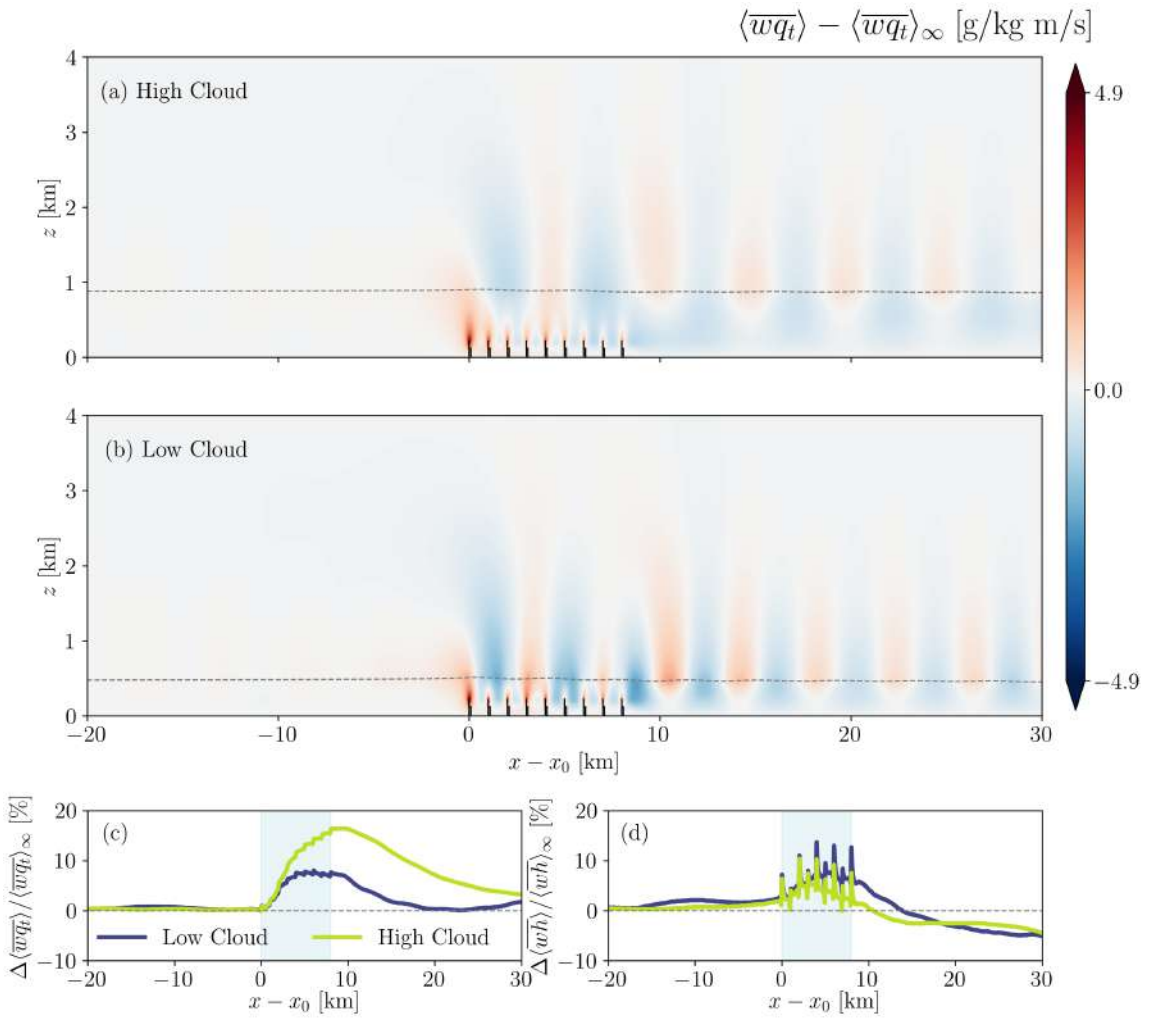

Figure 2: Influence of wind farm-induced gravity waves on atmospheric moisture flux in the *low cloud* and *high cloud* cases shown in panels (a) and (b). The dashed line indicates the cloud-top height, defined by the midpoint relative humidity in the cloud-top region (77.5% in panel (a) and 85% in panel (b)). Wind turbines are shown to scale. Panels (c) and (d) show the relative changes in latent and sensible heat fluxes at the ground compared with the inflow. The light-blue shading in panels (c) and (d) indicates the wind farm location. Only part of the simulation domain is shown.

Coupled model of wind-farm–induced gravity waves with atmospheric boundary layer

H. Amini Kafiabad [1], M. Bastankhah [2]

[1] Department of Mathematical Sciences, Durham University, Durham, United Kingdom
[2] Department of Engineering, Durham University, Durham, United Kingdom

email-adress of the corresponding authour: hossein.amini-kafiabad@durham.ac.uk, majid.bastankhah@durham.ac.uk

Abstract:
The dynamics of large-scale wind farms and the atmospheric boundary layer (ABL) are inherently coupled. The reduction of wind speed at hub height drives vertical motions that displace the capping inversion and excite gravity waves in the free atmosphere. These waves, in turn, impose pressure gradients that modulate the wind farm performance. Current state-of-the-art practices often treat wake modelling and gravity-wave generation in isolation, or approximate the two-way coupling by stitching together separate components through iterative algorithms [1, 2]. Furthermore, existing analytical models often neglect the vertical variability of the ABL, representing it as a single uniform layer [3] which compromises the physical consistency of the flow solution. In this work, we present a new modelling framework that captures the two-way coupling between turbulent farm wakes and gravity waves while retaining a realistic description of the ABL's vertical structure. Although this framework can be applied to ABL models of varying complexity, we consider the linearised two-dimensional incompressible boundary layer equations as a proof of concept. Crucially, our formulation retains the vertical momentum equation, allowing pressure to vary with height, a feature often neglected in shallow-water-type approximations but essential for capturing the complex vertical dynamics of wake-wave interactions. The coupling between the boundary layer flow and the overlying stratified atmosphere is achieved via a new dynamic boundary condition applied at the capping inversion. We model the inversion layer as a pliant interface where the pressure perturbation is determined by both hydrostatic interfacial waves and internal gravity waves in the free atmosphere. This yields a spectral Robin boundary condition for the vertical velocity $\hat{w}$:

$$\frac{\partial \hat{w}}{\partial z} = \frac{g' + i\,U_0(H)\,N\,\mathrm{sgn}(k)}{U_0(H)^2}\,\hat{w}, \tag{1}$$

where g' is the reduced gravity, k is the wave number, N is the Brunt-Väisälä frequency of the free atmosphere, and $U_0(H)$ is the background velocity at the inversion height H. The system is solved efficiently using a spectral method in the streamwise direction and finite differences in the vertical direction. Figure 1 illustrates preliminary results for a tandem wind farm interacting with a conventionally neutral ABL. The model successfully captures the farm-to-farm interaction, the complex vertical structure of the velocity perturbations, and the displacement of the capping inversion. Future work will extend this formulation to three dimensions, nonlinear dynamics, and non-neutral boundary-layer conditions.

References

[1] Stipa S. et al., (2024), The multi-scale coupled model: A new framework for capturing the impact of gravity waves, *Wind Energ. Sci., 9, pp. 1123–1152.*

[2] Devesse K. et al., (2024), A meso–micro atmospheric perturbation model for wind farm blockage, *J. Fluid Mech., 998, A63.*

[3] Smith R. B., (2010): Gravity wave effects on wind farm efficiency, *Wind Energy, 13, pp. 449-458.*

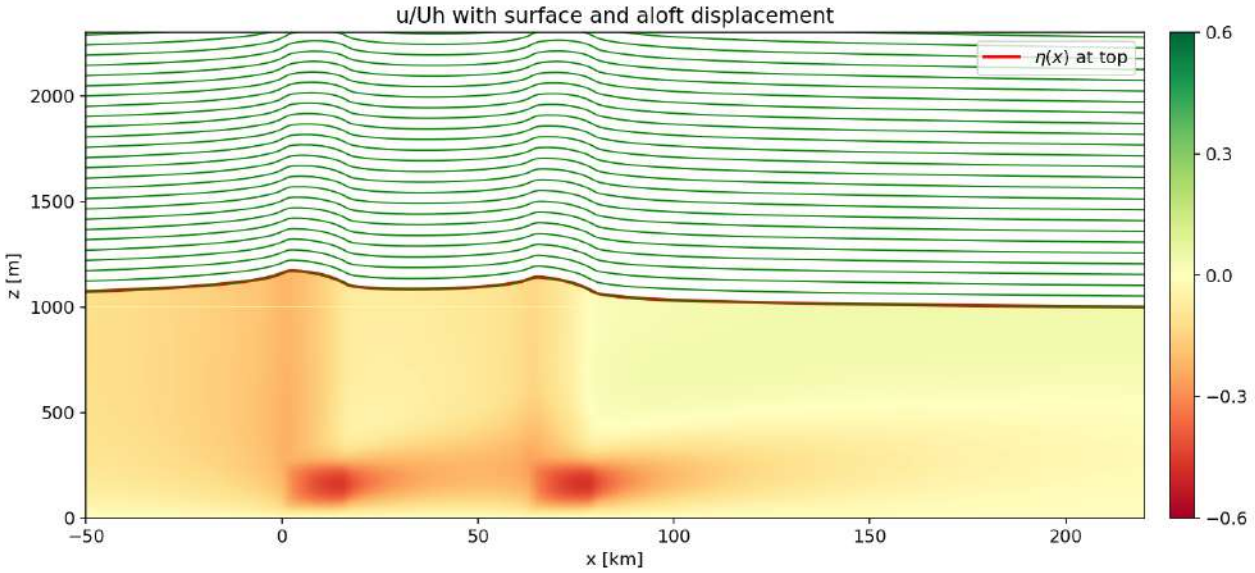

Figure 1: The red middle curve indicates the displaced capping inversion. Below the inversion, streamwise velocity perturbations induced by a tandem wind farm interacting with a conventional neutral boundary layer are shown, with the colour scale indicated on the right. Above the inversion, the displacement of vertical layers resulting from the interaction with the boundary layer is displayed. The figure highlights both the wake interaction between the upstream and downstream wind farms and the associated coupling with the free atmosphere.

A wind farm modeling paradigm for stratified atmospheric boundary layers

Michael F. Howland [1]

[1] Department of Civil and Environmental Engineering, Massachusetts Institute of Technology, Cambridge, USA

email-address of the corresponding author: mhowland@mit.edu

Abstract:

As wind turbines and farms grow larger, consideration of stratified atmospheric boundary layer (ABL) processes in wind power models becomes increasingly important. Together, Coriolis effects and atmospheric stratification and buoyancy control the boundary layer structure and flow characteristics. In addition, stratification will result in a direct buoyant forcing within the wake region. Engineering models of wind farm flow and power production combine models of rotor aerodynamics, wakes, and the large-scale atmospheric response to wind farms. Such models typically capture wind turbine rotor thrust and power using lookup tables that neglect the influence of rotor-inflow misalignment, wind speed shear and direction shear, and turbulence or using the rotor equivalent model which only captures geometric effects of these mechanisms. Further, engineering models of mean wake velocity typically utilize empirical turbulence models that do not explicitly account for ABL shear and stability. Here, we develop a new fast-running wind farm modeling paradigm for stratified ABLs where we generalize classical momentum theory to capture the diverse operating regimes for modern wind turbines rotor aerodynamics and we integrate it into new wake model based on coupled wake turbulence kinetic energy and wake momentum parabolized Reynolds Averaged Navier Stokes (RANS) equations. Comparing the model predictions to large eddy simulations (LES) across stabilities (Obukhov lengths) and surface roughness lengths, we find lower prediction error than standard wake models across the ABL conditions and error metrics investigated. The new model also yields three-dimensional predictions of turbulence kinetic energy in the wake.

At the wind turbine rotor scale, we develop a Unified Momentum Model [1] depicted in Figure 1 for rotor aerodynamics that is valid across operating regimes, from low to high thrust coefficient magnitudes, including positive and negative thrust, and at arbitrary misalignment angles between inflow and rotor. The Unified Momentum Model overcomes limitations of classical one-dimensional momentum theory by accounting for both misalignment between the rotor and inflow and the pressure deficit in the rotor wake, as predicted by a solution to the differential Euler equations. The resulting aerodynamic model predicts rotor thrust, power, and wake velocities at arbitrary misalignments and thrust coefficients without empirical corrections. Additionally, the model is coupled with blade element modeling to yield a new first-principles blade element momentum (BEM) model without empirical corrections. Predictions from the new BEM model are validated against LES and experiments.

At the wake scale, we investigate the flow physics mechanisms that govern the momentum and turbulence within the wake of a wind turbine operating in stratified ABLs. We conduct analysis of the streamwise momentum wake deficit and wake-added turbulence kinetic energy (TKE) budgets to study wind turbine wakes under neutrally and stably stratified ABL conditions. To separate the turbulence in the wake from the turbulent, incident ABL flow, we decompose the flow into the base ABL flow and the deficit flow produced by the presence of a turbine. Building on budget analysis of the deficit flow, we develop a fast-running model of wind turbine wakes based on the parabolized RANS equations for both velocity deficit and wake-added TKE [2] with initial conditions provided by the Unified Momentum Model. By predicting the wake based on the Unified Momentum Model integrated into a parabolized RANS wake model, the mean wake velocity deficit is coupled to both the turbulent ABL inflow and also the wake added turbulence. The proposed model lowers prediction error compared to widely used wake models by coupling the wake recovery to the spatially evolving wake turbulence and by accounting for wind shear and stability, with predictions shown in Figure 2.

References

[1] Liew, Jaime, Kirby S. Heck, and Michael F. Howland. Unified momentum model for rotor aerodynamics across operating regimes, *Nature Communications, 15, no. 1 (2024): 6658*

[2] Klemmer, Kerry S., and Michael F. Howland. "Wake turbulence modeling in stratified atmospheric flows using a novel $k - \ell$ model." *Journal of Renewable and Sustainable Energy 17, no. 3 (2025).*

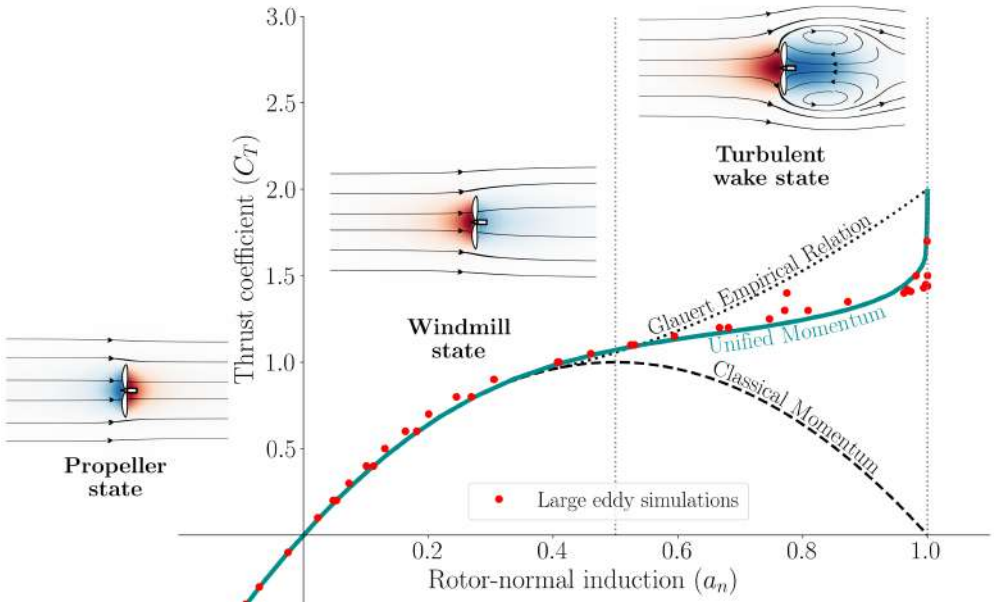

Figure 1: Schematic illustrating the rotor thrust coefficient variations with rotor-normal induction across various operational scenarios for a yaw-aligned wind turbine. Model predictions are shown using classical one-dimensional momentum modeling, Glauert's empirical relation, and the Unified Momentum Model introduced in this abstract.

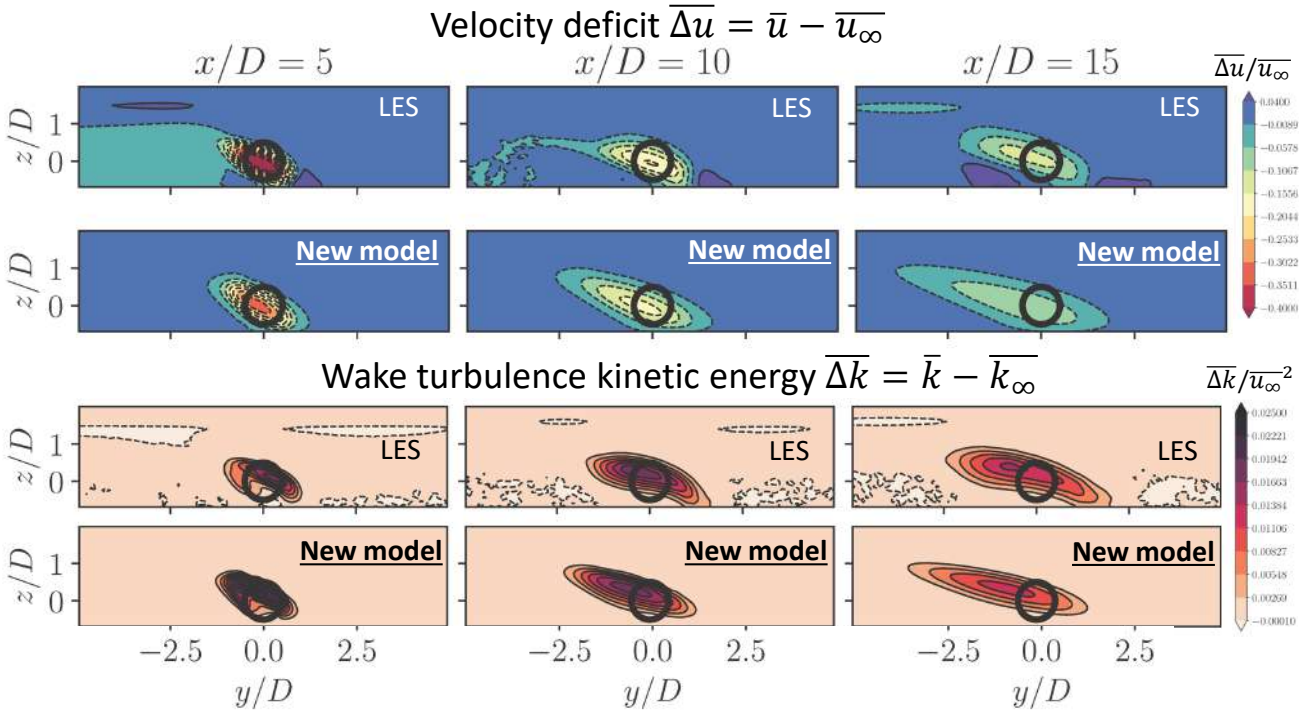

Figure 2: Contours of mean wake velocity deficit $\overline{\Delta u}$ and wake-added turbulence kinetic energy $\overline{\Delta k}$ from the $k-\ell$ model compared with LES for a stable boundary layer (SBL) flow. The freestream velocity and turbulence kinetic energy are $\overline{u_\infty}$ and $\overline{k_\infty}$, respectively.

Differences in cluster and internal wake effects from mesoscale and large-eddy simulations off the U.S. East Coast

Miguel Sanchez-Gomez [1], Georgios Deskos [1], Mike Optis [2], Julie K. Lundquist [3], Michael Sinner [1], Geng Xia [1], Walter Musial [1]

[1] National Laboratory of the Rockies, Golden, Colorado, USA
[2] Veer Renewables, Courtenay, British Columbia, Canada
[3] Ralph O'Connor Sustainable Energy Institute, Johns Hopkins University, Baltimore, Maryland, USA

email-address of the corresponding author: Julie.Lundquist@JHU.edu

Abstract:
Mesoscale simulations are increasingly used to estimate wake effects within and between large wind farms, despite limited validation for large-scale wake effects. This study, based on [1], evaluates the capabilities and limitations of mesoscale simulations in capturing wake-induced impacts on wind turbine power production through a direct comparison with large-domain large-eddy simulations (LES) for three planned offshore wind farms under realistic atmospheric conditions and a range of atmospheric stability. We assess mesoscale performance of the [2] wind farm parameterization in replicating wake characteristics behind single and multiple turbine clusters and quantify the resulting variability in mean turbine power. Results show that mesoscale Weather Research and Forecasting simulations with the Fitch wind farm parameterization capture key features of the velocity deficit downstream of both single and multiple wind farms, with mean root-mean-square errors near 5% and good agreement with stability-driven wake behavior. However, in these simulations, the mesoscale Fitch parameterization underestimates power losses from internal wake effects, particularly when turbines align with the prevailing wind direction or under stable stratification. In these conditions, individual wakes persist and dominate downstream power deficits. The coarse resolution of the mesoscale simulations limits their ability to resolve individual wind turbine wakes that drive power fluctuations within wind farms. Nonetheless, mesoscale simulations can yield accurate estimates of combined wake losses from internal and cluster effects across some wind direction sectors, where errors in wake representation may cancel out. These findings underscore the strengths of mesoscale simulations for capturing broader wake patterns, while highlighting their limitations for modeling turbine-level power losses. Future work should explore hybrid modeling approaches to capture both long-range cluster wake propagation and localized internal wake dynamics.

References

[1] Sanchez-Gomez, Miguel and Deskos, Georgios and Optis, Mike and Lundquist, Julie K. and Sinner, Michael and Xia, Geng and Musial, Walter, (2025), Differences in cluster and internal wake effects from mesoscale and large-eddy simulations off the U.S. East Coast, *Wind Energy Science Discussions*, https://wes.copernicus.org/preprints/wes-2025-152/

[2] Fitch, Anna C. and Olson, Joseph B. and Lundquist, Julie K. and Dudhia, Jimy and Gupta, Alok K. and Michalakes, John and Barstad, Idar, (2012), Local and Mesoscale Impacts of Wind Farms as Parameterized in a Mesoscale NWP Model, *Monthly Weather Review*, vol. 140, pp. 3017–3038

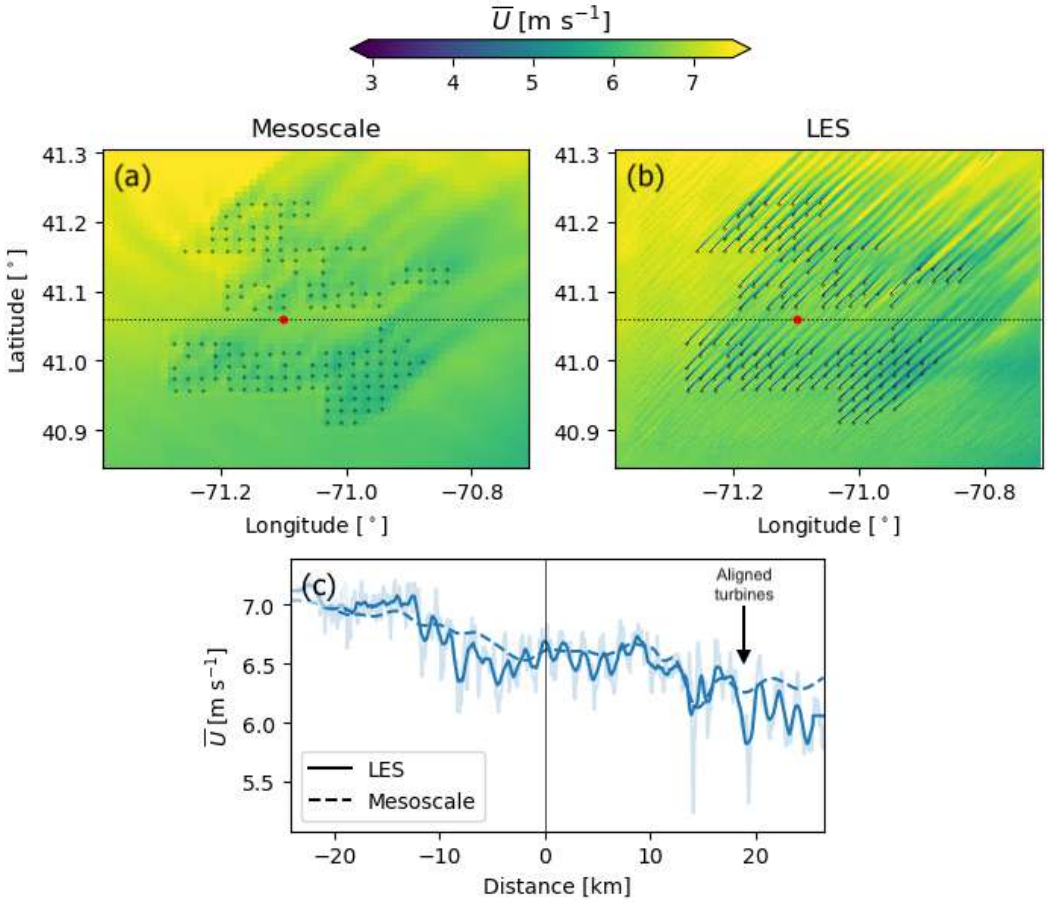

Figure 1: *Time-averaged velocity field at hub height for the mesoscale (a) and LES (b) simulations under stable atmospheric conditions. The velocity fields are averaged in time between 14:30 and 14:45 UTC on 26 November 2019. The dotted black lines in each panel illustrate the locations of the velocity transects, and the red dots indicate the midpoint distance of each transect. Panel (c) shows the velocity along the transect for the LES and mesoscale simulation. For reference, the mean wind direction across the region is* 219°.

A Lagrangian Tracer System Using Balloons to Study Wind Farm Interactions with the Atmospheric Boundary Layer

A. Borra[1], F. Falkinhoff[1], M. Grunwald[1,2], E. Bodenschatz[1,2], G. Bagheri[1] and C. E. Brunner[1]

[1] Max Planck Institute for Dynamics and Self-Organization, Göttingen, Germany
[2] Georg-August-University Göttingen, Göttingen, Germany

email-address of the corresponding author: claudia.brunner@ds.mpg.de

Abstract:
As wind farms increase in size, their interactions with the atmospheric boundary layer (ABL) become increasingly important for accurate predictions of power output. However, due to the large range of scales involved, these processes are challenging to study, both numerically and in the field, and are therefore not sufficiently understood.

Traditionally, wind farm flows have been studied from an Eulerian perspective, meaning that the flow field is observed from a fixed reference frame as a function of time. However, many important processes such as mixing, dispersion and turbulent transport are inherently Lagrangian processes, meaning that they depend on the paths of individual fluid particles moving through the flow field. As such, studying them from a Lagrangian perspective may provide deeper insight. Unlike the traditional Eulerian approach, which records fluid properties at fixed spatial locations, Lagrangian particle tracking (LPT) records fluid properties along the particle trajectory, providing more detailed information about a fluid parcel as it evolves in space and time. The resulting data typically have the necessary spatiotemporal resolution to study turbulent fluctuations, but are spatially sparse, meaning that the density of the recorded tracks within the volume of interest is low. Creating tracer objects in the atmospheric boundary layer is particularly challenging because changes in pressure, temperature and humidity all affect the local density of the flow and thus the buoyancy of the tracer objects.

Here, we present a novel measurement technique for collecting Lagrangian information in the ABL, using neutrally-buoyant radiosondes that follow the flow over many kilometers while recording meteorological properties at high spatial and temporal resolution. Ideally, they remain neutrally buoyant at all times, which means that the weight of the radiosonde must be balanced by lift. The radiosondes used here weigh 12 g and were attached to balloons filled with the precise amount of helium to achieve neutral buoyancy at ground level. The positions of the radiosondes are determined using GPS at a sampling frequency of 1 Hz. Wind speed and direction, temperature, pressure and relative humidity are recorded at 0.16 Hz. While line-of-sight is maintained, this information is continuously transmitted to a ground-based receiver station with a range of 45 km. The on-board battery allows for 1.5 hours of data transmission. Multiple tracer objects are simultaneously released from a predetermined position in the flow using a DJI Matrice 350 drone (Fig. 1a).

We present the tracer design as well as results from a proof-of-concept field campaign deploying them in the wake of a wind turbine at the WINSENT wind farm test site near Stuttgart, Germany [1] in October 2025. Seven tracers were successfully launched at mean wind speeds of 7 m/s $\leq \overline{u} \leq$ 9 m/s and neutral stability conditions. We show the tracks of the tracers as they travel through two small wind farms (Fig. 1b) as well as temperature, humidity and altitude along these tracks (Fig. 2). We conclude that this technique has the ability to provide valuable information on wind farm flows, particularly when a large number of tracers are released. We discuss successes and shortcoming of this first field campaign and propose improvements for future campaigns.

References

[1] Zentrum für Sonnenenergie- und Wasserstoff-Forschung (ZSW), (2023), Research Test Site WINSENT, https://www.zsw-bw.de/en/research/wind-energy/topics/research-test-site-winsent.html

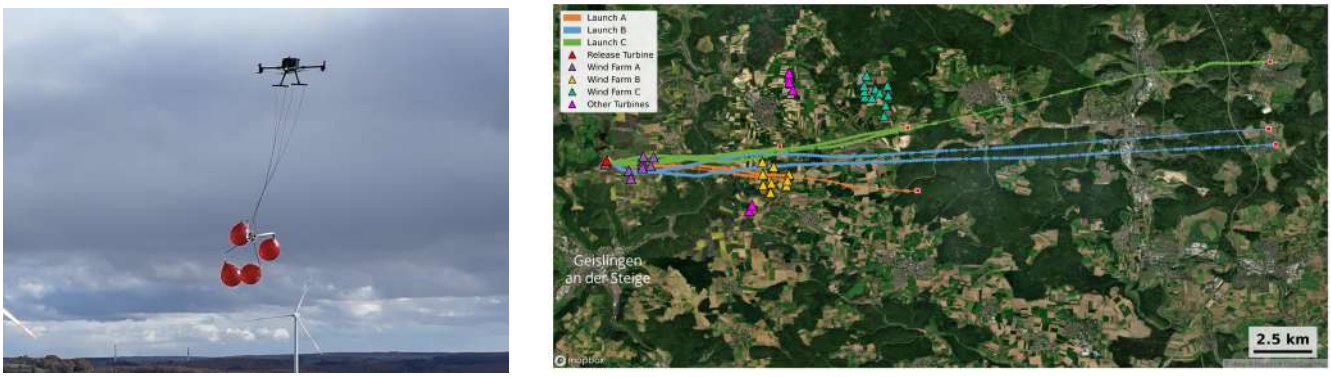

(a) (b)

Figure 1: *(a) release mechanism with Lagrangian tracer objects hanging below DJI Matrice 350 and (b) overhead view of tracks of the Lagrangian tracers*

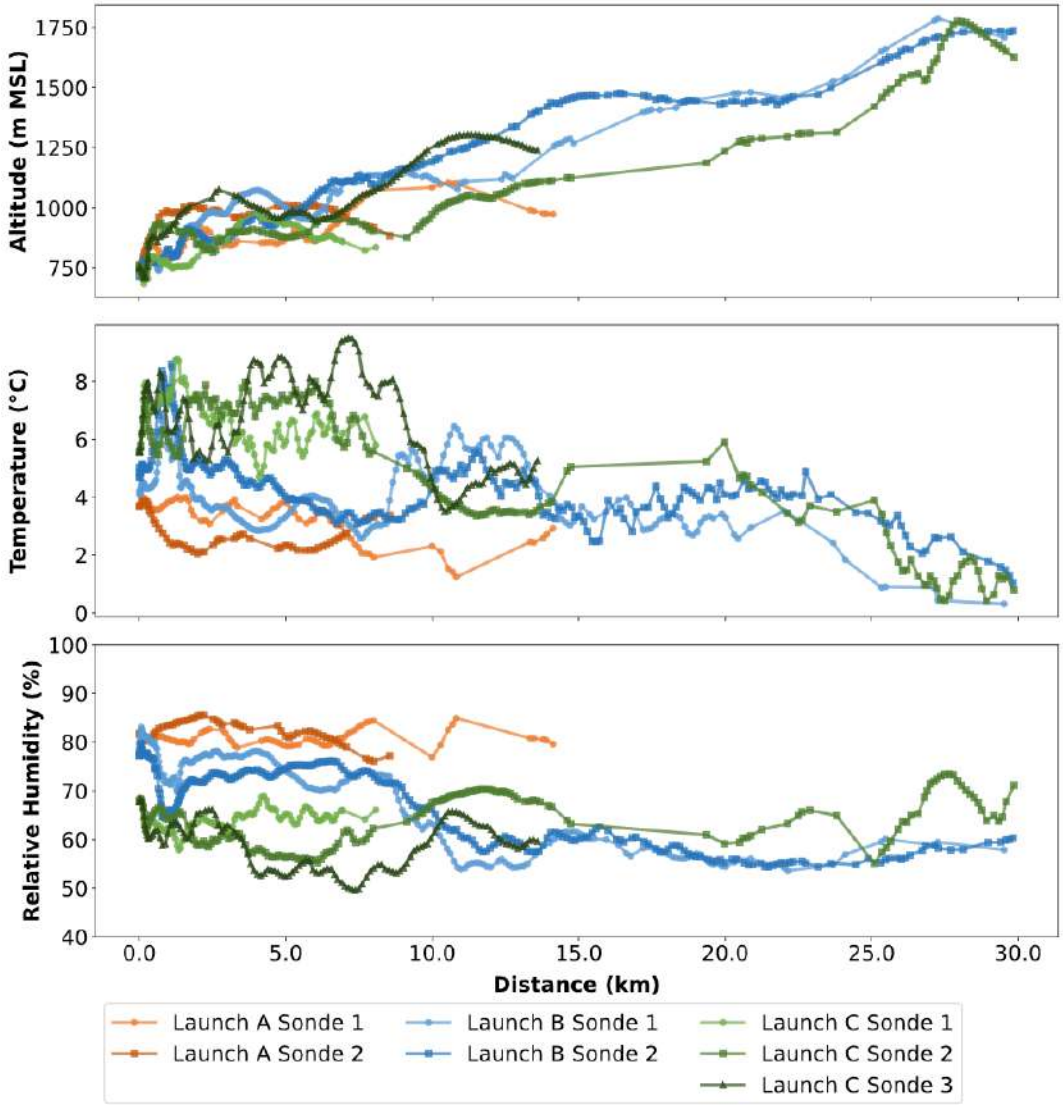

Figure 2: *(a) Altitude, (b) temperature, and (c) relative humidity profiles along the Lagrangian tracks*

Validating a three-year high-resolution mesoscale simulation of a multi-gigawatt offshore wind farm cluster with lidar and satellite observations

Wim Munters[1], A. Palatos-Plexidas[1,2], S. Gremmo[1], L. De Cruz[2,3] and J. van Beeck[1]

[1] von Karman Institute for Fluid Dynamics, Sint-Genesius-Rode, Belgium
[2] Vrije Universiteit Brussel, Brussels, Belgium
[3] Royal Meteorological Institute of Belgium, Brussels, Belgium

email-address of the corresponding author: wim.munters@vki.ac.be

Abstract:
With an increasing amount of large offshore wind farms being installed, interactions between neighboring farms have raised increased interest from both research and industry in recent years. Specifically, individual turbine wakes merge to form coherent wind farm wakes that can persist for several tens of kilometers, thus impacting the wind conditions of neighboring farms. As such, accurately quantifying farm wake effects from both existing and future wind farms has become increasingly pertinent for all stages of a wind farm project, from planning through operations to decommissioning.

Mesoscale weather simulations equipped with wind farm parameterizations have emerged as the current state-of-the-art numerical methodology to quantify these wake effects. Although validation of simulated wake effects has been undertaken in several studies (see [1] for an overview), long-term validations of high-resolution mesoscale models are scarce in literature. To address this gap, we present a high-resolution three-year mesoscale wind farm wake study and validate simulation results with Synthetic Radar Aperture satellite imagery and strategically located profiling lidars [2]. Wind farm wake simulations are performed with the Fitch [3] wind farm parameterization implemented in the Weather Research and Forecasting model for the period from 2021 to 2023 with a fine horizontal grid spacing of 1 km.

We focus on the Belgian-Dutch cluster in the Southern Bight of the North Sea, which is the largest operational offshore wind farm cluster with an installed capacity of more than 3.7 GW. Long-term lidar campaigns oriented both upstream and downstream of the cluster along the prevailing southwesterly wind direction provide a unique test case for long-duration validation of simulated wake effects (see Figure 1a). Simulated hub-height wind speeds are observed to match well with lidar observations, and the analysis of specific events show farm wakes persisting for tens of kilometers in both simulations and SAR images (see Figure 1b,c), further justifying the methodology as a useful tool for quantifying wind farm wake effects in large wind farm clusters.

This work was supported by the European Union through Horizon Europe project DTWO (grant no. 101146689). Furthermore, we acknowledge support from VLAIO and De Blauwe Cluster (project HBC.2022.0549 Cloud4Wake).

References

[1] Fischereit, J., Brown, R., Larsén, X.G., Badger, J. and Hawkes, G., 2022. Review of mesoscale wind-farm parametrizations and their applications. *Boundary-Layer Meteorology, 182(2), pp.175-224.*

[2] Palatos-Plexidas, A., Gremmo, S., van Beeck, J., De Cruz, L. and Munters, W., 2025, Assessing the Accuracy of a Three-Year High-Resolution Mesoscale Wind Farm Wake Simulation with Lidar and Satellite Radar Data., *Wind Energy Science Discussions, 2025, pp.1-33.*

[3] Fitch, A.C., Olson, J.B., Lundquist, J.K., Dudhia, J., Gupta, A.K., Michalakes, J. and Barstad, I., 2012. Local and mesoscale impacts of wind farms as parameterized in a mesoscale NWP model. *Monthly Weather Review, 140(9), pp.3017-3038.*

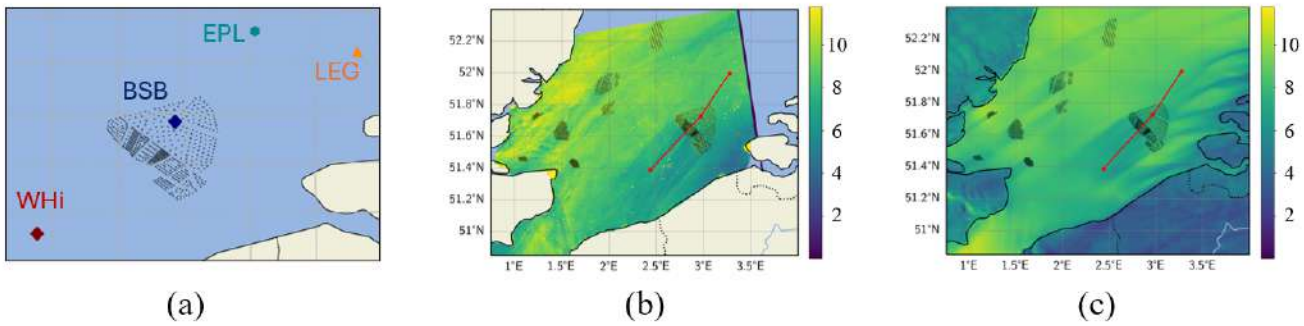

Figure 1: *(a): Belgian-Dutch wind farm cluster layout. Four lidar locations inside and around the cluster are shown. (b), (c): Planview of 10 m wind speed on 19 September 2020 17:40 UTC in SAR (b) and WRF (c). Coloring is in units of m/s.*

Assessing turbulent wind farm flows with dual-Doppler radar measurements

Julia Gottschall [1,2], Q. Zheng [1], L. Hung [1] and A. Jordan [1]

[1] Fraunhofer Institute for Wind Energy Systems IWES, Bremerhaven/Bremen, Germany
[2] Faculty of Geosciences, University of Bremen, Bremen, Germany

email-address of the corresponding author: julia.gottschall@iwes.fraunhofer.de

Abstract:
Dual-Doppler radar systems have recently emerged as a next-generation method for wind measurement, yet their application to wind wake characterization remains limited by data quality challenges, including measurement artifacts and low data availability. In [1], we have presented a comprehensive post-processing framework for dual-Doppler radar data to comprehensively identify and discard measurements with unphysical flow patterns, which is demonstrated for the AWAKEN field campaign. The developed pipeline enables the first systematic application of radar-measured wind fields to investigate wakes that extend over 10 km using over one year of continuous observational data with engineering wake simulation at a two-wind-farm scale, a scale and duration only made possible by robust quality control procedures. Analysis of 82,516 individual radar scans over 12 months reveals that external factors such as precipitation, season and diurnal trends critically influence radar data quality. Using the high-quality cases identified by the pipeline, we validate TurbOPark and Bastankhah2016 engineering wake models against radar-derived wind fields and characterize wake evolution across different atmospheric stability regimes. Results demonstrate that atmospheric stability exerts substantial control on inter-farm wake interactions: stable conditions produce persistent velocity deficits (5–6% at 52.5D downstream) with severe power losses in downstream turbines (up to 76%), while neutral conditions enable faster wake recovery and improved downstream performance.

The work in [1] has established a practical methodology for extracting reliable wind field observations from dual-Doppler radar systems and demonstrated their value for generating wake model validation datasets and improving wind farm performance prediction under diverse atmospheric conditions. In a next step, we are going to apply the framework to an offshore wind farm dataset similar to the one described on [2]. For this contribution, we discuss the emerging opportunity not just with regard to studying the complex wake deficit patterns of large wind farms but also the increase in turbulence within and around them.

References

[1] Zheng Q., Hung L., Jordan A., and Gottschall J., 2026, An Extensive Framework for Preparing Dual-Doppler Radar Measurements for Wake Model Validation: Application to the AWAKEN Large-scale Field Experiment, *Journal of Renewable and Sustainable Energy (JRSE)* (submitted)

[2] Nygaard N. G. and Newcombe A. C., 2018, Wake behind an offshore wind farm observed with dual-Doppler radars, *IOP Conf. Series: Journal of Physics: Conf. Series* 1037; doi :10.1088/1742-6596/1037/7/072008

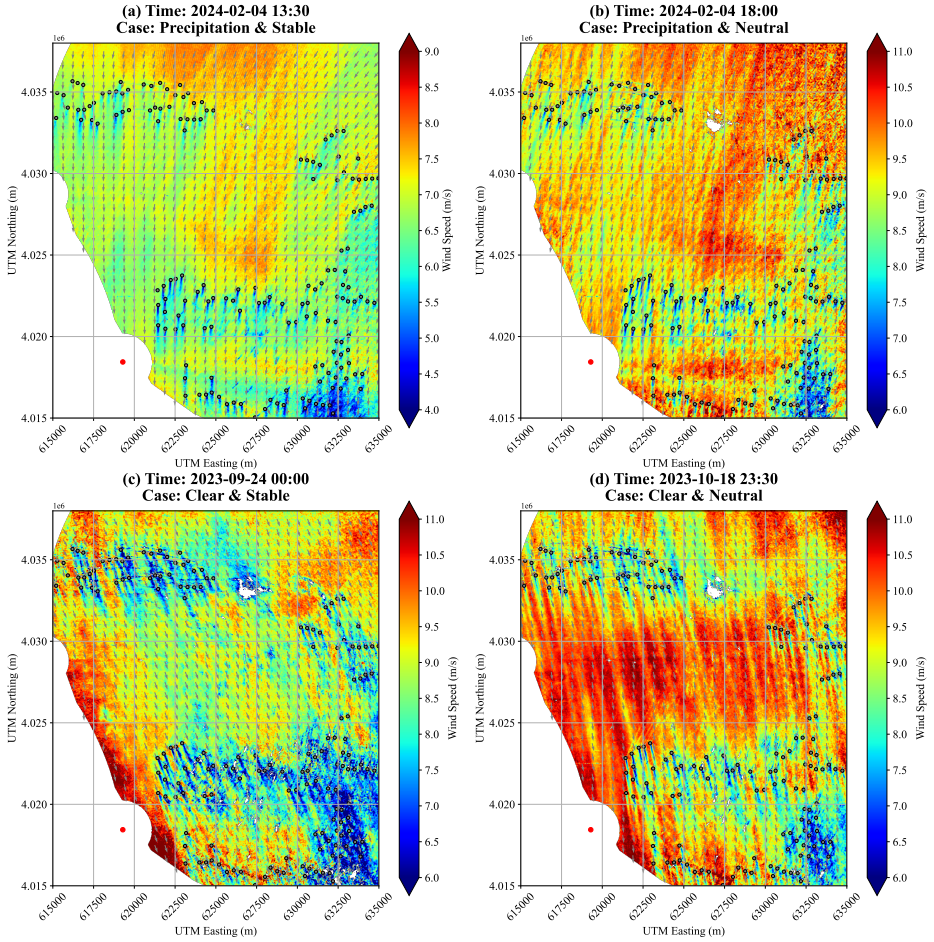

Figure 1: *Radar-measured wind speed fields at hub height for four selected atmospheric cases.* Arrows indicate the wind direction; turbines are represented as gray circles with a black edge. The four cases represent different atmospheric and precipitation conditions: (a) precipitation with stable stratification, (b) precipitation with neutral stratification, (c) clear skies with stable stratification, and (d) clear skies with neutral stratification [1].

Offshore wind farms in a turbulent atmosphere - when models meet reality

Nicolai Gayle Nygaard [1]

[1] Ørsted, Fredericia, Denmark

email-address of the corresponding author: ©nicny@orsted.com

Abstract:
The global buildout of offshore wind energy now approaches 90 GW of installed capacity worldwide. This remarkable growth has been enabled not only by huge advances in turbines technology, but also by the widespread use of engineering models that describe the atmospheric boundary layer and the complex flow interactions within and between wind farms, including wake and blockage effects.

Despite their relative simplicity, these models have provided bankable energy yield assessments and risk estimates robust enough to underpin investments of hundreds of billions of dollars. While idealized by design and subject to known limitations, such engineering models have demonstrated notable resilience. As deployment of offshore wind energy has expanded with larger turbines and wind farm clusters, and new climatic regimes, model shortcomings exposed by field data have driven iterative refinement rather than obsolescence. Their continued evolution illustrates how simplified, physically grounded representations of atmospheric flow can successfully guide investment decisions.

In this presentation, I present examples comparing engineering model predictions with observations from offshore wind farms. The models span a wide range of scales: from detailed representations of atmospheric profiles that influence the power performance of an individual turbine rotor, to wake interactions within wind farms, and ultimately to wakes between wind farms separated by tens of kilometers. These interactions can extend beyond the farms themselves, as atmospheric back-action modifies the surrounding boundary layer flow, including the generation of gravity waves that feed back on wind farm performance.

The examples highlight both the strengths of current best-practice modeling approaches and their limitations when confronted with real-world data. Together, they help chart a path toward the next generation of models, developed through close collaboration between industry and academia. I will argue that delivering unbiased, low-uncertainty energy yield estimates in the future will require the adoption of a quasi-dynamic modeling framework that accounts for the evolving atmospheric state and its two-way interaction with turbines and wind farms.

Simulation and modelling of wind-farm blockage

Johan Meyers [1]

[1] Department of Mechanical Engineering, KU Leuven, Leuven, Belgium

email-address of the corresponding author: johan.meyers@kuleuven.be

Abstract:

With the construction of large wind farms with high power densities in recent years, wind-farm blockage has become a major concern for developers. In the current talk, the physics of wind-farm blockage is discussed, highlighting the importance of hydrostatic blockage associated with the stratification of the free atmosphere. Large-eddy simulations are used to explore the relevant parameter space, focusing both on detrimental effects of blockage related to an unfavorable pressure gradient and flow slow-down in front of the farm, and beneficial effects related to favorable pressure gradients in the farm. In a second part of the talk, the development of fast methods that enrich classical wake models with a blockage correction is presented. We discuss the open-source package WAYVE that has been developed to that end, including recent extensions that allow for significant speed-ups by exploiting ideas from two-scale momentum theory.

Exploring the potential and limits of wake mixing

S. Tamaro, D. Bortolin, F.V. Mühle, F. Campagnolo and C.L. Bottasso

Wind Energy Institute, Technical University of Munich, 85748 Garching b. München, Germany

email-adress of the corresponding author: carlo.bottasso@tum.de

Abstract:
Wake mixing has recently gained significant attention in the recent literature. It includes passive approaches – based on modifying the design of the rotor – and active strategies where the rotor is commanded to inject perturbations in the wake, in both cases with the goal of enhancing wake recovery and benefit downstream turbines. Early studies ([1]) have shown that the effectiveness of wake mixing can – under particular conditions – rival that of the well-established wake steering approach ([2]), thereby sparking considerable interest in the research community. However, wake mixing typically leads to increased fatigue loading ([3]) and a consequent reduction in turbine lifetime, effects that must be carefully balanced against the potential power benefits.
In this work, we present a summary and outlook of the research activities conducted by the Wind Energy Institute at the Technical University of Munich on wake mixing. We consider one passive approach – rotor asymmetry – and two active ones: the helix and dynamic yaw (DY).

Rotor asymmetry: Asymmetric rotors feature one or more blades that are different from the others. The goal of this approach is to perturb the equilibrium of the blade tip vortices in the near wake of the turbine ([4]), to ultimately accelerate its recovery. Recently, we performed a study ([5]) that featured one blade with a 6% increase in blade length and showed an anticipated onset of the leapfrogging instability of the tip vortices, both experimentally and numerically. Figure 1 presents a visualization of the tip vortices in the wind tunnel for the symmetric and asymmetric rotors, obtained by phase-locking velocity measurements with the rotor azimuth angle. The modified interaction of the tip vortices, however, did not result in a faster wake recovery in the far wake, which – on the contrary – was seen to recover at a slower rate than for the symmetric rotor.

The helix: The helix approach is a particular type of individual pitch control, where the pitch of each blade follows a sinusoidal motion with a constant phase offset among blades, resulting in a characteristic helical shape of the wake ([6]). We have performed experimental and numerical work on the helix ([3]), where the effectiveness of the helix was generally higher than that of DY. However, the helix was outperformed by wake steering in almost all scenarios considered. The combination of wake steering and the helix was also examined in a dedicated wind tunnel campaign. Time-resolved particle tracking velocimetry was used to measure the near-wake of a rotor under simultaneous wake mixing and yaw misalignment. Figure 2 presents a visualization of the tip vortices in the near wake. Overall, the combined control strategy was found to be less effective than either technique applied individually, resulting in no net power benefit.

Dynamic yaw: DY consists of enforcing a periodic lateral meandering of the wake by varying the nacelle yaw angle in a sinusoidal fashion. We have presented wind tunnel testing and numerical validation of this method in [3], where the effectiveness of DY was characterized in terms of the actuation frequency and amplitude, as well as of the inflow turbulence level. Recently, a new study by [7] has expanded on this work by applying DY to three aligned rotors, demonstrating the existence of an optimal actuation phase difference that ultimately amplifies the lateral meandering of the wake.
The investigated wake-mixing strategies show that both passive and active perturbations affect the wake through different mechanisms, with particularly noticeable effects in the near-wake region. Among the considered approaches, the helix appears the most promising. However, for all techniques, power gains approach wake steering only under very limited conditions, namely low ambient turbulence and near-full waking. When accounting for the additional structural loading imposed on the driving turbine and the practical complexities associated with implementation on commercial machines, the results suggest that current wake-mixing approaches are unlikely to provide a broadly applicable alternative to wake steering. While these strategies remain highly relevant for advancing the understanding of wake physics, a genuine breakthrough in wake mixing still appears elusive.

References

[1] Taschner E., Becker M., Verzijlbergh R. and van Wingerden J.-W., (2024), Comparison of helix and wake steering control for varying turbine spacing and wind direction, *Journal of Physics: Conference Series, vol. 2767, pp. 032-023*

[2] Fleming P., Gebraad P., Lee S., van Wingerden J.-W., Johnson K., Churchfield M., Michalakes J., Spalart P., and Moriarty P., (2014), Evaluating techniques for redirecting turbine wakes using SOWFA, *Renewable Energy, vol. 70, pp. 211-218*

[3] Bortolin D., Tamaro S., Campagnolo F., Mühle F.V., Manolesos M., Croce C., and Bottasso C.L., (2026), An experimental investigation on wake mixing and steering techniques, *Journal of Physics: Conference Series (under review)*

[4] Lignarolo L.E.M., Ragni, D., Scarano, F., Simão Ferreira C.J. and van Bussel G.J.W., (2015), Tip-vortex instability and turbulent mixing in wind-turbine wakes, *Journal of Fluid Mechanics, vol. 781*

[5] Tamaro S., Stegmüller J., Bortolin D., Campagnolo F., Mühle F.V., Breitsamter C., and Bottasso C.L., (2026), Experimental and numerical characterization of blade tip vortices for an asymmetric rotor, *Journal of Physics: Conference Series (under review)*

[6] Frederik J., (2021): *Pitch control for wind turbine load mitigation and enhanced wake mixing: A simulation and experimental validation study*, TU Delft Repository

[7] Mühle F.V., Tamaro S., Bortolin D., Campagnolo F. and Bottasso C.L., (2026), Wake mixing wind farm control with synchronized dynamic yaw for power optimization, *Journal of Physics: Conference Series (under review)*

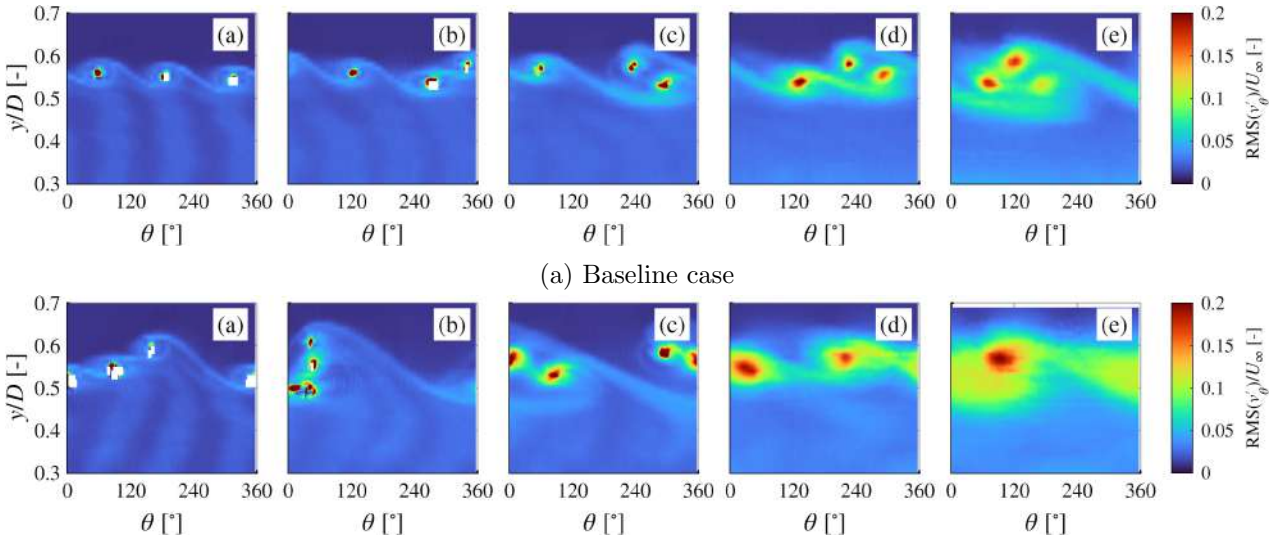

(a) Baseline case

(b) Asymmetric case

Figure 1: *Rotor asymmetry: root mean square of the lateral velocity fluctuations, phase locked with the rotor azimuth. Measurements are acquired at hub height at the downstream distances of $x/D = 0.5$ (a), $x/D = 0.75$ (b), $x/D = 1$ (c), $x/D = 1.5$ (d), $x/D = 2$ (e). White areas in the plot indicate a lack of data due to large inflow angles.*

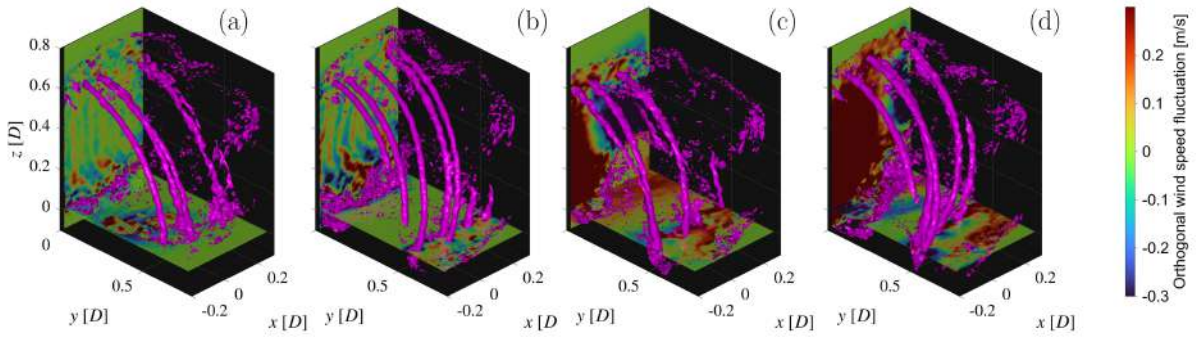

Figure 2: *Instantaneous iso-vorticity surfaces (magenta), and wind velocity fluctuation on vertical and horizontal planes from particle tracking velocimetry experiments in four control scenarios: baseline (a), static yaw (b), helix (c), helix and static yaw (d). The hub is located at $x, y, z = (-0.77D, 0, 0)$.*

Dynamic wind farm flow and cluster wake control

Jan-Willem van Wingerden [1]

[1] DCSC, Delft University of Technology, Delft, The Netherlands

email-address of the corresponding author: j.w.vanwingerden@tudelft.nl

Abstract:
This presentation addresses our current research in dynamic wind farm flow control and cluster wake control: enabling wind turbines to actively cooperate in order to maximize collective performance (energy yield and loads). Conventional wind farm control approaches, such as wake steering, have demonstrated that deliberate manipulation of turbine orientation can mitigate wake losses and increase overall power production [3]. However, these strategies largely rely on quasi-static models and optimization and do not fully exploit the dynamic nature of the problem at hand. The central theme of this talk is that a big step forward lies in dynamically controlling wake and cluster wake interactions.

A key innovation discussed is the Helix concept [1], a novel flow control technology designed to actively mix the wake behind a single turbine. By enhancing wake mixing, the Helix approach shortens and weakens downstream wake deficits, thereby reducing their adverse impact on neighboring turbines. Experimental [5] and modeling results [4] indicate that this targeted manipulation of the flow can significantly improve energy capture at the wind farm level. Beyond demonstrating its individual effectiveness, the Helix concept serves as a foundation for more advanced control paradigms that extend from single-turbine optimization to coordinated, farm-wide strategies using synchronization [6]. Inspired by the Helix, the presentation introduces the concept of dynamic cluster wake control [2]. In this framework, the ideas behind the Helix are extend to the cluster wake problem.

Despite promising advances, wind farm flow control remains at an early stage relative to its theoretical and practical potential. Significant research challenges persist, particularly in designing robust, scalable control architectures capable of handling time-varying environmental conditions and complex turbine interactions. Addressing these challenges is essential for reducing the cost of valued energy and enhancing the competitiveness of wind power. The integration of dynamic control methods—most notably the combination of the Helix approach with established wake steering techniques—offers a compelling pathway forward, paving the way toward fully cooperative and adaptive wind farms.

References

[1] Joeri A Frederik, Bart M Doekemeijer, Sebastiaan P Mulders, and Jan-Willem van Wingerden. The helix approach: Using dynamic individual pitch control to enhance wake mixing in wind farms. *Wind energy*, 23(8):1739–1751, 2020.

[2] Jonas Gutknecht, Emanuel Taschner, Marcus Becker, Axelle Viré, and Jan-Willem van Wingerden. Mitigating cluster wake induced power losses at neighboring wind farms through cluster-wide coordinated control. 2025.

[3] Johan Meyers, Carlo Bottasso, Katherine Dykes, Paul Fleming, Pieter Gebraad, Gregor Giebel, Tuhfe Göçmen, and Jan-Willem Van Wingerden. Wind farm flow control: prospects and challenges. *Wind Energy Science Discussions*, 2022:1–56, 2022.

[4] Emanuel Taschner, Aemilius AW van Vondelen, Remco Verzijlbergh, and Jan-Willem van Wingerden. On the performance of the helix wind farm control approach in the conventionally neutral atmospheric boundary layer. In *Journal of physics: conference series*, volume 2505, page 012006. IOP Publishing, 2023.

[5] Daan Van der Hoek, Bert Van den Abbeele, Carlos Simao Ferreira, and Jan-Willem van Wingerden. Maximizing wind farm power output with the helix approach: Experimental validation and wake analysis using tomographic particle image velocimetry. *Wind Energy*, 27(5):463–482, 2024.

[6] AAW Van Vondelen, DC Van Der Hoek, ST Navalkar, and JW Van Wingerden. Synchronized dynamic induction control: An experimental investigation. In *Journal of physics: conference series*, volume 2767, page 032027. IOP Publishing, 2024.

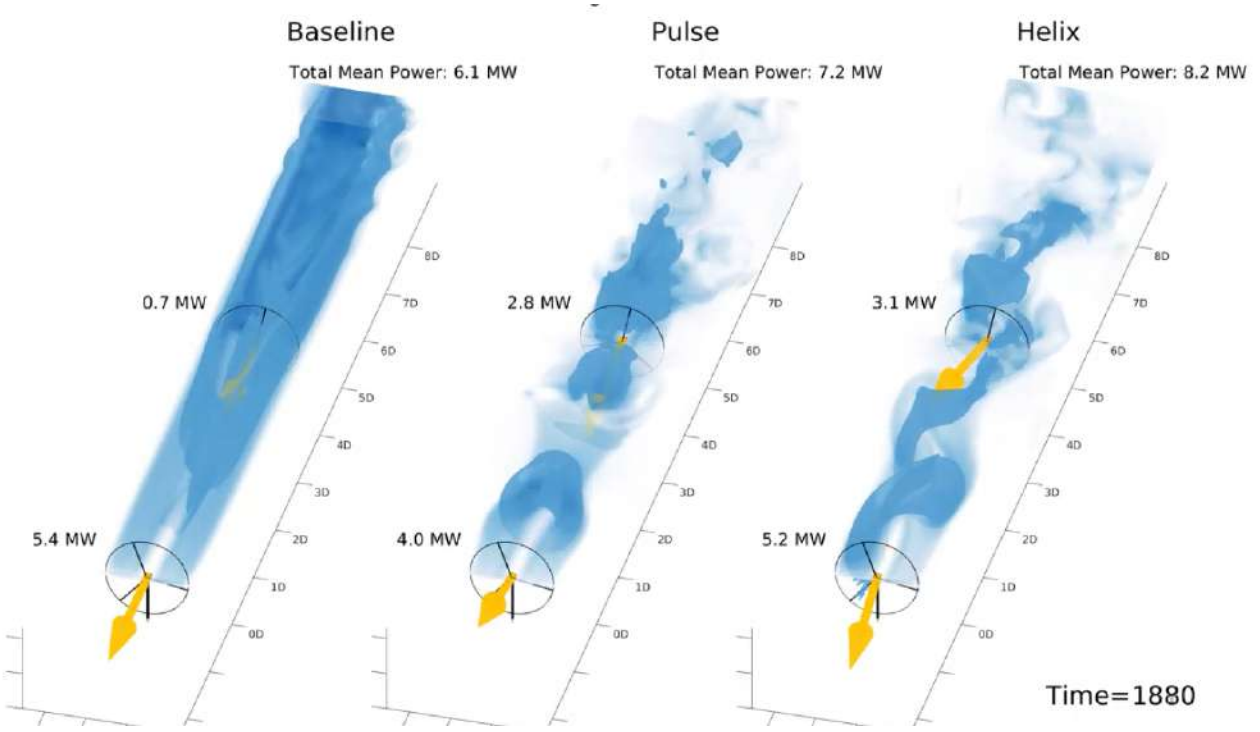

Figure 1: *Simulation result of the Helix [1]*

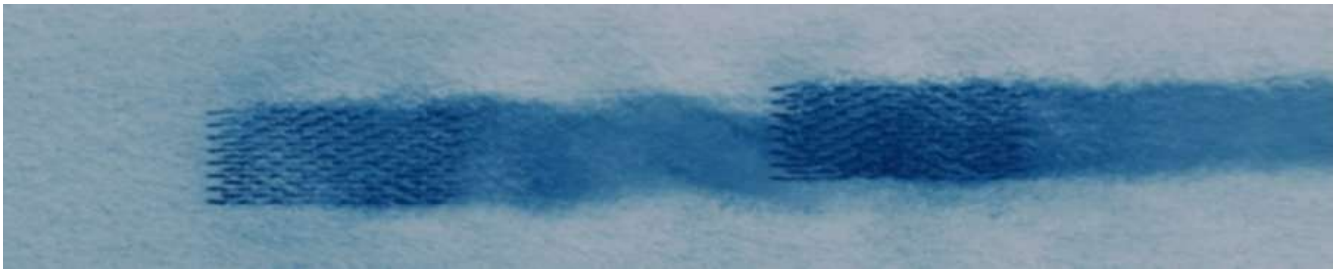

Figure 2: *Simulation result of active cluster wake mixing [2]*

Reinforcement Learning for Real-Time Closed-Loop Collaborative Wind Farm Control and Power Optimisation

S. Laizet [1], A. Mole[1], M. Weissenbacher[1] and G. Rigas[1]

[1] Department of Aeronautics, Imperial College London, UK

email-address of the corresponding author: s.laizet@imperial.ac.uk

Abstract:

Maximising the energy output of existing wind farms through wind farm control is a key strategy to enhance the efficiency of renewable energy systems. Modern large–scale offshore wind farms consist of multiple turbines grouped together, usually in well-structured formations. Wind turbines are typically operated with a greedy strategy, optimising their individual power generation whilst ignoring the effect on other wind turbines. This leads to individual wind turbines often operating in suboptimal conditions due to aerodynamic interactions between the wind turbines, resulting in a reduction in total power output. Instead, by implementing a collective wind farm control approach that accounts for aerodynamic interactions between turbines, wake effects can be mitigated, leading to improved wind farm efficiency.

Control strategies for wind farms fall broadly into two categories: *static* (or *quasi-static*), where fixed optimal parameters are obtained for given conditions, and *dynamic*, where parameters change as a function of time. Dynamic wind farm control can be further divided into *open-loop control*, where control strategies follow a predetermined dynamic behaviour, and *closed-loop control*, where the controller senses and actively responds to changing flow conditions.

In this work, we present a reinforcement learning (RL) controller trained within a high-fidelity large-eddy simulation (LES) environment that fully resolves atmospheric turbulence. Unlike static controllers that respond only to mean wind conditions, our approach learns collaborative dynamic control strategies that adapt in real time to the continuously evolving turbulent flow field. The LES are performed with the wind farm simulator Winc3d [1], which is part of the framework Xcompact3d, dedicated to the study of turbulent flows on supercomputers. In this work a Soft Actor Critic (SAC) implementation for the RL algorithm is used, based on the PyTorch machine learning library. The LES solver and the RL controller components are coupled through the SmartSim library. The static control approach used as a reference is based on a Bayesian Optimisation (BO) strategy using BoTorch.

We evaluate the performance of the RL controller in a three-turbine test case, where it achieves a 4.30% increase in total wind farm power output relative to the greedy operation of the baseline (95% CI: [4.10%, 4.49%]). This nearly doubles the 2.19% gain delivered by static optimal yaw control based on the BO approach (95% CI: [1.98%, 2.39%]), and substantially outperforms the 2.67% gain (95% CI: [2.47%, 2.87%]) achieved by a dynamic controller based on global wind direction, optimised via BO [2].

An overview of our control framework can be seen in Figure 1. The progress of RL training is also shown in this figure, with the RL control initially reducing farm power output, including two pronounced troughs below –20%, as the agent explores the policy space driven by the regularisation of the objective entropy. The optimisation progress from the static BO approach initially exhibits substantial fluctuations with peaks below −30% farm power, reflecting the exploration as BO samples broadly across the parameter space.

The performance gap between our RL controller and these baselines demonstrates that learning directly from turbulence-resolved simulations enables the discovery of richer, flow-responsive control strategies that static or low-fidelity approaches cannot access.

References

[1] Deskos, G., Laizet, S., & Palacios, R. (2020), WInc3D: A novel framework for turbulence-resolving simulations of wind farm wake interactions, *Wind Energy*.

[2] Mole, A., Weissenbacher, M., Rigas, G., & Laizet, S. (2026), Reinforcement learning increases wind farm power production by enabling closed-loop collaborative control, *Communications Engineering*.

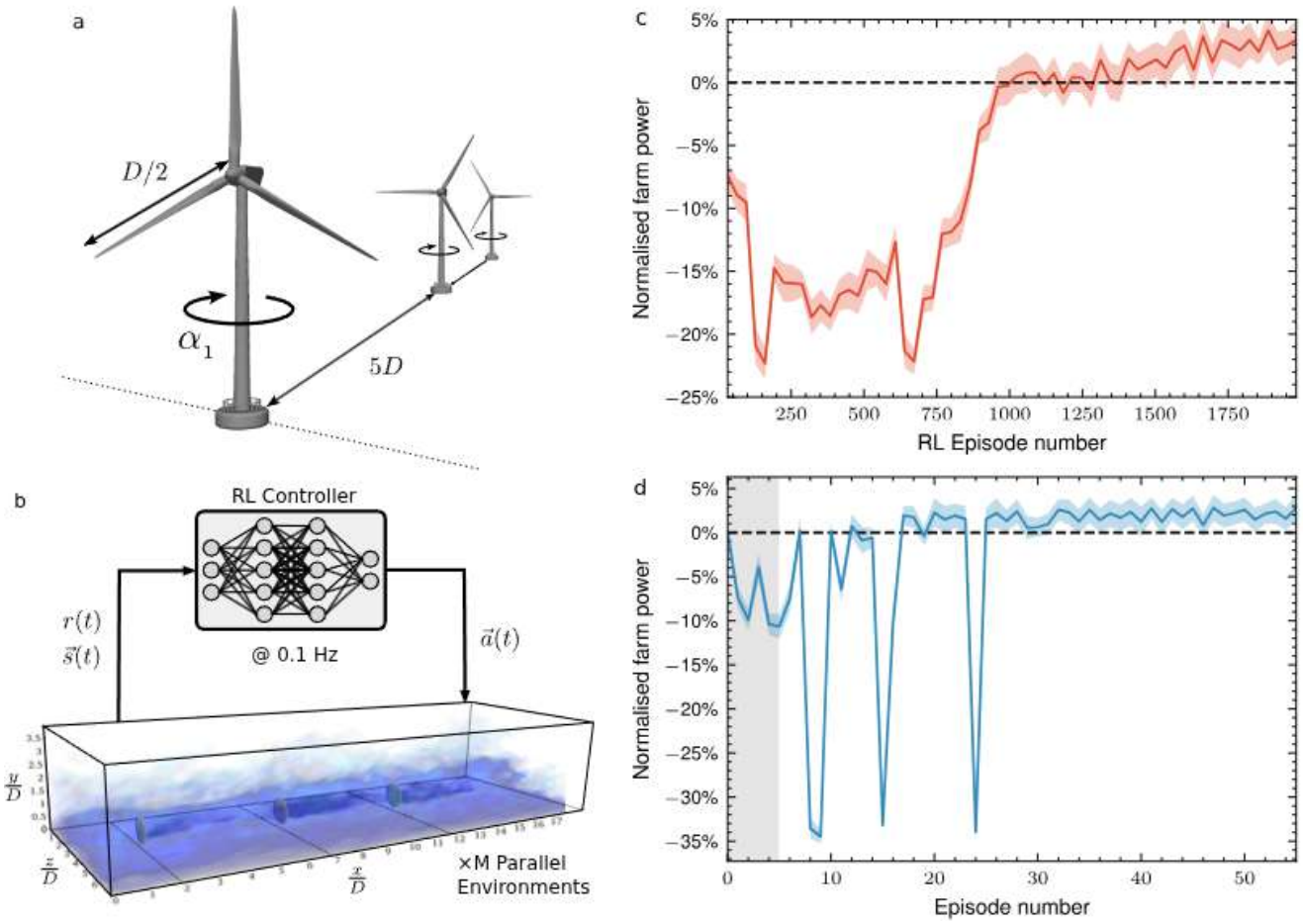

Figure 1: *(a)*: Schematic of the simulated wind farm. Three in-line turbines with diameter $D = 126m$ in an atmospheric boundary layer are simulated using a high-fidelity 3D-LES solver. The turbines are aligned along the direction of the flow and the yaw angle is dynamically adjusted. *(b)*: Schematic of the RL control loop. The controller receives velocity sensor observations from $M = 32$ LES environments and determines the yaw angles of three in-line turbines. Angles are updated by the controller every $10s$ of simulated time. *(c)*: Mean farm power during RL training relative to the greedy baseline with 95% CI computed over $n = 32$ training environments as a function of episode number. *(d)*: Mean relative farm power with 95% CI computed over $n = 32$ training environments during Bayesian optimization to find optimal static yaw angles.

Toward Predictive Offshore Wind Farm Simulations

Fotis Sotiropoulos [1], Christian Santoni [2], Tor Viren [3], Lian Shen [3], Hossein Seyedzadeh [4], and Ali Khosronejad [4]

[1] Department of Mechanical Engineering, The Pennsylvania State University, University Park, PA, USA
[2] Department of Mechanical Engineering, North Carolina A&T State University, Greensboro, NC, USA
[3] Department of Mechanical Engineering and St. Anthony Falls Laboratory, University of Minnesota, Minneapolis, MN, USA
[4] Department of Civil Engineering, Stony Brook University, Stony Brook, NY, USA

email-adress of the corresponding authour: fotis@psu.edu

Abstract:
Accurate prediction of wake dynamics and power production in offshore wind farms remains a central challenge for wind farm design, optimization, and control—particularly under realistic marine atmospheric boundary layer conditions where wind–wave interactions play a critical role [2]. Over the past fifteen years, our group has developed and systematically validated a suite of high-fidelity large-eddy simulation (LES) tools that enable predictive, physics-based modeling of utility-scale wind farms under realistic atmospheric and oceanic forcing. This contribution presents the culmination of this effort through LES of a full-scale offshore wind farm incorporating advanced wave-aware sea-surface boundary conditions and rigorous validation against field measurements.

We report large-eddy simulations of a 111-turbine utility-scale offshore wind farm (fig. 1) operating under neutral atmospheric conditions, using actuator-line and actuator-surface representations for turbine blades and nacelles, respectively [3]. Two classes of sea-surface boundary conditions are examined: (i) a conventional wave-phase-averaged approach based on roughness-length parameterization, and (ii) a wave-phase-aware formulation in which ocean-wave kinematics are obtained from a high-order spectral wave model and coupled to the atmospheric flow through dynamically varying shear stresses at the sea surface (fig. 2). The latter approach accounts for the relative motion between wind and waves without resorting to surface-resolving grids [1]. The wave-phase-aware simulations exhibit enhanced wake recovery and increased downward transport of mean kinetic energy into turbine wakes. These flow differences lead to substantially improved power predictions. Validation against LiDAR and SCADA data shows that the wave-phase-aware LES predicts turbine power with relative errors of approximately 3-10% across the wind farm, compared to 10-20% for the wave-phase-averaged approach. This level of agreement at full wind-farm scale demonstrates that modern LES frameworks, when equipped with physically consistent boundary conditions, can serve as predictive tools rather than purely diagnostic ones.

We conclude by outlining how such validated LES databases enable the development of hybrid LES–AI reduced-order models for offshore wind farm design, optimization, and control. By fusing first-principles simulations with machine learning, these approaches promise rapid design-space exploration and real-time decision-making. decision-making while retaining a firm physical foundation.

References

[1] Santoni, C., Viren, T., Shen, L., Sotiropoulos, F., and Khosronejad, A. (2025), Large-eddy simulations of a utility-scale offshore wind farm under neutral atmospheric conditions, *Physical Review Fluids*, 10(5):054801.

[2] Zhang, Z., Hao, X., Santoni, C., Shen, L., Sotiropoulos, F., and Khosronejad, A. (2023), Toward prediction of turbulent atmospheric flows over propagating oceanic waves via machine-learning augmented large-eddy simulation, *Ocean Engineering*, 280:114759.

[3] Santoni, C., Sotiropoulos, F., and Khosronejad, A. (2024), A comparative analysis of actuator-based turbine structure parametrizations for high-fidelity modeling of utility-scale wind turbines under neutral atmospheric conditions, *Energies*, 17(3):753.

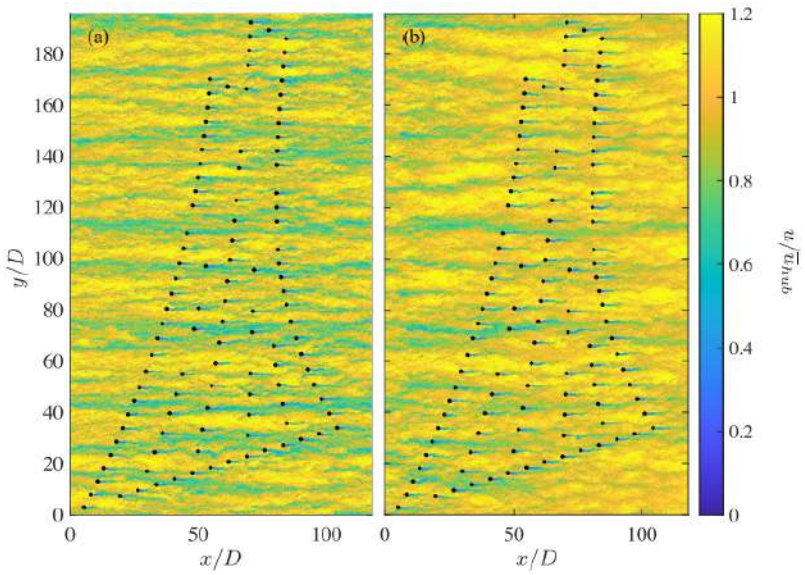

Figure 1: *Instantaneous streamwise velocity fields, u/u_{hub}, on the hub-height plane for the (a) wave-phase-averaged and (b) wave-phase-aware sea-surface boundary conditions. Wind flows from left to right, and turbine positions are marked by black circles. These visualizations highlight the influence of surface boundary-layer treatments on wake structure and downstream flow organization [1].*

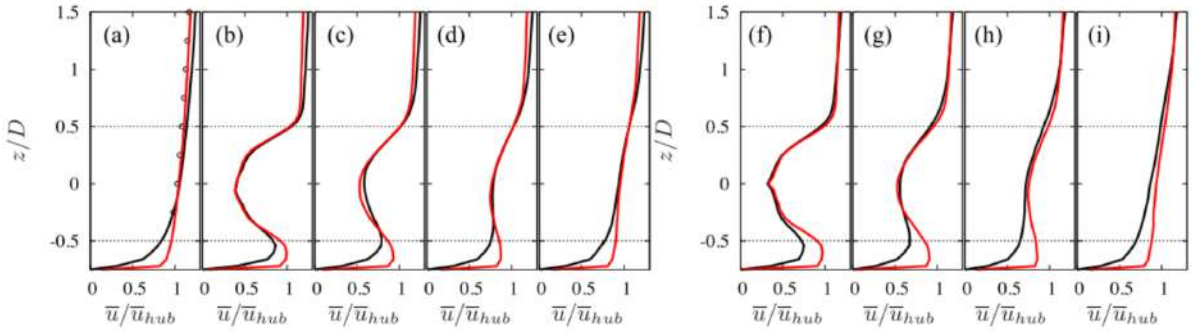

Figure 2: *Vertical profiles of normalized mean streamwise velocity $\overline{u}/\overline{u}_{hub}$ at downstream locations of $-1D$, $1D$, $3D$, $5D$, and $10D$ behind turbine $T01$ (panels a–e), and at $1D$, $3D$, $5D$, and $10D$ downstream of turbine $T02$ (panels f–i). Results compare the wave-phase-averaged (———) and wave-phase-aware (———) boundary treatments, alongside LiDAR measurements (○). The dashed horizontal markers indicate the rotor-swept region. These comparisons illustrate how incorporating wave-resolved sea-surface dynamics modifies wake structure and improves agreement with observations [1].*

Numerical analysis of the ocean circulation induced by off-shore wind farms

S. Leonardi [1], M. A Guzmán Hernández[1], M. Della Monica[2] and M. Bernardini [2]

[1] Department of Mechanical Engineering, The University of Texas at Dallas, Richardson, Texas, USA
[2] Dipartimento di Ingegneria Meccanica, Universitá di Roma "La Sapienza"

email-address of the corresponding author: stefano.leonardi@utdallas.edu

Abstract:
By 2050, it is projected that wind capacity will quadruple to over 400 GW in the United States. Much of this increase will mostly come from offshore wind energy. Although some isolated turbines may not significantly affect ocean circulation and the atmosphere, the effect due to a major deployment of wind turbines on local to regional physical processes of the ocean is for the most part still unknown. To assess the influence of wind farms on the secondary motion in the ocean we have developed a one-way numerical coupling of our in-house code UTD-WF solver,used to model the atmospheric boundary layer and the wind turbines, and FVCOM (Finite Volume Community Ocean Model) used to model the ocean domain.

A wind farm composed of 8 NREL 5 MW reference turbines, arranged in 4 rows and 2 columns, is considered (Fig.1). The turbines are equally spaced by $5D$ and $3D$ in the streamwise and spanwise directions, respectively. The turbines have a rotor diameter of $D = 126$ m, a rated wind speed of $U_{rated} = U_{ref} = 11.4$ m s^{-1}, and a rated power of $P_{rated} = 5$ MW. The angular velocity is determined according to the rotor dynamics and controlled using a standard region II control law to maximize the power capture (Bernardoni *et al.* [1]). The first row of turbines is placed at $x = 7D$ to allow for the development of the incoming flow and avoid reflection of pressure waves at the inlet (Santoni *et al.* [2]).

Color contours of time-averaged velocity components in horizontal sections above and below the sea level, and cross sections in the ocean are shown in Fig.1. The flow patterns in the streamwise direction in the ocean are consistent to those in the atmosphere. The velocity and shear stress on the ocean around the tower is larger due to the blockage. The towers also induce a spanwise motion that propagates far downstream due to the larger inertia of the ocean as opposed to the atmosphere. Due to the mixing and wake recovery promoted by turbulence, the velocity gradients between the wake region and the surrounding flow are smeared and not sharp as in the case of uniform incoming flow (not shown here for lack of space). The wake region and the gradients of velocities in spanwise direction induce upwelling and downwelling across the ocean depth, as shown in Fig.1(g-k). However, as the wake entrains and expands after the third row of wind turbines, there is a transition region where the wake dominates and this leads to a decreased wind stress at the sea surface. The spanwise variation (or convergence) generates a downwelling, or negative vertical $\overline{U}_y$ region behind the turbine tower, and a reversed direction of circulation.

References

[1] Bernardoni F, Ciri U, Rotea M A and Leonardi S 2021 *Journal of Renewable and Sustainable Energy* **13** 043301 ISSN 1941-7012 URL https://pubs.aip.org/jrse/article/13/4/043301/364088/Identification-of-wind-turbine-clusters-for

[2] Santoni C, García-Cartagena E J, Ciri U, Zhan L, Valerio Iungo G and Leonardi S 2020 *Wind Energy* **23** 691–710 ISSN 1095-4244, 1099-1824 URL https://onlinelibrary.wiley.com/doi/10.1002/we.2452

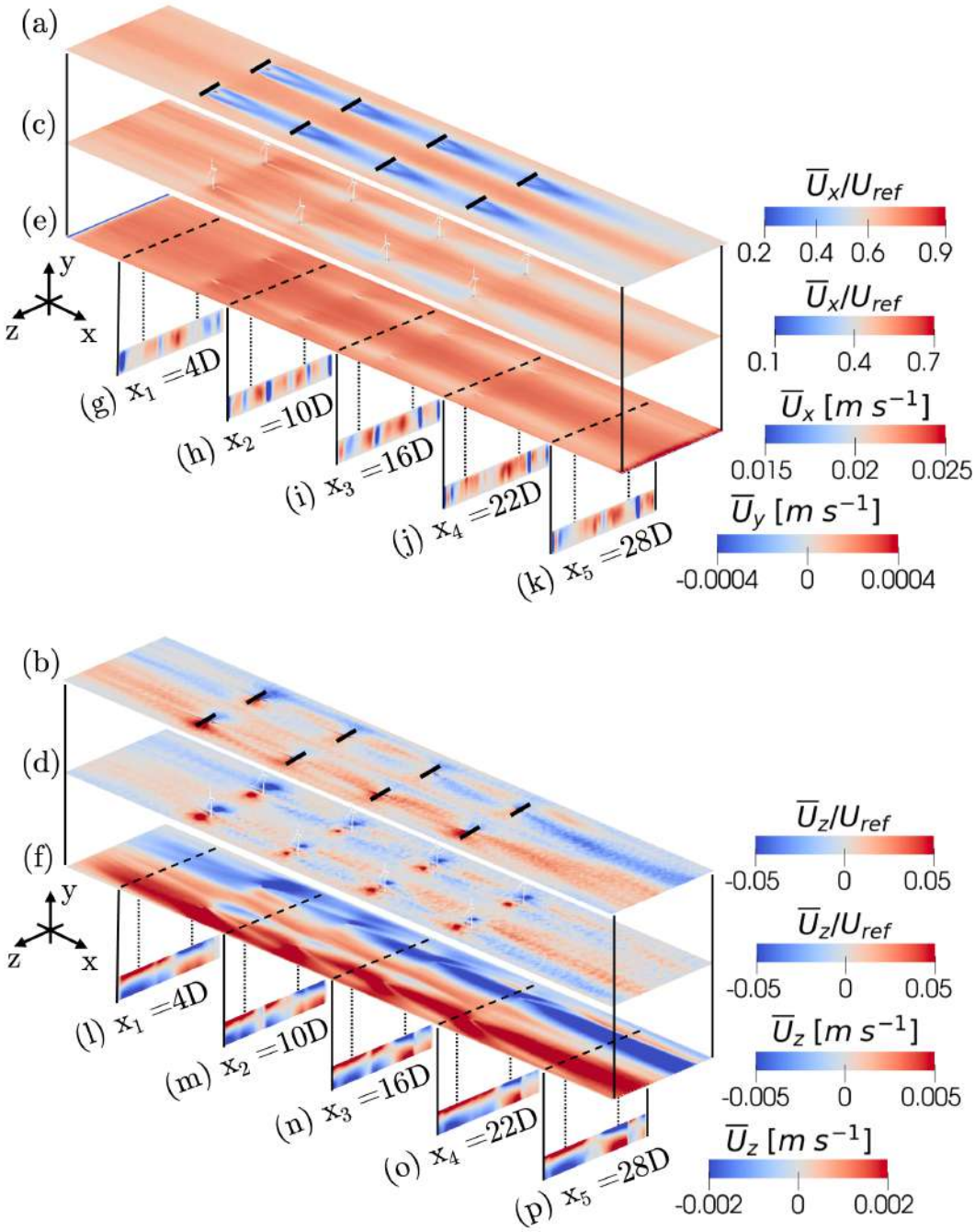

Figure 1: *Color contours of time-averaged: (a) streamwise velocity* $\overline{U}_{hub,x}/U_{ref}$ *and (b) spanwise velocity* $\overline{U}_{hub,z}/U_{ref}$ *at* $y_{hub} = 90$ *m, (c) streamwise velocity* $\overline{U}_{10,x}/U_{ref}$ *and (d) spanwise velocity* $\overline{U}_{10,z}/U_{ref}$ *at* $y_{10} = 10$ *m; (e) streamwise velocity* $\overline{U}_{0,x}$ *and (f) spanwise velocity* $\overline{U}_{0,z}$ *at* $y_0 = -0.7$ *m; (g-k) vertical velocity* $\overline{U}_y$ *and (l-p) spanwise velocity* $\overline{U}_z$ *at* x_i*. The black lines indicate turbine rotors.*

Predictions of the Underwater Acoustic Footprint of Large Offshore Wind Turbines

Esteban Ferrer [1], Laura Botero-Bolívar [2], Martín de Frutos [1], David Huergo[1] and Abbas Ballout [1]

[1] ETSIAE-UPM-School of Aeronautics, Universidad Politécnica de Madrid,
Plaza Cardenal Cisneros 3, E-28040 Madrid, Spain
[2] Mechanical Engineering Department, Universidad Industrial de Santander, Carrera 27 Calle 9, 680001 Bucaramanga, Colombia

email-adress of the corresponding authour: esteban.ferrer@upm.es

Abstract:
The rapid expansion of offshore wind energy has led to the deployment of large wind farms comprising more than 150 turbines [1]. We propose a framework to quantify the aerodynamic noise generated by offshore wind turbines, which is dominated by broadband contributions from leading-edge noise, produced by the interaction of atmospheric turbulence with the blade, and trailing edge noise, generated by the turbulent boundary layer convecting past the blade trailing edge [2]. To compute these sources, the turbine blade is discretized into two-dimensional airfoil segments and modeled using blade element momentum theory coupled with Amiet's formulation, including corrections for finite-chord effects [3]. Leading- and trailing-edge contributions are treated as uncorrelated sources and summed along the blade span, with Doppler corrections accounting for blade rotation. The resulting airborne noise is transmitted into the ocean following Snell's law, which restricts effective refraction to a narrow cone of approximately 13° relative to the normal to the sea surface, as illustrated in Fig. 1. A transmission loss of 29.5 dB is applied at the air–water interface, atmospheric attenuation is included in the air, and underwater propagation is modeled using cylindrical spreading, appropriate for shallow-water environments [4]. For wind farms, turbines are assumed to be non-correlated noise sources, resulting in an overall increase of $10\log_{10}(N)$ in the level of underwater noise.

This framework is applied to the offshore wind turbine IEA 22 MW [5], which features a rotor diameter of 284 m and a hub height of 170 m. Operating at a nominal wind speed of 11.78 m/s and a rotational speed of 7.1 rpm, the turbine reaches blade tip speeds exceeding 100 m/s, leading to significant broadband aerodynamic noise, particularly at low frequencies relevant to marine mammal hearing. The predicted far-field spectra for a single turbine and for wind farms of 100 and 150 turbines are shown in Fig. 1, together with the hearing thresholds of low-, mid- and high-frequency cetaceans and pinnipeds [6]. Even a single turbine exceeds the low-frequency hearing threshold, while large wind farms can generate underwater noise levels up to 25 dB above the auditory thresholds of some marine species, indicating a strong potential for acoustic masking.

To address the limitations of semi-analytical approaches and capture the full complexity of offshore wind farm environments, we are developing the open-source high-order solver `HORSES3D` [7, 8]. This discontinuous Galerkin solver supports compressible and incompressible flows, turbulence modeling, and aeroacoustics, and achieves high efficiency through exponential error convergence with polynomial order. Rotating turbine blades are modeled using actuator-line methods or sliding meshes, while complex structures such as towers and platforms are incorporated using immersed boundary techniques [9, 10]. The air–water interface is resolved using a Cahn–Hilliard multiphase formulation capable of accurately transmitting acoustic waves across the interface, as shown in Fig. 1 [11]. The solver is parallelized with MPI, exhibits near-ideal scaling up to 10^4 CPU cores, and has been ported to GPUs, achieving excellent performance on large-scale architectures (e.g., ideal scaling for up to 256 Nvidia H100).

This work provides the first quantitative assessment of the underwater aerodynamic noise footprint of a 22 MW offshore wind turbine and its scaling to large wind farms [12]. The results demonstrate that aerodynamic noise, particularly trailing-edge noise, represents a previously overlooked environmental challenge for offshore wind energy. The ongoing development of `HORSES3D` will enable more accurate predictions of underwater acoustic emissions and support the design of offshore wind farms that are both energy-efficient and environmentally sustainable.

Acknowledgments

This research has received funding from the European Union (ERC, Off-coustics, project number 101086075). Views and opinions expressed are, however, those of the authors only and do not necessarily reflect those of the European Union or the European Research Council. Neither the European Union nor the granting authority can be held responsible for them.

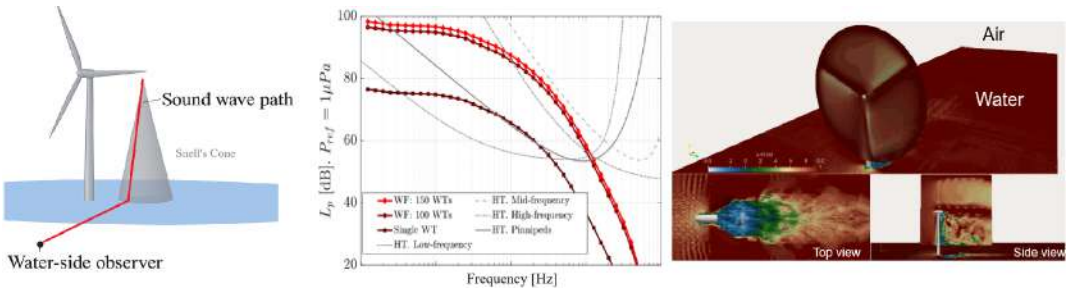

Figure 1: (Left) Sketch of wind turbine with Snell's cone for air and water: cone of 13° angle with respect to the air-water interface normal vector, that encompasses acoustic waves that penetrate underwater. (Middle) IEA 22 MW wind turbine: One-third octave far-field noise spectra for a Water observer (10 m deep) at 100 m downwind of the turbine. Overlaid are hearing threshold of marine animals. WT: wind turbine; WF: wind farm with 100 and 150 WTs; HT: hearing threshold. (Right) Offshore wind turbine simulated with actuator lines and free-surface using a Cahn-Hilliard formulation.

References

[1] Ørsted 2024 Hornsea 1 offshore wind farm https://orsted.co.uk/energy-solutions/offshore-wind/our-wind-farms/hornsea1 accessed: 2024-10-01

[2] Oerlemans S, Sijtsma P and Méndez López B 2007 *Journal of Sound and Vibration* **299** 869–883 ISSN 0022-460X

[3] Amiet R 1976 *Journal of Sound and Vibration* **47** 387–393 ISSN 0022-460X

[4] Hansen C H, Doolan C J and Hansen K L 2017 *John Wiley & Sons*

[5] Zahle F, Barlas A, Lønbæk K, Bortolotti P, Zalkind D, Wang L, Labuschagne C, Sethuraman L and Barter G 2024 *Technical University of Denmark*

[6] Tougaard J 2021 *Journal of Aeroacoustics Society of America* **118** 3154–3163

[7] Ferrer E, Rubio G, Ntoukas G, Laskowski W, Mariño O, Colombo S, Mateo-Gabín A, Marbona H, Manrique de Lara F, Huergo D, Manzanero J, Rueda-Ramírez A, Kopriva D and Valero E 2023 *Computer Physics Communications* **287** 108700 ISSN 0010-4655 URL `https://www.sciencedirect.com/science/article/pii/S0010465523000450`

[8] Botero-Bolívar L, Marino O A, Venner C H, de Santana L D and Ferrer E 2024 *Renewable Energy* **227** 120476 ISSN 0960-1481

[9] Kou J, Joshi S, de Mendoza A H, Puri K, Hirsch C and Ferrer E 2022 *Journal of Computational Physics* **448** 110721 ISSN 0021-9991

[10] Colombo S, Rubio G, Kou J, Valero E, Codina R and Ferrer E 2025 *Journal of Computational Physics* **528** 113807 ISSN 0021-9991

[11] Ballout A, Marino O A, Ntoukas G, Rubio G and Ferrer E 2026 *Journal of Computational Physics* **545** 114478 ISSN 0021-9991 URL `https://www.sciencedirect.com/science/article/pii/S0021999125007600`

[12] Bolívar L B, Sánchez O A M, de Frutos M and Ferrer E 2025 On the prediction of underwater aerodynamic noise of offshore wind turbines (*Preprint* `2501.12404`)

LES of the AWAKEN benchmark wind farm with complex topography, mesoscale atmospheric forcing, and variable thermal stratification

Joshua Brinkerhoff [1], A. Ajay [1], J. Singh [1] and S. Stipa [2]

[1] School of Engineering, University of British Columbia–Okanagan, Kelowna, Canada
[2] Von Kármán Institute for Fluid Dynamics, Sint-Genesius-Rode, Belgium

Address for correspondence: joshua.brinkerhoff@ubc.ca

Abstract:
Onshore wind farm performance is governed by the dynamic interactions of synoptic and mesoscale atmospheric forcing, boundary-layer turbulence, terrain-induced flow heterogeneity, and turbine-scale wake dynamics. Understanding these multiscale interactions remains a major scientific and computational challenge, particularly in thermally-stratified atmospheric boundary layers and topographically complex environments.

Aiming to overcome these limitations, we have developed a multiscale simulation framework for large eddy simulations (LES) of onshore wind farms under realistic ground topography and mesoscale atmospheric variability. All methods are implemented in the open-source LES code TOSCA (Toolbox fOr Stratified Convective Atmospheres), providing a unified and extensible platform for wind energy simulations in complex environments [1]. Complex terrain is modeled using a hybrid wall-modeled immersed boundary method that captures the dominant influence of complex ground topography while maintaining numerical stability and computational efficiency. Mesoscale atmospheric variability is introduced through a profile-assimilation-based coupling strategy using multiresolution analysis with wavelet basis functions and a hybrid geostrophic–wavelet forcing formulation [2], enabling time-varying meteorological forcing and diurnal boundary-layer evolution to be consistently imposed. Turbulence representation on coarse grids is enhanced by developing a mixed subgrid-scale modeling approach combined with higher-order numerical discretization, enabling improved representation of anisotropy and non-equilibrium effects in stratified and terrain-influenced boundary layers.

To demonstrate the utility of the developed framework, we conduct an LES of a realistic wind farm located in King Plains, Oklahoma, USA over an entire diurnal period on August 23-24, 2023, validated against measurements from the American WAKE ExperimeNt (AWAKEN) field campaign [3]. Elevation map of the test site is shown in fig. 1(a). The present framework is unique in its application to wind-farm simulations, as it simultaneously resolves mesoscale atmospheric forcing, diurnal variations in the thermal stratification, terrain-induced spatial flow variations, and wind turbine wake dynamics. Three case scenarios are simulated: (i) flow over hilly terrain with wind turbines; (ii) flow over flat terrain with wind turbines; (iii) flow over hilly terrain without turbines. The instantaneous velocity magnitude corresponding to case (i) is shown in fig. 1(b). The relative effects of diurnal stratification and complex terrain on the turbine wake dynamics and power is investigated via comparison across the three cases. Our results show that during unstable atmospheric conditions, power production experiences limited spatial variability across the farm, while stable conditions produce pronounced spatial and temporal variability in both flow properties and turbine power. Wake velocity deficit under unstable and stable conditions is shown in fig 2. While upstream turbines produce higher power than downstream rows during unstable and transition regimes, under stable conditions downstream turbines outperform the first row despite experiencing stronger wakes. This behavior originates from a dynamic interaction between the complex terrain and a nocturnal low-level-jet, and highlights the benefit of our simulation framework for elucidating the multi-scale physics of onshore wind farms.

References

[1] Stipa S., Ajay A., Allaerts A., and Brinkerhoff J., (2024), TOSCA – an open-source, finite-volume, large-eddy simulation (LES) environment for wind farm flows, *Wind Energy Science, vol. 9, p. 297-320.*

[2] Ajay, A., Singh, J., Stipa, S., Beaucage P., and Brinkerhoff J., (2026), Development of profile assimilation methods for data-driven large eddy simulations, *Boundary-Layer Meteorology, vol. 192, p. 20.*

[3] Moriarty P., Bodini N., Cheung L., Hamilton N., Herges T., Kaul C., Letizia S., Pekpour M., and Simley E., (2023), Overview of recent observations and simulations from the American WAKe ExperimeNt (AWAKEN) field campaign, *Journal of Physics: Conference Series, vol. 2505, p. 012049.*

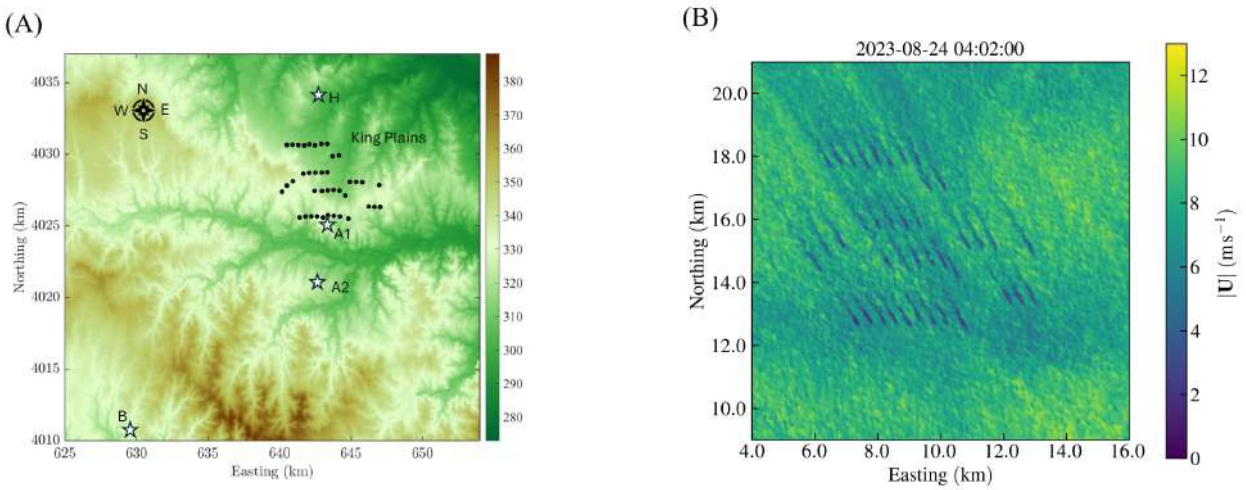

Figure 1: *(a) Elevation map of the simulated site, showing the wind-farm turbines located on the eastern side of the King Plains farm and the field data instrumentation sites. (b) Instantaneous velocity magnitude at the hub-height (89 m) above ground level at UTC 04:02 on Aug. 24, 2023, showing large- and small-scale spatial variations in the flow field.*

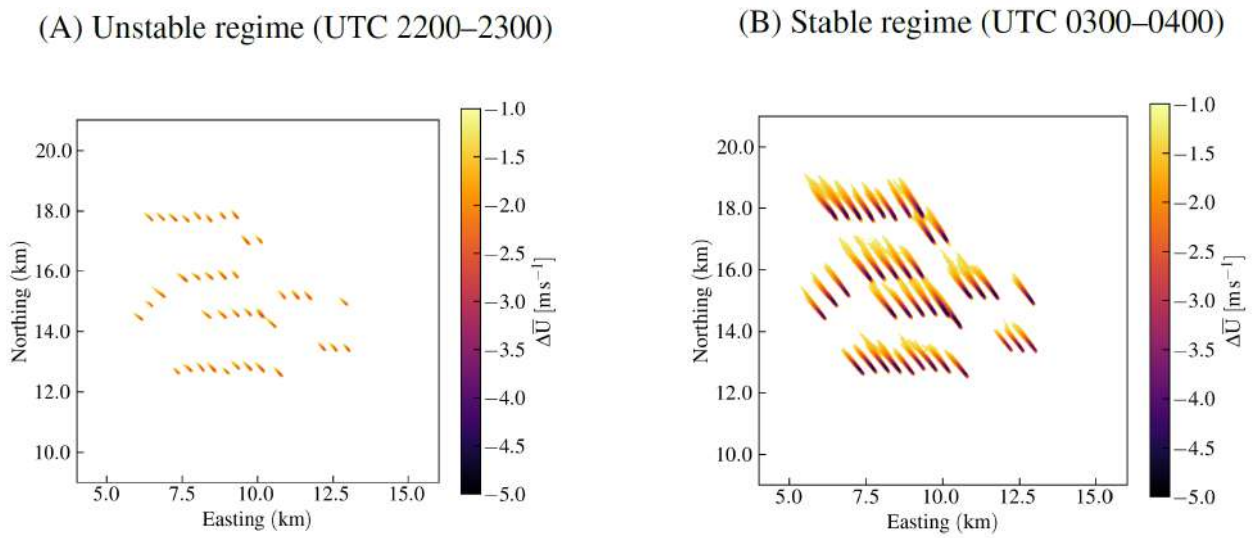

Figure 2: *Time-averaged (over one hour period) hub-height velocity deficit ($\Delta\overline{U}$) due to turbine wakes in (a) unstable and (b) stable conditions.*

Coupled Wave-Atmosphere Effects on the Wake of Offshore Wind Farm Clusters

Sebastiano Stipa [1], Wim Munters [1]

[1] Environmental and Applied Fluid Dynamics Dept., von Karman Institute for Fluid Dynamics, Sint-Genesius-Rode, Belgium

email-address of the corresponding author: sebastiano.stipa@vki.ac.be

Abstract:
Offshore environments exhibit a nearly constant sea surface temperature over the diurnal cycle and a markedly lower aerodynamic roughness compared to land. These characteristics promote stronger and more persistent winds, making coastal seas particularly attractive for wind energy production. In the North Sea, the additional advantage of relatively shallow waters has enabled the widespread deployment of fixed-bottom turbines, and governments have accelerated the construction of large-scale wind farms over the past decade. As these farms expand in both size and turbine number, they increasingly interact, both mutually and with the marine atmospheric boundary layer. One consequence of this interaction is the formation of wind farm wakes, which can substantially influence the energy yield and structural loading of downstream turbines. The low surface roughness typical of offshore conditions further amplifies this effect, allowing wakes to persist for several kilometers downstream of a cluster.

The extent and longevity of these wakes depend on multiple factors, including surface-layer stability, ambient turbulence levels, boundary-layer height, and the prevailing sea state. In particular, the sea state contributes in modulating the effective surface roughness experienced by the atmospheric flow, thereby influencing wake evolution. While the roles of stability and turbulence intensity have been extensively investigated through observations and numerical models, the effect of sea state on wake behavior has received less attention.

Large-eddy simulations (LESs) have been used in [1, 2, 3] to investigate the effect of waves on the wake of an isolated wind turbine, finding that aligned wind-waves increase power production and decrease turbulence mixing, thus increasing wake length. For instance, this has also been shown at the wind farm level in [4] using mesoscale models. Here, the authors also found instantaneous differences of 20% in power between the uncoupled (only atmosphere) and coupled (wave-atmosphere) models, with mean differences over two weeks of 9%. Notably, the two simulated week were purposely chosen here so that wave impact was large. In [5], a similar model was used to investigate wake effects on waves. The authors concluded that, although results can be dependent on the setup, a decrease in wave height is generally observed in the wake of a wind farm. However, these effects may strongly depend on the presence of spatial variability of the background wave field, e.g. in relation to fetch. Interestingly, none of the above study looked at the effect of waves on wakes for a longer, statistically representative time period.

To address this gap, we conducted a year-long mesoscale simulations for 2022, using both an uncoupled atmospheric model (WRF v4.5 [6]) and a wave–atmosphere coupled system (COAWST [7]). In the uncoupled model, surface roughness is solely based on the friction velocity [8], while in the coupled configuration, the SWAN wave model (v41.45 [9]) provides sea-state-dependent surface roughness to the atmospheric component via the Drennan et al. [10] formulation. The latter depends on friction velocity, wave height, wave age, but does not explicitly account for wind–wave misalignment. However, this limitation is not expected to greatly influence our results, as the North Sea is shallow and semi-enclosed, with limited fetch and predominantly wind-sea rather than swell conditions [11].

Our analysis shows that, on an annual basis, incorporating sea-state-dependent surface roughness has a negligible influence on the cluster-wake velocity deficit, independent of wind direction or distance from the cluster center (Fig. 1-left). Figure 1-right presents the directional distribution of wind speed, wake deficit, turbulence intensity, roughness, and significant wave height at a point 33 km downstream of the cluster, located on the innermost circle of Fig. 1-left and always aligned opposite to the incoming wind. Despite the substantial differences in surface roughness predicted by the two models, both with and without turbines, the resulting wind speed and turbulence intensity remain nearly identical. COAWST predicts slightly higher wind speeds for the northerly wind sector (large wind and wave fetch), which occur infrequently but is consistent with the lower roughness values generally produced by the coupled system. Concerning wave response, our results confirm the finding of [5] on a broader statistical scale: significant wave height within the wake is systematically reduced relative to unperturbed conditions.

In the future, we plan to extend this analysis to the power output predicted by each model and to examine velocity and roughness differences across the entire domain rather than focusing solely on the wake. We also intend to investigate specific events within the year where larger model discrepancies are expected, for example during strong winter storms with rapidly evolving sea states.

Acknowledgments:
The authors acknowledge support from the Horizon Europe DTWO project, funded by the EU (grant no. 101146689). Compute resources were provided by the VSC (Flemish Supercomputer Center).

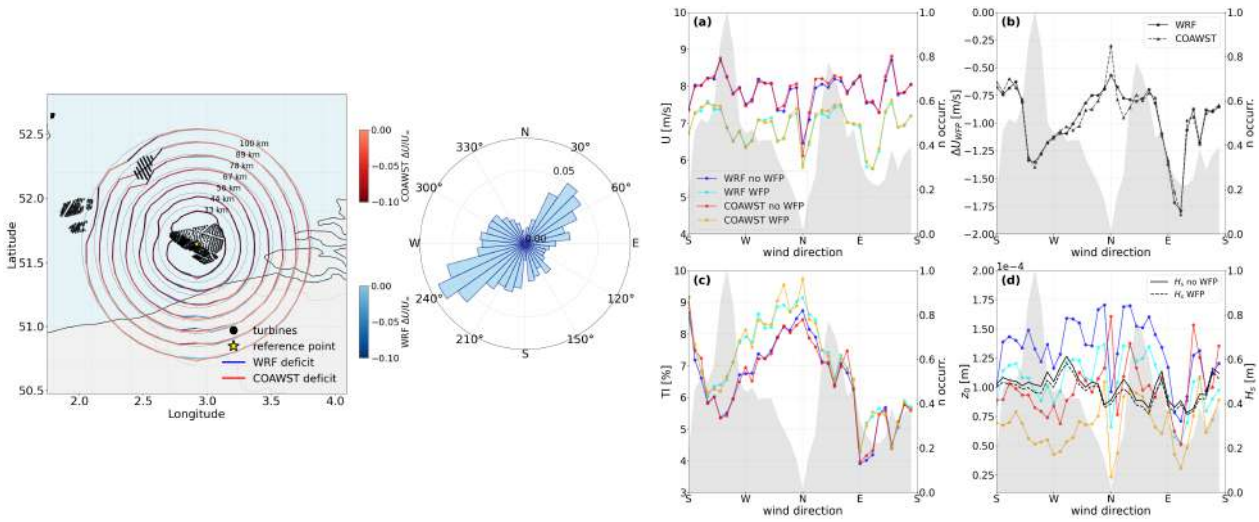

Figure 1: **Left:** wake deficit plot, data on each circle are independent of the directional PDF and refer only to waked situations, where the wind is diametrically opposed to the selected point. For each flow snapshot, the mean wind direction on the inner-circle is used to identify, on every circle, the point lying directly in the cluster wake. The wake deficit accumulated at this point is then normalized by the number of occurrences in which it is actually waked. **Center:** directional wind PDF. **Right:** (a) wind speed, (b) wind speed deficit, (c) turbulence intensity (d) surface roughness and significant wave height. Data on (a), (c) and (d) are with and without wind farm parameterization (WFP). Quantities are shown as a function of wind direction and correspond to the inner circle of the left panel (33 km downwind from the wind farm center). The number of occurrences for each wind direction is shown in shaded gray.

References

[1] Yang D, Meneveau C and Shen L 2014 *Renewable Energy* **70** 11–23 ISSN 0960-1481 special issue on aerodynamics of offshore wind energy systems and wakes URL https://www.sciencedirect.com/science/article/pii/S0960148114002444

[2] AlSam A, Szasz R and Revstedt J 2015 *Journal of Energy Resources Technology* **137** 051209 ISSN 0195-0738 URL https://doi.org/10.1115/1.4031005

[3] Kalvig S M, Manger E and Kverneland R 2013 *Energy Procedia* **35** 148–156 ISSN 1876-6102 deepWind 2013 – Selected papers from 10th Deep Sea Offshore Wind R&D Conference, Trondheim, Norway, 24 – 25 January 2013 URL https://www.sciencedirect.com/science/article/pii/S187661021301254X

[4] Porchetta S, Muñoz-Esparza D, Munters W, van Beeck J and van Lipzig N 2021 *Renewable Energy* **180** 1179–1193 ISSN 0960-1481 URL https://www.sciencedirect.com/science/article/pii/S0960148121012799

[5] Larsén X G, Fischereit J, Hamzeloo S, Bärfuss K and Lampert A 2024 *Renewable Energy* **237** 121671 ISSN 0960-1481 URL https://www.sciencedirect.com/science/article/pii/S0960148124017397

[6] Skamarock W C, Klemp J B, Dudhia J, Gill G O, Liu Z, Berner J, Wang W, Powers J G, Duda M G, Barker D M and Huang X Y 2019 *(No. NCAR/TN-556+STR)* 145

[7] Warner J C, Armstrong B, He R and Zambon J B 2010 *Ocean Modelling* **35** 230–244 ISSN 1463-5003 URL https://www.sciencedirect.com/science/article/pii/S1463500310001113

[8] Charnock H 1955 *Quarterly Journal of the Royal Meteorological Society* **81** 639–640 URL https://rmets.onlinelibrary.wiley.com/doi/abs/10.1002/qj.49708135027

[9] Booij N, Ris R and Holthuijsen L 1999 *J. Geophys. Res.* **104** 7649–7656

[10] Drennan W M, Graber H C, Hauser D and Quentin C 2003 *Journal of Geophysical Research: Oceans* **108** URL https://agupubs.onlinelibrary.wiley.com/doi/abs/10.1029/2000JC000715

[11] Porchetta S, Temel O, Muñoz Esparza D, Reuder J, Monbaliu J, van Beeck J and van Lipzig N 2019 *Atmospheric Chemistry and Physics* **19** 6681–6700 URL https://acp.copernicus.org/articles/19/6681/2019/

Breaking the barrier of sound: Can wind turbines operate safely in transonic flow?

D. von Terzi,[1] D. de Tavernier,[1] A. Aditya,[1] M.C. Vitulano,[1] G. de Stefano,[2] F. Schrijer,[1] B. van Oudheusden,[1] and M. Zaaijer[1]

[1] Flow Physics and Technology, Aerospace Engineering, Delft University of Technology, The Netherlands
[2] Engineering Department, University of Campania Luigi Vanvitelli, Italy

email-address of the corresponding author: D.A.vonTerzi@tudelft.nl

Abstract:
Over the past few decades, concomitant with the rising share of wind energy in the global energy supply, sizes of wind turbines have been increasing significantly. Offshore wind turbines deployed today are the largest rotating machines mankind has ever built. There size is of the order of the IEA 15 MW reference wind turbine (RWT) [1] with a rotor diameter of 240 m and first prototypes exist of the order of the even larger IEA 22 MW RWT [2] with 284 m rotor size. For aviation, when the first airplanes reached transonic flow, the so-called barrier of sound seemed unbreakable due to a drastic rise in drag. Moreover, airplanes experienced buffeting and strong vibrations that led to severe structural and control problems. With improved understanding of the transonic flow physics and the resulting design evolutions, however, airplanes are now routinely flying within or through the transonic flow regime with little or no difficulty [3].

In this presentation, following an intial simplified analysis for the IEA 15 MW RWT [4], we will investigate for what operating conditions, where on the blade and why the IEA 22 MW RWT is at risk of operating in a transonic flow regime. Typical results are provided in figure 1. For the outboard airfoil at highest risk, the FFA-W3-211, our recent numerical study using Unsteady Reynolds-Averaged Navier-Stokes (URANS) simulations confirmed that local supersonic flow and shocks could appear on this airfoil for the identified critical operating conditions [5]. While these conditions can not be reproduced in a wind tunnel, an equivalent situation (at different Mach and Reynolds numbers) also confirmed experimentally the numerical analysis [6]. We will also present recent experimental results that identify shock oscillations and the corresponding frequencies (see figure2) and dive into how transonic flow characteristics on wind turbine airoils differ from those employed in aviation. Moreover, we will show results from a numerical study that identifies a hysteresis loop associated with entering and leaving the transonic flow regime due to angle of attack oscillations (see figure 3 and [7]). Some of our results show, that the airfoil can enter the supersonic flow region without shock formation. In addition, we will introduce the Transonic Safe Mode [8], an operating strategy that allows for safe operation of wind turbines in the transonic flow regime. Finally, we will discuss open questions regarding wind turbine transonic flow physics and their relevance for safe operation.

References

[1] Gaertner E. et al., (2020), Definition of the IEA Wind 15-megawatt offshore reference wind turbine. *Report NREL/TP-5000-75698*, National Renewable Energy Laboratory, USA

[2] Zahle F. et al., (2024), Definition of the IEA Wind 22-megawatt offshore reference wind turbine. *Report E-0243*, DTU Wind Energy, Denmark

[3] Talay T.A. (1975): *Introduction to the aerodynamics of flight*, NASA SP-367, NASA History Division, Langley Research Center, USA

[4] de Tavernier D.A.M. and von Terzi D.A., (2022), The emergence of supersonic flow on wind turbines, *J. Phys.: Conf. Ser., vol. 2265, 042068*

[5] Vitulano M.C., de Tavernier D., de Stefano G. and von Terzi D., (2025), Numerical analysis of transonic flow over the FFA-W3-211 wind turbine tip airfoil, *Wind Energ. Sci., vol. 9, pp. 141-163*

[6] Aditya A., Vitulano M.C., de Tavernier D., Schrijer F., van Oudheusden B. and von Terzi D., (2025), Experimental study of transonic flow over a wind turbine airfoil, *Wind Energ. Sci., vol. 10, pp. 2925–2946*

[7] Vitulano M.C., de Tavernier D., de Stefano G. and von Terzi D., (2026), Numerical analysis of dynamic wind turbine airfoil characteristics in transonic flow, *Wind Energ. Sci., vol. 11, pp. 643-660*

[8] de Tavernier D.A.M., Zaaijer M. and von Terzi D.A., (2026), The Transonic Safe Mode as an enabler of next-generation wind turbines, *Nature Comms. Eng.*, accepted

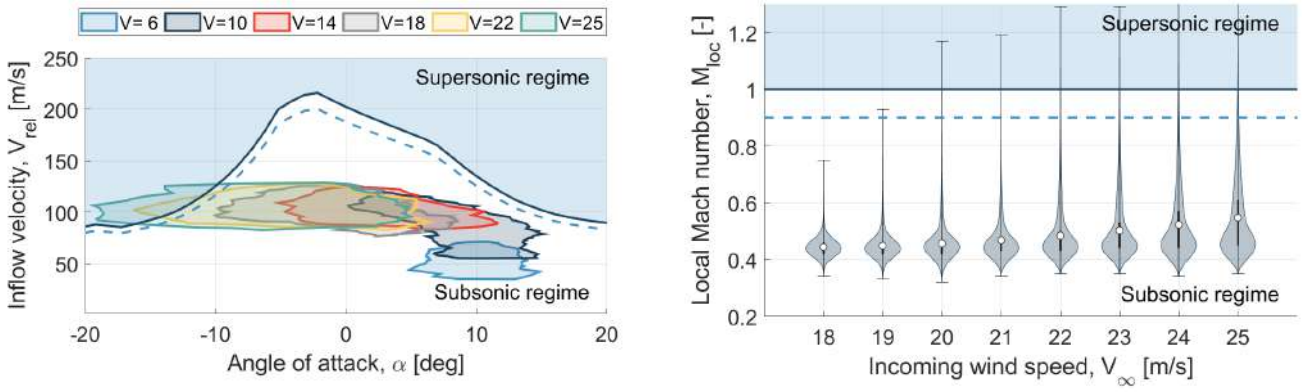

Figure 1: Comparison of the effect of incoming wind speed on the operation of the IEA 22 MW and the possibility of transonic flow. On the left, the outer boundary of the inflow conditions (specified by angle of attack and relative inflow velocity), obtained within a 1-hour simulation. On the right, the statistical distribution of the maximum local Mach number in time using a violin box, including the median, 1st and 3rd quartiles. $TI = 20\%$ and $r/R = 98\%$. The transonic onset boundary is indicated for a critical Mach number $M_{cr} = 1$ (solid line) and for $M_{cr} = 0.9$ (dashed line).

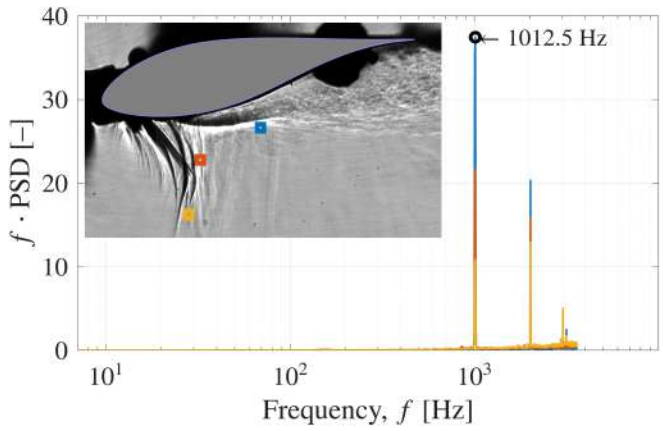

Figure 2: Instantaneous schlieren frame marked with interrogation windows (inset image) and the corresponding dominant frequencies from wind tunnel experiments of the FFA-W3-211 airfoil (IEA-22MW tip); $M_\infty = 0.65$ and $\mathrm{Re} = 1.6 \times 10^6$.

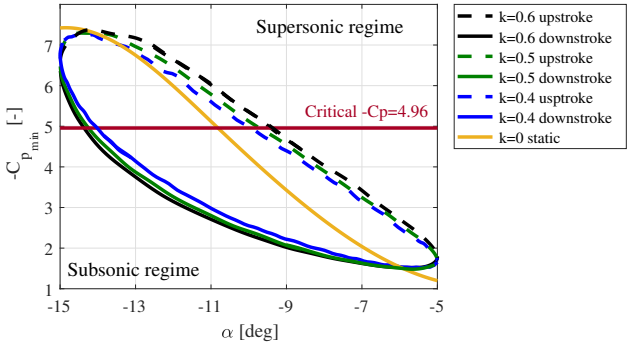

Figure 3: Minimum pressure coefficient as a function of the effective angle of attack for the FFA-W3-211 airfoil (IEA-22MW tip) obtained via URANS simulations [7], for inflow oscillations with reduced frequencies k = 0.4 (blue lines), k = 0.5 (green lines), k = 0.6 (black lines), k = 0 (yellow line, static reference): downstroke (solid lines), upstroke (dashed lines); red line marks critical pressure coefficient for reaching sonic speed; $M_\infty = 0.35$ and $\mathrm{Re} = 9 \times 10^6$.

Unsteady Wake Dynamics and Rotor-Wake Interactions in Floating Offshore Wind Farms: Comprehensive Insights from the NETTUNO Project

Alessandro Bianchini[1], Alessandro Fontanella[2], Marco Belloli[2], Francesco Papi[1]

[1] Department of Industrial Engineering, University of Florence, Firenze, Italy

[1] Dipartimento di Energia, Politecnico di Milano, Milano, Italy

Email-address of the corresponding author: alessandro.bianchini@unifi.it

Abstract:

The transition of offshore wind energy toward deep-water regions necessitates the deployment of floating offshore wind turbines (FOWTs), which operate as fully coupled aero-hydro-servo-elastic systems. Unlike bottom-fixed counterparts, FOWTs are subject to large-amplitude platform motions that alter rotor aerodynamics and induce complex, unsteady wake structures. The NETTUNO research project (www.nettuno-project.it) has addressed the current knowledge gap regarding turbine-wake interactions through a synergic approach involving 1:75 scaled wind tunnel experiments of the DTU 10 MW reference turbine (both in isolation and in an array configuration, with one upstream turbine moving on a 6-DOF robot and the second one fixed) and multi-fidelity numerical simulations, ranging from Free-Vortex Wake (FVW) methods to Actuator Line Models (both with Unsteady Reynolds-Averaged Navier-Stokes (URANS) and Large-Eddy Simulations (LES) approaches), to blade-resolved CFD.

Key findings regarding wake development confirmed that platform surge and pitch motions induce periodic thrust fluctuations (already seen during the OC6 Phaser III research program by the IEA), which are advected downstream as coherent velocity oscillations. For the test case at hand, these fluctuations were maximized at a reduced frequency of 0.6, where the periodic perturbations to the wake structure are most pronounced. While preliminary hypotheses suggested that motion-induced mixing could significantly accelerate wake recovery, experimental evidence demonstrates that such gains are highly sensitive to inflow conditions; while enhanced mixing is observed in nearly laminar flows, the impact of platform motion on wake deficit is substantially diminished at realistic inflow turbulence intensities (e.g., 1.5%–3%), as atmospheric turbulence dominates the recovery process. Furthermore, high-fidelity simulations revealed that both platform motion and inflow turbulence anticipate the breakdown of tip vortices, promoting an earlier transition to a fully developed wake compared to static conditions.

In terms of downstream impacts, turbines operating within the wake of a moving upstream rotor experience periodic aerodynamic excitations in thrust and torque coherent with the platform motion frequency. These dynamic loads reach their maximum in aligned configurations, where the entire downstream rotor-swept area is immersed in the pulsating wake, while every time the two turbines are staggered, the overall impact of the wake on downstream rotors is partially flattened out. However, the spectral signature of these motion-induced loads tends to dissipate beyond a downstream distance of 5D as wake turbulence masks the periodic structures. Notably, crosswind and yaw motions of the upstream turbine were found to facilitate modest relative power increases for downstream turbines (up to 26% in specific 3D aligned scenarios) by enhancing lateral wake meandering and mixing.

Numerical benchmarking highlighted that while engineering methods like FVW can accurately predict rotor integral loads, they often overpredict velocity oscillations and struggle to capture wake dissipation beyond 3D without extensive tuning of vortex filament parameters. Conversely, ALM-LES models proved essential for capturing the interaction between free-stream turbulence and the wake shear layer.

The talk will present a comprehensive overview of the most relevant results of the project, both from an experimental and numerical point of view, and will put them into perspective with respect to the upcoming work package 3 of the OC7 project that will make use of the same dataset.

References

[1] Cioni, S., Papi, F., Balduzzi, F., Fontanella, A., Bianchini, A. (2025). "Blade-resolved CFD analysis of a floating wind turbine: new insights on unsteady aerodynamics, loads, and wake". Ocean Engineering, 341, 122746.

[2] Fontanella, A., Fusetti, A., Cioni, S., Papi, F., Muggiasca, S., Persico, G., Dossena, V., Bianchini, A., Belloli, M. (2025). "Wake development in floating wind turbines: new insights and an open dataset from wind tunnel experiments". Wind Energy Science, 10, 1369–1387.

[3] Pagamonci, L., Papi, F., Cojocaru, G., Belloli, M., Bianchini, A. (2025). "How does turbulence affect wake development in floating wind turbines? Some insights from comparative large-eddy simulations and wind tunnel experiments". Wind Energy Science, 10, 1707–1736.

[4] Fontanella, A., Cioni, S., Papi, F., Muggiasca, S., Bianchini, A., Belloli, M. (2025). "Experimental investigation of the effects of floating wind turbine motion on a downstream turbine performance and loads". Wind Energy Science Discussions [Preprint], DOI: 10.5194/wes-2025-106.

[5] Cioni, S., Papi, F., Melani, P. F., Fontanella, A., Firpo, A., Sanvito, A. G., Persico, G., Dossena, V., Muggiasca, S., Belloli, M., Bianchini, A. (2025). "How accurately do engineering methods capture floating wind turbine performance and wake? A critical perspective using multi-fidelity simulations". Wind Energy Science Discussions [Preprint/Revised], DOI: 10.5194/wes-2025-149

Analytical limit for extraction of offshore wind energy using a minimalistic model approach

Jens N. Sørensen [1], Gunner C. Larsen [2], Mads M. Pedersen [2] and Carlos S. Ferreira [3]

[1] Flows Section, DTU Wind and Energy Systems, Lyngby, Denmark
[2] Load Response Section, DTU Wind and Energy Systems, Roskilde, Denmark
[3] Faculty Aerospace Engineering, TU Delft, Delft, The Netherlands

Corresponding author: jnso@dtu.dk

Abstract:
A minimalistic model for prediction of offshore wind energy has recently been developed and validated against performance data of several operating wind farms [1]. The basis of the approach is an atmospheric boundary layer model assuming a fully developed wind farm array boundary layer, combining a two-level roughness model with the geostrophic drag law and momentum theory. This approach was originally developed by Templin [2] to determine the impact of large-scale utilization of wind power on the available wind resources and later refined by Frandsen [3]. Connected to development of the simplistic model in [1], the boundary layer model was further adapted to a finite size wind farm, and the Weibull distribution, describing the site wind speed resource, was transformed from the ambient inflow distribution to the wind farm flow distribution, which is the decisive distribution needed for correct estimation of the wind farm energy production from larger wind farms. The model is referred to as minimalistic, as it requires a minimum of input variables. Hence, the wind turbines are characterized by diameter, hub height, and installed power; the wind farm topology is characterized by area and the number of wind turbines; and the wind climate is characterized by two Weibull distribution parameters and the site latitude. The model implicitly includes wake effects of the turbines and does not require knowledge of the turbine brand or the actual layout of the farm. Recent work has focused on further refinement and validation of the production part of the simplistic model complex. The finiteness correction factor is redefined and included in the Weibull convolution as a function of number of wind turbines and the average distance between the turbines. In addition, a simple model describing the dependence of sea surface roughness on wind speed is introduced to refine the CFD-simulated correction factor, and the simplified version of the Geostrophic Drag Law previously derived in [3] has been revised to gain increased accuracy as well as including the effect of site latitude on the wind characteristics [4]. Lately, the minimalistic model approach has been exploited to derive an analytical expression for the upper limit of extraction of offshore wind energy [5]. Some of the results obtained are shown in Fig.1, which shows the annual production data for the Horns Rev 1 (left) and Horns Rev 2 (right) wind farms as function of year (upper) and average annual wind speed (lower). We show how the energy production, in accordance with the annual wind speed statistics, varies from year to year (upper figures). The spread of the production gives an indication of the uncertainty of the production for a given average wind speed (lower figures). Two very different production data for Horns Rev 2 are seen at a wind speed of about 10.2 m/s. These are obtained in 2011 and 2015, with the latter being an outlier due to a two month cable breakdown i 2015. Besides this, there is in general a lot of scatter in the measured data, which can be due to differences in humidity, atmospheric boundary stability properties, wind farm curtailment (experiments), or changes in the predominant wind direction from year to year. All these are features that are not included in the minimalistic model. Comparing the scatter to the computed values, excluding the Horns Rev 2 outlier, the computed values are within the uncertainty of the energy production from year to year. For Horns Rev 1 the maximum relative error is about 6 %, and the mean relative error is 3.6 %. For Horns Rev 2, excluding the outlier in year 2015, the corresponding values are 5 % and 3.1 %. For these two wind farms, the uncertainty of the predictions is within the spread of the production data. In the presentation, we give an overview of the latest refinements, show some results, and discuss the implications of the analytic upper limit.

References

[1] Sørensen, J.N. and Larsen, G.C., (2021), A Minimalistic Prediction Model to Determine Energy Production and Costs of Offshore Wind Farms, *Energies, vol. 14, pp. 448-474.*

[2] Templin, R.J., (1974): An estimate of the interaction of windmills in widespread arrays. *Technical report, N.A.E. Report LTR-LA-171; National Research Council of Canada.*

[3] Frandsen, S., (1992), On the wind speed reduction in the center of large clusters of wind turbines, *Journal of Wind Engineering and Industrial Aerodynamics, vol. 39, pp. 251–265.*

[4] Larsen, G.C., Pedersen, M.M., Sørensen, J.N. (2026), Why bother on Model Complexity? – Refinement and Validation of a Simplistic Model for Prediction of Energy Production of Offshore Wind Farms, *To be submitted to Energies.*

[5] Simao Ferreira, C., Larsen, G.C., Sørensen, J.N., (2026), A theoretical upper limit for offshore wind energy extraction. *Cell Reports Sustainability. Article number: 100573. DOIs: 10.1016/j.crsus.2025.100573.*

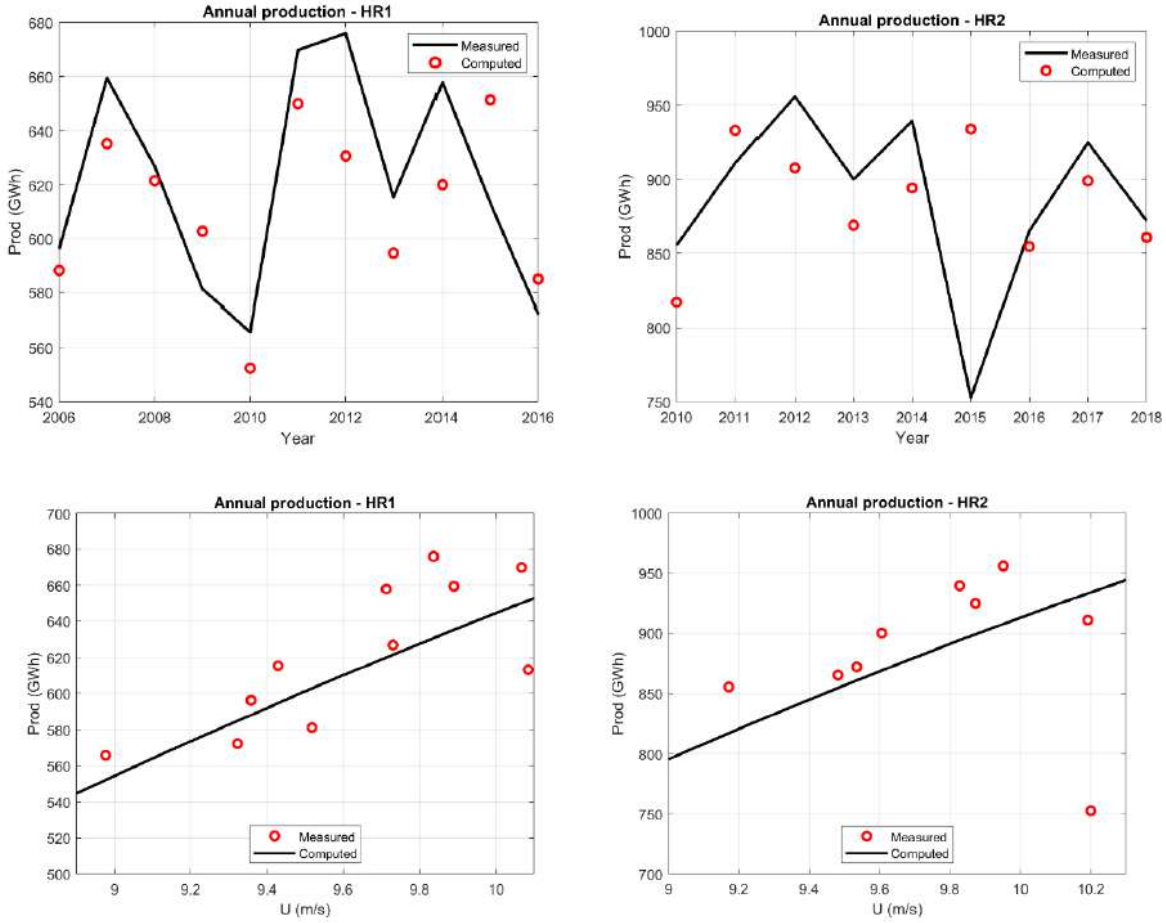

Figure 1: Production data for Horns Rev 1 (left) and Horns Rev 2 (right) wind farms as function of year (upper) and average annual wind speed (lower).

Analysis of Wind Turbine Wake Instabilities Induced by External Perturbations

Ali Ata Adam [1], Amanda S.M. Smyth [1] and Christopher R. Vogel [1]

[1] Department of Engineering Science, University of Oxford, Oxford OX1 3PJ, UK

email-adress of the corresponding author: ata.adam@eng.ox.ac.uk

Abstract:
Wakes have a significant impact on the power output of a wind farm because the velocity deficit in the wakes of upstream turbines reduces the power available to downstream turbines. Wind farm efficiency could be increased by inducing wake breakdown and enhancing energy flux into the wake through amplifying wake instabilities. However, the complexity of wake instabilities requires a deeper understanding of the underlying flow physics to develop effective mitigation strategies, such as optimised turbine spacing, wake steering techniques, and advanced control systems that minimise energy losses and enhance overall wind farm performance [1].

This study examines the impact of well-defined external perturbations on wind turbine wake dynamics using high-fidelity Large Eddy Simulations (LES) in OpenFOAM to capture the complex unsteady flow features within the wake shear layer. The wind turbine is modelled using an in-house actuator disc (AD) model, which provides a simplified, controllable parametrisation while preserving the essential wake dynamics.

Figure 1 shows that lateral inflow perturbations generally promote wake recovery more effectively than thrust perturbations across different baseline thrust coefficients and perturbation amplitudes. Thrust perturbations generate coherent annular vortex rings, which are illustrated in Fig. 2, that block energy entrainment into the wake, similar to the effects of tip vortices [2]. In contrast, as shown in Fig. 3, lateral inflow perturbations produce vortex rings around the shear layer of the wake that are tilted due to a fluctuating transverse velocity. The rings are further distorted due to their mutual interactions in the wake. Similar behaviour has been reported for actuator discs at lower Reynolds numbers [3] and for floating wind turbines under heave motion [4]. This work demonstrates that simplified perturbation cases can be meaningfully extended to more realistic wind turbine configurations, providing fundamental insights into the mechanisms governing wake instability and how to control such instabilities to mitigate wake effects.

References

[1] Meyers J., Bottasso C., Dykes K., Fleming P., Gebraad P., Giebel G., Göçmen T. and van Wingerden J., (2022), Wind farm flow control: prospects and challenges, *Wind Energy Science, vol. 7, pp. 2271-2306*

[2] Lignarolo L.E.M., Ragni D., Scarano F., Simão Ferreira C.J. and van Bussel G.J.W., (2015), Tip–vortex instability and turbulent mixing in wind–turbine wakes, *Journal of Fluid Mechanics, vol. 781, pp. 467-493*

[3] Mao X. and Sørensen J. N., (2018): Far-wake meandering induced by atmospheric eddies in flow past a wind turbine, *Journal of Fluid Mechanics, vol. 846, pp. 190-209*

[4] Li W., Zhao Z., Dong G., Liu Y., Liu H., Wei S., Ali K., Liu Y. and Ma Y., (2025), Effects of heave frequency and amplitude on wake evolution of floating offshore wind turbine in smooth flow conditions, *Ocean Engineering, vol. 340, pp. 122401*

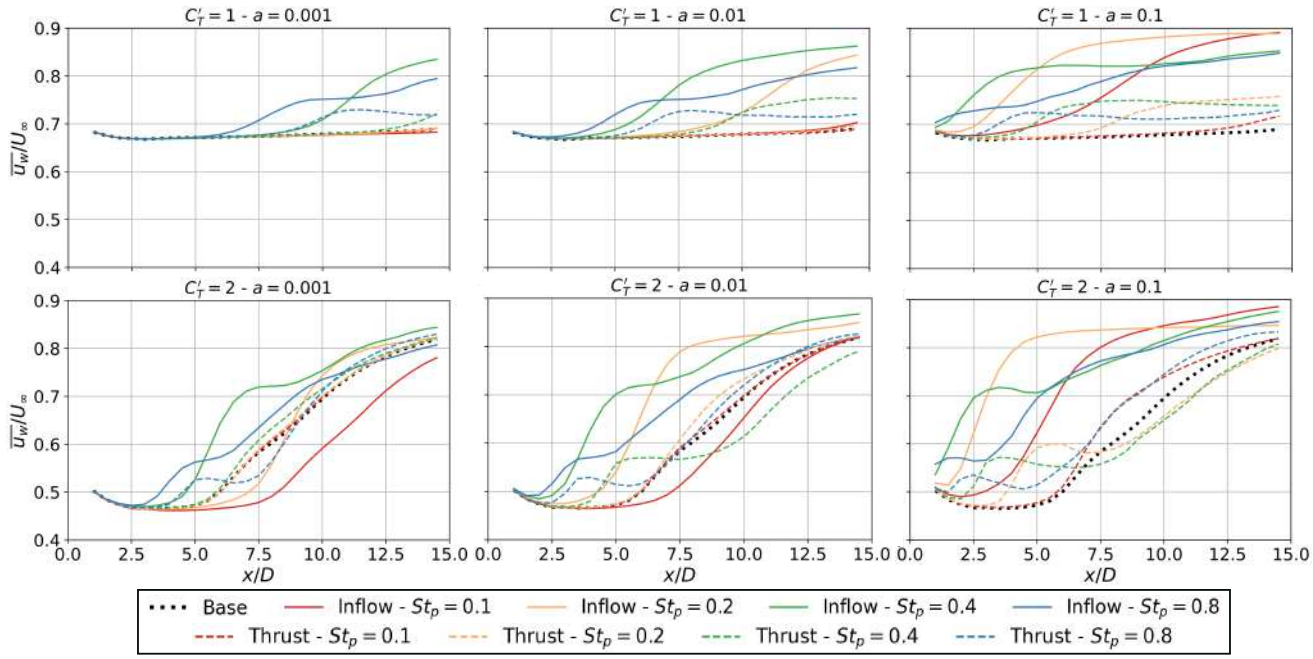

Figure 1: Average wake velocity for time-averaged local thrust coefficients (top) $\overline{C_T'} = 1$ and (bottom) $\overline{C_T'} = 2$, with perturbations of relative amplitudes (left) $a = 0.001$, (middle) $a = 0.01$ and (right) $a = 0.1$.

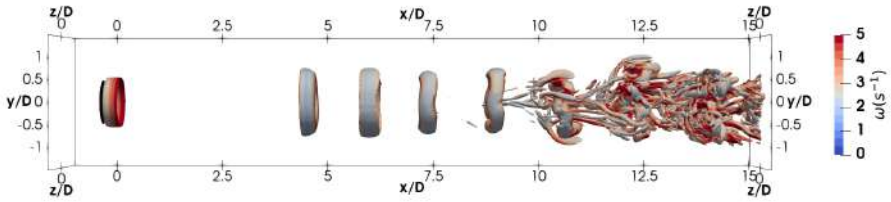

Figure 2: Instantaneous isosurfaces of Q-criterion coloured by vorticity magnitude under thrust perturbations of $St_p = 0.4$ and $a = 0.01$.

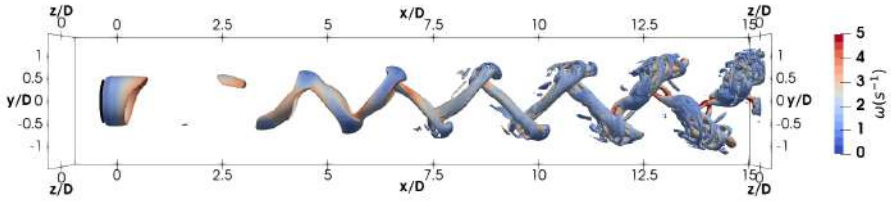

Figure 3: Instantaneous isosurfaces of Q-criterion coloured by vorticity magnitude under transverse inflow perturbations of $St_p = 0.4$ and $a = 0.01$.

Field-scale Lagrangian particle tracking measurements of tip vortices using soap bubbles

Akhileshwar Borra[1], Mano Grunwald[1,2] and Claudia E. Brunner[1]

[1] Turbulence and Wind Energy, Max Planck Institute Dynamics and Self-Organization, Göttingen, Germany
[2] Department of Physics, Georg-August-University, Göttingen, Germany

email-address of the corresponding author: akhileshwar.borra@ds.mpg.de

Abstract:

Tip vortices affect both the aerodynamic forces generated in the outer region of the rotor blades (and hence the performance of wind turbines) and the characteristics of the wake (and hence the performance of wind farms). The behaviour of tip vortices depends on the characteristics of the atmospheric flow, such as turbulence intensity, shear, and turbulence length scales. However, there is still a gap in the scientific understanding of the effects of atmospheric turbulent conditions on tip vortex formation and breakdown in the near wake region.

Furthermore, it is nearly impossible to generate atmospheric turbulence conditions in a wind tunnel due to the high Reynolds numbers required, and most previous studies were conducted under laminar inflow conditions, or in the presence of turbulence that lacked the required large-scale flow features. Therefore, it has not previously been possible to investigate the effects of atmospheric turbulence on tip vortex formation and breakdown despite its significance. This means that field measurements are required. However, commercially available atmospheric flow measurement techniques such as anemometers or LIDAR lack either the spatial information or the temporal resolution to provide the required insights into tip vortex dynamics. Particle-based methods have been recently used at field-scale to study atmospheric turbulence and tip vortices of wind turbines [1, 2]. In this work, we will discuss our field-scale Lagrangian particle tracking (LPT) method and data collected during our field campaign in February 2026 at the OST Aventa 6.5 kW wind turbine in Winterthur, Switzerland.

The LPT system consists of three key components: (1) flow seeding, (2) illumination, and (3) high-speed cameras. The goal is to obtain high-speed images with easily identifiable particles that can be tracked across the frames, which represents the behaviour of the fluid particles. In our field-scale LPT setup, we use helium-filled soap bubbles (HFSB) as the flow seeding, natural sunlight or a 10 kW xenon arc lamp as the illumination and four Phantom VEO4K-990 cameras as the high-speed cameras. HSFBs are produced with a custom-made bubble generator that is lifted to the desired position using a DJI Matrice 350 drone. Light from the sun (daytime) or the xenon arc lamp (nighttime) reflects off the surface of the soap bubble creating glare points which are captured by the high-speed cameras. The field of view, defined as the volume which is intersected by all four cameras, is located 15 m above ground and is 8 m in the direction of the wake, and 10 in the vertical direction and 6 m in the lateral direction. The data is collected at 900 Hz. These images will be processed using an open-source LPT tracking software from Johns Hopkins University: OpenLPT [3]. An initial test campaign was performed at the OST wind turbine and the experimental setup is shown in Figure 1. The OST wind turbine has a rotor diameter of 12.8 m and hub height of 18 m. Figure 2 shows the experimental setup at night with the xenon arc lamp emitting light and HFSBs being generated in the measurement volume. A sample dataset taken in freestream atmospheric turbulence is shown in Figure 3.

References

[1] Hong, J., Toloui, M., Chamorro, L., Guala, M., Howard, K., Riley, S., Tucker, J. and Sotiropoulos, F., (2014), Natural snowfall reveals large-scale flow structures in the wake of a 2.5-MW wind turbine, *Nature communications, vol. 5 pp. 4216*

[2] Conlin, N., Even, H., Wei, N., Balantrapu, A. and Hultmark, M., (2024), Lagrangian particle tracking in the atmospheric surface layer, *Meaurement science and technology*, vol. 35 pp. 095803

[3] Tan, S., Salibindla, A., Masuk, A., and Ni, R. (2020), Introducing OpenLPT: new method of removing ghost particles and high-concentration particle shadow tracking, *Experiments in Fluids, vol. 61 pp. 47*

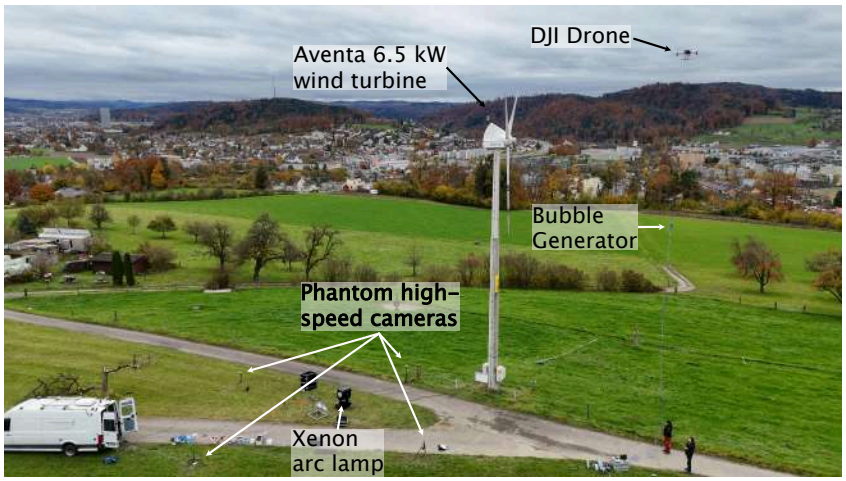

Figure 1: Field-scale LPT setup in Winterthur, Switzerland

Figure 2: LPT setup at night with helium-filled soap bubbles

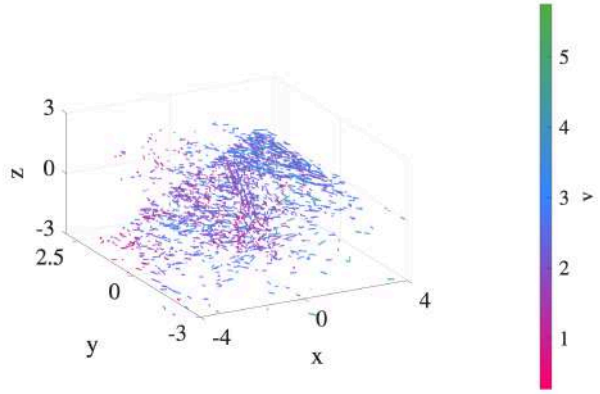

Figure 3: Sample data of atmospheric turbulence from LPT

Interaction between an ABL and a model wind farm

Adrian Thomas Mc Glade [1], and Oliver R. H. Buxton [1]

[1] Department of Aeronautics, Imperial College London, London, UK

email address of the corresponding author: a.mcglade23@imperial.ac.uk

Abstract:
Wind energy is a cornerstone of renewable electricity generation, with wind farms critical for decarbonisation. As farms grow, aerodynamic interactions—both between turbines and with the surrounding flow—become increasingly important. In particular, global blockage, where multiple turbines reduce upstream wind speeds, affects both farm performance and the incoming atmospheric boundary layer (ABL) [1, 2]. This study investigates global blockage and its impact on the ABL using wind tunnel experiments with a model wind farm.

The experiment was conducted in Imperial's T2 wind tunnel illustrated in Figure 1. Two farm layouts (aligned and staggered) were considered, along with a characterisation of the flow without the farm, with streamwise and spanwise spacing of 5 and 4 disc diameters $D = 50\,\text{mm}$. Wind turbines are approximated using porous discs, a modified version of the porous disc model of [3], with a $C_T \approx C_D = 0.94$. The hub-height was $0.8D$. Two model-scale ABLs were created using Irwin spires, resulting in boundary layer depths of $\delta_{99} \approx 1.9D$ and $3.6D$. Due to the small scale of the farm, 60-grit sandpaper was effectively used as roughness. The resulting ABL-profiles are shown in figures 2, successfully reproducing the salient features of an ABL, despite their diminutive size. Measurements were taken in front of the farm with a hot wire (HW), the principal quantities of interest are normalised mean velocity ($U = \overline{U}/U_{\text{ref}}$) and turbulence intensity ($TI = \sqrt{\overline{u'^2}}/U_{\text{ref}}$). U_{ref} is the mean velocity measured at $(x/D, y/D, z/D) = (-8, 0, 10)$. To develop an understanding of the impact of the farm, U and TI were averaged across the span (Y). Figures 3a) and b) show the streamwise evolution of these span-averaged quantities. Figure 3a) demonstrates that there is a significant reduction in the hub-height mean velocity due to the presence of the farm. The characterisation of the inflow shows that the boundary layer is still evolving in the streamwise direction, but relative to the baseline inflow, the mean velocity is reduced by 5% and 4% for the $\delta_{99} \approx 1.9D$ and $3.6D$ ABLs at $x/D = -1.7$, respectively. There is only a small difference between the staggered and aligned configurations. Similarly, 3 b) shows an increase of TI 6 and 5.5% for the $\delta_{99} \approx 1.9D$ and $3.6D$ ABLs at $x/D = -1.7$. These results illustrate how the presence of the farm impacts farm performance. This impact, however, extends beyond the hub-height. Using the spanwise averaged mean velocity $U = U(x, z)$, the evolution of the displacement thickness, δ^*, can be considered:

$$\delta^*(x) = \int_0^\infty \left(1 - \frac{U(x,z)}{U_{\text{ref}}}\right) dz \qquad P(x) = \frac{1}{2}\,\rho\, C_p\, D \int_{z_{\text{Hub}}-D/2}^{z_{\text{Hub}}+D/2} U^3(x,z)\, dz \tag{1}$$

Figure 3c) shows the streamwise evolution of the displacement thickness, showing that the farm is effectively thickening the ABL, reducing the available energy for extraction. To quantify this effect, consider the basic one-dimensional turbine power of equation 1 which estimates the available turbine power at each streamwise position. This power is normalised by the characterisation or 'no farm' case. The results of which are shown in figure 3d). Figure 3d) shows an 13% and 11% reduction in power for the $\delta_{99} \approx 1.9D$ and $3.6D$ ABLs at $x/D = -1.7$. This power reduction extends far upstream of what would be expected for the induction region of a single disc or turbine, indicating that this is indeed a farm-scale effect.

References

[1] Bleeg J., Purcell M., Ruisi R. and Traiger E, (2018), Wind Farm Blockage and the Consequences of Neglecting Its Impact on Energy Production, *Energies 11, no. 6: 1609.*

[2] Abraham A., Puccioni M.,Jordan A.,Maric, E.,Bodini N.,Hamilton N.,Letizia S., Klein P. M., Smith E. N., Wharton S., Gero J.,Jacob J. D.,Krishnamurthy R., Newsom R. K.,Pekour M.,Radünz W. and Moriarty P., (2025): Operational wind plants increase planetary boundary layer height: an observational study *Wind Energy Science 11, no. 8, pp 1681-1705*

[3] Camp E. and Cal R.B. (2016), Mean kinetic energy transport and event classification in a model wind turbine array versus an array of porous disks: Energy budget and octant analysis, *Physical Review Fluids 1*

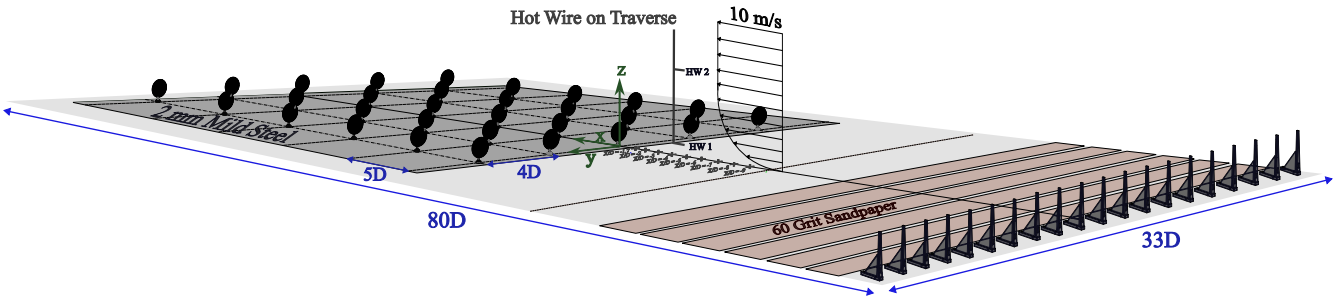

Figure 1: *Experimental setup for the aligned layout*

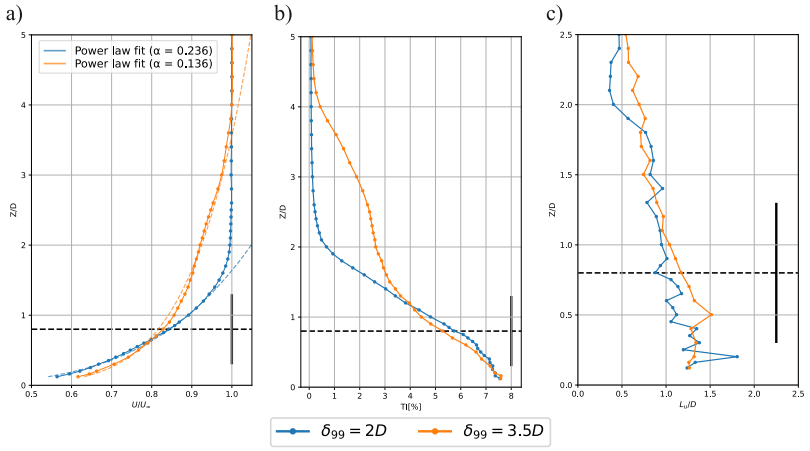

Figure 2: *The generated a) Velocity profile, b) Turbulence Intensity (TI) profile, c) integral length scale (estimated using autocorrelation and Taylor's frozen turbulence hypothesis) of the regular spires. Taken at the leading disc plane*

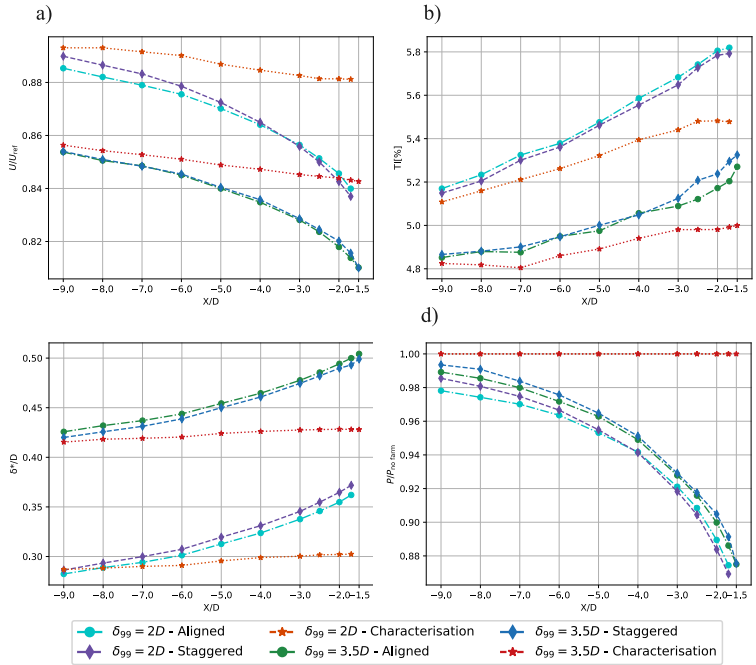

Figure 3: *Streamwise evolution of the a) spanwise averaged hub-height velocity, U b) spanwise averaged hub-height TI c) displacement thickness $\delta^\star$ and d) turbine power $P/P_{no\ farm}$*

Spanwise-resolved wind turbine blade dynamics

Francisco J. G. de Oliveira [1], Zahra Sharif Khodaei [1] and Oliver R. H. Buxton [1]

[1] Department of Aeronautics, Imperial College London, London, UK

email-address of the corresponding author: f.oliveira22@imperial.ac.uk

Abstract:

As wind farms increase in density to meet 2050 climate targets, downstream turbines increasingly operate within the wakes of upstream machines. These wakes introduce velocity deficits, enhanced turbulence, and coherent vortex structures that significantly alter power capture and accelerate fatigue loading and damage [1]. Understanding the fundamental mechanisms by which wake dynamics couple to blade structural response is critical for predicting fatigue lifetime and optimising turbine performance in realistic operating environments. Experiments were conducted in the large test section of the $10' \times 5'$ wind tunnel at Imperial College London using a 3-bladed 1-metre-diameter wind turbine model ($R = 0.5$m), operating at a free-stream velocity of $U_\infty = 2.8$[m/s] [2]. Blade dynamics were measured with Rayleigh backscattering sensors (RBS) providing spanwise strain measurements (ε) with a spatial resolution of $\delta_f = 2.6$ mm, coupled to a fibre-optic slip-ring routed through the rotor's base (see 1 *a)*) [3, 4]. The sensors were set in a sinusoidal layout to retrieve both flapwise (ε^f) and edgewise (ε^e) strain components (see figure 1 *b)*). The turbine was connected to a MAXON generator, allowing operation across a large number of tip-speed-ratios (λ) encompassing below, above and design ($\lambda_d = 4$) operating conditions. Free-stream turbulence (FST) was generated using a turbulence grid placed at 3 upstream locations, producing different FST "flavours" $\{\mathrm{A}, \mathrm{B}, \mathrm{C}\}$ characterised by TI[%] $\in \{3.8, 5.3, 8.2\}$. Prior to each acquisition, an independent acquisition was performed where the turbine was set to rotate at corresponding speed for each λ under a quiescent atmosphere ($U_\infty = 0$), allowing us to infer the gravitational and centrifugally driven strain (ε_{g+c}). The aerodynamic induced strain (ε_a) at each operating condition with $U_\infty = 2.8$[m/s] is then estimated by removing the contribution of ε_{g+c} acquired *a priori* ($\varepsilon_a = \varepsilon - \varepsilon_{g+c}$). Figures 1 *c)* and *d)* present the distributions of $\overline{\varepsilon_a^f}(s/R)$ (where $\bar{\cdot}$ denotes time averaging) across the blade's extent. The magnitude of $\overline{\varepsilon_a^f}(s/R)$ shows a clear dependence on λ. At below-design ($\lambda = 2$), $\overline{\varepsilon_a^f}(s/R)$ presents smaller magnitudes consistent with a smaller thrust acting across the rotor. As λ increases, so does the thrust experienced by the turbine and the magnitude of $\overline{\varepsilon_a^f}(s/R)$ increases across the blade. The increase of TI increases the magnitude of $\overline{\varepsilon_a^f}(s/R)$, particularly for $\lambda = 2$. We define the flapwise bending proxy Δ_f from peak-trough differences across blades sections to quantify induced variations of the time-averaged load acting on the blade. The distributions of Δ_f as a function of λ and blade section (see figure 1 *d)*) show a general increase with λ, at the ROOT and MIDSPAN, with the latter exhibiting the steepest growth. The TIP shows less sensitivity and a larger standard deviation—attributed to the fact that this blade region is characterised by thinner blade profiles. Finally, the distributions of root-mean-squared (RMS) of aerodynamic-induced strain fluctuations ($\varepsilon'_a = \varepsilon_a - \overline{\varepsilon_a}$) presented in figure 1 *f)* peak in magnitude at $\lambda = 3.5$, suggesting that fatigue-relevant damage is maximised near the transition to design operation. Increasing TI generally amplifies the response, but the dominant dynamic remains driven by λ.

References

[1] Thomsen, K. and Sørensen, P., (1999), Fatigue loads for wind turbines operating in wakes, *Journal of Wind Engineering and Industrial Aerodynamics, vol. 80 pp. 16*

[2] G. de Oliveira, F. J., Bourhis, M., Khodaei, Z. S., Buxton, O. R. H. (2025), The effect of tip-speed ratio and free-stream turbulence on the coupled wind turbine blade/wake dynamics, *Wind Energy Science, preprint under review*

[3] Wen, B., Li, Z., Jiang, Z., Tian, X., Dong, X. and Peng, Z. (2020), Blade Loading Performance of a Floating Wind Turbine in Wave Basin Model Tests, *Ocean Engineering, vol. 199 pp 107061*

[4] Shroff, S., *et. al.* (2017), Manufactured and laboratory tested scaled blades and parts of the blade, *Deliverable D2.24, INNWIND.EU*

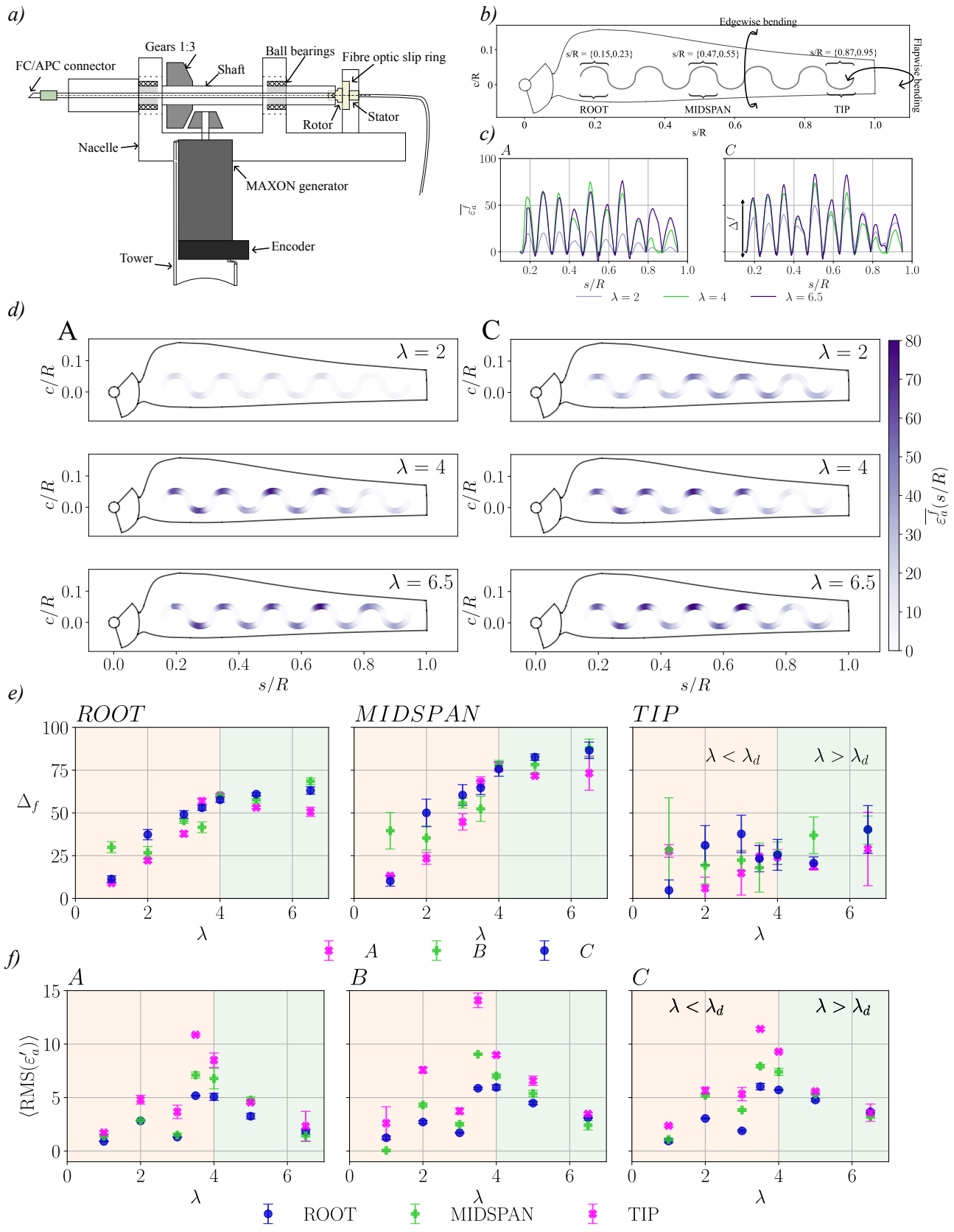

Figure 1: *a)*: Schematic of the nacelle layout and the wind turbine's control system. *b)*: Schematic of the fibre-optic sensing layout used, and blade sections nomenclature. *c)*: spanwise distributions of time-averaged aerodynamic induced flapwise strain. *d)*: blade-projected flapwise distributions of time-averaged aerodynamic induced strain. *e)*: Evolution of flapwise bending proxy Δ_f at the different blade sections for different FST and λ. *f)*: $\langle \mathrm{RMS}(\varepsilon'_a) \rangle$ as a function of λ, FST and blade section.

Laboratory Recreation of Atmospheric Turbulence

Hyunseok Kim [1] and Claudia E. Brunner [1]

[1] Max Planck Institute for Dynamics and Self-Organization, Göttingen, Germany

email-adress of the corresponding author: hyunseok.kim@ds.mpg.de

Abstract:
Atmospheric turbulence fundamentally impacts the flow physics of wind turbines and wind farms. It is often unsteady over a wide range of scales, which makes the interactions between the flow and a wind turbine complex [1]. In the context of wind energy research, the effect of inflow turbulence has often been reduced to a few parameters, such as turbulence intensity and integral scales [2, 3], which are insufficient to capture the rich nature of atmospheric turbulence. Despite its importance, the effect of unsteady inflow with wide scale separation on wind turbine fluid dynamics has remained relatively unexplored, partly due to the difficulty of generating such flow systematically. In this research, we designed, generated, and validated an unsteady flow with wide scale separation. We leveraged two special facilities that enable wide scale separation and flexible modulation of the inflow: the Variable Density Turbulence Tunnel (VDTT) and an active grid. The VDTT is a special wind tunnel capable of being pressurized with SF_6. The maximum pressure of the system is 15 bar, which leads to high density (113.26 kg/m^3 at 21°C) with a dynamic viscosity similar to air, resulting in an extremely low kinematic viscosity [4]. Since low kinematic viscosity extends the high-frequency end of the turbulence scales, the VDTT can achieve extremely large scale separation, represented by a high turbulence Reynolds number ($Re_\lambda = u_{rms}\lambda/\nu$, where, u_{rms}: the root-mean squared velocity fluctuation, λ: the Taylor-microscale, and ν: the kinematic viscosity). $Re_\lambda > 5000$ have been achieved in the case of homogeneous isotropic turbulence [5]. The active grid consists of 111 individually programmable flaps [6]. It is located at the inlet of the VDTT test section and generates the desired inflow condition. The protocol for the active grid is determined by low-pass filtered sonic anemometer data acquired at the site A1 in Oklahoma, USA, as part of the AWAKEN project [7]. The flow velocity inside the wind tunnel was measured using a hot-wire probe at 60 kHz. The representative instantaneous velocity profile in the wind tunnel accurately tracks the grid protocol derived from the field data (Figure 1). The velocity fluctuations span six orders of magnitude in temporal scale (Figure 2). This study demonstrates the potential for more realistic wind turbine testing conditions in a laboratory.

References

[1] Veers P., Dykes K., Lantz E., Barth S., Bottasso C. L., Carlson O., Clifton A., Green J., Green P., Holttinen H. et al., (2019), Grand challenges in the science of wind energy, *Science, vol. 366, no. 6464, pp. eaau2027*

[2] Talavera M. and Shu F., (2017), Experimental study of turbulence intensity influence on wind turbine performance and wake recovery in a low-speed wind tunnel, *Renewable Energy, vol. 109, pp. 363–371*

[3] Gambuzza S. and Ganapathisubramani B., (2021), The effects of free-stream turbulence on the performance of a model wind turbine, *Journal of Renewable and Sustainable Energy, vol. 13, no. 2*

[4] Bodenschatz E., Bewley G. P., Nobach H., Sinhuber M. and Xu H., (2014), Variable density turbulence tunnel facility, *Review of Scientific Instruments, vol. 85, no. 9*

[5] Küchler C., Bewley G. P. and Bodenschatz E., (2023), Universal velocity statistics in decaying turbulence, *Physical Review Letters, vol. 131, no. 2, pp. 024001*

[6] Griffin K. P., Wei N. J., Bodenschatz E. and Bewley G. P., (2019), Control of long-range correlations in turbulence, *Experiments in Fluids, vol. 60, no. 4, pp. 55*

[7] Goldberger L., (2025), *AWAKEN Site A1 - PNNL Surface Met Station / Raw Data*, United States, DOI: 10.21947/1988081. Available at: https://www.osti.gov/biblio/1988081

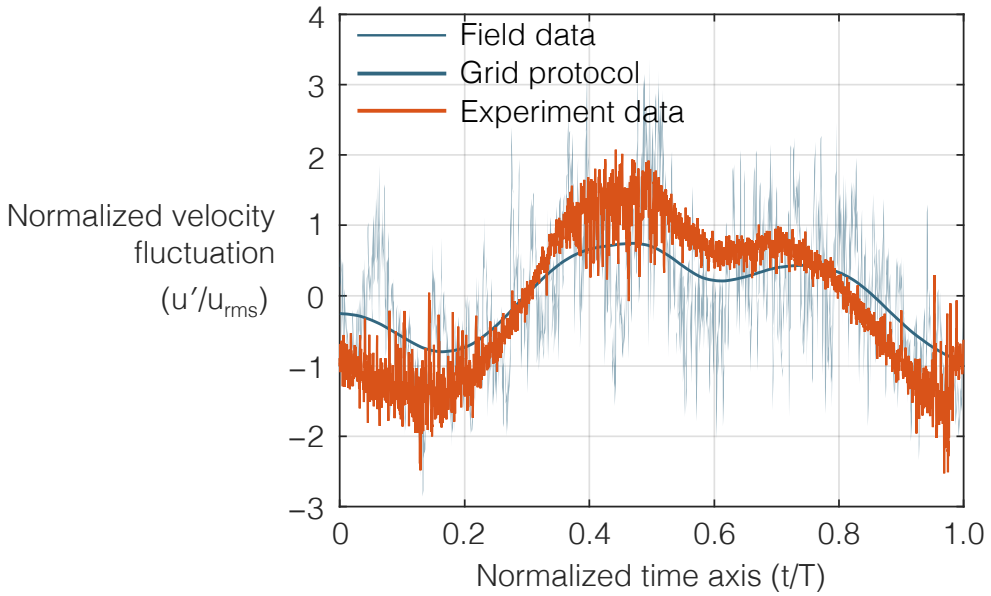

Figure 1: *A comparison of the normalized velocity fluctuation of the field measurement data and the recreated profile in the wind tunnel*

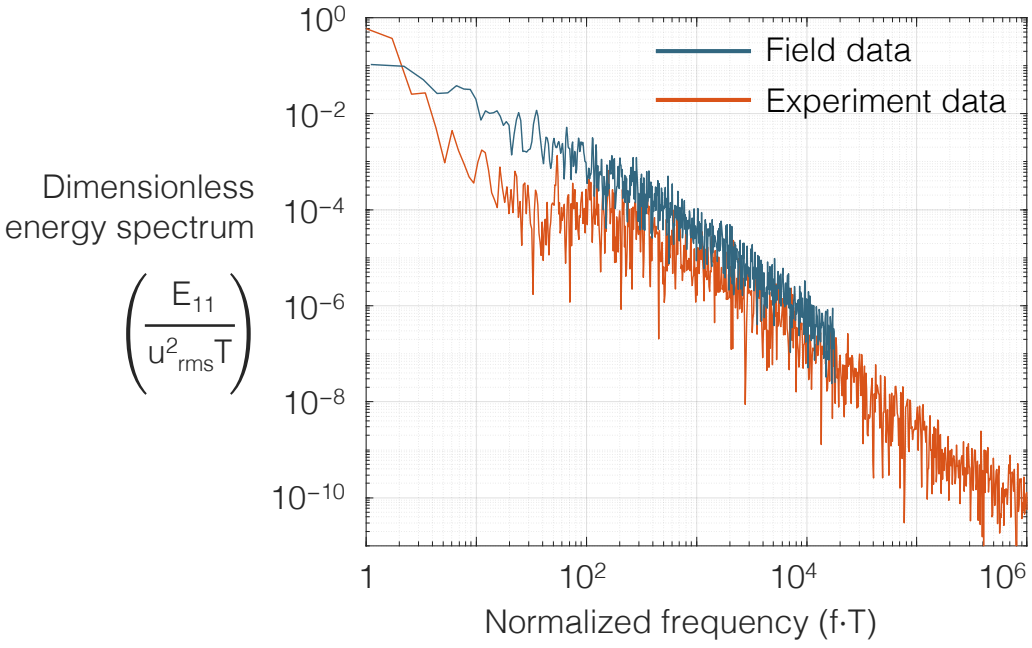

Figure 2: *A comparison of the dimensionless velocity energy spectrum*

A new joint yaw and induction control paradigm revealed by Unified rotor modeling and validation

Ilan M. L. Upfal[1], John W. Kurelek[2], Supun Pieris[2], Kirby S. Heck[1], Marcus Hultmark[3], and Michael F. Howland [1]

[1] Civil and Environmental Engineering, Massachusetts Institute of Technology, Cambridge, USA
[2] Mechanical and Materials Engineering, Queen's University, Kingston, Canada
[3] Mechanical and Aerospace Engineering, Princeton University, Princeton, USA

email-address of the corresponding author: iupfal@mit.edu

Abstract:
Field experiments have demonstrated the potential to increase array energy production using flow control, but the realized gains are limited by empiricism used to model the effects of inflow-rotor misalignment and high thrust coefficient operation [1, 2]. By capturing the transverse velocity generated by inflow-rotor misalignment and the wake pressure deficit in high thrust from first principles, the recently developed Unified Momentum Model reduces error and uncertainty in the predictions of the velocities induced by rotor thrust [3]. We couple this momentum model with a blade element model to yield a fully predictive Unified Wind Turbine (UWT) model for induction, thrust, and power across arbitrary tip speed ratio, pitch angle, yaw misalignment, and rotor design.

Furthermore, validation of control-oriented engineering models has been limited by a lack of controlled experiments for yaw-misaligned rotors that systematically vary control setpoints—tip-speed ratio and pitch angle—while remaining representative of the Reynolds number, Mach number, and tip-speed ratios of utility-scale turbines. We present first-of-their-kind high pressure wind tunnel experiments of a yaw-misaligned model turbine across a range of tip-speed ratios at a diameter-based Reynolds number of 4×10^6 (Figure 1). These experiments achieve full dynamic similarity with field scale turbines while spanning a wide range of control setpoints, enabling rigorous validation of the UWT model. In Figure 2, UWT model predictions for normalized thrust and power coefficients show excellent agreement with experiments for a near-optimal tip speed ratio of 4.5. The experiments further reveal in Figure 3 that the power-maximizing tip-speed ratio varies with yaw angle, a behavior that empirical cosine models cannot capture. We show that the UWT model accurately predicts the power-maximizing control strategy λ^* at each yaw angle γ within experimental uncertainty, and predicts the corresponding optimal power C_P^* for $-15^\circ \leq \gamma \leq 15^\circ$.

These predictive capabilities enable a new wind farm flow control paradigm in which the pitch angle and tip speed ratio can be co-optimized with the turbine yaw angle to minimize power degradation in yaw misalignment. Finally, we leverage the UWT model to perform wind farm flow control optimizations using this new joint yaw and induction control paradigm and validate the performance against high-fidelity large eddy simulations in atmospheric boundary layer flow.

References:

[1] Howland M.F., Quesada J.B., Martínez J.J.P., et al., (2022), Collective wind farm operation based on a predictive model increases utility-scale energy production, *Nat. Energy 7, 818-827.*

[2] Gebraad P.M.O., Teeuwisse F.W., van Wingerden J.W., Fleming P.A., Ruben S.D., Marden J.R., and Pao L.Y., (2016), Wind plant power optimization through yaw control using a parametric model for wake effects—a CFD simulation study, *Wind Energy, 19: 95–114.*

[3] Liew J., Heck K.S., and Howland M.F., (2024), Unified momentum model for rotor aerodynamics across operating regimes, *Nat. Commun., 15(1):6658.*

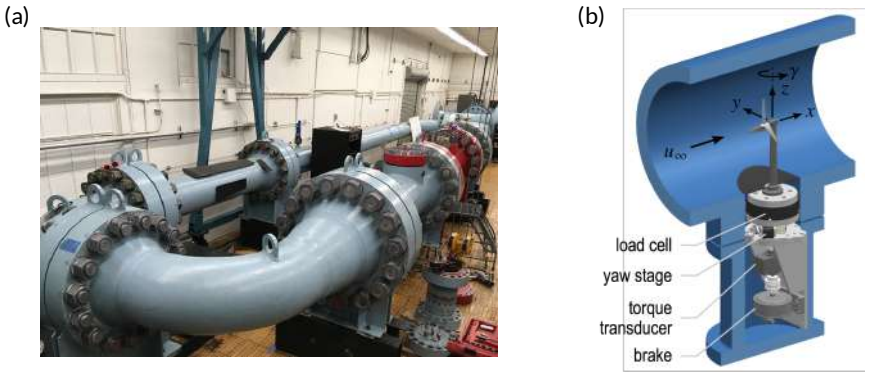

Figure 1: Experimental setup of the pressurized wind tunnel experiments. (a) A photo of the High Reynolds number Test Facility (HRTF) at Princeton University and (b) a schematic of the turbine test section.

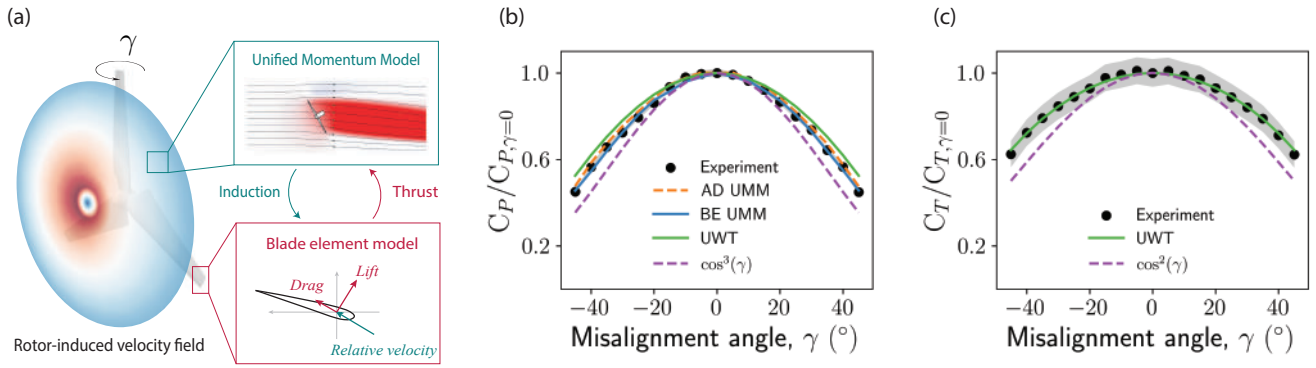

Figure 2: The Unified Wind Turbine (UWT) model is compared to controlled experiments at dynamic similarity with commercial wind turbines. (a) The UWT model is developed by coupling the Unified Momentum Model (UMM) with a blade element model. (b) Power coefficient normalized by the yaw aligned value for a tip speed ratio of 4.5, comparing the UWT model to the experiments. The green line shows the fully predictive UWT result without knowledge of the measured C_T. The blue line shows C_P computed by providing the measured C_T, revealing the Unified model performance without the error incurred by the blade element model coupling. The dashed orange line is the actuator disk power ($P = \vec{F}_T \cdot \vec{u}_d$) from the UMM using the measured C_T. (c) Same as (b) but for thrust coefficient.

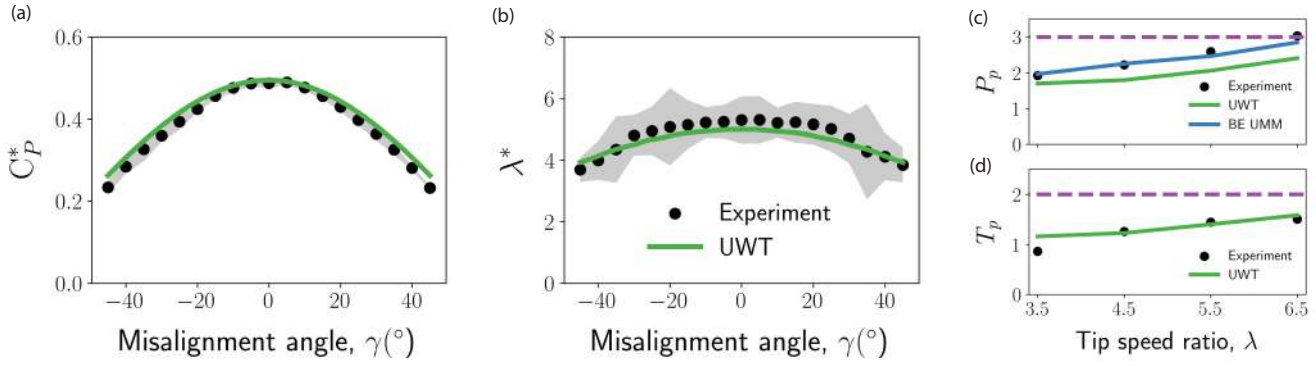

Figure 3: The Unified Wind Turbine (UWT) model predictions of the power maximizing control strategy at each yaw misalignment angle compared to the experiments. (a) The maximum coefficient of power at each yaw angle C_P^*, evaluated at at the optimal tip speed ratio λ^*. (b) The power maximizing tip speed ratio λ^* depending on the yaw misalignment angle γ. (c) Power-yaw exponent using the form $C_P/C_P(\gamma = 0) = \cos^{P_p}(\gamma)$ fit to the experiments and model results using least-squares regression. A standard value of $P_p = 3$ is shown for reference, which is the loss anticipated by geometry. (d) Same as (c) but for $C_T/C_T(\gamma = 0) = \cos^{T_p}(\gamma)$. A standard value of $T_p = 2$ is shown for reference, which is the loss anticipated by geometry.

Resolving a Wind Turbine Wake With Lagrangian Particle Tracking

Lorenn Le Turnier [1,2], Hyunseok Kim [1] and Claudia E. Brunner [1]

[1] Max Planck Institute for Dynamics and Self-Organization, Göttingen, Germany
[2] Georg-August-Universität, Göttingen, Germany

email-adress of the corresponding author: lorenn.le-turnier@ds.mpg.de

Abstract:
Wind turbine wakes are dominated by highly turbulent flows and characterized by the presence of coherent structures like the hub vortex and tip vortices. The breakdown of these structures generates turbulence within the core of the wake, thus affecting wake recovery. Moreover, it results in additional loads on the blades and the tower of downwind turbines, reducing their lifespan. Understanding the formation and breakdown mechanisms of these coherent structures is crucial for enhancing wind turbine performance.

We use a Lagrangian Particle Tracking (LPT) setup [1] (see Fig. 1 (left)). LPT allows for volumetric measurements of highly turbulent flows by following tracer particles within a predefined volume over an extended period of time. Illumination is provided by four LEDs and we achieve high temporal resolution using four Phantom high-speed cameras. These cameras have a frame rate of up to 10 kHz and a resolution of 2560×1664 pixels. The wind turbine model has a rotor diameter of 16 cm. The measurement volume has a size of the order of 10 cm^3.

To recreate high Reynolds number conditions, we used the Variable Density Turbulence Tunnel (VDTT) [2] (see Fig. 1 (right)) at the Max Planck Institute for Dynamics and Self-Organization (MPI-DS). The wind tunnel is filled with sulfur hexafluoride (SF_6) and pressurized to 6 bars. These conditions create a flow with a diameter-based Reynolds number of 1 million. To inject turbulence in the flow, we used an active grid located at the entrance of the upper section. This grid consists of 111 paddles which can be individually controlled, allowing spatial and temporal correlation of the turbulence injection [3].

In this work, the wind turbine wake is investigated at various downstream positions and for different turbulence conditions. The time-resolved three-dimensional positions of the particles are obtained using a shake-the-box code [4] developed at the MPI-DS. A sample of these trajectories is represented in Fig. 2. By temporally and azimuthally averging the 3D trajectories we derived the profiles of the three velocity components in the wake at different downstream positions. Fig. 3 shows preliminary analysis but measurements from 0 to 5.25 D have been done. We aim to understand how the existence and break down of the coherent structures influence the turbulence development in the wake and how different inflow conditions influence the generation of coherent structures.

References

[1] Küchler C., Landeta A. I., Moláček J. and Bodenschatz E., (2024), Lagrangian particle tracking at large Reynolds numbers, *Rev. Sci. Instrum. 95, 105110*

[2] Bodenschatz E., Bewley G. P., Nobach H., Sinhuber M. and Xu H., (2014), Variable density turbulence tunnel facility, *Rev. Sci. Instrum. 85, 093908*

[3] Griffin K. P., Wei N. J., Bodenschatz E. and Bewley G. P., (2019), Control of long-range correlations in turbulence, *Exp. Fluids 60, 55*

[4] Bertens G., Bagheri G., Xu H., Bodenschatz E. and Moláček J., (2021), In situ cloud particle tracking experiment, *Rev. Sci. Instrum. 92, 125105*

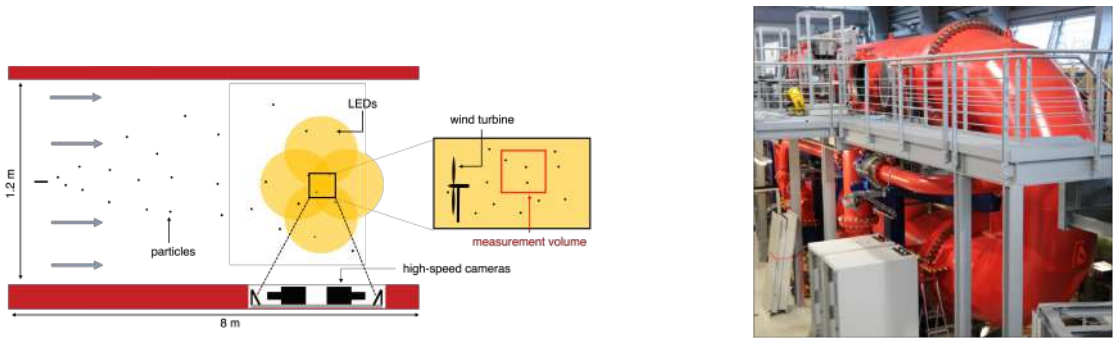

Figure 1: *Lagrangian Particle Tracking setup (left) and picture of the Variable Density Turbulence Tunnel (right)*

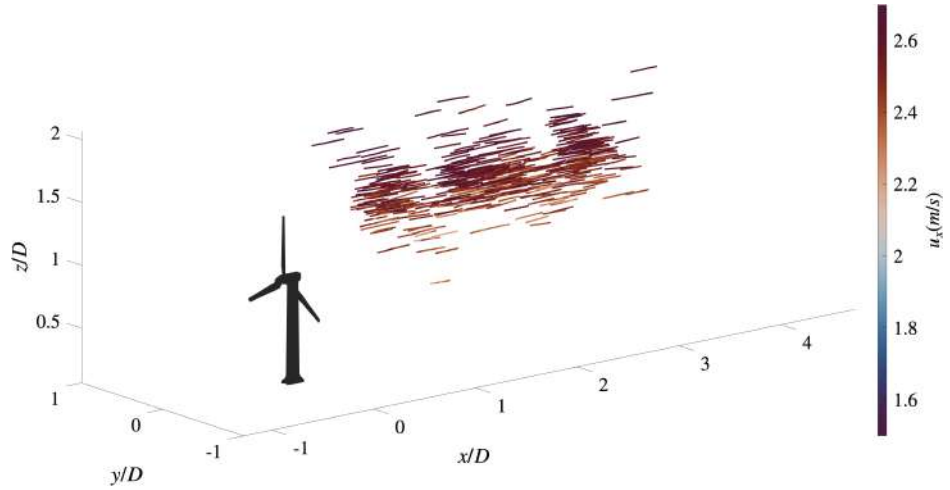

Figure 2: *Sample of three-dimensional particle trajectories in the wind turbine wake*

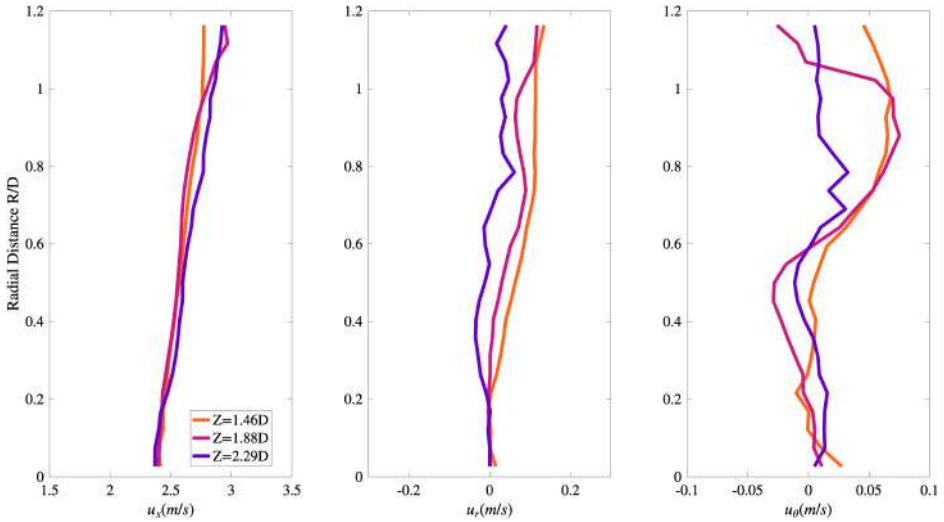

Figure 3: *Mean profiles of the three velocity components in the wind turbine wake at different downstream positions*

Surrogate POD-Based Model of an Isolated Wind Turbine

M. Rosales [1], M. Ávila [1] and O. Lehmkuhl [1]

[1] CASE, Barcelona Supercomputing Center (BSC-CNS), Barcelona, Spain

Email-adress of the corresponding author: maria.rosales@bsc.es

Abstract:
This study employs computational fluid dynamics (CFD) simulations in conjunction with a reduced-order model, such as the Proper Orthogonal Decomposition (POD) [1], to retain the most relevant coherent modes and to couple the reconstruction of the temporal evolution of the wind via a sensor-driven deep learning model, such as SHRED [2].

A dataset is generated from a CFD simulation of the single-wake wind turbine VESTAS V80 (Fig. 1). The simulations are performed using the in-house solver SOD2D [3], with inflow conditions corresponding to the fourth roughness case in [4]. A total of $N = 8148$ snapshots of the streamwise velocity u_x are collected over a time horizon of $T = 7705$ s. The spatial domain is reduced from 84.96 million nodes to 839,421 nodes by restricting the analysis to a subdomain of interest in the (x, y, z) directions.

Any turbulent flow field $\mathbf{X}(\mathbf{x}, t)$ can be decomposed into spatial modes and temporal coefficients using Proper Orthogonal Decomposition (POD): $\mathbf{X} = USV^T$ where U contains spatial modes, V temporal coefficients, and S the singular values. To retain the most energetic coherent structures while reducing dimensionality, several POD energy truncation levels are considered (Fig. 2), computed from the fluctuations u'_x. The POD basis is computed from the training set and used to project the validation and test data.

For each truncation level, a SHRED model is trained to reconstruct the flow from sparse sensor measurements. For each case, the dataset is split into 70/15/15 for training, validation, and testing using randomly selected snapshots. The SHRED model learns a mapping from sparse sensor measurements to the reduced temporal coefficients cases: V_i^T and $(SV^T)_i$. A single architecture is used across all POD truncation levels to ensure consistency. To improve robustness, an ensemble of n independently trained models is used, and the final prediction is the average output across the ensemble.

The loss function is defined as an energy-weighted reconstruction error:

$$\mathcal{L} = \sum_{i=1}^{r} \|y_i - \tilde{y}_i\|_2^2 \cdot \frac{S_i}{\sum_{j=1}^{r} S_j} \tag{1}$$

The lowest root mean square error on reconstruction is found for energy recoveries of $\sum S = [60, 70]\%$ on both procedures: V_i^T and $(SV^T)_i$. The highest error occurs at high energy recovery levels (cases 90% and 99%). Compared with LES data, as shown in Fig. 3 and Fig. 4, there are difficulties reproducing small scales. Initial results showed that although dimensionality reduction has been applied successfully, it is still open to research alternative approaches to this ROM technique to achieve higher compression rates and, if possible, improve small-scale representation.

References:

[1] B. Eiximeno, A. Miró, B. Begiashvili, E. Valero, I. Rodriguez, and O. Lehmkhul. "PyLOM: A HPC open source reduced order model suite for fluid dynamics applications". In: *Computer Physics Communications* 308 (2025), p. 109459.

[2] J. P. Williams, O. Zahn, and J. N. Kutz. "Sensing with shallow recurrent decoder networks". In: *Proceedings of the Royal Society A: Mathematical, Physical and Engineering Sciences* 480.2298 (2024), p. 20240054.

[3] L. Gasparino, F. Spiga, and O. Lehmkuhl. "SOD2D: A GPU-enabled Spectral Finite Elements Method for compressible scale-resolving simulations". In: *Computer Physics Communications* 297 (2024), p. 109067.

[4] Y.-T. Wu and F. Porté-Agel. "Atmospheric Turbulence Effects on Wind-Turbine Wakes: An LES Study". In: *Energies* 5.12 (2012), pp. 5340–5362.

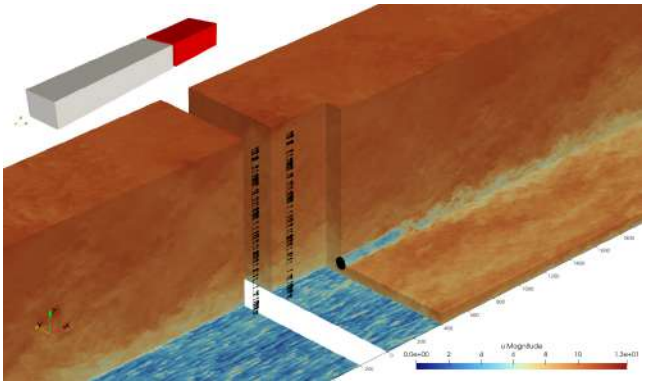

Figure 1: Reference of concurrent precursor-mesh simulation.

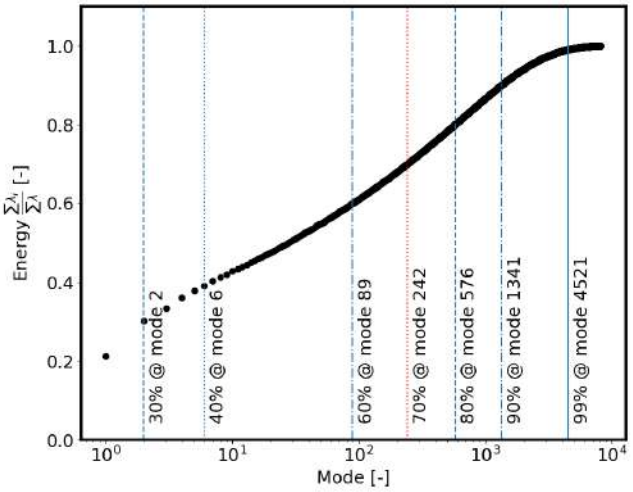

Figure 2: Energy distribution from POD modes.

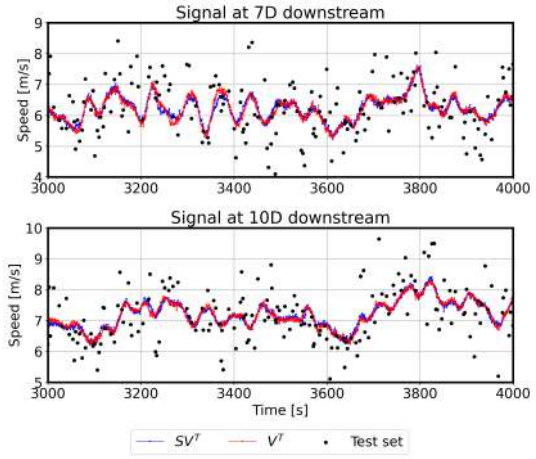

Figure 3: Comparison of ground truth and reconstruction of u_x using models $\sum S = 70\%$.

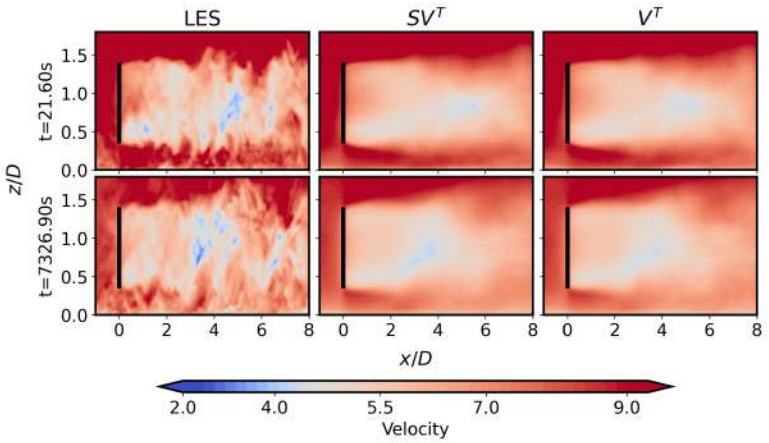

Figure 4: Instantaneous u_x snapshots and reconstruction from test set using model $\sum S = 70\%$.

Interaction of neighboring wind farms in shallow atmospheric boundary layers

M.A. Khan [1], and S.J. Watson [2]

[1,2] Wind Energy Section, Faculty of Aerospace Engineering, Delft University of Technology, Delft, Netherlands

email-adress of the corresponding authour: m.a.khan-2@tudelft.nl

Abstract:
A recent study on wind-farm wake recovery [1] identified a distinct mechanism in shallow atmospheric boundary layers (ABLs). In such conditions, wind-farm wakes recover more slowly, grow narrower instead of expanding, and bend due to the Coriolis effect. Across all ABL depths, wake recovery within approximately 10 km downstream of the wind farm is primarily driven by vertical entrainment, leading to full recovery in deep boundary layers. In contrast, wakes in shallow boundary layers extend beyond 10 km, where spanwise mean advection contributes more significantly, though relatively inefficiently, to far-wake recovery. These findings raise important questions for wind farm clusters, particularly regarding the performance of a downstream wind farm operating within the near wake of an upstream farm in shallow ABLs.

Beyond wake interactions, neighboring wind farms in shallow offshore ABLs may also interact through atmospheric gravity waves (AGWs). Such boundary layers are often capped by a temperature inversion and a stably stratified free atmosphere, which support AGW propagation in multiple directions depending on atmospheric conditions [2]. AGWs generated by individual wind farms may interact constructively, potentially influencing even the upstream wind farm. Motivated by this, we investigate the interaction of two neighboring wind farms in shallow, conventionally neutral ABLs accounting for AGWs.

We perform large-eddy simulations (LES) of two hypothetical aligned wind farms, comparing with an isolated wind farm. The inter-farm spacing is set equal to the interfacial gravity-wave wavelength (4.3 km), enabling constructive wave superposition and increased wave amplitude at the downstream wind farm. Since interfacial wave amplitude is directly linked to boundary-layer thickening and enhanced blockage effects [2], we systematically vary the free-atmospheric lapse rate, capping inversion strength, and boundary-layer height. Three ABL heights are considered: 250 m, 500 m, and 750 m.

Figure 1 shows the temporally and row-averaged power output of both wind farms relative to the isolated case. The upstream wind farm gains up to 1.2% under milder lapse rates and up to 1% with increasing ABL height. For all but the shallowest ABL, the downstream wind farm produces 23–28% less power than the isolated case; in the 250 m ABL, the deficit increases to 52%. Moreover, in this shallowest case, the upstream wind farm produces 0.7% less power than the isolated farm. These results demonstrate that closely spaced wind farms in shallow ABLs are adversely affected by AGW interactions, with the downstream wind farm suffering most due to slow inter-farm wake recovery. We are currently extending this study by simulating ABL heights in the range of 200 m to 500 m to better understand the interaction of neighboring wind farms in shallow ABLs.

References

[1] Lanzilao L. and Meyers J., (2025), Wind-farm wake recovery mechanisms in conventionally neutral boundary layers, *Journal of Fluid Mechanics, vol. 1015, pp. A5*

[2] Khan M.A., Churchfield M.J. and Watson S.J., (2025), Dependence of Wind-Farm-Induced Gravity Waves and Wind-Farm Performance on Non-Dimensional Atmospheric Parameters and Simulation Configuration, *Wind Energy Science Discussions, vol. 2025, pp. 1–34*

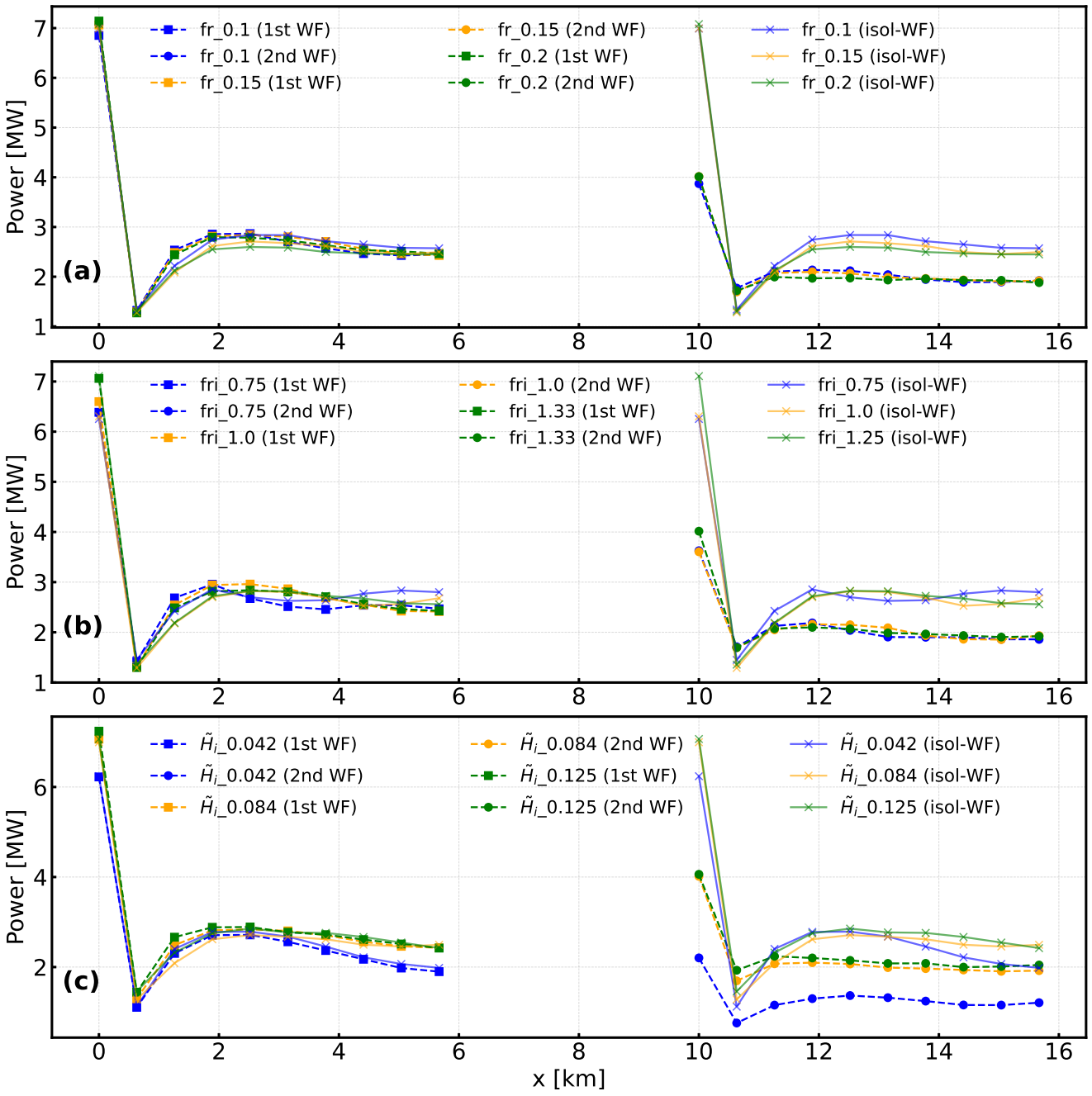

Figure 1: *Temporal and row-averaged wind turbine power output as a function of (a) Fr, (b) Fr_i, and (c) $\tilde{H}_i$; each compared to that of the isolated wind farm. Where ($Fr = U/NL$ and $Fr_i = U/\sqrt{g'H_i}$) are the Froude numbers of free atmosphere and the capping inversion, and ($\tilde{H}_i = H_i/L$) is the aspect ratio of the ABL. These non-dimensional parameters relate the flow conditions, i.e. U: geostrophic wind speed, N:Brunt-Väisälä frequency that is a function of lapse rate, g': reduced gravity as a function of potential temperature jump across the capping inversion, $\Delta\theta$, and H_i: capping inversion height, to wind farm length (L) in the streamwise direction.*

Coupling Large Eddy Simulations and Aeroelastic Blade Response for Wind Farm Optimisation

Andrew Mole [1], Luca Magri [1,2]

[1] Department of Aeronautics, Imperial College London, London, UK
[2] Politecnico di Torino, DIMEAS, Torino, Italy

email-address of the corresponding author: a.mole@imperial.ac.uk

Abstract:
Understanding and controlling turbulent flow interactions within wind farms is central to improving their performance and longevity [5]. In large arrays, the unsteady turbulent wakes of the turbines propagate downstream, reducing power extraction and increasing structural loading on subsequent turbines. These coupled aerodynamic and structural effects present a key challenge for wind farm control.

In this work, we investigate how turbulent wake dynamics interact with the turbines structural response using a high-fidelity simulation framework. The Actuator Line Method (ALM) is deployed within Large Eddy Simulations (LES) to resolve the turbulent flow within a wind farm. The flow solver Xcompact3d [1] is coupled with the aeroelastic solver BeamDyn [6] to account for blade deformation as shown in Figure 1. When applied under realistic wind conditions, this enables a detailed characterisation of the effect the deformation has on downstream wind turbines under unyawed and yawed scenarios.

Building on this high-fidelity framework, we explore how turbulent flow features influence the trade-off between power production and structural fatigue. Rather than optimising for power alone [4, 2], we adopt a multi-objective approach that accounts for both power production and fatigue-inducing loads arising from turbulence driven cyclic loading. To efficiently explore this high-dimensional and computationally expensive problem, we employ Multi-Objective Bayesian Optimisation (MOBO) [3], which leverages surrogate models to identify Pareto-optimal operating strategies as shown in Figure 2.

This approach provides new insight into how turbulent wake dynamics can be managed to balance competing objectives in wind farm operation. The results highlight the importance of incorporating turbulence-resolving simulations and aeroelastic effects into the optimisation framework, and demonstrate a pathway toward adaptable wind farm control strategies.

References

[1] Paul Bartholomew et al. "Xcompact3D: An open-source framework for solving turbulence problems on a Cartesian mesh". In: *SoftwareX* 12 (2020), p. 100550.

[2] Nikolaos Bempedelis et al. "Data-driven optimisation of wind farm layout and wake steering with large-eddy simulations". In: *Wind Energy Science* 9.4 (2024), pp. 869–882.

[3] Samuel Daulton, Maximilian Balandat, and Eytan Bakshy. "Differentiable expected hypervolume improvement for parallel multi-objective Bayesian optimization". In: *Advances in neural information processing systems* 33 (2020), pp. 9851–9864.

[4] Andrew Mole and Sylvain Laizet. "Multi-Fidelity Bayesian Optimisation of Wind Farm Wake Steering Using Wake Models and Large Eddy Simulations". In: *Flow, Turbulence and Combustion* (2024).

[5] Paul Veers et al. "Grand Challenges in the Design, Manufacture, and Operation of Future Wind Turbine Systems". In: *Wind Energy Science* 8.7 (2023), pp. 1071–1131.

[6] Qi Wang et al. "BeamDyn: a high-fidelity wind turbine blade solver in the FAST modular framework". In: *Wind Energy* 20.8 (2017), pp. 1439–1462.

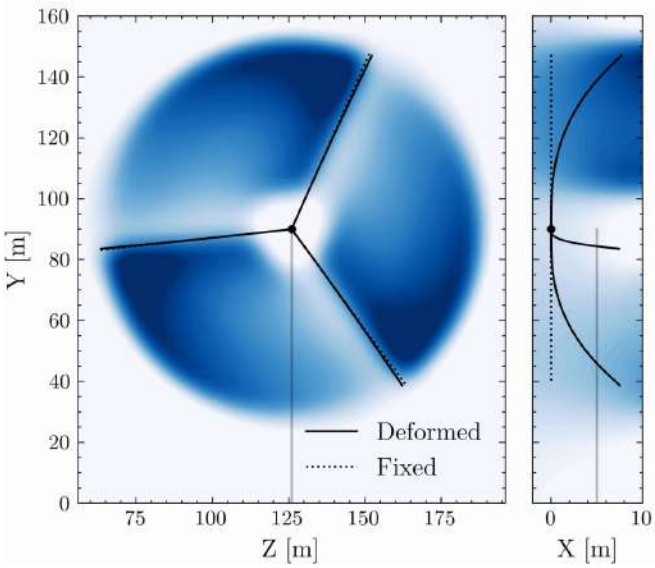

Figure 1: *Caption for the figure on the left side*

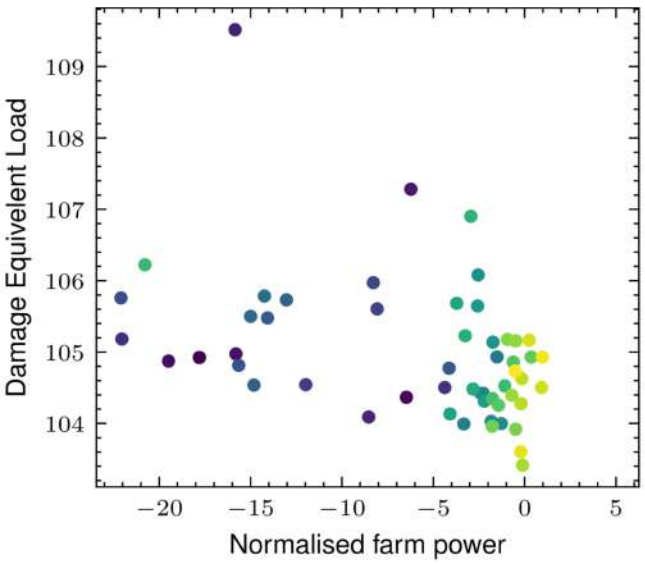

Figure 2: *Caption for the figure on the right side*

Turbulent/turbulent interfaces: building blocks for understanding the connection between scales

Pedro D. Alves [1], Oliver R. H. Buxton [2] and Carlos B. da Silva [1]

[1] IDMEC, Instituto Superior Técnico, Universidade de Lisboa, Lisboa, Portugal

[2] Department of Aeronautics, Imperial College London, London, UK

email-adress of the corresponding authour: pedrodalves@tecnico.ulisboa.pt

Abstract:

The interaction between wind farms and the atmospheric boundary layer consists of a multiscale complex problem with several regions of interest [1]. A particularly relevant one is the inhomogeneous layer that separates the bulk flow from the background, denominated as turbulent/turbulent interface (TTI) [2]. At a fundamental level, the TTI mediates the processes of scalar, momentum and energy exchanges which are believed to be influenced by the large-scale properties. Indeed, turbulence intensity controls the entrainment flux of wakes with a turbulent background [2], and dictates the dominance of scalar layers with different turbulent properties [3]. Simultaneously, there is compelling evidence pointing towards an important role of the small scales of motion, as they universally describe enstrophy profiles [3] and scale the entrainment velocity [4] in the vicinity of TTIs.

In this work we use direct numerical simulations (DNSs) of spatially-developing shearless layers with different turbulence properties to shed some light on the apparent quarrel concerning the role of small and large scales. These DNSs, with 2048×1024^2 detailed in [3], allow the inlet selection, for each layer, of integral length scale, turbulence intensity or enstrophy magnitude. In figure 1, a subdomain of a DNS is shown, where the inner layer presents a higher enstrophy level than the outer, and a similar integral length scale. The flow field shows different topologies in close proximity to the TTI, e.g. saddles or foci, which are usually quantified through an analysis of the velocity gradient tensor, a_{ij}, such as the ubiquitously studied (R_A,Q_A) map, i.e. composed of its invariants [5]. Figure 2 shows this joint probability density function for three interface-normal distances. Clearly, even though the classical tear-drop shape exists throughout the TTI, it shows deviations, especially in the first quadrant. Since viscous effects of velocity gradients are negligible near TTIs [3], this dynamical aspect of a_{ij} can only be caused by its own self-amplification mechanism, $a_{ik}a_{kj}$, or due to the pressure Hessian, $\partial^2 p/\partial x_i \partial x_j$. Interestingly, pressure exhibits a smooth evolution across the TTI (figure 3), contrasting with other small-scale quantities, ultimately conforming a possible pathway between small and large scales that shall be further explored in the presentation.

References

[1] Porté-Agel, F., Bastankhah M. and Shamsoddin, S., (2020), Wind-Turbine and Wind-Farm Flows: A Review, *Boundary-Layer Meteorology, 174:1–59*

[2] Kankanwadi, K. S. and Buxton, O. R. (2020), Turbulent entrainment into a cylinder wake from a turbulent background, *Journal of Fluid Mechanics, 905, A35*

[3] Alves, P. D., Zecchetto, M., Buxton, O. and Da Silva, C. B. (2025), Dynamics of spatially developing turbulent/turbulent interfaces in the absence of mean shear, *Journal of Fluid Mechanics, 1022, A9*

[4] Chen, J. and Buxton, O. R. (2024), Turbulent/turbulent entrainment in a planar wake, *Journal of Fluid Mechanics, 1000, A26*

[5] Meneveau, C. (2011), Lagrangian dynamics and models of the velocity gradient tensor in turbulent flows, *Annual Review of Fluid Mechanics, 43(1), 219-245*

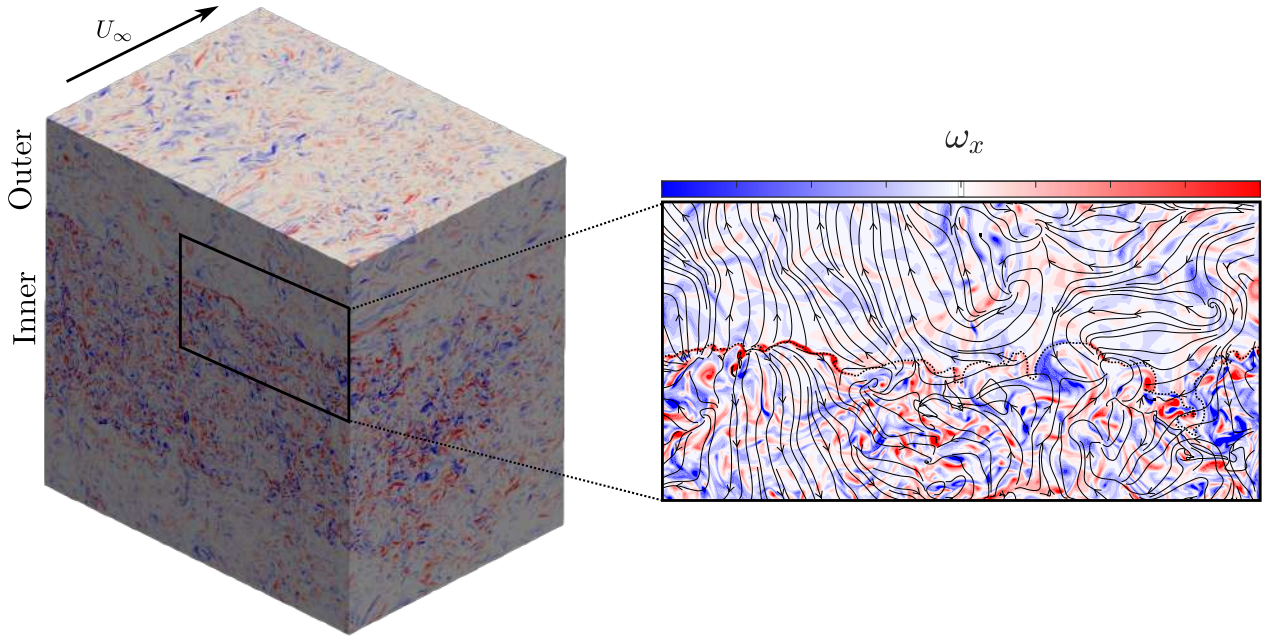

Figure 1: *Three-dimensional visualisation of $x-$component of the vorticity vector, ω_x, for a DNS subdomain (left) and detail of the flow streamlines projected onto a two-dimensional velocity plane (right). The arrow in the left figure points in the streamwise direction, where U_∞ is the convection velocity. Blue/red hues denote negative/positive values of ω_x.*

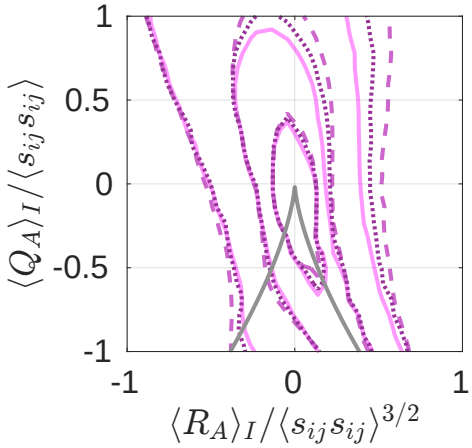

Figure 2: *Joint probability density function of R_A and Q_A normalised by the rate-of-strain tensor magnitude, $s_{ij}s_{ij}$. Lighter/darker colors refer to locations closer to/farther from the TTI.*

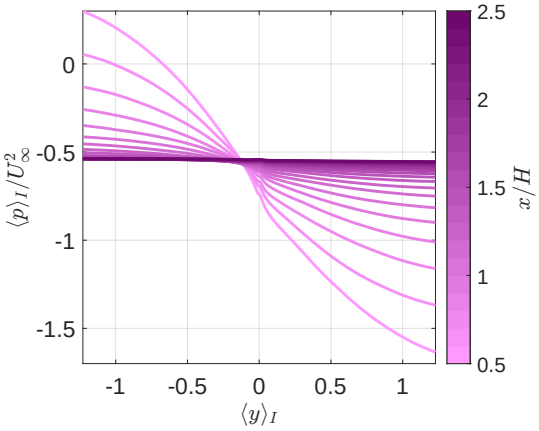

Figure 3: *Conditional profiles of pressure normalised by the convection velocity, U_∞. Lighter/darker colors refer to locations closer to/farther from the inlet. Adapted from [3].*

An actuatable porous disk for miniature active cluster wake control windtunnel experiments

S.A. Umans [1], B. de Vos [1], B.M. Harder [1], J. Gutknecht [1], S.J. Watson [1] and J.W. van Wingerden [1]

[1] Delft University of Technology, Delft, The Netherlands

email-adress of the corresponding author: s.a.umans@tudelft.nl

Abstract:
The number of offshore wind farms is increasing to achieve renewable energy production targets. Consequently, the distances between farms is decreasing and power losses resulting from inter-farm interactions have been a growing concern for industry, policy-makers, and scientists [1]. These power losses originate in the cluster wake of an upstream farm advecting far enough downstream to impede on a downstream farm, decreasing the amount of available power for this farm. Currently, there are few solutions to mitigate these power losses. One proposed solution is Active Cluster Wake Control (ACWC) [2], where the upstream farm would collectively change its induction dynamically to increase the available power for the downstream farm. Potentially, ACWC methods have the capacity to increase the collective energy yield, but this is yet to be shown.

To advance the development of ACWC, a tool to quickly make rough assessments of various methods would be valuable. The large scales of the problem make numerically analysing ACWC methods computationally expensive. Alternatively, scaled wind tunnel experiments could facilitate relatively quick assessment. This would require sufficiently small turbine models to fit a farm configuration in regular wind tunnels. Various small scale models exist, categorised as either bladed turbines or porous disks (PDs). However, bladed turbines are relatively difficult to scale to a farm configuration, and there exist no actuatable PDs that can be scaled down to small enough sizes [3].

Therefore, we developed such a small scale APD, shown in Fig. 1. This APD has a disk diameter of 10 cm and simulates induction control by varying the porosity. This is achieved by having two stacked PDs, where the rear is stationary, and the front can be given an angular offset. This yields a porosity curve as shown in Fig. 2, where the porosity decreases with increasing absolute angle, as long as the radial ribs overlap, and is constant otherwise.

A linear relation between the APD thrust coefficient and porosity is found, making it possible to indirectly set the thrust coefficient and to dynamically change it. Probing the wake with a sensor porous disk (SPD) at various locations, as shown in Fig. 3, also allows for the reconstruction of the free stream velocity, $u_{\mathrm{r}}^{\mathrm{S}}$, averaged over the SPD rotor at each position.

When the upstream APD sinusoidally varies its thrust coefficient, this can be measured in the wake by the SPD, as shown in the phase averages displayed in Fig. 4. This proves the feasibility of this model to dynamically alter the wake.

The application of this model is not limited to farm configurations, but could also be extended to situations such as turbine-to-turbine active wake mixing synchronisation problems.

References

[1] Finserås, E., Herrera Anchustegui, I., Cheynet, E., Gebhardt, C.G., Reuder, J., (2024), Gone with the wind? Wind farm-induced wakes and regulatory gaps, *Marine Policy, vol. 159, pp. 105897*

[2] Gutknecht, J., Taschner, E., Becker, M., Viré, A., Wingerden, J.-W.V., (2025), Mitigating cluster wake induced power losses at neighboring wind farms through cluster-wide coordinated control, *Research Square, Preprint version 1*

[3] Yu, W., Hong, V.W., Ferreira, C., van Kuik, G.A.M., (2017), Experimental analysis on the dynamic wake of an actuator disc undergoing transient loads, *Exp. Fluids, vol. 58, pp. 149*

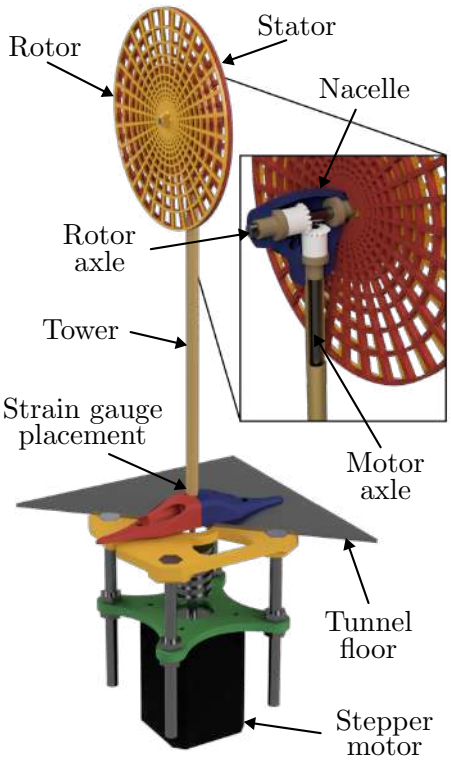

Figure 1: *Model render with internal nacelle details.*

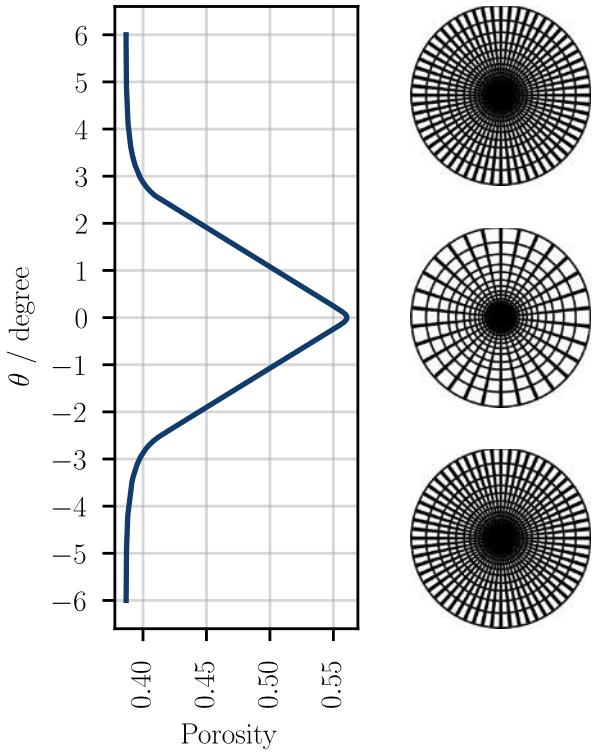

Figure 2: *Theoretical porosity curve as a function of angular offset, with the corresponding extreme and zero position frontal faces depicted on the right.*

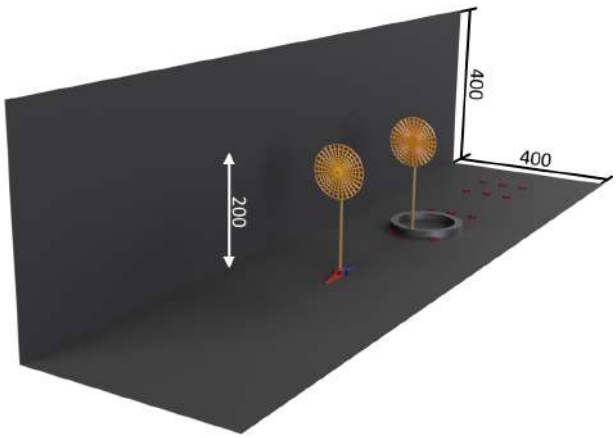

Figure 3: *Tunnel, APD, SPD, and red SPD placement markers to scale.*

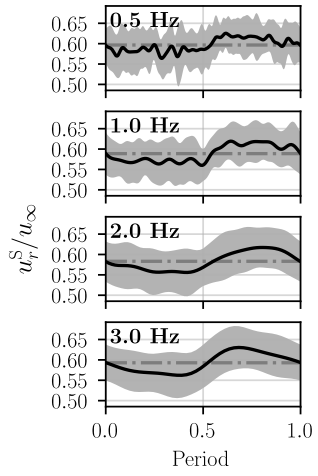

Figure 4: *Phase average with the SPD placed in the center wake and 3D downstream. The shaded area indicates the 95% confidence interval.*

The Leading Edge Paradox: A Story of Distortion and Noise

Sparsh Sharma, Alexandre Suryadi and Michaela Herr

Wind Energy, German Aerospace Center, Braunschweig, Germany

email-adress of the corresponding authour: sparsh.sharma@dlr.de

Abstract:
Turbulent inflow undergoes systematic distortion as it convects toward a lifting surface. In wind-farm environments this mechanism governs both the unsteady loading of turbine blades and the spectral transfer of energy from large-scale atmospheric structures to the smaller scales directly responsible for fatigue and noise. The present work develops and identifies a mathematically explicit distortion operator that maps upstream turbulence to its near–leading-edge counterpart, using high-fidelity Lattice Boltzmann simulations of grid-generated turbulence interacting with a finite-thickness airfoil as a controlled analogue for wind-turbine blades.

Let $\Phi_\infty(\mathbf{k},\omega)$ denote the upstream spectral tensor and $\Phi_{\mathrm{LE}}(\mathbf{k},\omega)$ the tensor measured a small distance upstream of the leading edge. The interaction is shown to be governed by a single non-dimensional distortion parameter $\theta = a\tau$ (with $a = \mathcal{O}(U_\infty/r_{\mathrm{LE}})$ the local stagnation strain and $\tau = r_{\mathrm{LE}}/U_\infty$ the flight time), leading to the closed-form Rapid Distortion mapping

$$\Phi_{\mathrm{LE}}(\mathbf{k},\omega) \approx \Pi(\mathbf{k})\, F(\theta)\, \Phi_\infty\big(F^\top(\theta)\mathbf{k},\omega\big)\, F^\top(\theta)\, \Pi(\mathbf{k})\, \mathcal{D}(\mathbf{k};\theta),$$

where $F(\theta) = \mathrm{diag}(e^\theta, e^{-\theta}, 1)$ encodes anisotropic wavevector shear, Π enforces incompressibility, and $\mathcal{D}$ captures scale-selective viscous damping. The operator implies a universal dependence on $\kappa = kr_{\mathrm{LE}}$: large eddies ($\kappa \ll 1$) experience amplification of wall-normal energy and increased coherence, while small eddies ($\kappa \gg 1$) are attenuated. The simulations confirm these asymptotics: near-nose spectra reveal low-frequency amplification, high-frequency suppression, and a coherence increase at scales comparable to r_{LE}.

This behavior mirrors the physics of turbine inflow in wind farms, where atmospheric eddies of size $\Lambda/D = \mathcal{O}(1)$ impose coherent loading, while smaller structures are filtered by blade geometry and local strain. The operator therefore provides a scale-aware, geometry-explicit framework for predicting how incoming turbulence is reshaped before interacting with the blade, without reliance on empirical tuning. Applications include (i) improved blade-loading and fatigue models through physically grounded spectral gains, (ii) coherence-aware formulations for wake-induced unsteadiness, and (iii) a path toward universal inflow-to-loading transfer functions valid across Reynolds number, turbulence intensity, and inflow topology. A second page supplies numerical evidence, including spectral gains, coherence trends, and vortical topology near the leading edge.

Supporting figures

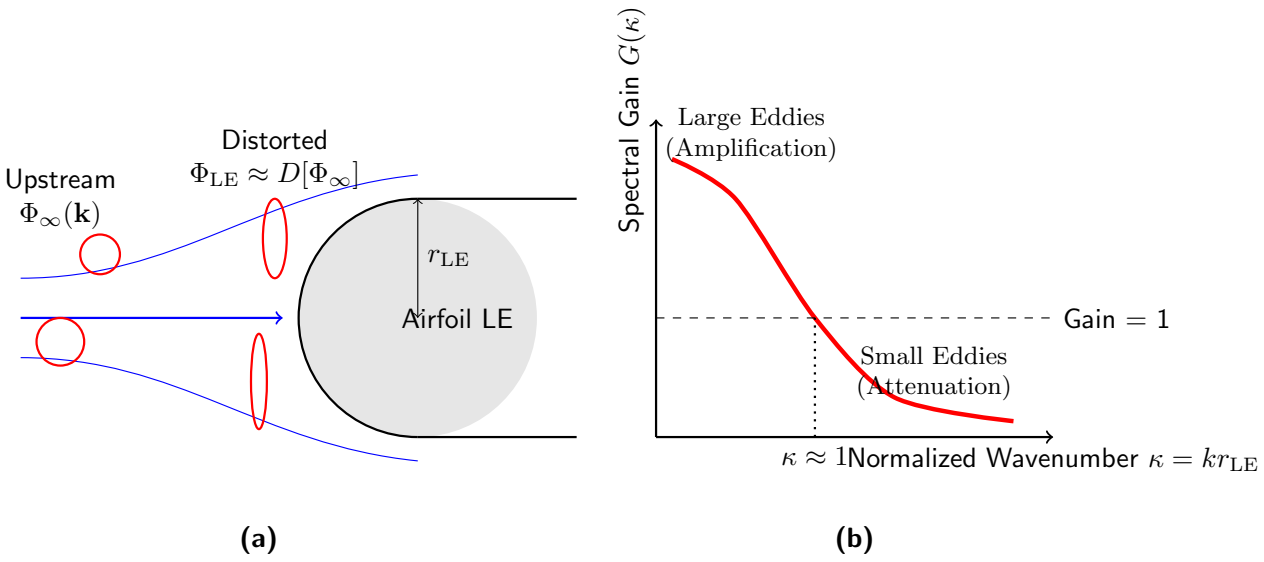

Figure 1: Scale-dependent distortion of upstream turbulence as it convects toward the leading edge. Panel (a) illustrates the mapping from the upstream spectrum $\Phi_\infty(\mathbf{k})$ to the distorted near–leading-edge field $\Phi_{\mathrm{LE}} \approx D[\Phi_\infty]$. Panel (b) shows the corresponding spectral gain $G(\kappa)$, revealing amplification of large eddies ($\kappa \ll 1$) and attenuation of small scales ($\kappa \gg 1$), with the strongest distortion around $\kappa \approx 1$.

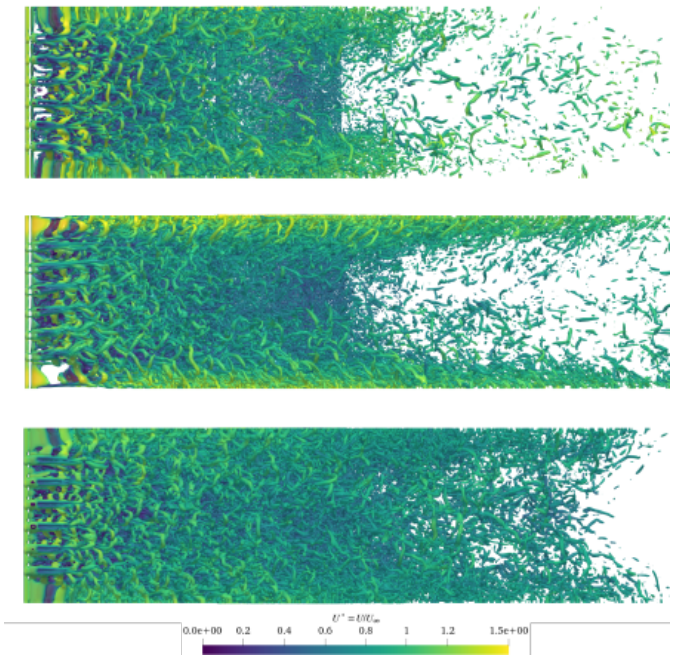

Figure 2: Instantaneous vortical structures visualised using a fixed Q–criterion threshold for three inflow velocities. The top, middle, and bottom panels correspond to $U_\infty = 20$, 30, and 40 m/s, respectively. Increasing inflow velocity produces stronger small-scale content and earlier breakdown downstream of the turbulence-generating grid. At lower velocity (20 m/s), the vortices remain more coherent and elongated, whereas at higher velocities (30–40 m/s) the field becomes progressively richer in fine-scale structures, indicating higher turbulent kinetic energy and more rapid cascade. All visualisations use the same colour map ($U^* = U/U_\infty$) to allow direct comparison across cases.

Sensitivity of wind farm-induced gravity waves to rotor diameter, farm aspect ratio and turbine spacing

Udhaya Chandiran Krishnan Paranjothi [1], Stefan Hickel [1] and Simon Watson [1]

[1] Faculty of Aerospace Engineering, Delft University of Technology, 2629HS Delft, The Netherlands

email-address of the corresponding author: u.c.krishnanparanjothi@tudelft.nl

Abstract:

Recent studies have revealed that large wind farms, operating in flat terrain such as offshore, can displace the flow enough to excite gravity waves in the stratified regions of the atmospheric boundary layer [1]. These wind farm-induced gravity waves (WFIGW) can intensify the pressure gradient in the streamwise direction of the wind farm, which in turn affects the performance of the wind turbines. Allaerts et al. [2] assessed the associated annual energy loss in the Belgian-Dutch wind farm cluster to be in the order of 4 - 6 %, establishing the importance of WFIGW. However, the sensitivity of WFIGW to many parameters remains unknown. Considering that parameters such as turbine diameter (D), farm aspect ratio (AR, which is defined here as the ratio of streamwise length to the spanwise length of the wind farm), and turbine spacing (S) are optimized for a proposed wind farm site, the sensitivity of WFIGW to these parameters is the primary research question that this study addresses through large eddy simulations.

A wind farm consisting of IEA 22MW reference wind turbines ($D = 284\,\mathrm{m}$), arranged with a turbine spacing of $5D$ in 10 rows and 10 columns (each row is oriented perpendicular to the inflow wind direction and each column is aligned with it), is taken as reference. Each parameter is varied separately ($D =$ 241.94 m and 126.91 m; $S = 7D$ and $9D$; $AR = 0.5$ and 2) resulting in six additional simulations. The turbines with smaller rotor diameters are configured to have the same hub height as the reference turbine in order to isolate the effect of rotor diameter. The simulations are carried out in a conventionally neutral boundary layer with an inversion height of 500 m, an inversion strength of 2 K, a free atmospheric lapse rate of 3 K/km, a velocity at hub height of 10 m/s and at a latitude of 51.6°.

The time-averaged results from some of the simulations are discussed here. The normalized vertical component of velocity along a vertical plane aligned with the mean wind direction for the different rotor diameter cases are displayed in fig. 1. The larger turbines displace the flow more, resulting in the excitation of higher amplitude gravity waves. In fig. 2, which compares different aspect ratios, the longer wind farm gives rise to gravity waves at the start and the end of the wind farm, which then interact. Fig. 3 compares the pressure perturbation fields in a horizontal plane at the hub height for two different rotor diameter cases. It is evident that the higher flow displacement caused by larger rotor diameter results in a stronger pressure feedback. Similarly, fig. 4 shows that a longer wind farm encounters a marginally higher pressure feedback. The same behaviour is observed in the normalized horizontal velocity along the sixth column of wind turbines, as shown in fig. 5. Finally, the row averaged turbine power outputs for the various cases are presented in fig. 6. The larger turbines mostly generate lower normalized power. This can be explained by the reduction in the region available in the boundary layer for momentum entrainment. A more detailed analysis of all the cases will be presented at the colloquium.

References

[1] Allaerts D., and Meyer J., (2017), Boundary-layer development and gravity waves in conventionally neutral wind farms, *Journal of Fluid Mechanics, vol. 814, pp. 95-130*

[2] Allaerts D., Broucke S. V., van Lipzig N., and Meyer J., (2018), Annual impact of wind-farm gravity waves on the Belgian–Dutch offshore wind-farm cluster, *Journal of Physics: Conference Series, vol. 1037, pp. 072006*

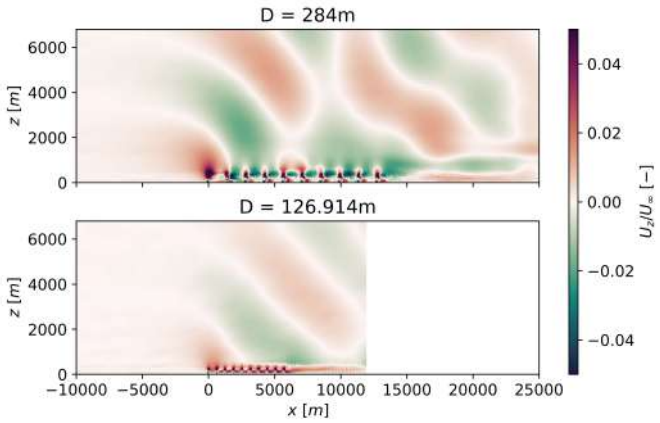

Figure 1: *Time averaged vertical velocity, normalized using the hub height inflow velocity, along a vertical plane aligned with the mean wind direction for different rotor diameter cases*

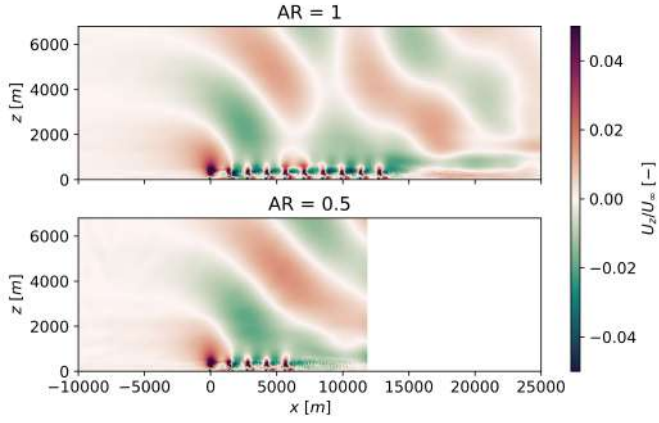

Figure 2: *Time averaged vertical velocity, normalized using the hub height inflow velocity, along a vertical plane aligned with the mean wind direction for different aspect ratio cases*

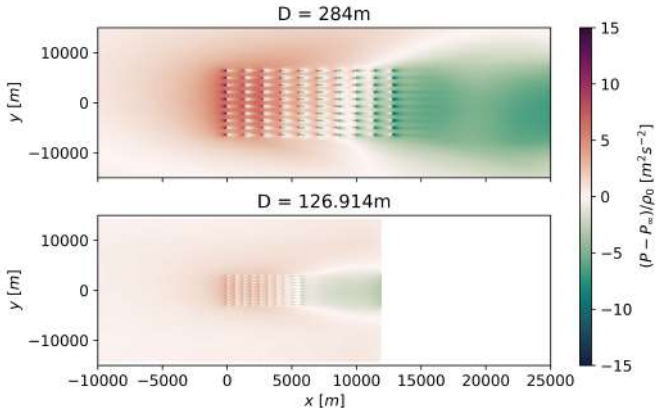

Figure 3: *Time averaged pressure perturbation, normalized using the density, along a horizontal plane at the hub height for different rotor diameter cases*

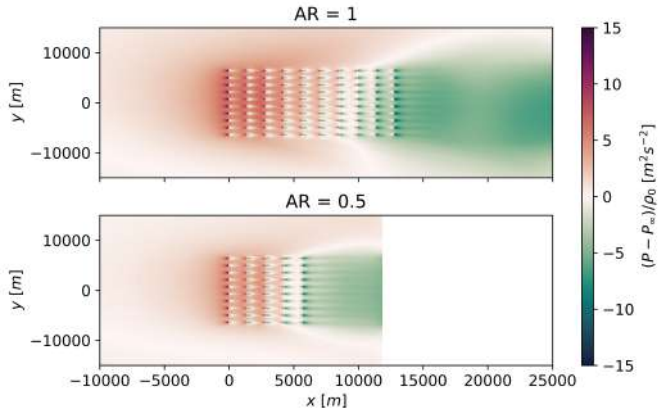

Figure 4: *Time averaged pressure perturbation, normalized using the density, along a horizontal plane at the hub height for different aspect ratio cases*

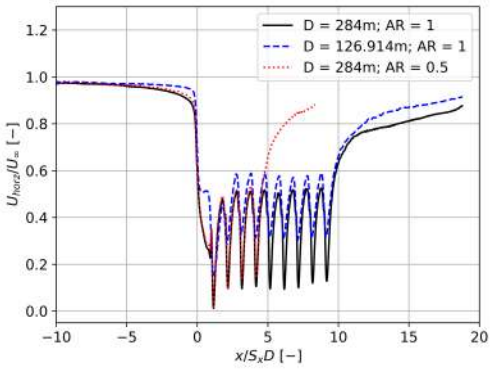

Figure 5: *Time averaged horizontal velocity, normalized using the hub height inflow velocity, along the sixth turbine column*

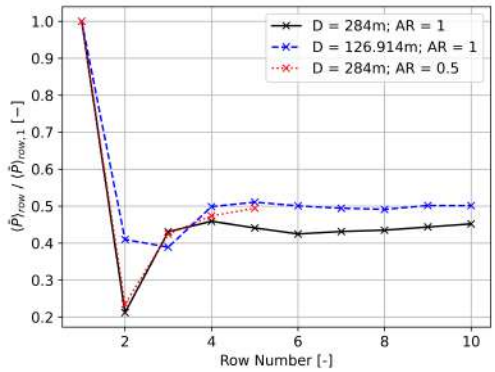

Figure 6: *Time and row averaged turbine power output, normalized by the first row power output*

Assessment using LES simulations of the wake meandering predictions by the OnWaRDS wake model

Elisa Valepyn [1], Maud Moens [1], Maxime Lejeune [1*], Matthieu Duponcheel [1], Ariane Frère [2] and Philippe Chatelain [1]

[1] UCLouvain, Institute of Mechanics, Materials and Civil Engineering (iMMC), Louvain-la-Neuve, Belgium
[2] Engie Research & Innovations, Laborelec, Linkebeek, Belgium

email-adress of the corresponding authour: elisa.valepyn@uclouvain.be

Abstract:
Accurate prediction of wind farm flows under realistic atmospheric and operational conditions remains a major challenge for both wind farm modelling and control. Wake dynamics are inherently multi-scale and strongly influenced by ambient turbulence, leading to complex phenomena such as wake meandering. Consequently, enhancing our understanding of wind turbine wakes is imperative to improve the efficiency of the control strategies in wind farms. In order to deal with flow unsteadiness, time delays involved in wake propagation and transient operating conditions, model-based wind farm control schemes have been gaining interest. Those rely on the information provided by an underlying model of the wind farm dynamics which predicts the turbines-wakes interactions.

However, in order to make it suitable for control applications, the model must be fast enough to be used online, and achieve sufficient accuracy as the fidelity of the model always bounds the performance of the control scheme. Medium-fidelity dynamic models fill this gap by providing a dynamic and reasonably faithful representation of the flow while remaining computationally tractable.

In this work, we assess the capability of a medium-fidelity, physics-based dynamic wake model, called OnWaRDS [1], to reproduce the main dynamic features of the wake across a range of inflow and operational conditions. OnWaRDS has been implemented in the OFF framework [2], a dynamic open-source wake model designed for wind farm flow control and wake model development. In this context, OnWaRDS constitutes a computationally efficient formulation specifically designed to enable scalable data assimilation for large wind farms. OnWaRDS combines a rotor-based flow sensing with a Lagrangian flow modelling into a unified framework. A Kalman filter is coupled to a Blade Element Momentum (BEM) theory solver [3] to estimate the rotor-normal component while an Artificial Neural Network (ANN) regressor, trained on high-fidelity Large Eddy Simulations (LES) data, is used to compute the transverse velocity component. Then, the Lagrangian flow model reconstructs the farm flow field using a series of particles and propagates them across the wind farm in a physics-informed fashion. High-fidelity LES will be used as a reference to evaluate the model performance. The flow solver used is an in-house 4th-order finite difference LES solver coupled with Actuator Disks (LES-AD) [4].

The assessment of OnWaRDS focuses on the reproduction of wake meandering characteristics 1, the estimation of turbulence intensity within the wake, the ambient turbulence intensity and the response of the model to changes in operating conditions, including transient and static yaw misalignment. By validating the model predictions against LES data, this work aims to quantify the range of conditions under which such medium-fidelity approaches can reliably represent wind turbine wake dynamics. The results provide insight into the strengths and limitations of dynamic wake models for operational wind farm applications and constitute an important step toward their deployment in model-based wind farm control strategies.

References

[1] Lejeune M., Moens M., and Chatelain P., (2022): A Meandering-Capturing Wake Model Coupled to Rotor-Based Flow-Sensing for Operational Wind Farm Flow Prediction, *Frontiers in Energy Research*

[2] Becker M., Lejeune M., Chatelain P., Allaerts D., Mudafort R. and van Wingerden J. W., (2025): A dynamic open-source model to investigate wake dynamics in response to wind farm flow control strategies, *Wind Energy Science* 10, 1055–1075

[3] Bottasso C. L., Cacciola S. and Schreiber J., (2018): Local wind speed estimation, with application to wake impingement detection, *Renewable Energy* 116, 155–168

[4] Moens M., Duponcheel M., Winckelmans G. and Chatelain P., (2018): An actuator disk method with tip-loss correction based on local effective upstream velocities, *Wind Energy* 21, 766–782

*Present affiliation: von Karman Institute for Fluid Dynamics, Rhode-Saint-Genèse, Belgium

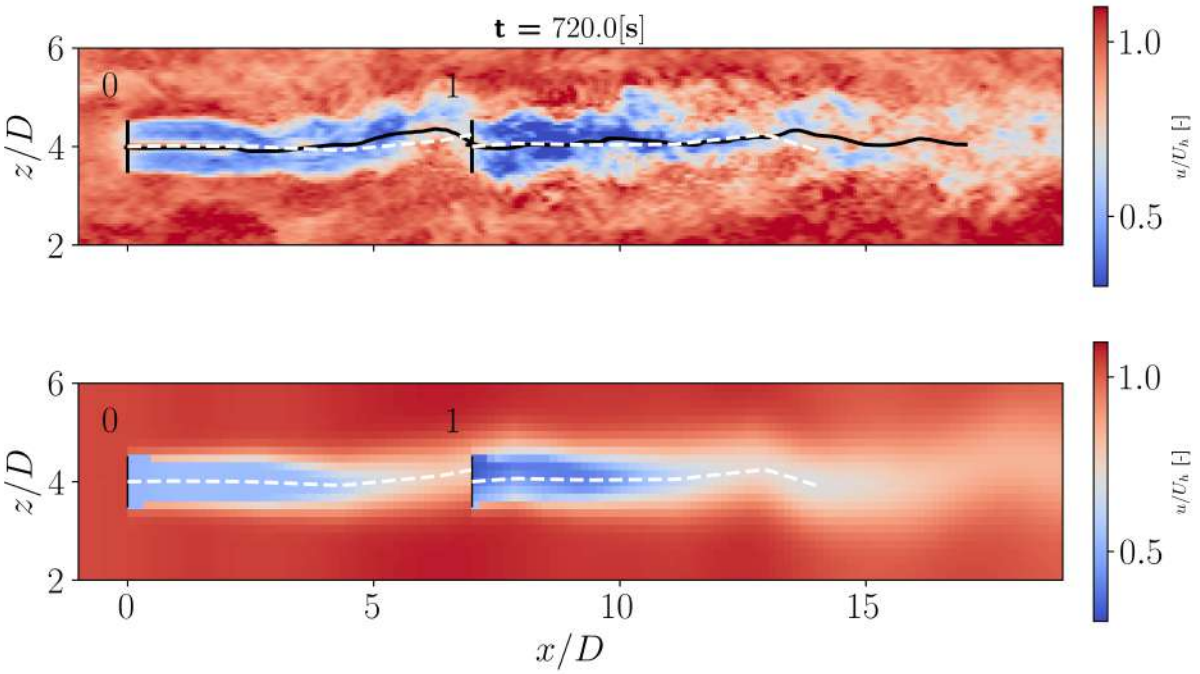

Figure 1: *OnWaRDS wake model (bottom), compared to a realistic representation of the wind farm flow (LES-AD) (top). The white lines are the center of the wakes modeled in OnWaRDS while black lines are the ones captured in the LES-AD framework.*

IMPERIAL

Department of Aeronautics

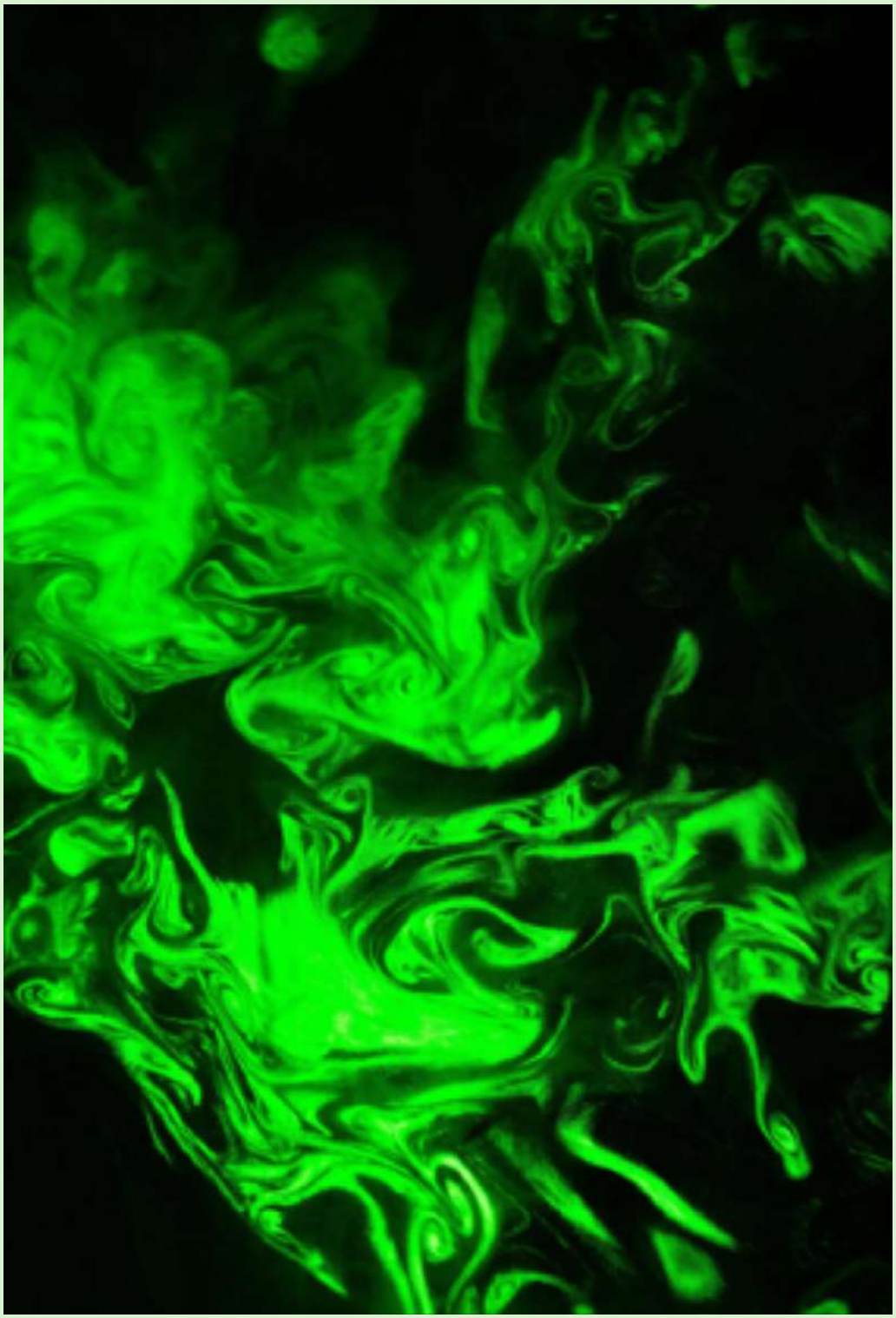

Engineering and Physical Sciences Research Council

ERCOFTAC

EUROPEAN MECHANICS SOCIETY